CHPM2030

CHPM2030 DELIVERABLE D6.2.1.

REPORT ON PILOTS: EVALUATION OF THE CHPM POTENTIAL OF CORNWALL, SOUTH WEST ENGLAND

Summary:
This report investigates the potential for combined heat and metal production from south-west England, considering availability of legacy geoscience information, the geological environment, geothermal characteristics, potential for deep metal enrichment, and technical, environmental, social and regulatory factors that could influence the future development of this technology in the region.

Authors:

Paul A J Lusty, British Geological Survey, Principal Economic Geologist
Richard B Haslam, British Geological Survey, Structural Geologist
Richard A Shaw, British Geological Survey, Economic Geologist
Eimear A Deady, British Geological Survey, Minerals Geoscientist
Paul Williamson, British Geological Survey, Senior Geophysicist

This project has received funding from the European Union's Horizon 2020 research and innovation programme under grant agreement nº 654100.

TABLE OF CONTENTS

LIST OF FIGURES

LIST OF TABLES

1 Executive summary

The CHPM2030 project aims to develop a novel technological solution of Combined Heat, Power and Metal (CHPM) extraction from ultra-deep ore bodies, which will pave the way for pilot-scale systems to be operational by 2030. This technology will help increase the attractiveness of renewable geothermal energy and also reduce Europe's dependency on the import of metals and fossil fuels. In the envisioned technology, an engineered geothermal system (EGS) is established within a metal-bearing geological formation at depths of 4 km or greater, which will be manipulated in such a way that the co-production of energy and metals will be possible. Critical to this, is an understanding of the natural networks of hydraulically-conductive mineral veins that could function as heat-exchange surfaces, and sources of metals. If metals can be leached from the orebodies in high concentrations, and over a prolonged period of time, then their recovery may substantially influence the economics of engineered geothermal systems. Furthermore, leaching of metals from subsurface pathways in a controlled way has the potential to improve fluid flow, and so increase system performance over time.

The CHPM2030 project examined the potential of four areas in Europe for CHPM systems, namely the Precambrian Fennoscandian Shield province, in Sweden; the late Palaeozoic Variscan province, of south-west England and southern Portugal; and the Mesozoic-Cenozoic Alpine province, in north-west Romania. This report covers south-west England, considering the availability of geoscience information, the geological environment, geothermal characteristics, potential for deep metal enrichment, and technical, environmental, social and regulatory factors that could influence the future development of CHPM extraction technology in the region.

The geothermal energy potential of the UK was investigated by research funded by the UK government and European Commission between 1977 and 1994. The UK has a fairly uniform background heat flow field, with areas of greater heat flow associated with the radiogenic Permian granites in south-west England, buried Caledonian granites of northern England and the batholith in the Eastern Highlands of Scotland. South-west England was selected as the UK CHPM2030 study area as it is a major magmatic province, with high heat production, and hosts extensive polymetallic mineralisation. Its long history of metal production, and economic geology research means it is a data-rich region. It is also the focus for contemporary deep geothermal research and development in the UK.

South-west England forms an integral part of the European Variscides and has been influenced by rifting, convergence and passive margin inversion and extensional reactivation. Crustal extension and orogenic collapse during the late Carboniferous and lower Permian resulted in extensive granitic magmatism in the region, forming the Cornubian Batholith. The granites were emplaced into largely Devonian sedimentary rocks, hosted in fault-bound basins. Crustal extension and shortening resulted in large-scale faulting and folding across the region. A major structural feature of south-west England is approximately NW-SE-trending fracture systems, locally termed 'cross-courses', which are considered to play a significant role in the overall permeability of the region. Extensive, internationally renowned granite-related mineralisation occurred during the early to mid-Permian, which contains metals including tin, tungsten, copper, zinc, and arsenic. A separate, Mid-Triassic phase of mineralisation related to basinal fluids, and containing lead, zinc, silver, fluorite and barite developed in the cross-course fractures.

This review whilst considering the broader scale geological context, principally focuses on a study area covering the northern part of the Carnmenellis granite, one of the six exposed granite plutons that form the Cornubian Batholith. At surface the Carnmenellis granite is roughly circular in shape and covers an area of

some 135 km^2. However, in common with the other plutons its shape at depth and thickness remains uncertain. This project used borehole data in conjunction with existing gravity models to better constrain the position of the upper granite surface.

Geological research in south-west England spans over two hundred and fifty years and has been greatly enhanced by geophysical surveys. Gravity modelling of the Cornubian Batholith has resulted in variable estimates of its thickness. The most recent interpretation suggests that the batholith consists of two sheets, with an upper granite, with a base at 6–8 km, and a lower more extensive granite sheet, with a base at 12–15 km. This is supported by the magnetotelluric (MT) and seismic data. Modelling of the Carnmenellis granite suggests it may have a centrally located feeder zone. Seismic surveys have been conducted across south-west England and its adjacent areas. However, no reflectors were identified in the granite, the granite/country rock contact was not imaged, and it was concluded that the granite is seismically featureless. MT data from the Carnmenellis granite indicates a very homogenous body, with joint closure by a depth of 7 km, and a change to pore-dominated resistivity below this depth. High resolution magnetic and radiometric datasets for south-west England were obtained during the recent Tellus South West survey. This data has been widely used in research projects, resulting in new structural interpretations, improved correlations of stratigraphic units and a re-evaluation of the heat production across the batholith.

The study area is extensively mineralised, hosting the highly productive Camborne-Redruth mining district. The granite-related mineralisation can be broadly defined as quartz–wolframite and tourmaline–quartz–cassiterite veins, with subordinate copper, arsenic, and minor bismuth, silver, and lead, which typically occur in swarms in both the granite and the metasedimentary country rock. Grade and tonnage of these deposits are comparable to significant vein-stockwork tin-tungsten deposits globally. Cobalt has been produced from this type of mineralisation in the Redruth area. The Mid-Triassic, variably metalliferous, cross-course veins cross-cut and displace the granite-related mineralisation in this area. They are primarily lead, zinc, silver, fluorite and baryte-bearing, and virtually all the mineralised veins occur in the metasedimentary rocks.

The Carnmenellis granite was the focus of a major geothermal experiment, the UK hot dry rock (HDR) research and development programme that ran for more than 15 years, and produced a huge amount of data and analysis on the geothermal energy potential of south-west England. The project, based at Rosemanowes Quarry, near Penryn in west Cornwall, aimed to demonstrate the feasibility of establishing a 'full-scale prototype' HDR power station in Cornwall. A contemporary project, operated by operated by Geothermal Engineering Ltd (GEL), is the United Downs Deep Geothermal Power (UDDGP) project, located near Redruth and about 7 km north of the old HDR project site. The HDR project focussed on engineering an underground heat exchanger in the low porosity and permeability rock mass using reservoir stimulation. In contrast the UDDGP project is based on a new concept of exploiting the natural permeability that may exist in major fault zones in Cornwall, eliminating the requirement for artificial stimulation of the rock mass. Much of the data, information and analysis presented this review arises from these two deep geothermal development projects.

The temperature of the Carnmenellis granite at 5 km depth is estimated to be 200°C. This estimate is consistent with the actual temperatures measured in the HDR project boreholes. Heat production maps define clear zones of greater heat production in the Carnmenellis granite outcrop. In the United Downs project area, heatflow modelling predicts that at a vertical depth of 4500 m the temperature will be between 180–220°C.

Cornish granites typically have very low primary permeability, but relatively high hydraulic conductivity as a result of faults and joints. The latter are particularly important for controlling fluid flow in Cornish granites. Fluid circulation has been a continuous feature of the Carnmenellis granite and its host rocks since emplacement. Fluid circulation is evident in the local mines where thermal, saline brines discharge from

crosscourse structures. It is concluded that a dynamic system driven by convective and hydrodynamic forces has allowed continuous water-rock reaction to occur within the upper 3–4 km of the currently exposed pluton. It is thought that a large reservoir of probable diluted palaeobrines exists at depth in this area. However, these are not viewed as static, trapped palaeofluids, but rather part of a dynamic system of fluid circulation, involving continuous mixing of saline and meteoric waters, and water-rock reaction that continues today. These brines contain lithium concentrations of up to 125 mg/l^{-1}, probably as a result of the mica breakdown during fluid-rock interaction.

An extensive programme of both direct and indirect stress measurement was undertaken in the Carnmenellis granite during the HDR project in an attempt to understand how the stress regime would influence the shape, extent and orientation of the growth of a geothermal reservoir. Initial tests to develop a 'commercial-scale' heat exchanger at the Rosemanowes site were largely unsuccessful, as when water circulation commenced fluids losses were excessive and the pumping pressures required to maintain circulation were excessive, due to the poor connectivity between the boreholes. A configuration, involving a third borehole orientated to maximise the number of joint intersections and use of viscous gel to open up the rock volume had lower impedance and water losses, and injection and production flow rates in the system were measured over a continuous four year period. It was concluded that the 'optimum hydraulic performance' that could be achieved at the Rosemanowes site was an injection flow rate of 24l/s, with impedance of 0.6 MPa per l/s and with a water loss of 21 per cent. A decline in the thermal performance of the system was also observed over the monitoring period, due to a short circuit between the boreholes. The UDDGP project is currently working on the basis that if the PTFZ is assumed to have a width of about 200 m and two fractures occur every metre that have an aperture of 90 µm, the entire zone would have a transmissivity of 123 mD, resulting in a transmissivity of about 25 Dm. Based on this and heat flow modelling the project aims to produce water at the surface at about 175°C, with a circulation flow rate of between 20–60 l/s.

It has been demonstrated that the stress regime in Cornwall means fluid injected into a deep borehole will migrate downwards, along favourably orientated joints, hence the requirement for the injection borehole to be shallower than the production hole. The UDDGP project boreholes have a large (c. 2000 m) separation, in order to exploit a sufficiently large heat exchanger and reduce the risk of short-circuiting of flow, and will be driven by a downhole pump that will create a pressure sink above the production well. It is predicted that even at moderate injection pressures shearing will occur on favourably orientated fractures.

Preliminary modelling of the Cornubian Batholith has been undertaken to improve understanding of its properties relevant to geothermal energy development. A regional model was constructed to understand the spatial relationship of key geological parameters that were used for the development of subsequent site-scale models. One of the site-scale models is based on data from the HDR project site, and covers a volume of 2.6 km^3, with a depth range of -1000 to -3000 mbsl. The model is centred on the HDR project boreholes, incorporating fracture data from two of the deep boreholes and site-specific hydrological properties. Data and assumptions about the fracture network were used to generate three discreet fracture network (DFN) models for the HDR project reservoir. These were up-scaled to include porosity and permeability in order to understand the potential flow pathways within the reservoir. The second site-scale model considers an area located to the NW of the Carnmenellis granite, where the current UDDGP project is located. The target geothermal reservoir is still considered to be the Carnmenellis granite, and the model covers a volume of 12 km^3, with a depth range of -1500 to -5500 mbsl. In the absence of any published data on the fracture network in the UDDGP project target reservoir and given the consistency of fractures mapped at surface in the Carnmenellis granite the two fracture sets identified and characterised in the HDR project site model were

also used in this model. Due to the uncertainty associated with the location and scale of the fault that the UDDGP project is targeting it was represented in the model as a fractured volume of rock, based on DFN modelling methods. An additional fracture set that is parallel to the fault strike was added to the two regional fracture sets in the UDDGP project site model. Compared to the HDR site project model the modelled volume shows a clear increase in permeability within the fault zone, despite the background permeability being similar. However, the model is likely to overestimate the permeability in the UDDGP project reservoir as the fracture apertures used in the modelling are based on the measured flow within the shallower HDR project boreholes. Although this modelling informs our understanding of the properties of two potential deep geothermal reservoirs in contrasting structural settings in the Carnmenellis granite, there are a number of uncertainties and limitations to these models, which future research will have to address.

The presence of mineralisation at EGS depths (≥4 km) in Cornwall is highly uncertain due to a lack of direct evidence. The deepest mine workings in Cornwall extend to about 1000 m depth, and until 2019 the deepest drilling in Cornwall reached about 2600 m, with only trace quantities of sulfide identified in the core. Significantly, the drilling at the UDDGP project has encountered a number of mineral lodes and cross-course structures. However, the CHPM concept does not necessarily rely an ore body in the traditional sense. Any metal enriched geological formation is a potential target for leaching. The Cornubian Batholith is notable globally for its high bismuth concentrations and the granite is strongly enriched in lithium. Disseminated niobium and tantalum phases also occur in some of the granites. The Carnmenellis granite predominantly comprises quartz, orthoclase feldspar, biotite and muscovite. Micas represent sinks for many minor metals. Preliminary leaching experiments on a mica concentrate produced from a Carnmenellis granite sample were disappointing in terms of the concentrations of metals recovered.

The UDDGP project provides the best indications of the potential environmental impacts of future geothermal resource development in Cornwall. There is a strong preference for new developments to utilise brownfield sites in the region. Proximity to the National Grid and network availability to connect new generation projects will also be a major consideration in the location of future developments. The planning permission application for geothermal exploration and development on the UDDGP project site received no objections from both statutory consultees and local residents. Private housing exists along the western, northern and eastern perimeters of the industrial estate, and the nearest village is less than 1 km away. Background monitoring and predictive modelling was undertaken to predict the noise levels in the area surrounding the site. The drilling rig being used has been designed to minimise environmental impact in urban and noise-sensitive environments, and a range of noise mitigation and attenuation measures have been implemented at the drilling site. Induced seismicity is a concern in all projects that involve deep drilling and water circulation through fractures. During the HDR project tens of thousands of micro-events were recorded, however, very few were felt at surface. In the planning consent for the project the local planning authority included a requirement for both seismic monitoring and a control protocol. Data from the monitoring system is made publically available. Mining in south-west England stretches back millennia, and the mining landscape is testament to the impact mineral extraction has had on the development of the region. The last decade has seen a renewed interest in metals and mining in south-west England. The extent of mineral extraction in south-west England and its impact on the heritage of the region probably means local communities have a relatively receptive attitude towards natural resource development. GEL have undertaken an extensive education and community outreach programme targeting the full cross-section of potential stakeholders. The UDDGP project consultation programme suggests that the local community and politicians are supportive of deep geothermal power development in Cornwall. Plymouth University, in south-west England are researching the issues relating to public perception of geothermal energy exploitation in the UK.

Geothermal heat is considered to have the potential to make a significant contribution to meeting the emissions targets set out in the UK Climate Change Act. One of the key challenges with ownership and regulation of geothermal heat in the UK is that it is regarded as a physical property, not a recoverable material such as a metallic mineral ore. As such, 'heat' is not a legally-defined entity and this causes some difficulties for assigning legal ownership and regulating it. Revision of geothermal regulations is one of a number of measures required to encourage the exploitation of geothermal resources in the UK. The current regulatory approach in the UK for deep geothermal developments requires environmental permissions and licences from the Environment Agency. Development falls under environmental permitting and groundwater regulations, as defined by the Water Framework Directive.

The National Planning Policy Framework in England states that Local Planning Authorities should develop positive strategies to help increase the use and supply of renewables and low carbon energy and heat. The Overarching National Policy Statement for Energy, sets out national policy for the delivery of major energy infrastructure, and indicates that the Government is committed to increasing dramatically the amount of renewable generation capacity. It includes a list of generic impacts that must be considered by energy development proposals. Cornwall Council are keen to understand the potential for geothermal resource development in the county, and strategies it could take to stimulate the deep geothermal sector. Cornwall has produced a 'Sustainable Energy Action Plan', which describes the importance of supporting and promoting geothermal opportunities. The Cornwall 'Local Plan' contains a specific 'Renewable and low carbon energy' policy, which seeks to increase the use and production of renewables and low carbon energy generation. The Council is particularly supportive of developments that 'create opportunities for co-location of energy producers with energy users, in particular heat, and facilitate renewable and low carbon energy innovation.

The mineral ownership situation in Great Britain could present a challenge for the CHPM2030 concept of recovering metals from a geothermal system. The rights to non-energy minerals in Great Britain, with the exception of gold and silver, are mainly in private ownership, and only the mineral rights owner can legally grant rights to explore and mine. Hence a critical stage in the exploration and development process is determination of mineral ownership. This can be difficult and time consuming in Great Britain, particularly in regions with a long history of mineral extraction such as Cornwall.

During the HDR project analysis was undertaken on the economic costs of HDR systems. The capital costs associated with a 'post-prototype' commercial-scale HDR power station in south-west England was estimated to be in the range of £71–100 million (equivalent 2018 prices). If an operational geothermal system can be established at the UDDGP project there are plans to construct a demonstration power plant to supply power to the UK national grid. Demand for renewables (and bio-fuels) is projected to increase in Cornwall, reaching 101 ktoe in 2030. Previous estimates of the electricity generation potential of deep geothermal in south-west England range from 100MW to 4GW, with significant by-product heat. It is suggested that development of this deep geothermal resource could result in Cornwall becoming an attractive destination for power dependent industries. The electricity grid in Cornwall has spare capacity on the network to take more locally generated renewable energy. However, there is very little capacity available for new connections.

In summary south-west England, and specifically Cornwall, is an excellent location for a pilot-scale CHPM system. It has the essential prerequisites of a proven geothermal energy resource and abundant polymetallic mineralisation. It is one of the best surveyed and most data-rich parts of the UK, with a long history of mineral development and geothermal research. The local government and communities appear supportive of deep geothermal resource development, and it has a major, active co-funded deep geothermal project.

2 Introduction

2.1 Objectives and role of the CHPM2030 project

The strategic objective of the CHPM2030 project is to develop a novel technological solution (Combined Heat, Power and Metal extraction from ultra-deep ore bodies), which will help reduce Europe's dependency on the import of metals and fossil fuels, and at the same time, lower the environmental impact of the energy supply.

In the envisioned technology, an Enhanced Geothermal System (EGS) is established on a metal-bearing geological formation, which will be manipulated in a way that the co-production of energy and metals will be possible. At a laboratory scale, the project intends to prove the concept that the composition and structure of ore bodies have certain characteristics that could be advantageous when developing an EGS.

2.2 UK CHPM2030 study area selection

Geological mapping of the UK commenced in the 1800s, and digital geological maps at a scale of 1:50 000 exist for all of the UK and 1:10 000 scale mapping is widely available. This information has supported extensive onshore exploration for metallic minerals, industrial minerals, coal, oil and gas, and geothermal resources. A 'National Geological Model' (NGM) has been constructed for the UK, and comprises an accurate, multi-scaled geospatial model of the subsurface geology. The NGM comprises a bedrock 'fence diagram' (UK3D) and a number of other 3D geological models. In terms of geophysical data, seismic data coverage is relatively good for regions underlain by sedimentary basins. Land gravity survey data covers all of Great Britain at an approximate resolution of one observation per 1.6 km^2. A series of regional aeromagnetic surveys of Great Britain provide complete coverage, typically at a flying height of about 300 m, with a 2 km line separation. More than a million onshore boreholes exist in Great Britain, with about 1760 boreholes that are over 1 km deep. Many bore holes have associated geochemical data, geophysical downhole log data and other records. There are 544 sites with a downhole temperature from 1 km or deeper. The geothermal energy potential of the UK was investigated by research funded by the UK government and European Commission between 1977 and 1994. This appraised heat flow, the potential for exploitation of radiothermal granites as hot dry rock (HDR) reservoirs and hot brines in deep sedimentary aquifers (Busby, 2010).

The United Kingdom is located on stable basement and is devoid of the active volcanism and high heat flows associated with tectonic activity. The average UK geothermal gradient is 26 °C km^{-1}, but locally it can exceed 35 °C km^{-1} (Busby, 2010). Temperatures at depth are determined by the heat flow and the thermal conductivities of the strata. The distribution of heat flow measurements across the UK is very uneven, and many of the boreholes from which data is derived were drilled for other purposes. The heat flow map of the UK is based on 212 observed heat flow measurements based on equilibrium temperatures and laboratory thermal conductivities, augmented by 504 heat flow estimates based on core borehole temperatures and estimated thermal conductivities (Figure 1A) (Busby and Terrington, 2017). There is a fairly uniform background heat flow field of about 55 mW m^{-2} with areas of greater heat flow associated with the radiogenic Permian granites in south-west England (117 ± 8 mW m^{-2}) and buried Caledonian granites of northern England (maximum values of 101 mW m^{-2}) (Figure 1A). Heat flow values also exceed the regional background over the batholith in the Eastern Highlands of Scotland (maximum values of 76 mW m^{-2}) (Beamish and Busby, 2016) (Figure 1B).

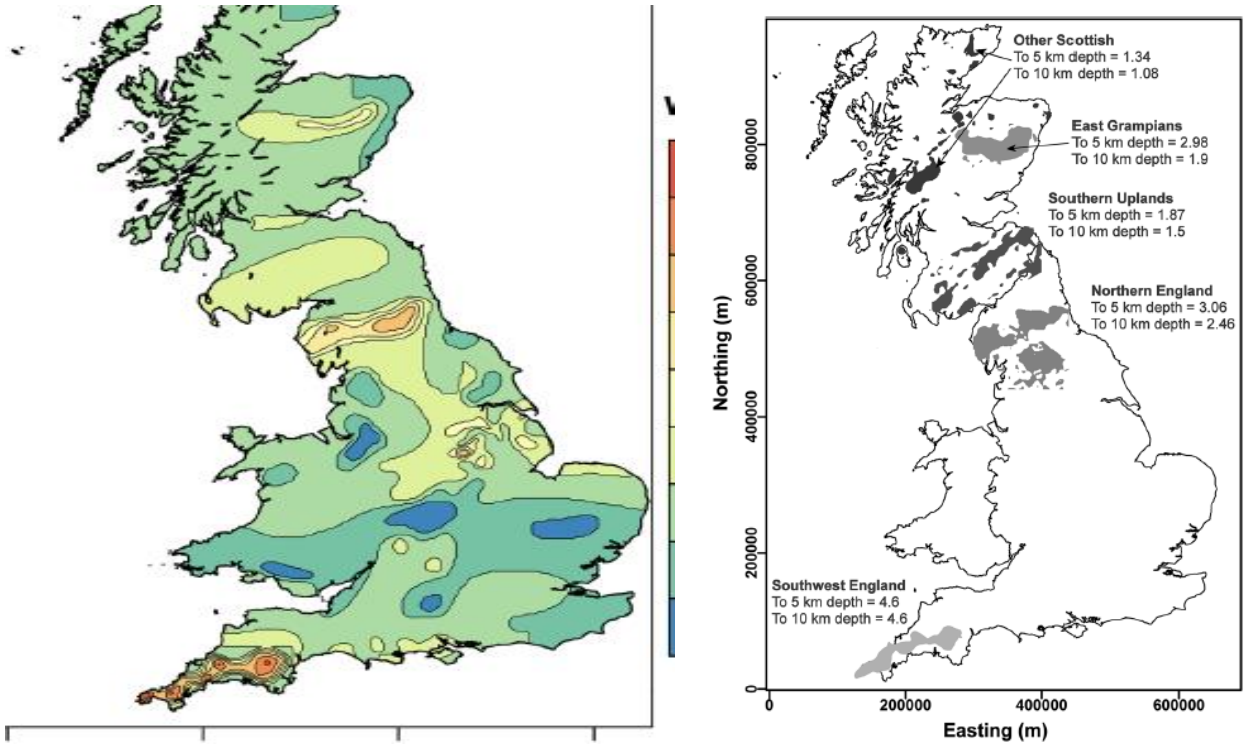

Figure 1: The deep geothermal energy potential of Great Britain. A. Surface heat flow map. B. The locations of significant high-level heat producing granites. Reproduced, unmodified from Busby and Terrington (2017), under Creative Commons Attribution 4.0 International License (http://creativecommons.org/licenses/by/4.0/). © The Author(s) 2017.

2.2.1 South-west England

An assessment of the EGS resource base for Great Britain identifies south-west England as having the greatest amount of 'technical potential power' at each 'depth slice' evaluated and in total, of all the English regions (Busby and Terrington, 2017). The high heat production of the region is associated with the Cornubian granite batholith, which extends across Devon and Cornwall (Figure 2). The Cornubian Batholith was the focus of a major geothermal experiment, the UK hot dry rock (HDR) research and development programme that ran from 1977 until the early 1990s (MacDonald et al., 1992; Richards et al., 1991) (Figure 3). There is currently significant renewed interest in the deep geothermal resource in Cornwall, with two advanced geothermal power projects in the county.

In addition to being one of the most prospective regions of Great Britain for deep geothermal heat south-west England hosts the Cornubian Orefield, part of the globally important Variscan metallogenic province (Figure 4). The orefield is a world-class Sn-W-Cu province and also contains As, Fe, Pb-Zn-Ag, U-Ni-Co and Sb-Au-rich mineralisation (Figure 5). It was a globally significant tin and copper producer during the late eighteenth century, and tin production continued up to late 1990s (Figure 6). During the last decade there has been a revival of interest in mineral exploration in the region, stimulated by the acquisition of high resolution airborne geophysical data, a LiDAR survey and geochemical sampling of soils and stream sediments (Yeomans, 2017), and development of the world-class Hemerdon W-Sn deposit (Shail et al., 2017). Growing interest in the security of supply of raw materials has stimulated research on the 'critical' metal potential the region, with an emphasis on tungsten, antimony, indium, cobalt and lithium (Simons et al., 2013a, b, 2014; 2017).

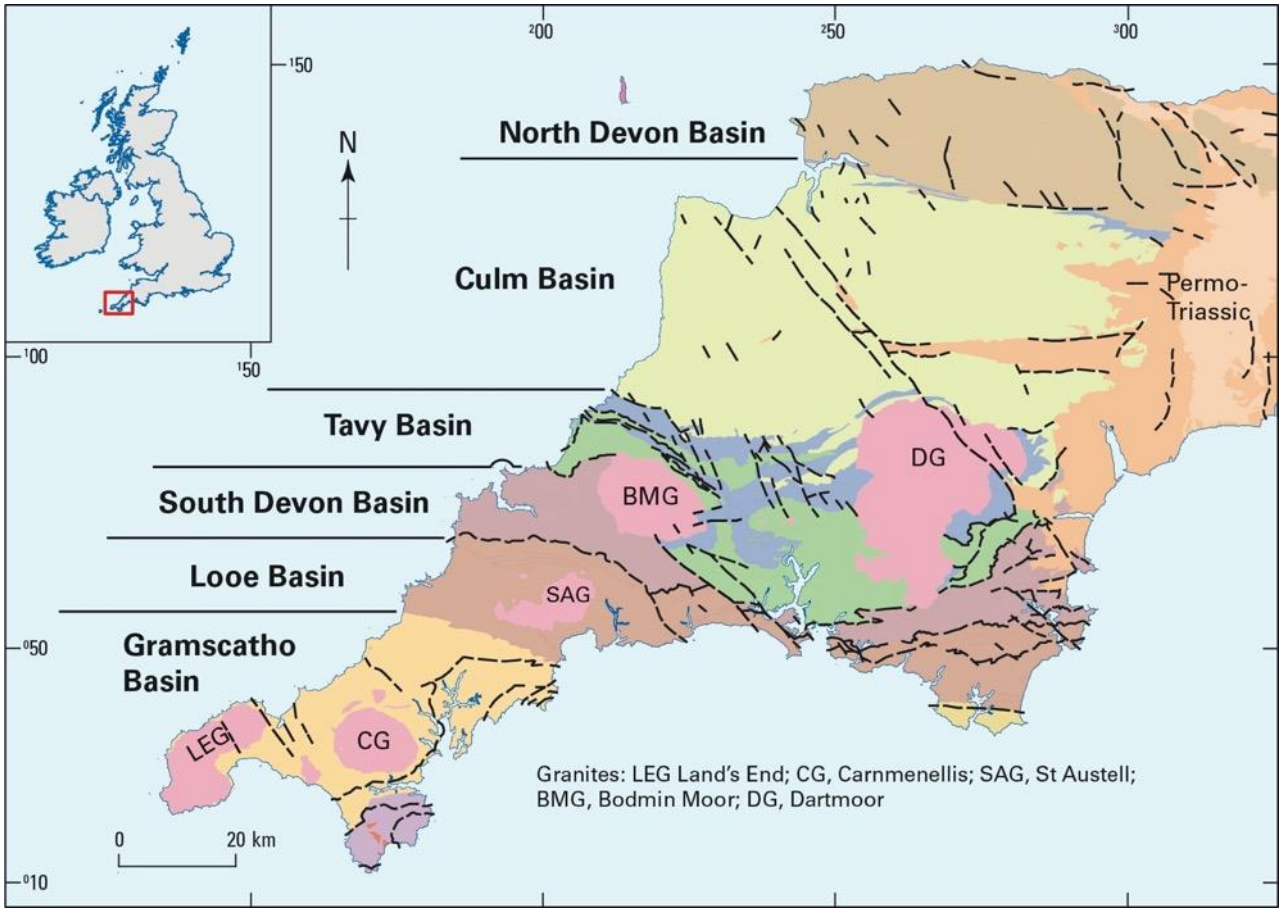

Figure 2: Simplified geological map of south-west England showing the distribution of sedimentary basins and the location of the granites of the Cornubian Batholith. The sedimentary basins typically comprise undifferentiated siltstones, mudstones and sandstones, with subordinate conglomerate. Modified from Shail and Leveridge (2009) with additional BGS data.

In summary the rationale for selection of south-west England as the UK CHPM2030 study area is due to a coincidence of geological phenomena and data availability:

i) The extensive exposed Permian granites result in it being one of the main high heat production and flow provinces in the UK;
ii) It hosts a major polymetallic ore field that is spatially associated and intrinsically linked to the granitic magmatism (Figure 5);
iii) It has a long history of metal production (surface and underground mining greatly enhance the geoscience knowledge base) and geothermal and economic geology research (geological research in south-west England has been undertaken for >250 years), meaning it is one of the best surveyed parts of the UK, and resulting in extensive data availability; and
iv) It is the focus for deep geothermal research and development in the UK, with ongoing mineral exploration programmes.

Figure 3: Rosemanowas Quarry, Cornwall, the Hot Dry Rock (HDR) project drilling site. A. Pump infrastructure used in the hydraulic stimulation experiments. B. Equipment used in the viscous fluid hydraulic stimulation experiments. Images reproduced from the HDR project photo archive held by the British Geological Survey. C. The quarry in 2017, which is used for testing geophysical equipment. D. The three HDR project borehole collars. E. Core from HDR project borehole RH12. F. Core from HDR project borehole RH15. British Geological Survey © UKRI.

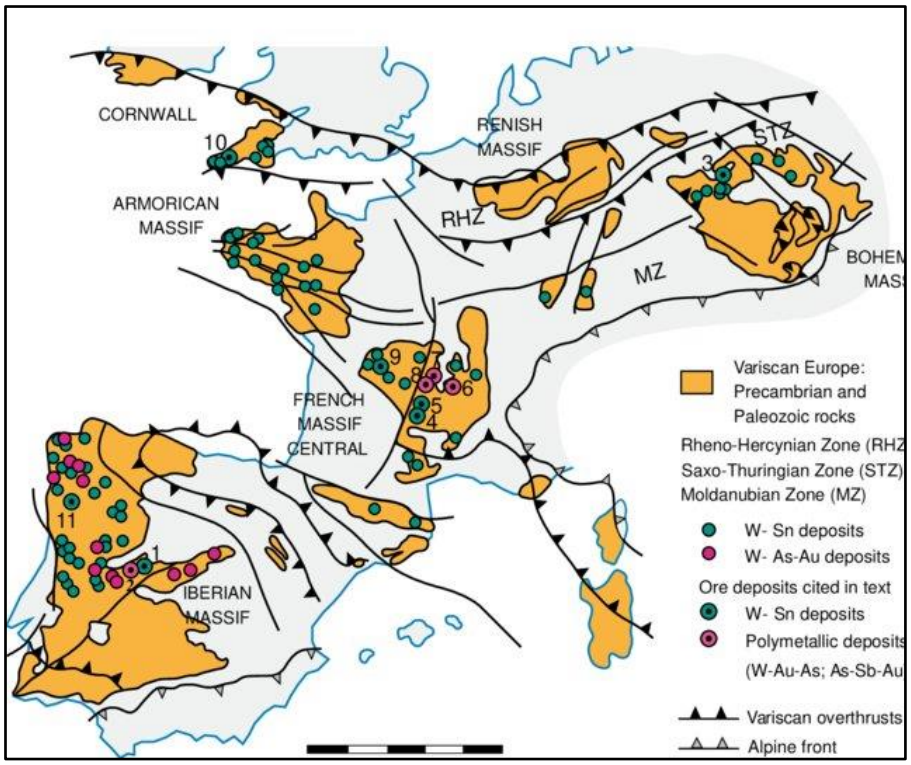

Figure 4: The Variscan belt in central and western Europe and major W-Sn and polymetallic minerals deposits. Reproduced, unmodified from Timón et al. (2019), under Creative Commons Attribution 4.0 International License (http://creativecommons.org/ licenses/by/4.0/).

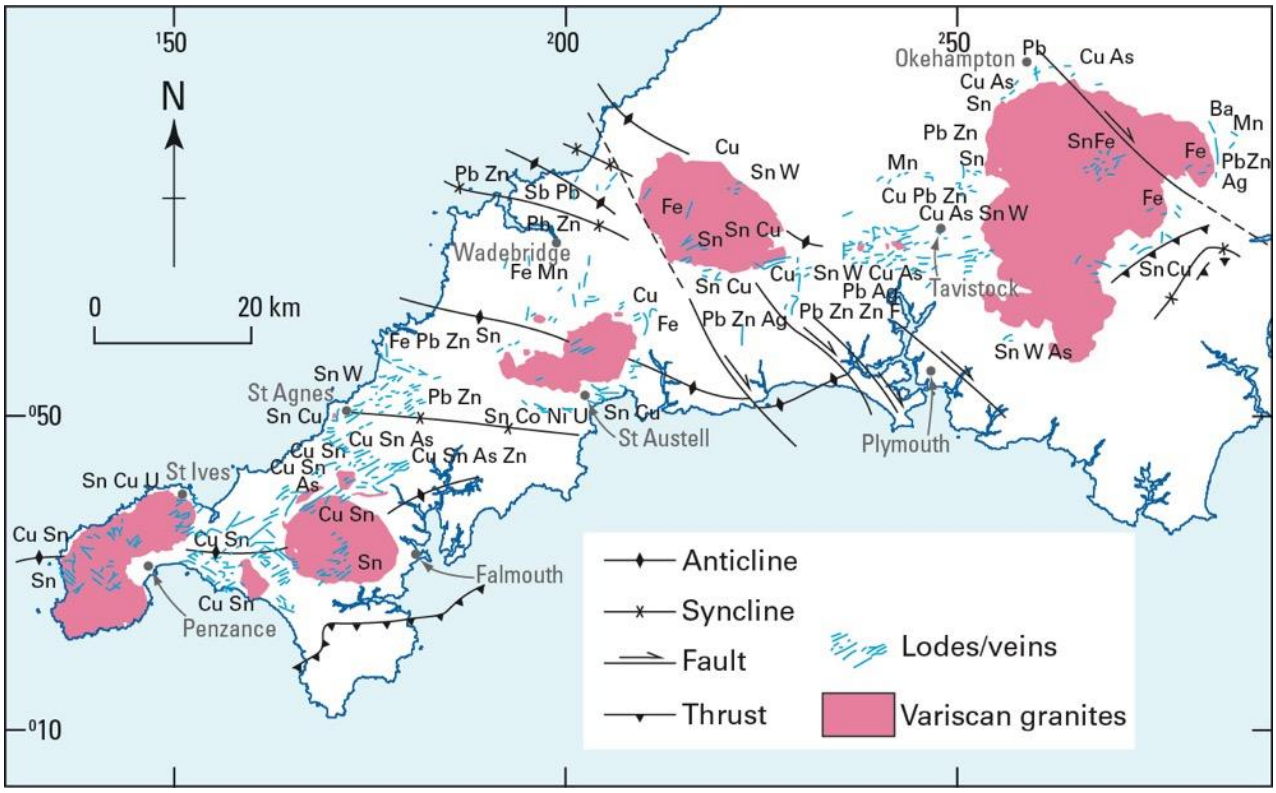

Figure 5: The Cornubian Orefield of south-west England. Modified from Dunham et al. (1978).

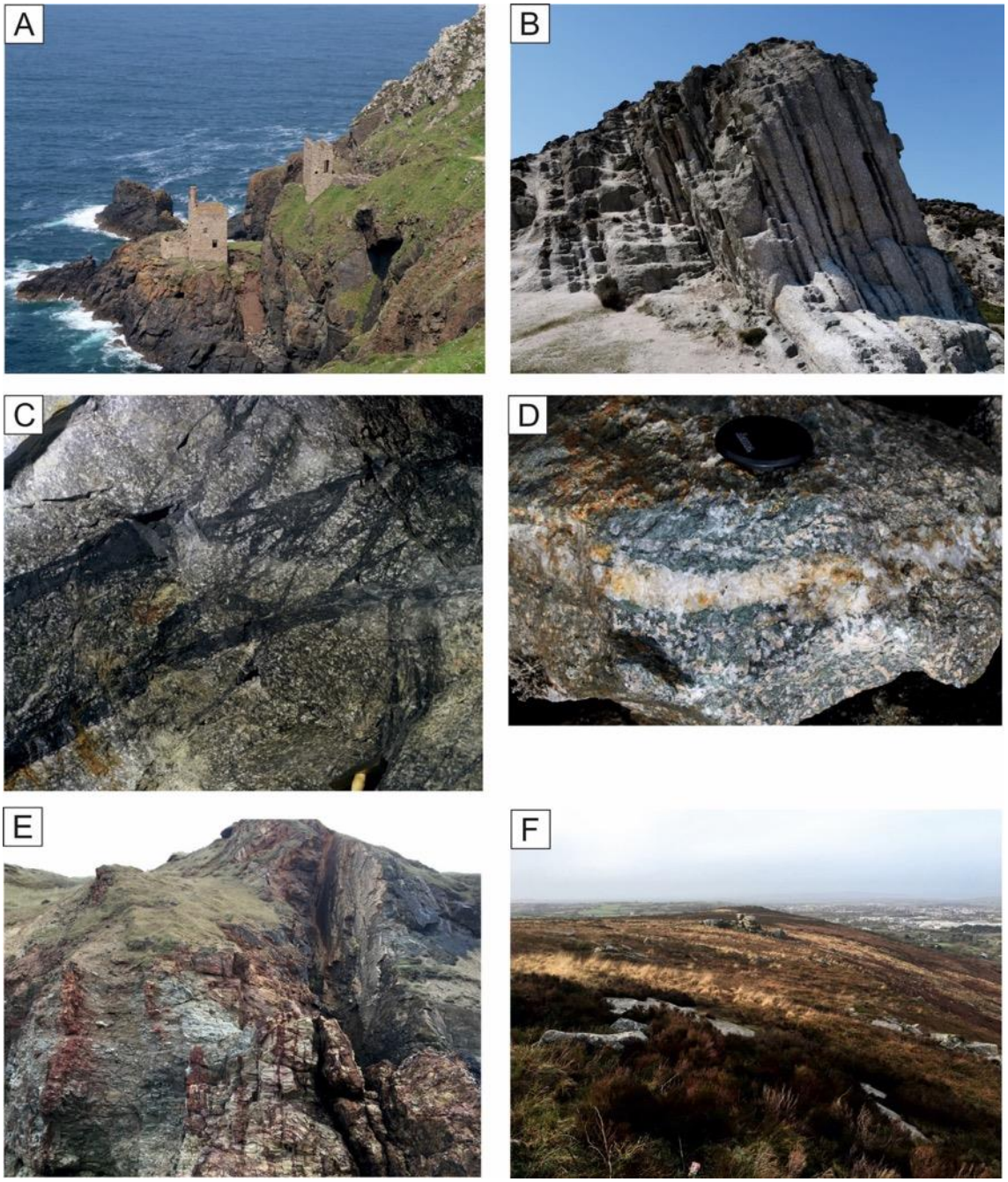

Figure 6: Typical Cornish mineralisation and exposures of granite. A. The Crowns Engine house, Botallack, Cornwall, evidence of the long history of mining in the region. B. Greisen bordered sheeted tin-tungsten veins occur in granite at Cligga Head on the north coast of Cornwall. C. South Crofty Mine, Robinson's Section, 380 fm. level, No. 4 lode west. Cassiterite/tourmaline filled fractures forming No. 4 lode seen in the roof of a drive in megacrystic, coarse-grained, biotite-granite. D. Main-stage mineralisation collected from a mine dump in the Minions area of Cornwall. E. A major zone of N-S-trending cross-course mineralisation, Cotty's Point, near Perranporth, north Cornwall. F. View westwards from close to the Carn Brea monument the along the exposure of the Carn Brea granite (a satellite granite of the Carnmenellis pluton), overlooking Camborne. British Geological Survey © UKRI.

2.2.2 The northern Carnmenellis CHPM2030 study area

The entire Cornubian Batholith is prospective for deep geothermal heat, with predicted average temperatures, at a depth of 5 km, ranging between 185 °C to 221 °C (Beamish and Busby, 2016). Mineralisation, the second criteria for CHPM, also occurs across much of the peninsula (Figure 6A). However, this pilot area assessment whilst considering the broader scale geological context and drawing on data from across Cornwall, principally focuses on a study area, of about 50 km^2, covering the northern part of the Carnmenellis granite (Figure 7). The reasons for selecting this area were:

i) The average temperature of the Carnmenellis granite, at 5 km depth, is predicted to be 200 °C (Beamish and Busby, 2016);
ii) Its hosts a well-defined mineralised belt, the Camborne-Redruth mining district, which passes along the northern edge of the Carnmenellis granite;
iii) Its complex structural geology, including major faults zones that are likely to enhance reservoir permeability, and a rheological contrast along the granite-country rock contact and metamorphic aureole;
iv) The presence of the legacy HDR research site (Figure 3), the boreholes from which provide the only published deep temperature measurements for the batholith, and confirm that the Carnmenellis granite has temperatures of 79 °C and 100 °C at 2.1 km and 2.6 km depeth, respectively; and
v) It contains the recently established United Downs Deep Geothermal Power (UDDGP) project, which is drilling two new deep boreholes into the granite.

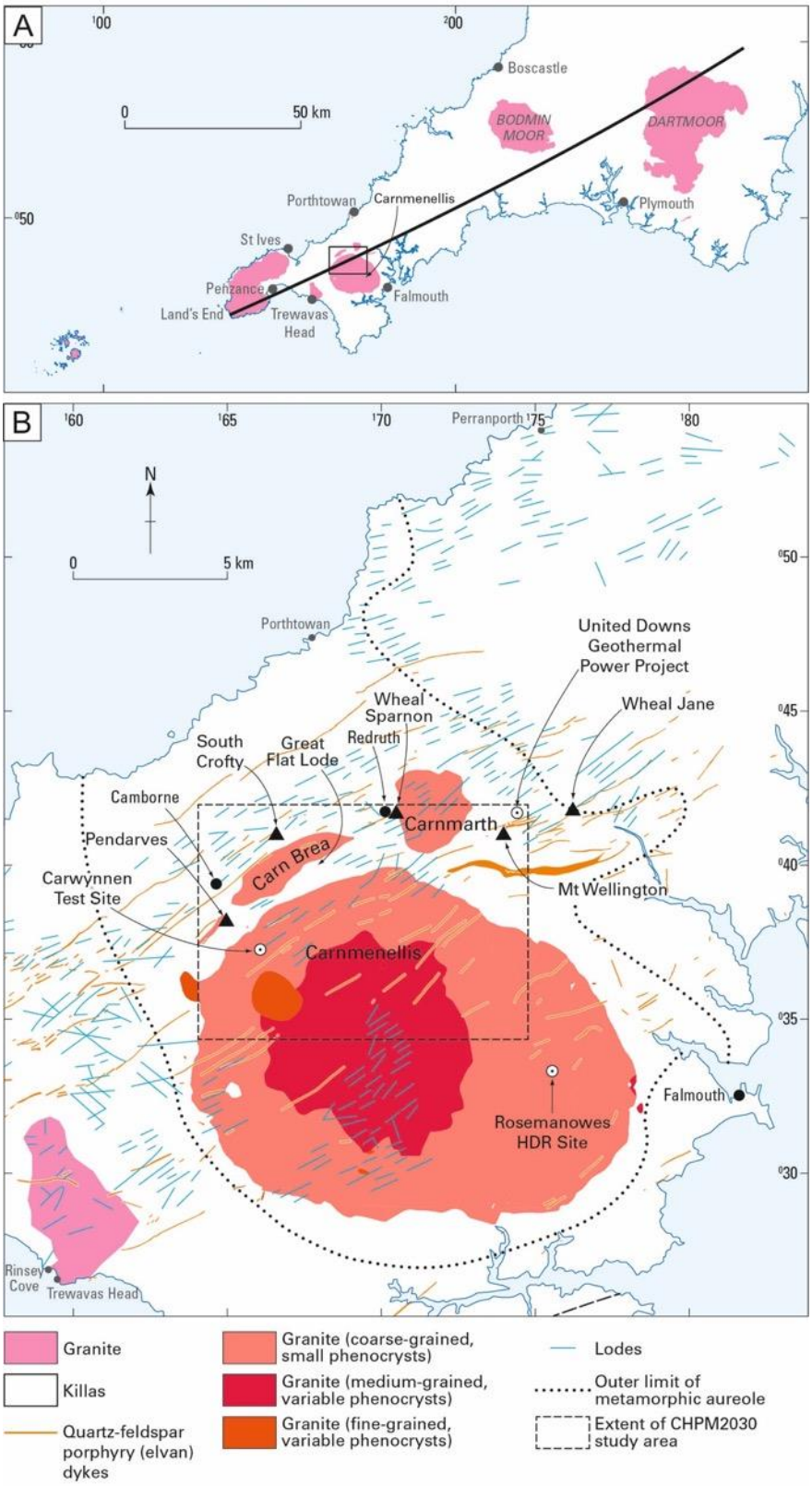

Figure 7: Location of the CHPM2030 south-west England study area. A. The position of the study area on the Cornubian peninsula of south-west England, with the major granite plutons shown. The black continuous line represents the approximate location of the cross-section shown in Figure 9. B. Simplified geology of the study area and its immediate surroundings, and key localities referred to in the text. British Geological Survey © UKRI.

3 Geology of the prospective area

3.1 Regional geological history

For a detailed review of the geology of the south-west England region the reader is referred to Westhead et al. (2017) and references herein. A brief chronology of major geological events in south-west England, from oldest to youngest, includes:

i) The development of a series of middle Palaeozoic (410–345 Ma), E–W-trending volcano-sedimentary basins (Figure 2) that have been inverted, deformed and subjected to low-grade metamorphism (Parker, 1989; Shail et al., 2014);
ii) Variscan continental collision, during the mid-Carboniferous (331–329 Ma), resulted in significant crustal shortening and the development of NNW-trending thrust sheets (Parker, 1989; Shail et al., 2014);
iii) Crustal extension and orogenic collapse during the late Carboniferous and lower Permian that resulted in extensive granitic magmatism (295–270 Ma) (Figure 2) and associated hypothermal (300–600°C) W-Sn greisens (Figure 6B), and mesothermal (200–300°C) Sn-Cu mineralisation hosted by E–W-trending mineral lodes (Figure 6C,D). Following granite emplacement widespread Pb-Zn-Ba-F-U mineralisation developed in N–S-trending cross-courses (Figure 6E), many of which are re-activated NNW-trending thrust sheets (LeBoutillier, 2002; Parker, 1989; Shail et al., 2014) (Table 1) and;
iv) Cyclic periods of uplift, erosion and sedimentation throughout the Jurassic and Cretaceous (Parker, 1989; Shail et al., 2014) resulting in the current landscape (e.g. exposure of granite roof zones at the existing land surface, Figure 6G).

3.1.1.1 Early Permian post-Variscan magmatism

The current surface expression (Figure 6F) of the Cornubian Batholith comprises six large granite plutons. From west to east these are: the offshore Isles of Scilly (120 km^2), Land's End (190 km^2), Carnmenellis (135 km^2), St Austell (85 km^2), Bodmin (220 km^2) (Figure 8A), and Dartmoor (650 km^2) (Figure 2, Figure 9). The subsurface extent of the Cornubian Batholith is estimated to be about 250 km in length and it has an approximate width of between 40–60 km (Scrivener, 2006; Willis-Richards and Jackson, 1989). However, there is uncertainty about the true size of the Cornubian Batholith because current models are based on limited geophysical data and very few deep drill holes. Similarly, there is some uncertainty about the true thickness and shape of the granite plutons. 2D-gravity modelling of the Carnmenellis, St Austell and Bodmin granites indicates they are tabular bodies with an estimated thickness of between three and four kilometres, whilst the larger Dartmoor pluton is estimated to be about nine kilometres thick (Taylor, 2007). However, seismic refraction data (discussed in Section 4.1.2.2) suggest that the depth of the base of the batholith (i.e. its lower contact with the killas) is variable, ranging from about 7–8 km beneath the Bodmin and Carnmenellis granites, respectively, to about ten kilometres beneath the Dartmoor granite (Brooks et al., 1984; Shail et al., 2014).

Radiometric dating (U-Pb in monazite and zircon) suggests that the extensive granitic magmatism in south-west England occurred over a period of about 20 million years, between about 293–274 Ma, although separate intrusive episodes can be identified in some of the individual plutons (Chen et al., 1993; Chesley et al., 1993; Clark et al., 1994). In terms of age, the plutons can be broadly divided into two groups: (i) the older (>290 Ma) Bodmin Moor, Isles of Scilly and Carnmenellis granites and; (ii) the younger (<286 Ma) Land's End, St Austell and Dartmoor granites (Figure 10).

Table 1: Summary of mineralisation styles in the south-west England. Adapted from Andersen et al. (2016).

Pre-granite mineralisation	Main ore minerals				
1) Rifting and passive margin development (early Devonian- Carboniferous) sedimentary-exhalative (SedEx) mineralisation	Haematite	Siderite	Galena	Sphalerite	
2) Variscan convergence and continental collision (late Devonian-Carboniferous) shear zone hosted Au-Sb + base metal mineralisation	Gold	Bournonite	Sphalerite	Chalcopyrite	Tetrahedrite
Granite-related mineralisation					
3) Early post-Variscan extension and magmatism (early Permian)					
a) Magnetite-silicate skarns developed in metabasaltic hosts	Magnetite	Cassiterite			
b) Sulfide-silicate skarns developed in calc-silicate granite hosts	Cassiterite	Arsenopyrite	Pyrite	Chalcopyrite	Pyrrhotite
c) Greisen-bordered sheeted vein complexes	Wolframite	Cassiterite	Chalcopyrite	Sphalerite	Bismuthinite
d) Quartz-tourmaline veins and breccias	Cassiterite	Haematite			
e) Polymetallic sulfide lodes	Cassiterite	Chalcopyrite	Wolframite	Arsenopyrite	Sphalerite
Post-granite mineralisation					
4) Episodic intraplate rifting and inversion (late Permian – Cenozoic)					
a) Crosscourse Pb-Zn ± F, Ba mineralisation	Galena	Sphalerite	Arsenopyrite	Chalcopyrite	

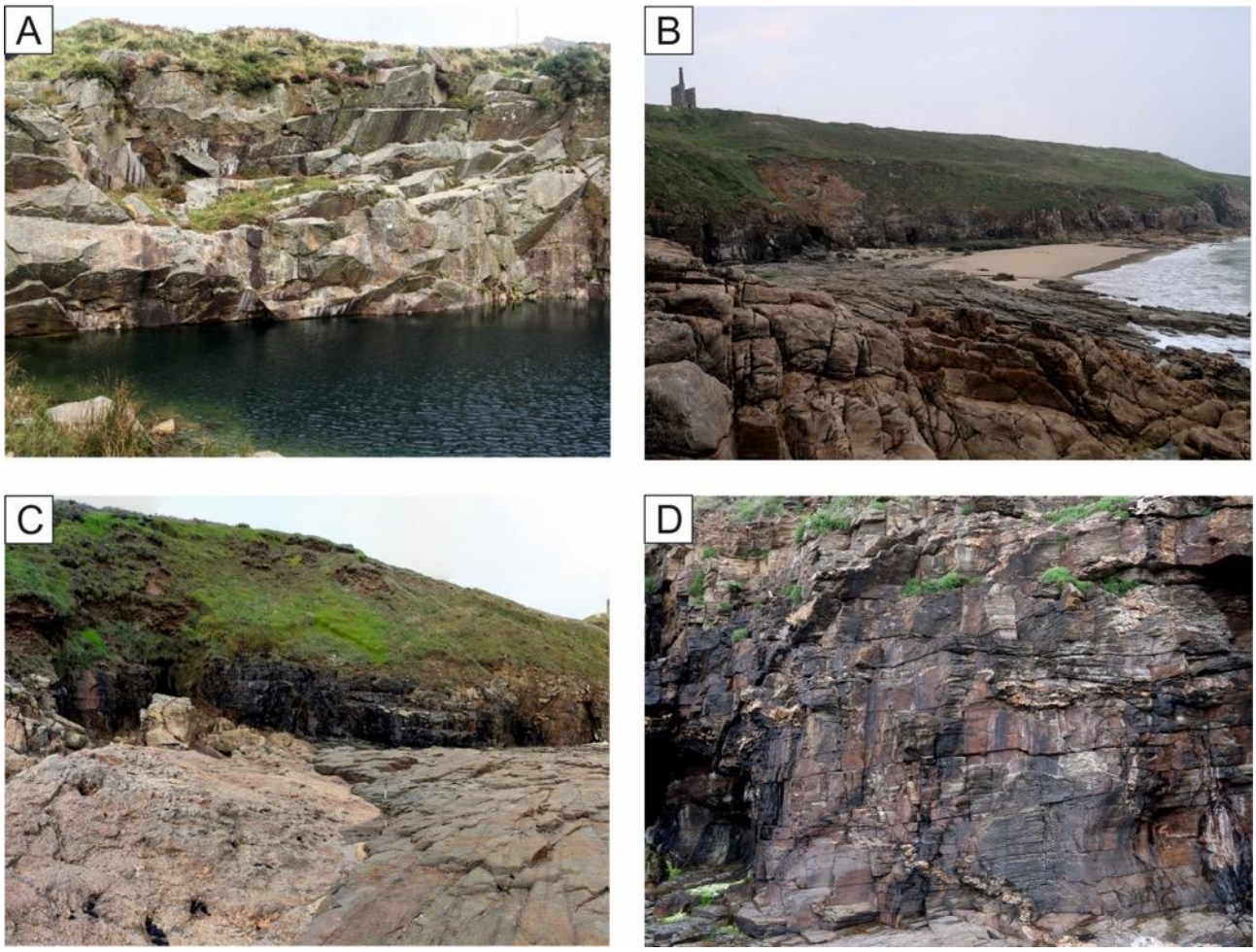

Figure 8: Typical exposures of granite and their country rocks in Cornwall. A. Quarried exposure in the Bodmin granite close to Minions, Cornwall. B. Exposure of granite intrusion (foreground), with rocks of the Mylor Slate Formation, locally termed 'killas' forming the wave-cut platform, at Rinsey Cove, south-west Cornwall. C. Contact between the granite and metasedimentary rocks (Mylor Slate Formation), at Rinsey Cove, south-west Cornwall. Deformed quartz veins in the metasedimentary rocks (Mylor Slate) at Rinsey Cove, south-west Cornwall. British Geological Survey © UKRI.

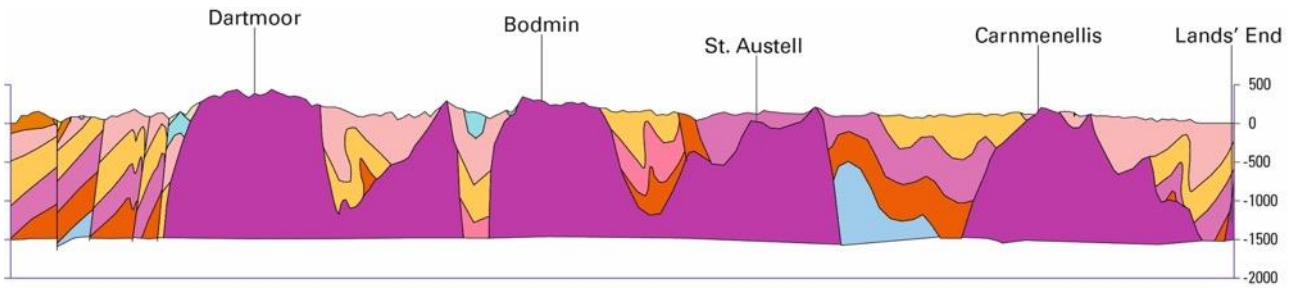

Figure 9: Schematic cross-section of the geology of the south-west region from St Just to Crewkerne. The major granite plutons are labelled and shown in purple with adjacent sedimentary basins. Adapted from Westhead et al. (2017).

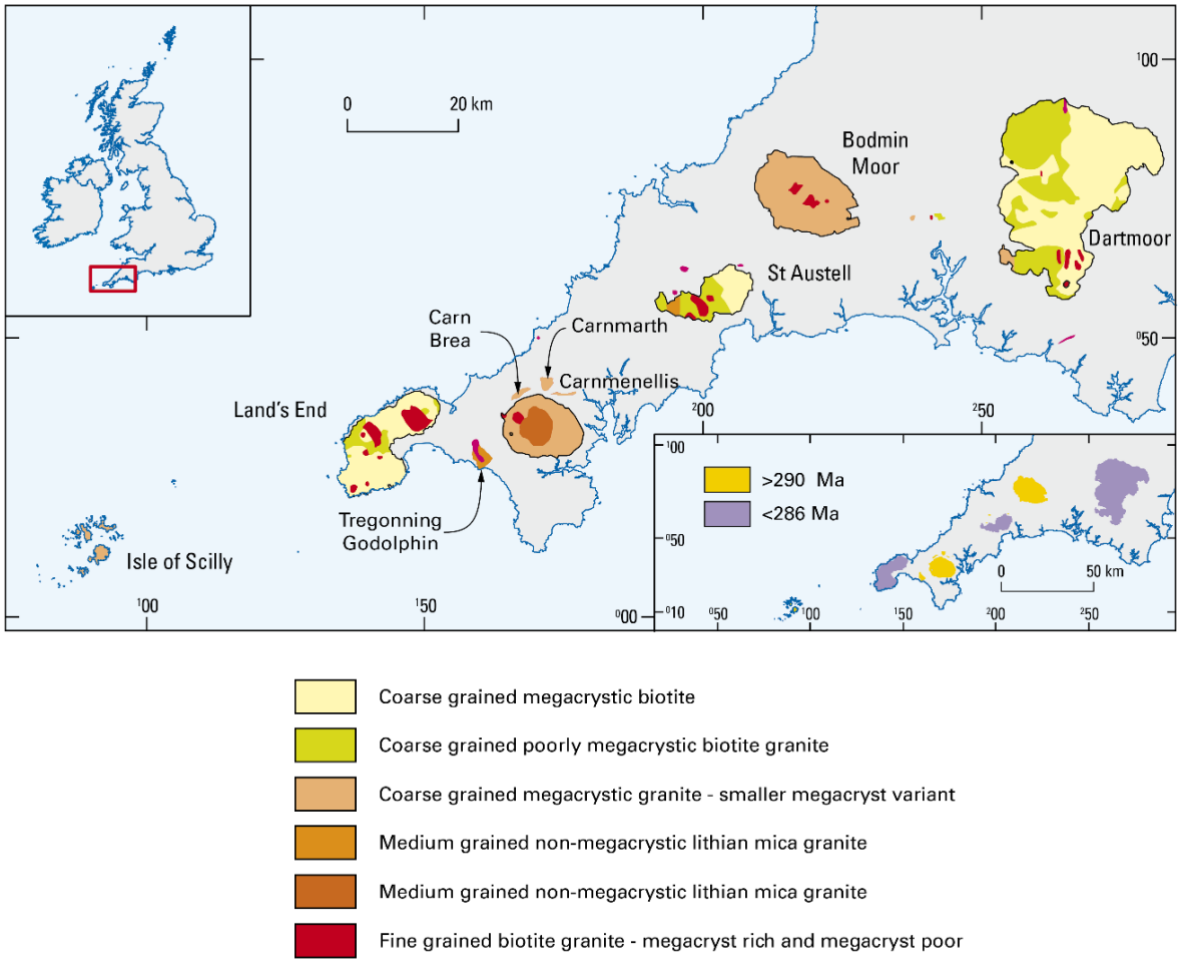

Figure 10: Map showing the principal mineralogical and textural variations in the Cornubian Batholith. It combines subdivisions into biotite and Li-mica granites with a textural scheme based primarily on mean matrix grainsize and the size and abundance of alkali feldspar megacrysts. Compiled from Bott and Scott (1964); Brooks et al. (1983); Dangerfield and Hawkes (1981); Exley and Stone (1982); Floyd et al. (1993), Hawkes and Dangerfield (1978); Manning (1998); Manning et al. (1996); Shail et al. (2014); Stone and Exley (1985); and Simons et al. (2016). In-set map shows the distribution of granite ages: Dartmoor, St Austell and Land's End (in purple) are <286 Ma, whereas Bodmin, Carnmenellis and Isle of Scilly (in yellow) are older (>290 Ma), based on Chen et al. (1993); Chesley et al. (1993); Clark et al. (1994); Darbyshire and Shepherd (1987). British Geological Survey © UKRI.

Compositionally the granites are all peraluminous, S-type granites that are enriched in elements such as K, B, F, Li, U, Th, Sn, Rb and Pb. A notable feature of Cornubian granites is their high uranium content (with an average content of about 12 ppm for all plutons), which is largely controlled by the distribution of accessory minerals such as uraninite and monazite (Chappell and Hine, 2006; Scrivener, 2006). Importantly it is the radioactive decay of uranium, thorium and potassium in the Cornubian granites that is responsible for their high heat production (Chappell and Hine, 2006). There have been many attempts to produce classification schemes, which describe the mineralogical and textural variations observed in the Cornish granites (Brooks et al., 1983; Floyd et al., 1993; Ghosh, 1934). The granites of south-west England have most recently been categorised by Simons et al. (2016) into five groups based on their mineralogy. These comprise the: two-mica granites such as Bodmin and Carnmenellis (G1); muscovite granites such as Hemerdon Ball and Cligga Head

(G2); biotite granites such as Land's End, St Austell and Dartmoor (G3); tourmaline granites that comprise parts of the St Austell granite (G4); and topaz granites such as Tregonning-Godolphin (G5). Other minor variants also exist, including Li-mica granite and fluorite granite (Brooks et al., 1983; Busby, 2010; Floyd et al., 1993; Manning et al., 1996). The older granites (Bodmin Moor, Isles of Scilly, and Carnmenellis) can be distinguished from the younger granites (Land's End, St Austell and Dartmoor) by their texture, composition (peraluminosity), isotopic signature ($^{\varepsilon}$Nd) and rare earth element (REE) patterns. These differences may reflect increased mantle-melting and possibly increased amounts of crustal melting during formation of the younger granites, probably in response to higher temperatures in the lower crust. However, it remains unclear why temperatures increased, and if this change was transitional, or an abrupt change in response to a discrete tectonic event (Shail et al., 2014; Stone, 1995, 1997, 2000a, b).

3.1.1.2 Country rocks

Emplacement of the Cornubian Batholith into largely Devonian sedimentary rocks caused large-scale heating and thermal alteration (Figure 8B,C). The resulting metamorphic rocks in south-west England are locally known as 'killas' (Figure 8D). Although these rocks are not economically important in themselves, fractures within them host a significant proportion of the region's mineral deposits (e.g. polymetallic mineral veins, or 'lodes'). The killas comprises a series of Devonian (410–355 Ma), marine deposited sandstones, siltstones, mudstones and rare carbonates that were regionally metamorphosed to sub-green schist facies during the Variscan Orogeny. As a result of granite emplacement, the low-grade regional metamorphism has been locally overprinted by higher-grade contact metamorphism, to produce a series of aluminosilicate and/or cordierite-bearing slates (Selwood et al., 1998).

3.2 Tectonic framework

The majority of the following section is based on Westhead et al. (2017). South-west England is located in the Variscan orogenic belt, which extends across southern England, a small part of southern Wales and Ireland, and across extensive areas of Europe (Figure 4). The region forms part of the Rhenohercynian Zone, which is interpreted as an oceanic collision belt (Franke, 1989; Holder and Leveridge, 1986). The sedimentary rocks of Devonian and Carboniferous age were deposited in fault-bounded basins (Figure 11), which are recognised as forming part of a passive margin sequence (Holder and Leveridge, 1994). The correlation of these rocks across north-western Europe (Holder and Leveridge, 1986) is indicative of a pattern of extensive E–W-trending sedimentary basins forming the northern passive margin of a laterally extensive Rhenohercynian oceanic basin (Franke, 1989). Remnants of oceanic crust and active margin sequences from this basin are preserved in southern Cornwall as the Lizard ophiolite. The sequence of extension and basin opening, followed by inversion and deformation within the Variscan rocks of the south-west England is considered to be related to the continental rifting and growth of the Rhenohercynian Ocean, followed by its closure during continental collision. Rifting of the passive margin occurred over a period of approximately 65 Ma, from the Early Devonian to the early Carboniferous, with extensional faulting becoming progressively younger northwards (Leveridge, 2002) (Figure 11).

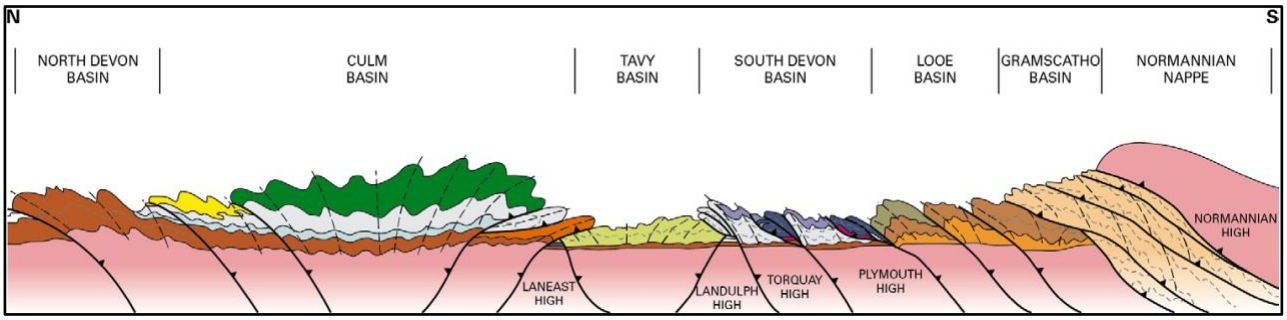

Figure 11: Sketch cross-section of the Variscan belt of south-west England, late Carboniferous. The sequence comprises six major E–W-trending fault-bounded basins: the Gramscatho, Looe, south Devon, Tavy, Culm and north Devon basins, with extensional faulting and intervening highs, getting progressively younger northwards. Redrawn from Leveridge and Hartley (2006).

The Rhenohercynian passive margin sequence within south-west England consists of six major E–W-trending fault-bounded basins: from east to west these are the: North Devon Basin; Culm Basin; Tavy Basin; South Devon Basin; Looe Basin and; Gramscatho Basin, together with the intervening highs (Figure 2, Figure 11). The synrift basin fill of the Gramscatho Basin is largely covered by sedimentation, resulting from subsequent Late Devonian synconvergence. To the north, the Looe Basin is overthrust to the south by sedimentary rocks of the Gramscatho Basin (Holder and Leveridge, 1986). Its northern boundary is defined by the interbasinal high deposits of the Plymouth Limestone Formation (Leveridge, 2002). The strata of the Looe basin constitute three major thrust nappes. At each thrust front, large-scale antiformal folding is present in the hanging wall, which suggests that internally the Looe Basin comprises three sub-basins with half-graben geometries.

The latest stages of the Carboniferous and the Permian are marked by a number of tectonic events related to a post-Variscan phase of regional extension (Holder and Leveridge, 1994). Extension and pressure release led to the melting of the lower crust–mantle boundary and the intrusion of the Dartmoor and Bodmin granites between 290 and 280 Ma (Chen et al., 1993; Chesley et al., 1993; Darbyshire and Shepherd, 1985). Related acid volcanic activity along the main NW-trending strike-slip faults, including the associated high-level quartz-feldspar porphyry dykes, which are locally termed ‘elvans’, and the intrusion of similar felsitic magma into E–W fractures, is compatible with N–S extension at the time. Similarly the formation of the E–W-trending, main stage, mineral veins, dated at 280 ± 20 Ma (Moorbath, 1962), indicates that the crust was undergoing N–S extension. The magnitude of this latest Carboniferous to Permian extension is indicated by the formation of sedimentary basins, containing several kilometres’ thickness of Permian sediments, above extensionally reactivated Variscan thrusts in Plymouth Bay (Evans, 1990), the Haig Fras, Melville and St Marys basins in the South-west Approaches (Hillis and Chapman, 1992), and the Crediton trough in Devon (Durrance, 1985b). Within south-west England, a number of gently dipping thrusts exhibit significant extensional reactivation, most of which can be ascribed to Permian extension.

Post-Variscan movements include sinistral fault displacements on the NW-trending faults during N–S extension in the Permian, the Late Triassic to Jurassic or the early Palaeogene. The dextral displacements of the NW-trending faults are related to N–S compression most probably of Late Cretaceous, late Palaeogene–Neogene or Miocene age (Leveridge, 2002) (Figure 8D).

3.2.1 Structural geology

South-west England is a structurally complex region whose geological past has been dominated by Variscan tectonics (Figure 2 and Figure 12). British Geological Survey (BGS) mapping, academic research and seismic surveys have led to the identification of three main deformational phases associated with Variscan orogenesis. Two phases are related to crustal shortening (D_1 and D_2) whilst the third (D_3) is associated with crustal extension during orogenic collapse (Alexander and Shail, 1996; Leveridge, 2002). The D_1 deformation event (c. 385 Ma) is characterised by: i) large-scale (10s km), NW-SE-trending strike-slip faults; ii) a NNW-trending mineral lineations; and iii) E-W-trending folds. Structures associated with the second deformation event (D_2) are similar to those formed during D_1, but D_2 structures are generally more steeply dipping. The D_3 event (c. 305–300 Ma) occurred in response to orogenic collapse and associated crustal extension. It resulted in the development of steep to gently inclined WNW-ESE-trending extensional faults (Alexander and Shail, 1996; Leveridge, 2002) (Figure 13). Regionally extensive NNW-SSE-trending cross-course structures formed during the Permian in response to a period of crustal extension (Scrivener et al., 1994; Shail and Alexander, 1997).

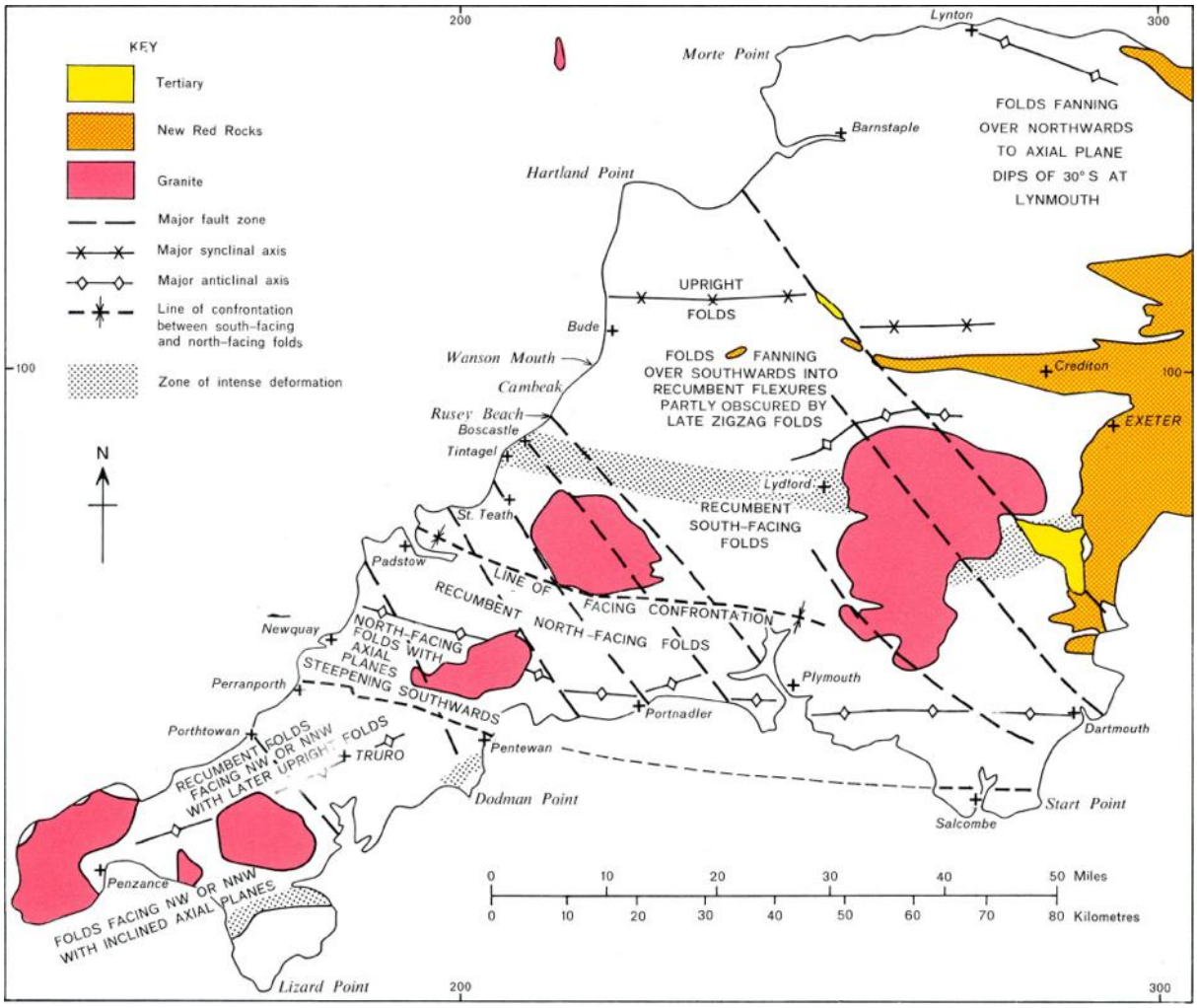

Figure 12: The major structures in south-west England, including the significant NW-SE-trending cross-courses. Reproduced from Edmonds et al. (1985).

Figure 13: Extensional fault (dashed white line) in the cliff at Gooden Heane Cove, near Portreath. British Geological Survey © UKRI.

In south-west England both granite and the killas have inherently poor permeability (Heath, 1985). Accordingly, fluid circulation in the region is largely controlled by regional-scale structures (e.g. NW-SE-trending faults) (Figure 2) and fractures (Bromley et al., 1989; Heath, 1985; Smedley et al., 1989). Fractures in the granite are primarily the result of magma chamber processes, for example cooling and hydro-fracturing (caused by the movement of magmatic fluids). In contrast fractures in the killas are principally the result of granite emplacement. Local zones of high-fracture density, in both granite and killas, may also be associated with episodes of late faulting. However, the permeability and connectivity of these fractures, particularly at depth, remains enigmatic (Heath, 1985).

3.3 Geology of the CHPM2030 study area

The geology of the south-west England study area (Figure 7) is dominated by the following lithologies: i) Devonian metasedimentary rocks of the Mylor Slate Formation; ii) the younger (Permian) Carnmenellis granite; and subordinate, iii) NE-SW-trending quartz-feldspar porphyry dykes (elvans). A description of these lithologies is provided below.

3.3.1 CHPM target formations

3.3.1.1 Mylor Slate Formation

The Mylor Slate Formation (MSF) (Figure 8B, C, D), or Mylor Series as it was previously known, extends over a large area of southern Cornwall, including the area around the northern edge of the Carnmenellis granite. The formation comprises two distinct sedimentary facies, which include interbedded slates and siltstones, and a breccia facies (the Porthleven Breccia Member, PBM). The MSF also includes a significant igneous component in the form of metamorphosed basic lavas and volcanic breccias (greenstones) that occur towards the base of the formation. The MSF typically comprises well-bedded dark grey slates with thin (c. 5 mm), finely spaced, siltstone laminae. Locally within the formation thin beds of siltstone (up to 15 cm thick) and fine-grained sandstone (up to 30 cm thick) are interbedded with the slate (Leveridge et al., 1990). The MSF was interpreted by Wilson and Taylor (1976) to be a low-energy, marine basinal sequence that contains distal turbidites, whereas the PBM formed in a higher energy environment, and is thought to represent a marine mass flow deposit (Middleton and Hampton, 1976).

The rocks of the MSF were initially regionally metamorphosed to greenschist facies at about 355 Ma (Hawkes, 1981), at a temperature of about 300°C and a pressure of at least 3 kbars (Barnes and Andrews, 1981), representing a burial depth of about 12 km (Holder and Leveridge, 1986). Emplacement of the Carnmenellis granite during the Permian (c. 313±3) (Neace et al., 2016) resulted in high-temperature contact metamorphism of the MSF, which resulted in the formation of hornfelsed slates and siltstones that typically contain coarse-grained andalusite. The metamorphic aureole around the northern edge of the Carnmenellis granite extends for approximately 1 km at its widest point (Leveridge et al., 1990) (Figure 7).

3.3.1.2 Carnmenellis granite

The Carnmenellis granite is a large (135 km^2), roughly circular granite body, with two satellite granites (the Carn Marth and Carn Brae granites) on its' northern edge (Figure 7). Emplacement of the Carnmenellis granite into the MSF occurred during the Permian (c. 293 Ma) (Chen et al., 1993; Chesley et al., 1993). It is a two-mica granite (G1), which exhibits variation in both grain size (coarse, medium and fine-grained), and the abundance and size of feldspar phenocrysts (Figure 10, Figure 14). The smaller of the two satellite granite bodies found at the northern edge of the Carnmenellis granite is also a coarse-grained, two-mica granite (G1), whereas the larger one is a fine- to coarse-grained muscovite granite (G2) (Simons et al., 2016). The Carnmenellis granite predominantly comprises alkali feldspar, plagioclase, quartz, biotite and muscovite, with accessory tourmaline, andalusite, ilmenite, apatite, monazite, zircon, xenotime and uraninite (Bromley et al., 1989). It is chemically similar to other Cornubian granites, being a peraluminous (A/CNK >1), S-type granite, enriched relative to the upper continental crust, in elements such as Li, Be, In, Sn, As, Pb and W (Bromley et al., 1989; Simons et al., 2016). The observed chemical and mineralogical characteristics of the Carnmenellis granite indicate formation by partial melting of a muscovite and biotite-rich greywacke source rock (Simons et al., 2016).

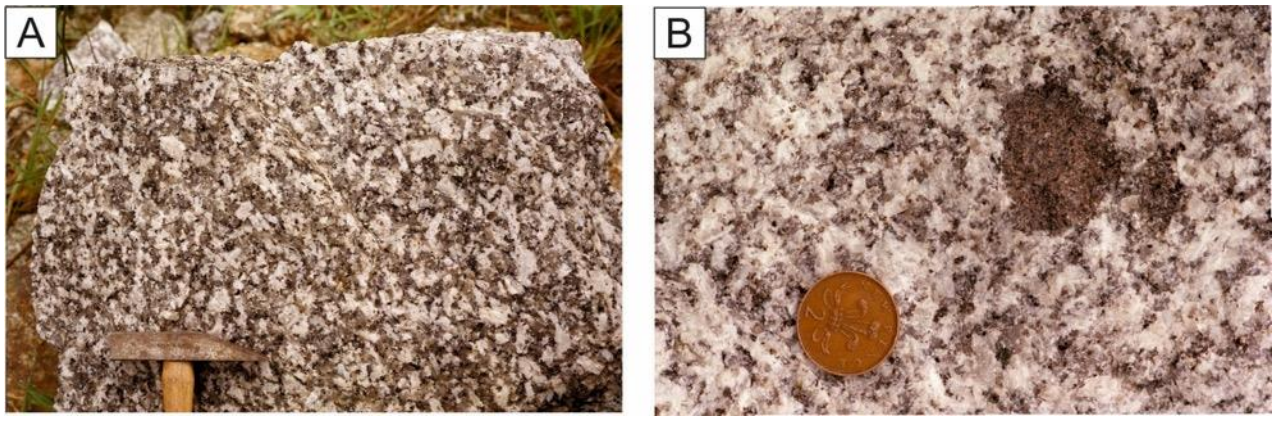

Figure 14: Carnmenellis granite. A. Trevone Quarry, near Longdowns. Unfoliated Carnmenellis granite. Carnmenellis Granite showing no significant alignment of the megacrysts. B. Carnsew Quarry, Penryn. A xenolith in the Carnmenellis granite. A biotite-rich xenolith of sedimentary origin lying within the Carnmenellis granite. British Geological Survey © UKRI.

The shape, thickness and size of the Cornubian Batholith has been the subject of significant scientific debate for almost 60 years. Early land-based gravity surveys confirmed (Bott et al., 1958) that the individual granite bodies exposed at surface are connected at depth. 2D-gravity modelling has been used to define the extent of the granite at depth (Beer et al., 1975; Rollin, 1988; Rollin et al., 1982; Tombs, 1977), and to define the thickness and shape of the individual plutons (Bott and Scott, 1964; Brooks et al., 1983; Edwards, 1984; Willis-

Richards and Baria, 1989). The most recent re-interpretation of gravity data by Taylor (2007) predicts that the Carnmenellis granite is an asymmetrical, tabular body approximately 3–4 km thick (Figure 15). The asymmetry of the Carnmenellis granite is mirrored in the width of the metamorphic aureole, which is significantly wider on the northern edge of the granite, where it can be up to 3 km wide. On the southern and eastern edges where the contact with the country rocks is steeper, the aureole rarely exceeds 1 km in width (Leveridge et al., 1990; Westhead et al., 2017). There are only limited seismic refraction data that cover the onshore extent of the Cornubian Batholith. However, these seismic refraction data do provide an indication of the depth of the base of the batholith (i.e. its lower contact with the killas), which is variable, and ranges between about seven and eight kilometres beneath the Carnmenellis granite (Brooks et al., 1984; Shail et al., 2014).

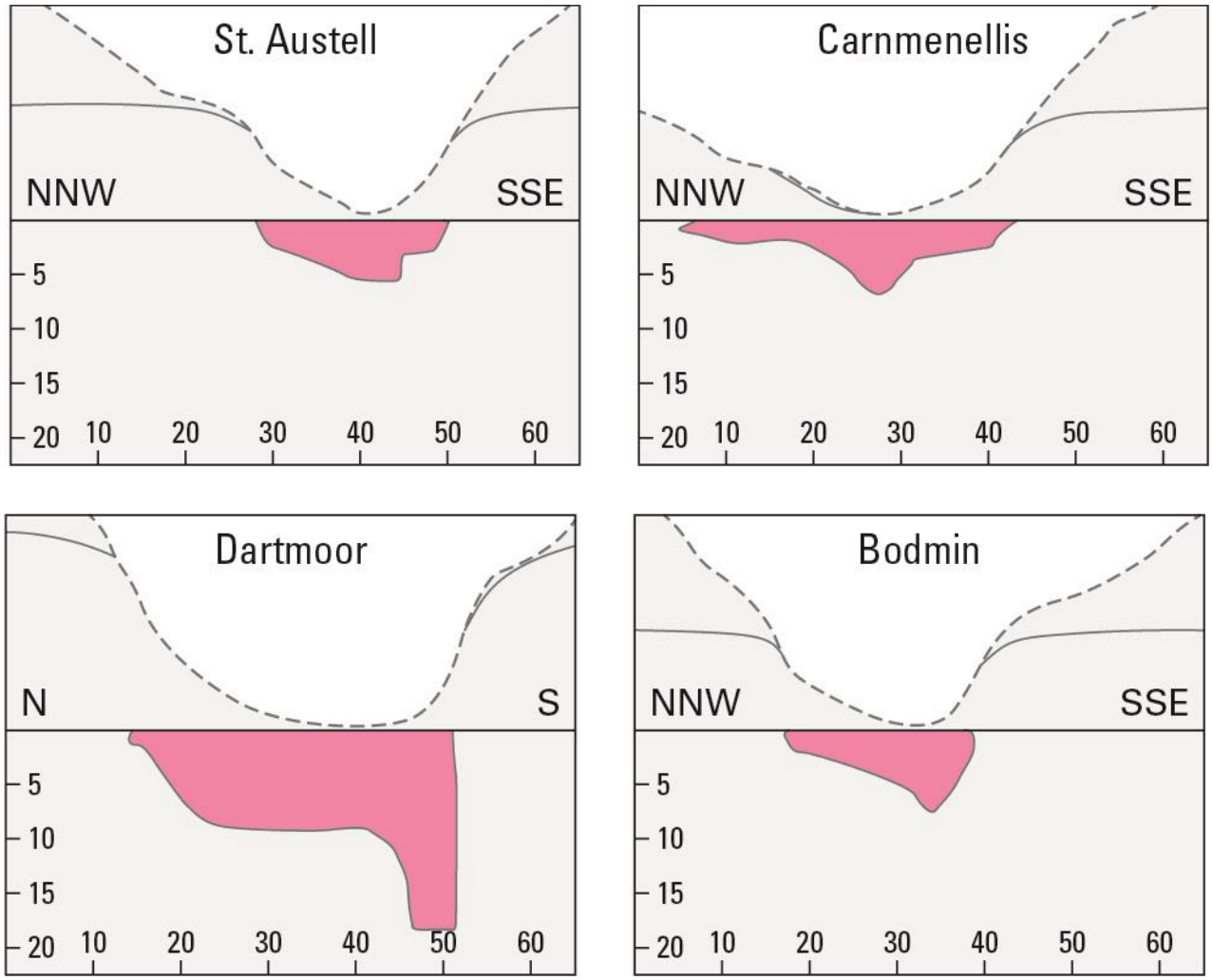

Figure 15: 2D gravity models for the St Austell, Carnmenellis, Dartmoor and Bodmin. Depths are in kilometres and horizontal scale has tick marks at 10 km intervals. Redrawn from Taylor (2007) Geological Society of London ©.

However, there is significant uncertainty about the actual shape and thickness of the Carnmenellis granite, and other plutons in south-west England, because of assumptions made during modelling (e.g. density contrasts) and the limited amount of data the models are based on. It is important to note that very few boreholes have been drilled to validate these models. However, two deep (2–2.5 km) boreholes in the

Carnmenellis granite, drilled during the HDR Programme, confirm that the granite extends to at least this depth and that it is chemically and mineralogically consistent over this depth range (Burgess et al., 1982a).

Constraining the Carnmenellis granite surface using borehole records

The BGS single onshore borehole database (SOBI) contains records produced by geologists or geotechnical engineers from drilling and site investigations. BGS holds a total of 2293 borehole records for the counties of Devon and Cornwall in south-west England (Figure 16). Of these records, 1414 have been digitised and 879 paper records are not yet available digitally. In an attempt improve the current topographic model for the granite surface, digital records of bore holes were reviewed and data on the depth of granite intersection were recorded (Appendix 1). For the purposes of this study only bore holes with a total depth greater than 100 m (500 in total) were considered (Figure 17). Of these, 88 boreholes encountered granite, with 37 being drilled directly into the granite at surface, and with the remaining 51 intersecting granite at depth. The following information was compiled for each of the bore holes: borehole name, BGS ID, hyperlink, approximate granite intersection depth in metres, total depth of bore hole, azimuth, inclination, easting and northing. The azimuth, inclination and depth of granite intersection have been used to define a revised granite surface for the modelling work (Section 7). All data are freely available from https://www.bgs.ac.uk/products/onshore/sobi.html.

3.3.1.3 Other rock types

Quartz-feldspar porphyry dykes (‘elvans’) are a relatively common intrusive feature found in the Carnmenellis granite and in the MSF around the northern-edge of the granite, especially in the mineralised zone around Camborne and Redruth (Figure 7). The dykes are typically steeply dipping and vary in thickness between a few tens of centimetres to more than 40 metres (Figure 18). They generally trend ENE-WSW, which is parallel to the strike direction of the hydrothermal mineral veins in the mineralised zone around Camborne and Redruth (Leveridge et al., 1990). Elvans are mineralogically simple, typically comprising alkali feldspar, quartz and plagioclase, and commonly display evidence of alteration of varying intensity, which resulted in the formation of secondary white mica, biotite and tourmaline. Geochemically elvans are granitic in composition, but with an enrichment in potassium. The similarity in mineralogy and chemistry of the elvans and granites has led some researchers to suggest a genetic link between the two (Shepherd et al., 1985).

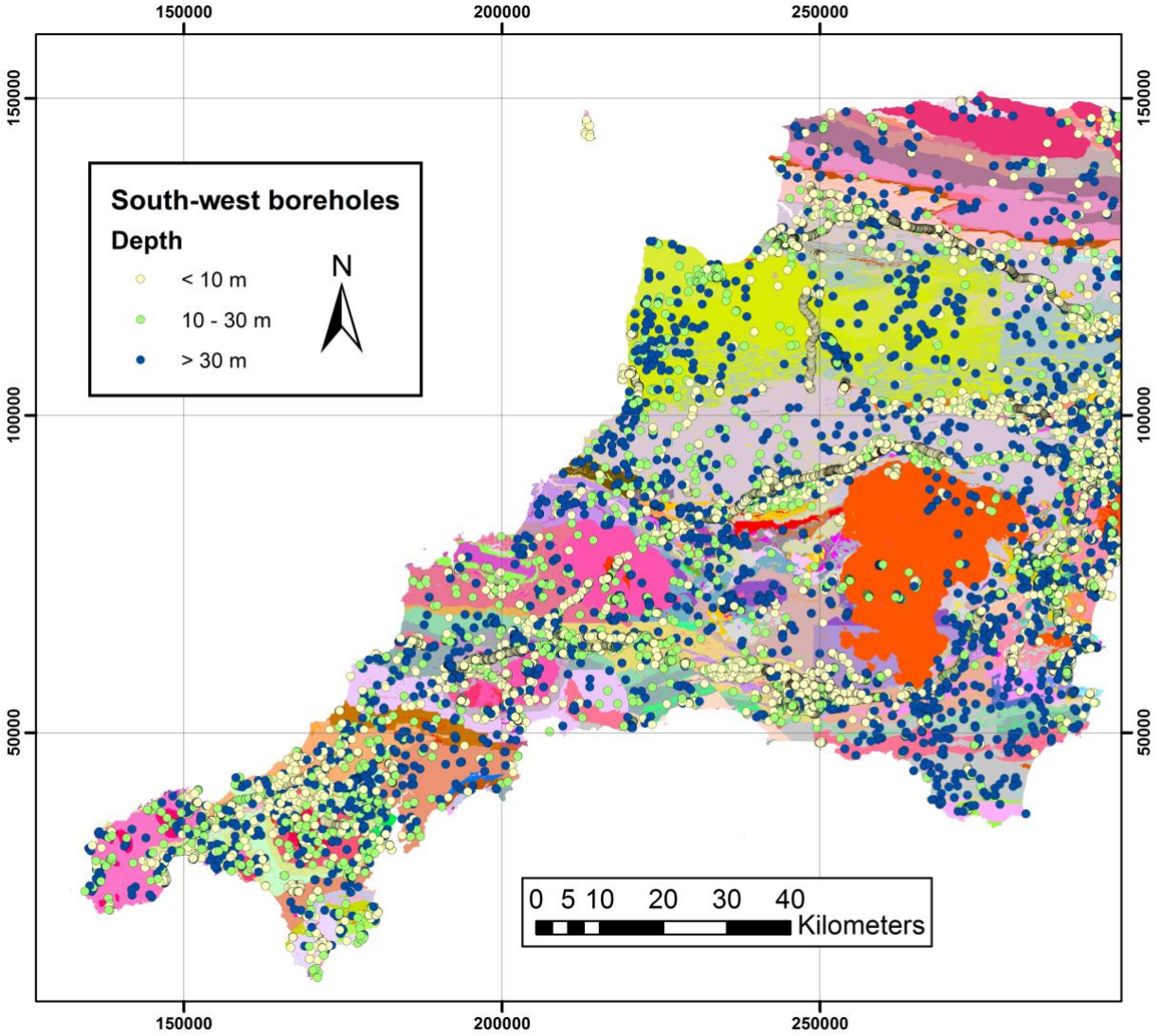

Figure 16: Distribution of bore holes that have been drilled in south-west England. Data for these bore holes are held at the British Geological Survey. British Geological Survey © UKRI.

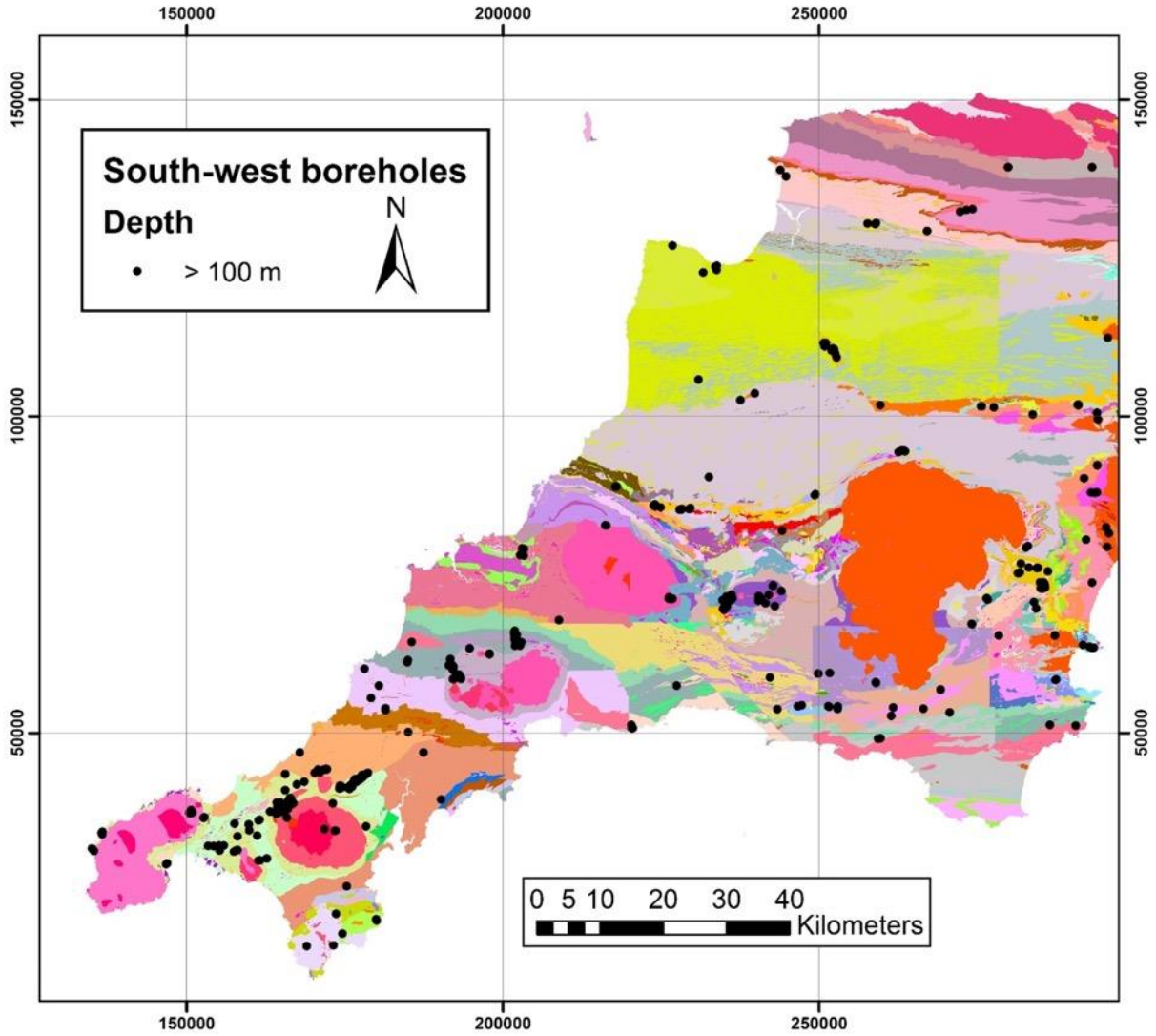

Figure 17: Boreholes deeper than 100 m (500 in total) that were reviewed in this study. British Geological Survey © UKRI.

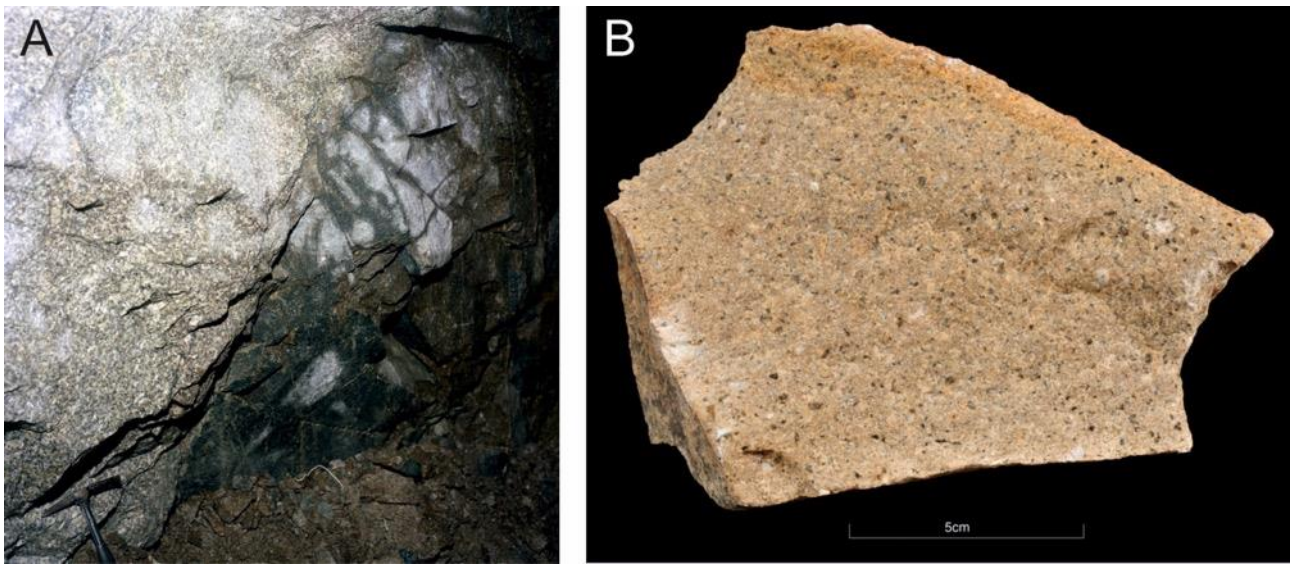

Figure 18: Quartz-feldspar porphyry dykes, which are locally termed 'elvans' in south-west England. A: South Crofty Mine, Robinson's Section, cross cut N. from No. 4 to No. 6 lode. Megacrystic, coarse-grained, biotite-granite/elvan contact in cross-cut. B: An elvan from DeLank Quarry, Bodmin, Cornwall. British Geological Survey © UKRI.

3.3.2 Key structural features

Cornish granites, including the Carnmenellis granite, typically have very low primary permeability, in the order of 10^{-8} to 10^{-10} D (Batchelor, 1978), but relatively high hydraulic conductivity (c. 20 mD;) according to Durrance (1985a) . The high hydraulic conductivity is driven by geological features in the granite such as joints, fractures, faults, mineral veins and heavily-fractured elvan dykes (Heath, 1985; Smedley et al., 1989).

3.3.2.1 Jointing in the granite

Jointing is particularly important for controlling fluid flow in Cornish granites (Figure 19), and the following four joint sets have been identified in the Carnmenellis granite (Bromley et al., 1989; Heath, 1985; Leveridge et al., 1990) (Figure 20):

i) Major joint set 1 is characterised by a set of steeply-dipping (60–85°) ENE-WSW-trending joints that contain tourmaline and quartz. They are parallel to the elvan dykes and hydrothermal mineral veins observed in the mineralised zone around Camborne and Redruth;
ii) Major joint set 2 is characterised by a set of vertical, variably mineralised (with galena and fluorspar) NNW-SSE-trending joints that are perpendicular to major joint set 1, but parallel to regional 'cross-course' structures;
iii) A subordinate set of unmineralised, vertical, NNE-SSW-trending joints; and
iv) A second set of subordinate, unmineralised, vertical E-W-trending joints.

Figure 19: Typical jointing in the Godolphin granite, exposed at Rinsey Cove, SW Cornwall. British Geological Survey © UKRI.

There are a number of lines of evidence to suggest that the joints in the Carnmenellis granite formed in response to externally applied regional stress: i) fractures in the country rock have a similar trend to that of the major joints sets in the granite; ii) joint sets with a similar orientation have been observed in the other major granite bodies in Cornwall; iii) a general lack of radial or concentric cooling joints in the granite; and iv) about 95 per cent of steeply-dipping joints in all granite bodies lie within a few tens of degrees of the dominant NNW-SSE trend (Bromley et al., 1989; Leveridge et al., 1990). It is also the regional stress field, orientated NNW-SSE that controls fluid flow, predominantly along stress-field parallel features such as joints and cross-courses. The horizontal stress regime ensures that these features remain dilated, permitting fluid movement. Evidence for this has been reported by a number of studies (Alderton and Sheppard, 1977; Smedley et al., 1989) that have sampled warm, saline fluids from springs issuing from NNW-SSE-trending features in the deep-mines at the northern edge of the Carnmenellis granite. Work by Batchelor (1978), as part of the HDR programme, also indicated that NNW-SSE-trending features occur at depths of 2.6 km in the Carnmenellis granite.

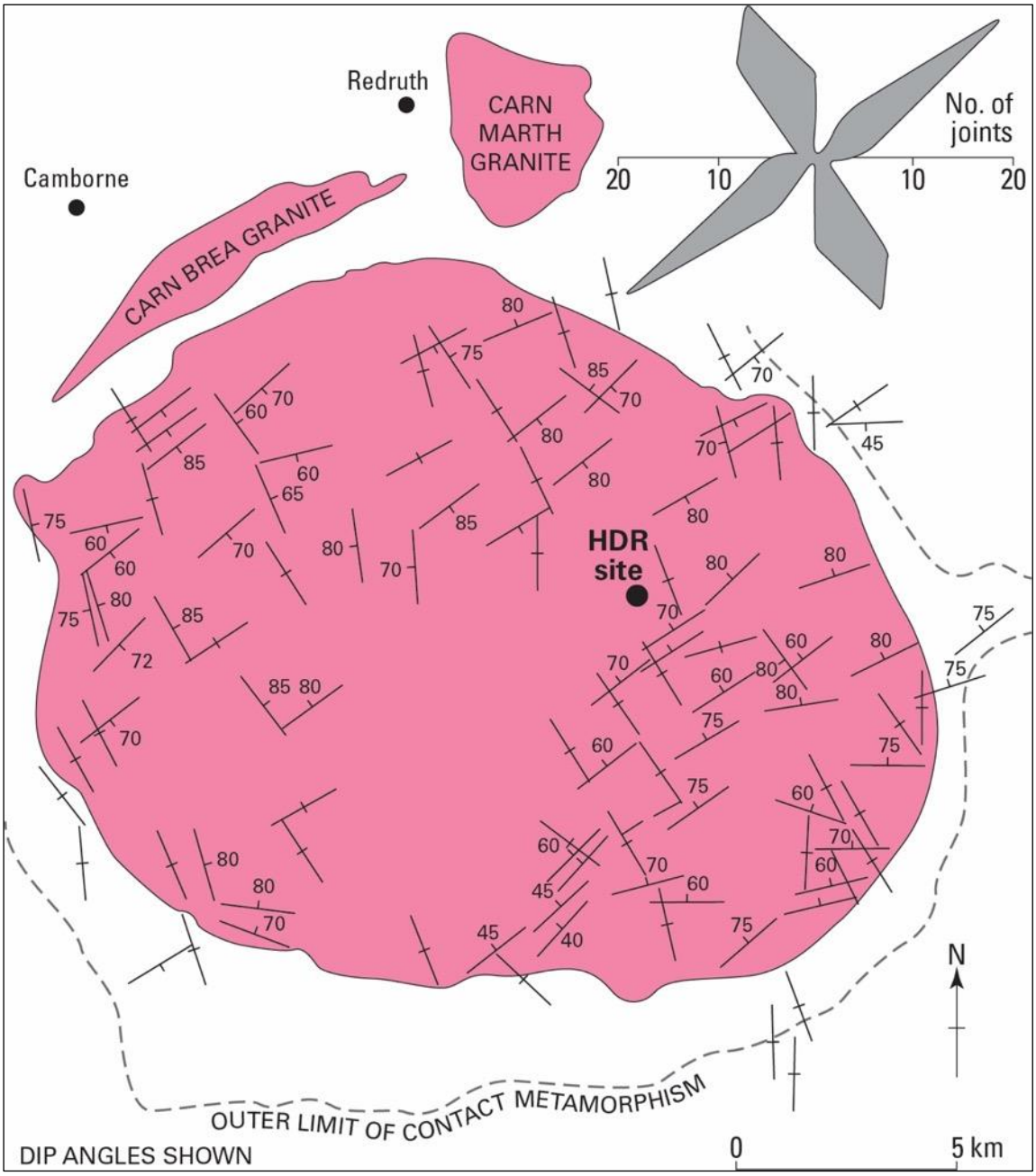

Figure 20: Sketch map of the Carnmenellis granite showing the strike and dip of the major joint sets Redrawn from Batchelor and Pine (1986), Figure 2, ©International Society for Rock Mechanics.

3.3.2.2 Faulting

A major feature of the region is the oblique dextral strike-slip faulting, striking between NW and NNW, which is locally associated with a subordinate complementary fault set striking between NNE and NE. In the CHPM2030 study area there is evidence for a period of N–S shearing followed by E–W crustal extension, which led to the development of extensive NW to N–S-trending fracture systems, throughout the Cornubian Orefield, locally termed 'cross-courses' (as strictly, they offset or cut across the earlier formed lode structures) (Figure 12). The Great Cross-course, the principal cross-course structure in the South Crofty Mine, is considered to represent a pre-granite strike-slip fault which was episodically reactivated during the Late Permian/Early

Triassic (Edmonds et al., 1985). The cross-course structures are likely to play a significant role in the overall permeability of the region. They are variably mineralised, with the vast majority of mineralised cross-courses occurring in the country rock, rather than granite (pers. comm.). The continuity of these structures in the study area remains ambiguous. BGS mapping from the mid-1800s shows these structures extending from the coast west of Porthtowan to the area SE of the Carn Marth granite (Figure 21A). However, subsequent revision of the mapping by the BGS (1990) whilst retaining inferred NW to N–S-trending faults, suggests these structures have more limited strike extent (Figure 21B). Whilst the cross-course structures can be clearly observed in coastal sections along the north Cornwall coast (Figure 22), and inland in underground mines exposures e.g. South Crofty (Figure 23), their position and continuity in the intervening zones remains conjectural.

Figure 21: Mapped cross-course structures to the north of the Carnmenellis granite. (A) NW-SE-trending cross-course structures are shown in white on the 1846 BGS map (de la Beche, 1846). (B) More recent BGS mapping (1990) of the same area depicts the cross-course structures as less continuous inferred faults (dashed black lines) (British Geological Survey, 1990). British Geological Survey © UKRI.

3.3.3 Data availability

The BGS is the world's longest established national geological survey, and is the UK's premier provider of objective and authoritative geoscientific data. It has been gathering geoscience data and information about the subsurface in the UK and other countries for more than 180 years. It is a data-rich organisation with more than 500 datasets in its care, including environmental monitoring data, digital databases, physical collections (e.g. borehole core, rocks and minerals), records and archives. Importantly, a great many of these datasets are openly available, many of which provide complete, seamless UK coverage at a number of scales. Certain other

datasets may be subject to confidentiality clauses and/or licencing fees. Information about how to access these datasets can be found here: http://www.bgs.ac.uk/data/home.html?src=topNav.

These national datasets are available to the CHPM2030 project, and can provide a very useful starting point to assess CHPM potential in south-west England. Many of the datasets cover much of the UK, whereas others are specific to south-west England (e.g. geophysical data conducted as part of the TELLUS project (http://www.tellusgb.ac.uk/). Most of the data stored relate to surface exposures or the near-surface environment. Although, the datasets do contain much information about a large number of boreholes and mines, most does not extend below 100 m, and there is limited data below 1,000 m. This places significant constraints on predictions when extrapolating the data to EGS depths (i.e. 4–6 km). The datasets are also of differing ages and levels of detail - reflecting changing national priorities over the past decades. In terms of geothermal development, much of the data are derived from a national programme of work in the 1980s and early 1990s. Therefore, the data reflect monitoring technology and ideas at that time, and much of the data are in analogue format. Details of BGS' data holdings are outlined CHPM2030 Deliverable D1.2 (Shaw et al., 2016).

Figure 22: Major cross-course structures exposed in the cliffs on the north Cornwall coast. A. Cross-course in the bay is traceable from water line up the beach and into the cliff face (dashed line) at Gooden Heane Cove, near Portreath. B. Cross-course viewed from the cliff top west of Porthtowan. This structure is shown on Figure 21B extending southward from the coast west of Porthtowan for a strike distance of about 2 km. C. Mineralised cross-course in the cliff face at St Agnes. The vein has multiple stage of development, open space and contains quartz-tourmaline-pyrite and minor chalcopyrite. D. Mineralised cross-course in the cliff at Cotty's Point, near Perranporth. The mineralisation comprises numerous episodes of chalcedonic and coarse quartz infill, which are evidence of multiple fluid flow events. Significant reddening of the host killas may be related to iron-rich fluids. British Geological Survey © UKRI.

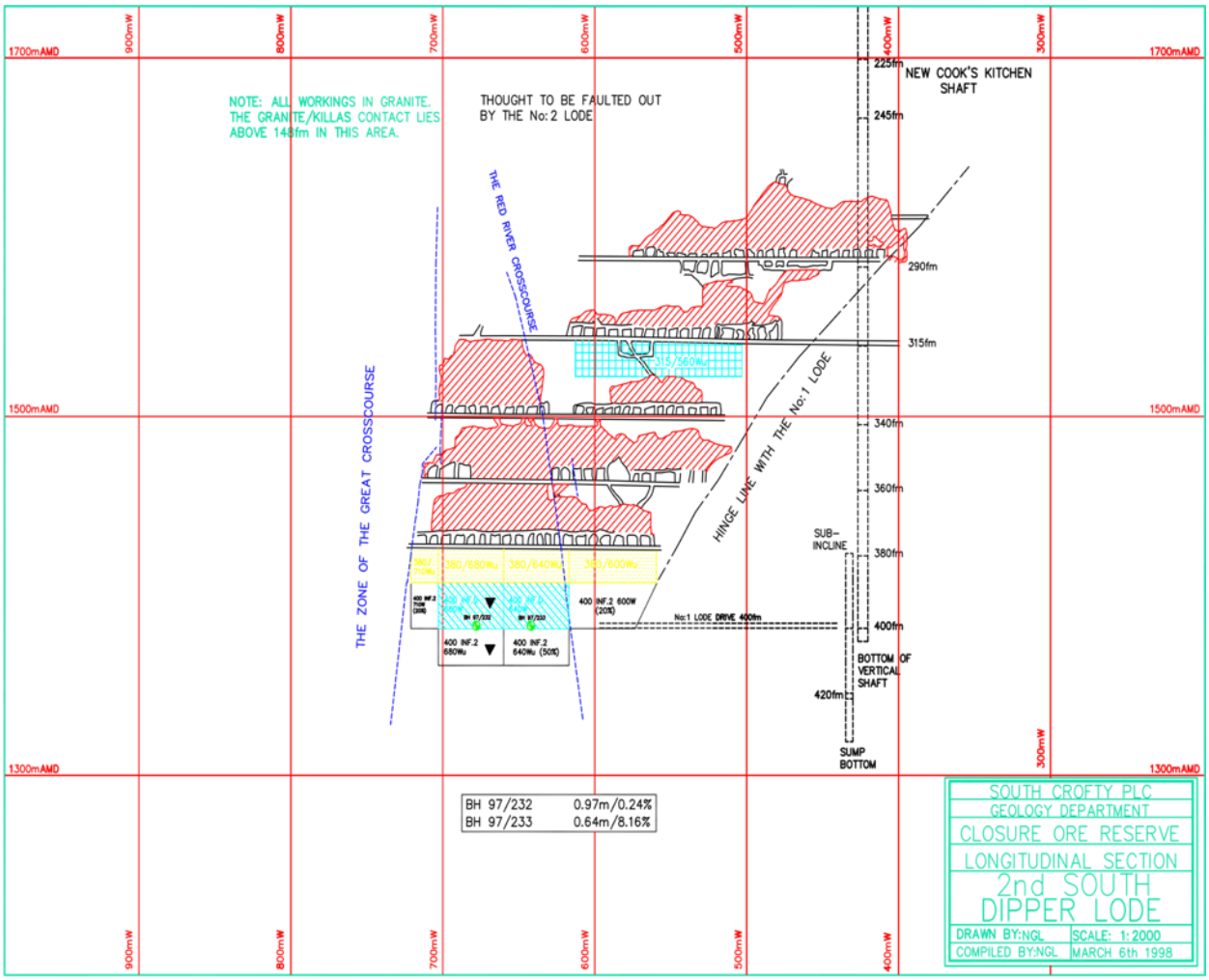

Figure 23: South Crofty Mine plan showing cross-courses identified in the mine. Reproduced with permission of Cornish Mines; credit: Dr Nick Le Boutillier (BSc PhD MCSM EurGeol CGeol FGS).

4 Geophysics of the prospective area

4.1 Previous work and data availability

4.1.1 Airborne data

In 1955 the British Geological Survey commenced the national aeromagnetic survey of the UK (altitude of 305 m and flight lines at 2 km). However, because of the mineral resource potential of south-west England, it was decided to combine the aeromagnetic survey with the UK Atomic Energy Agency uranium exploration programme and fly a more detailed co-funded survey over the region (Kimbell et al., 2003). The first part of the survey was flown in 1957, covering west and central Cornwall and used magnetic, electromagnetic (EM) and radiometric sensors. The EM results are strongly affected by cultural noise and equipment failure. The second phase, continuing eastward to cover the rest of Cornwall, most of Devon and part of Somerset, was flown in 1958–59 with only magnetic and radiometric sensors. The flight lines were flown parallel to the N–S National Grid lines and spaced 400 m (±200 m) apart and at an altitude of 150 m (± 30m). The principal aim of the radiometric survey was to identify vein-style uranium mineralisation. However, little attention was given to regional interpretation or other applications of the data (Kimbell et al., 2000; Kimbell et al., 2003). Iso-rad maps show a good correlation with the geology over the granites, surficial concentrations of radioactive minerals and mine dump material. The results of the aeromagnetic data have been included in published BGS maps of the region. The EM data has not been comprehensively interpreted, but many of the anomalies were considered topographical in origin or due to power infrastructure (Cornwell et al., 1995). In 1996 a decision was made to digitise the radiometric data from the 1957 survey to see if any new information could be gained (Kimbell et al., 2000). The digital data (Figure 24) provided new insights into the geology of the region, including the influence of granite mineralogy and alteration on the radiometric response, the characteristics of the Lizard Peninsula, changes in radiometric levels related to lithological units in the sedimentary rocks and the occurrences of uranium mineralisation (Kimbell et al., 2003).

This data has been superseded by that collected during the Tellus South West (TellusSW) survey (2013–2014), which encompasses the counties of Cornwall and parts of Devon and Somerset. The TellusSW survey had a number of components, but the most relevant to this review are a high resolution airborne geophysical survey, an airborne LiDAR survey, and geochemical sampling of soils and stream sediments. The maps and data produced show the soils, rocks and landscape at unprecedented depth and detail, and augment existing data to provide the two counties with among the best and most comprehensive environmental datasets anywhere in the world (www.tellusgb.ac.uk). The airborne geophysical data acquired during the second half of 2013 comprised a high resolution magnetic/magnetic gradient survey (Figure 25) combined with a multichannel (256 channel) radiometric survey (Figure 26). The survey was carried out using 200 m (N–S) line separations at a mean elevation of 91 m. Encompassing the counties of Cornwall and parts of Devon and Somerset, the survey provided 60,323 line-kilometres of data (www.tellusgb.ac.uk). The data is free to download and full details of the survey are provided in Beamish and White (2014). The LiDAR survey covers the same area as the geophysics and was flown during July to August 2013. Details of the survey can be found in Gerard (2014) and a high resolution digital terrain model was produced from the data by Ferraccioli et al. (2015) (see Appendix A in Gerard, 2014).

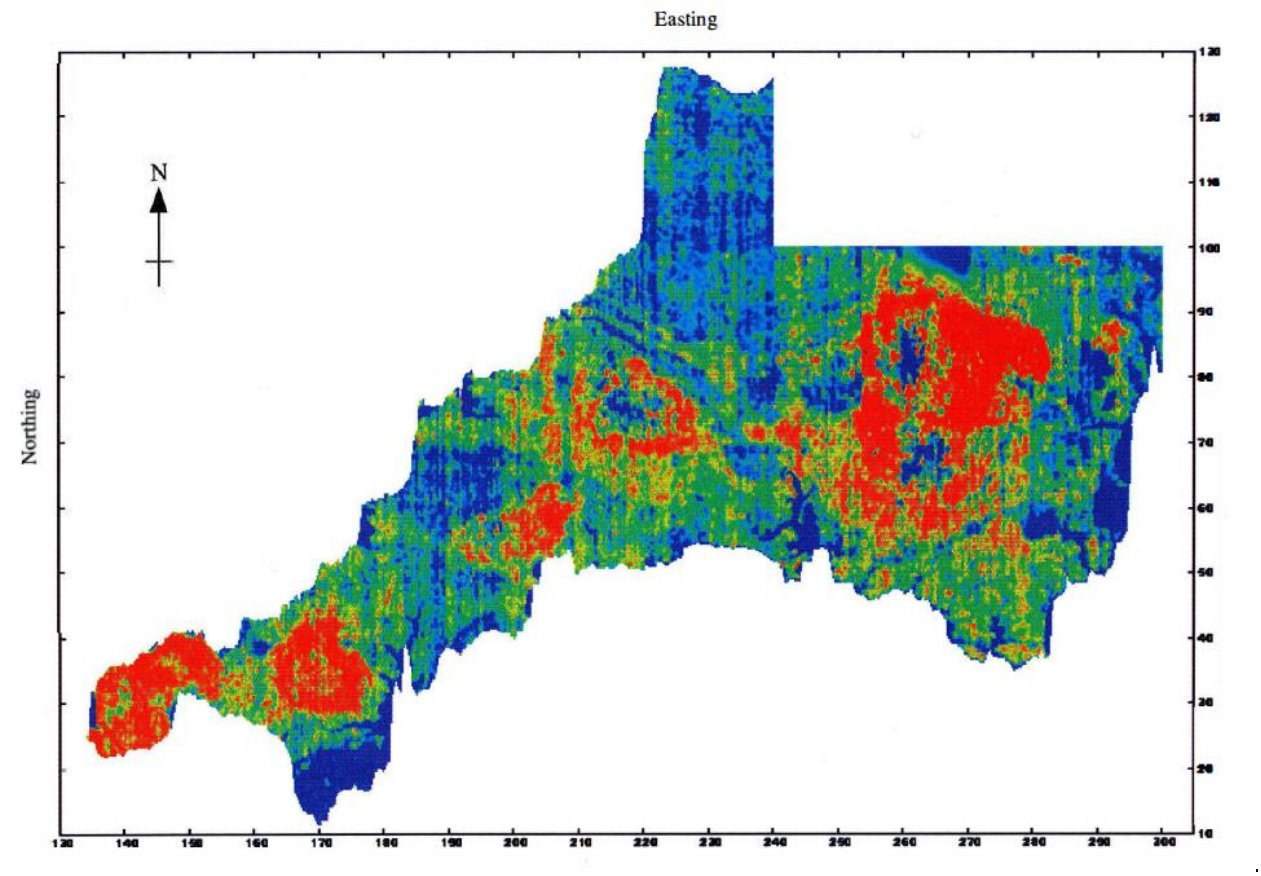

Figure 24: Total radiometric count map for south-west England. Red = high count, blue = low count. Shaded-relief map of the 1950s airborne radiometric data over south-west England. Reproduced from (Kimbell et al., 2000). British Geological Survey © UKRI.

Yeomans (2017) provides a summary of the potential applications of the TellusSW data for advancing our knowledge of the geology of south-west England. Simons et al. (2016) produced a new map for the Cornubian Batholith. However, it is based on mineralogical, geochemical and field relationships from a limited number of samples and selected areas of granite outcrop. Yeomans (2017) emphasises how the continuous nature of the airborne radiometric data (Figure 26) means it could be used for re-mapping these composite granites in a more objective way using their radioelement variation (which is a function of their geochemistry). This could be particularly valuable for enhancing our understanding in areas that may have low or no outcrop exposure. Yeomans (2018) used a machine learning approach (machine learning combine's statistical analyses and computer science to undertake automated pattern recognition in datasets), employing a range of algorithms to re-map and classify different granite types based on the airborne radiometric data and subsequently integrating the Tellus stream-sediment data. As the radiometric (gamma ray) data provide ground concentration estimates of the heat-producing radioelements it has also been used to revaluate heat production across the batholith (Beamish and Busby, 2016), which is discussed in Section 6.1.1. The TellusSW magnetic and LiDAR data have proved particularly useful for defining lineaments. This has permitted new structural interpretations in some areas and improved correlation of lithostratigraphic units across some map sheet boundaries (Yeomans, 2017). Yeomans et al. (2019) used the TellusSW magnetic, radiometric and LiDAR data and Object-Based Image Analysis (OBIA) (a tool for analysing spatially correlated groups of pixels) for semi-automated geological lineament detection in south-west England. This approach has generated a new comprehensive lineament network for the region (Figure 27).

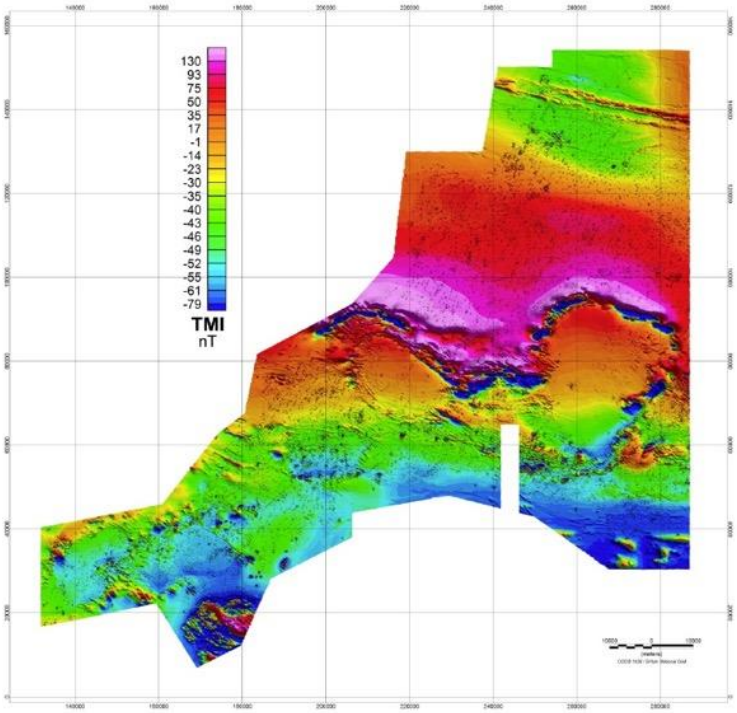

Figure 25: Total Magnetic Intensity (TMI), IGRF corrected to provide the final TMI anomaly data. Equal-area colour normalisation. Reproduced from Beamish and White (2014). British Geological Survey © UKRI.

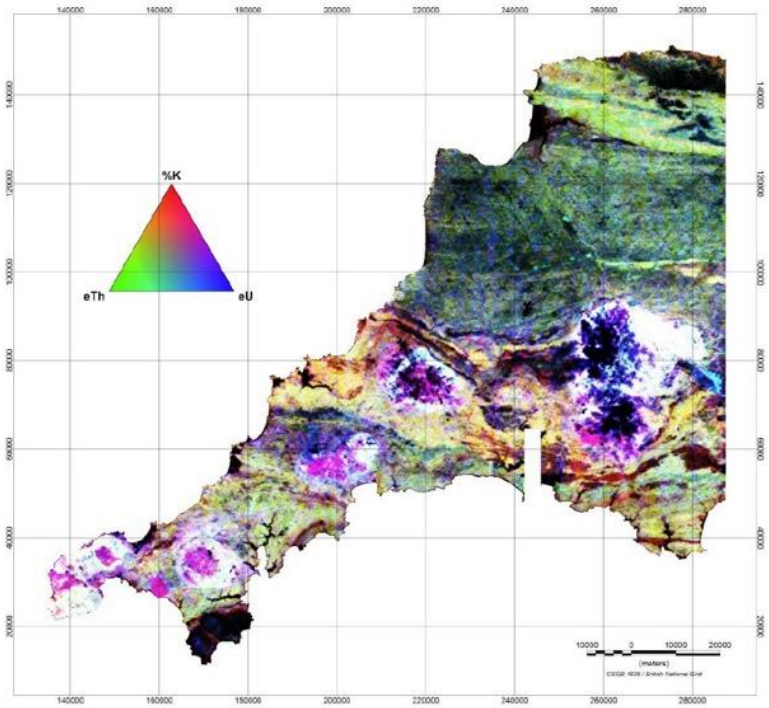

Figure 26: Ternary radiometric image formed from the Potassium (%K), Thorium (eTh) and Uranium (eU) ground concentration estimates. Reproduced from Beamish and White (2014). British Geological Survey © UKRI.

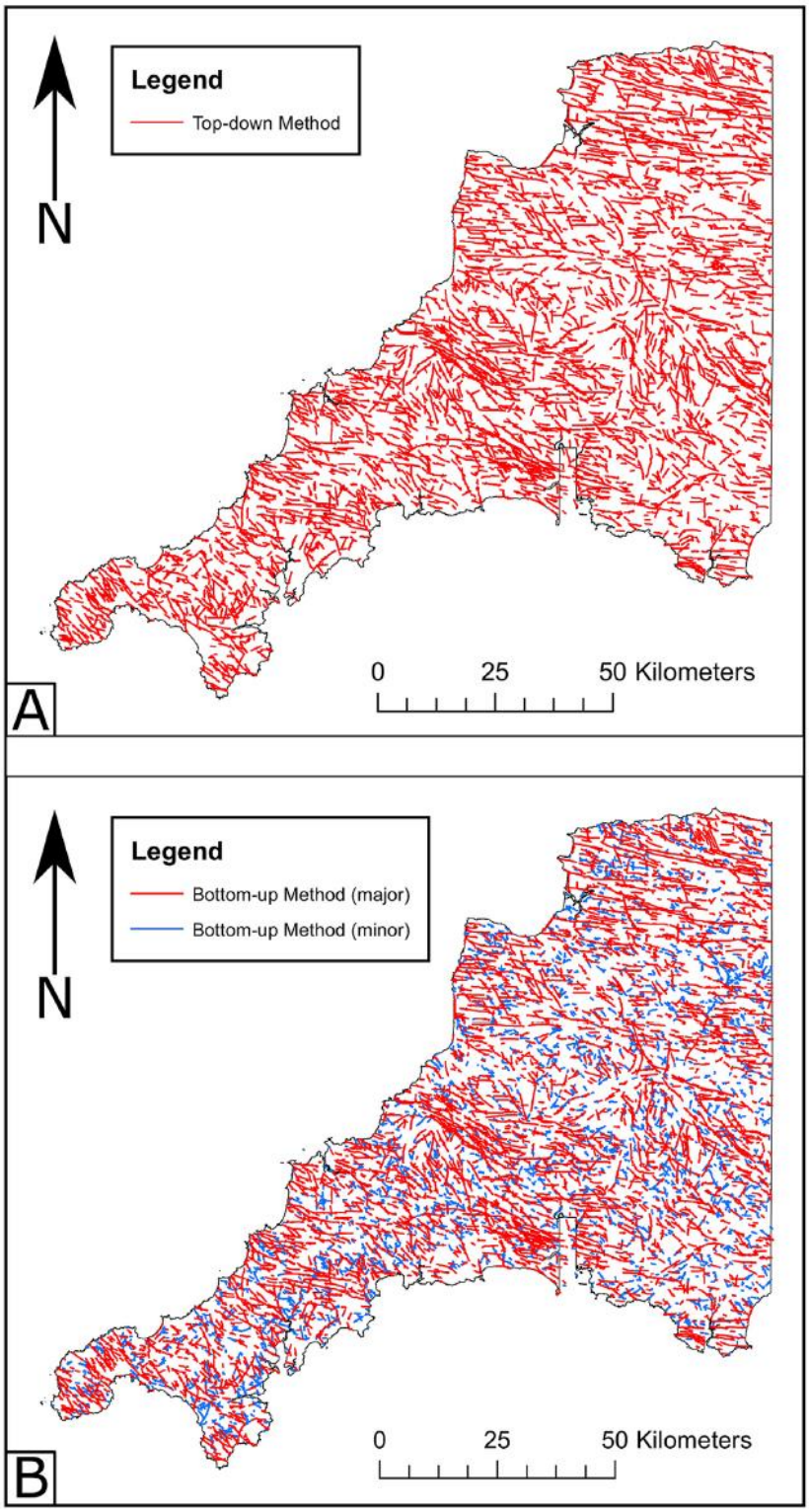

Figure 27: Regional lineament maps for south-west England. A. top-down methodology. B. Bottom-up methodology, see Yeomans et al. (2019) for a description of the lineament detection methodology. Reproduced from Yeomans et al. (2019), under Creative Commons Attribution 4.0 International License(http://creativecommons.org/ licenses/by/4.0/).

4.1.2 Ground-based data

4.1.2.1 Gravity data

There has been a long held view that the outcropping granites in south-west England were interconnected at depth (de la Beche, 1839). This was confirmed by gravity data derived in the 1950s, and the Bouguer gravity anomaly field in south-west England was first described and interpreted by Bott et al. (1958). Negative Bouguer gravity anomalies define the Cornubian peninsula, with significant lows associated with the exposed granite plutons (Figure 28). Bott et al. (1958) concluded that the exposed granites represented cupolas on a single elongated batholith that extended to a depth of at least 8 km and possibly as deep as 20 km. They considered the contacts between the granite and country rocks to typically slope outwards. Tombs (1977) used the gravity data to produce a three-dimensional model of the Cornubian Batholith, which suggested westward thinning of the batholith and the presence of shallow ridges connecting the exposed granite bodies.

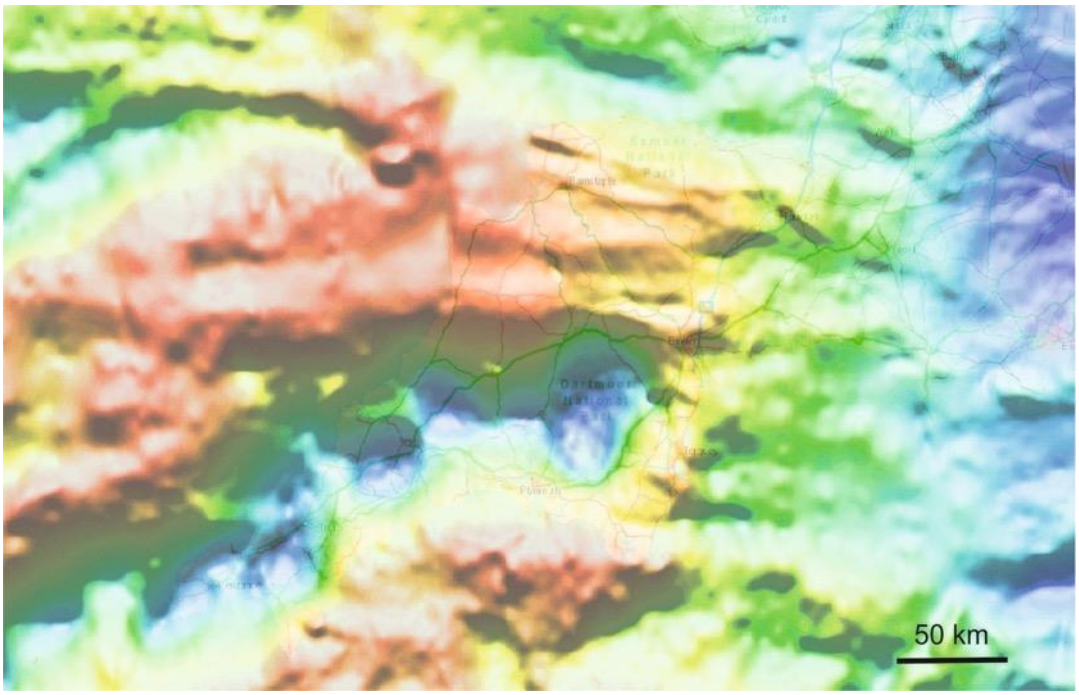

Figure 28: BGS gravity anomaly map over south-west England. The measured gravity values have been corrected in order to show the anomalies attributable to variations in crustal density. In broad terms the blues are attributable to large volumes of low density rocks, the reds to high density rocks. Significant lows occur, for instance, over areas of thick, low density sedimentary rocks, or large granites. Contains Ordnance Data © Crown Copyright and database rights [2019]. Ordnance Survey Licence no. 100021290. Contains British Geological Survey materials © NERC [2019].

The 'Camborne Geothermal Energy Project' carried out under contract as part of the Departments of Energy's Renewable Energy Research and Development Programme produced a three dimensional model of the shape of the Cornubian Batholith from gravity, density and wide angle seismic surveys (Willis-Richards et al., 1989). The gravity data (Figure 28 and Figure 29) were used to produce a three dimensional model covering the major granite outcrops from Dartmoor to Lands End (Willis-Richards and Jackson, 1989) (Figure 30). Details of the gravity modelling are described in Willis-Richards and Baria (1989) and summarised in Willis-Richards et al. (1989). Gravity derived estimates of batholith thickness are dependent on a number of assumptions, however,

the average batholith thickness under Lands End, Carnmenellis and the St Austell area was modelled to be about 13.5 km. The most significant features identified from the model were: i) that the batholith can be divided into two 'compartments', separated by a 3000 m deep, fault-bounded trough, extending between Carnmenelis and St Austell area; ii) all the major plutons are connected by saddles of granite in the roof of the batholith that are generally concealed by less than 2 km of cover rocks; iii) a buried granite ridge, under several hundred meters of cover rocks, extends northwards from the Carnmanellis granite towards Cligga Head; iv) a south-sloping base to the batholith, indicative of post-emplacement tilting to the south; and v) an estimated total volume of the batholith of about 68,000 km^3 (Figure 30) (Willis-Richards et al., 1989). A limitation with the gravity data is its spatial resolution, which makes features of less than about 2 km wavelength challenging to resolve. Despite this the model provided a limit to the total area and volume of the batholith (Willis-Richards et al., 1989). However, it was acknowledged that the estimated volume, based on the gravity modelled dimensions was significantly larger than previous estimates (Willis-Richards and Jackson, 1989). In fact the Cornubian Batholith appeared unusually thick relative most other granites globally, and more recent modelling of the gravity anomaly by Taylor (2007) has resulted in a significant reduction in the thickness of the Bodmin, St Austell and Carnmenellis plutons, and the confirmation of deeper, possible feeder zones towards the south of the Bodmin, St Austell and Dartmoor granites (Figure 15).

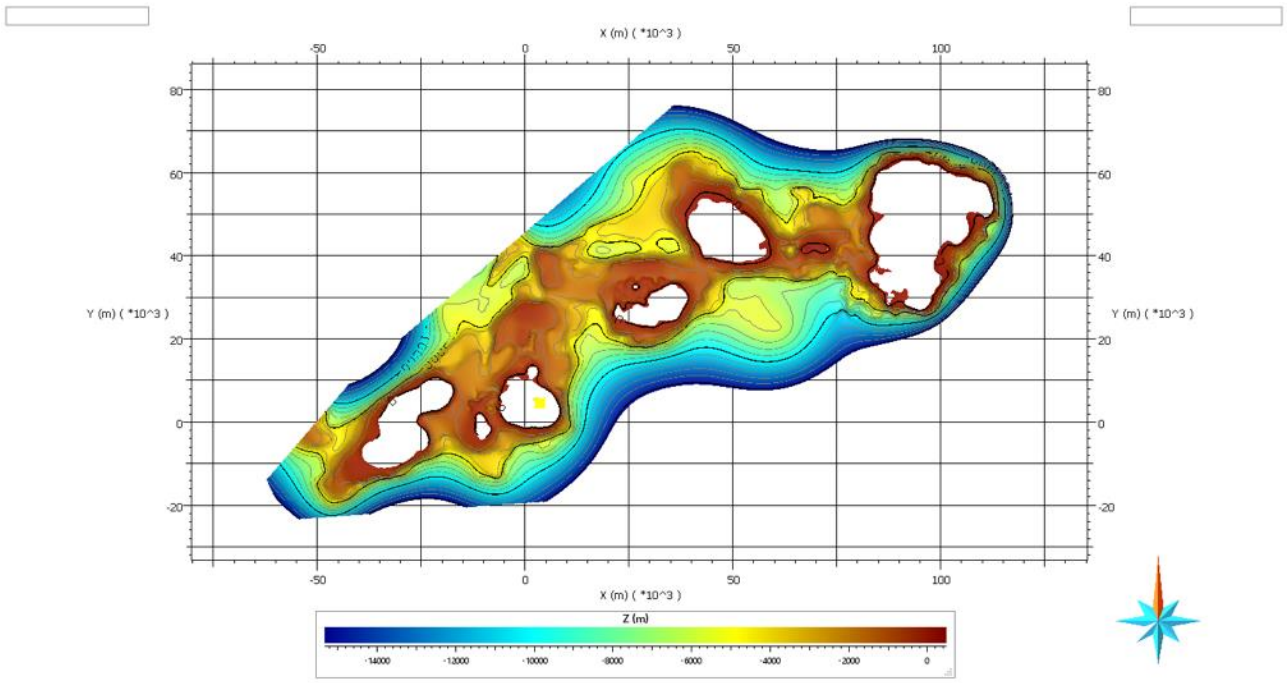

Figure 29: Plan view of the modelled top surface of the Cornubian Batholith (revised from CSM Report 2C-7, 1988; Willis-Richards and Baria, 1989; Tombs, 1980; Rollin, 1988 and Tombs, 1977). British Geological Survey © UKRI.

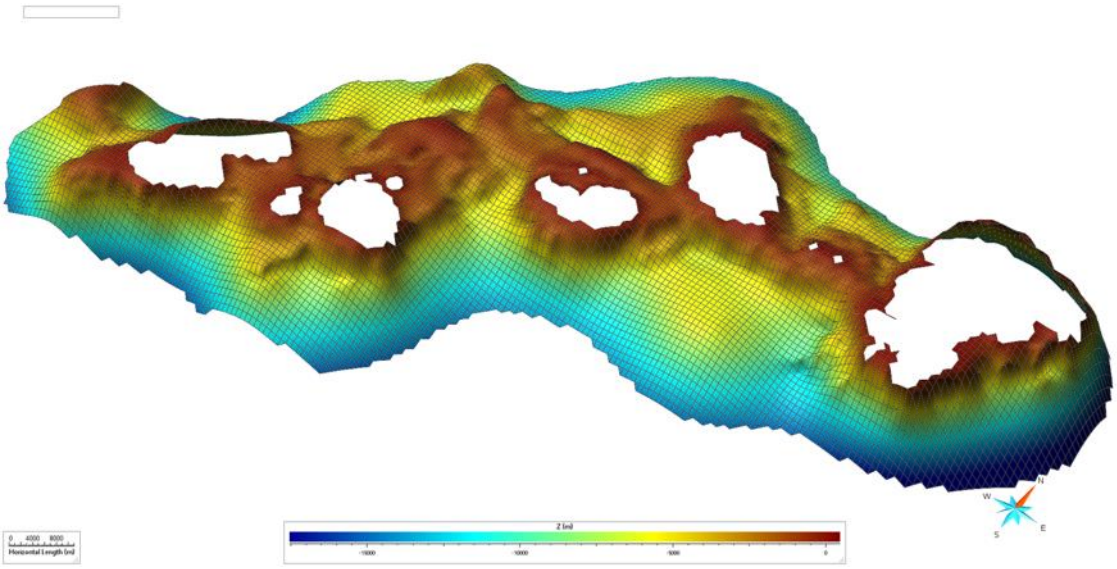

Figure 30: Perspective 3 dimensional view of the modelled top surface of the Cornubian Batholith (revised from CSM Report 2C-7, 1988; Willis-Richards and Baria, 1989; Tombs, 1980; Rollin, 1988 and Tombs, 1977). British Geological Survey © UKRI.

4.1.2.2 Seismic data

A seismic refraction experiment was undertaken in south-west England in 1966. One line was along the granite batholith and its seaward extension towards the WSW. The crustal structure along this line was initially described by Bott et al. (1970) and is discussed in detail by Holder and Bott (1971). The granite was interpreted to represents a 10–12 km thick upper crustal layer with a uniform velocity of 5.85 kms^{-1}. However, a near surface lower velocity layer of 2–3 km thickness can be distinguished. There is no sudden increase in velocity at the base of the upper crustal layer, but between 9–13 km velocity gradually increases, reaching 6.9 kms^{-1} at the base of the crust at 27 km (Figure 31).

A subsequent large-scale crustal refraction/wide angle reflection experiment (the Southwest England Seismic Experiment, SWESE) was carried out in 1979. The survey comprised a series of recording lines spanning the Cornubian peninsula (see Figure 1 in Brooks et al., 1984). Three crustal reflectors were identified (see Figure 6 in Brooks et al., 1984 and Figure 1.2 in Jones et al., 1989). The upper reflector (R1) lies at a depth of about 8 km ±1.15 km, and appears to be restricted to the interior of the granite batholith. It was considered to potentially represent the boundary between different intrusive phases of the granite, a zone of thrusting in the granite, or stoped blocks within the pluton. A deeper reflector (R2) is located at a depth of 10–15 km, and was interpreted to gradually shallow northwards. Although it coincides locally with the base of the granite as predicted by gravity modelling, this reflector extends well beyond the northern limit of the granite body. Accordingly, rather than representing the base of the batholith it was considered more likely that the R2 reflector was a thrust surface that is locally coincident with the gravity modelled base. The third reflector (R3) is located at a depth of 27–30 km and interpreted to represent the base of the crust. The experiment also imaged some shallow reflectors that coincide with the roof of the granite based on gravity modelling (Brooks et al., 1984). Rather than an internal batholith reflector, Shail et al. (2014) subsequently interpreted R1 to represent the lower contact of the granite with the host rock (i.e. the base of the batholith), which lies at a depth of c. 8 km below the southern parts of Carnmenellis.

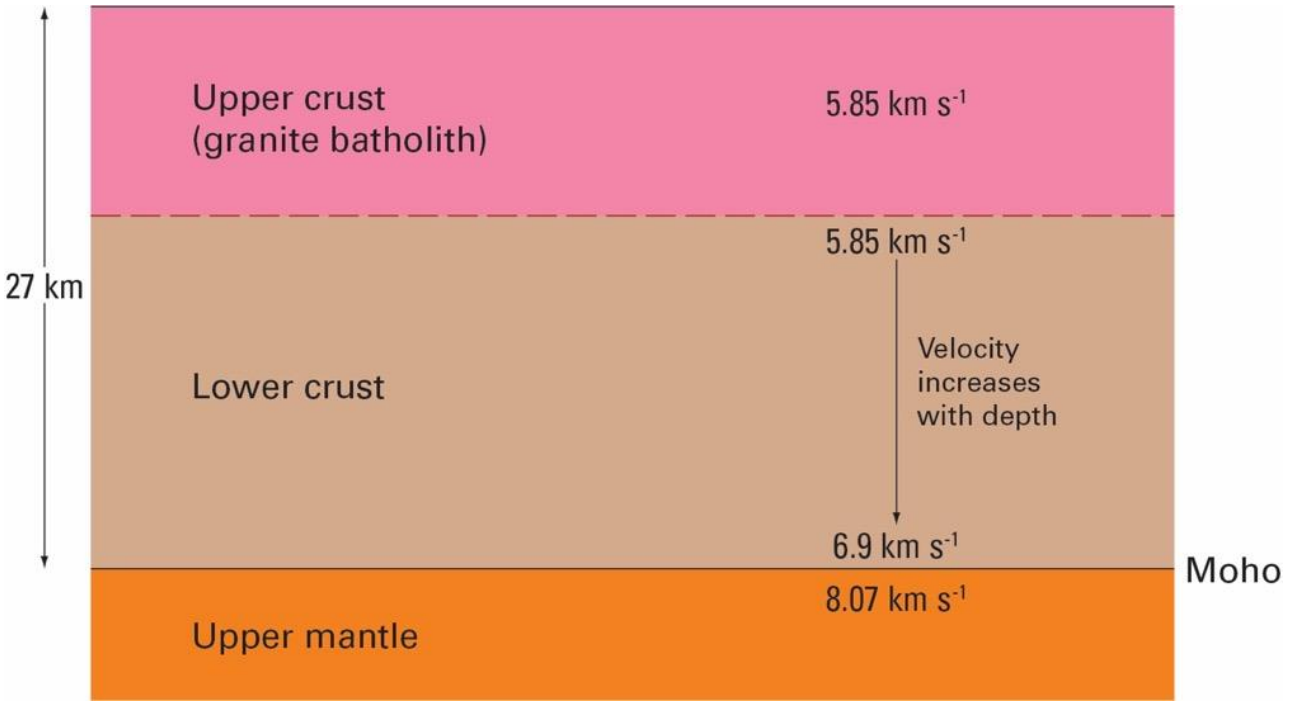

Figure 31: Model of the crustal structure for the seismic refraction line along the granite batholith. Reproduced from Fig 9. A. P. Holder & M. H. P. Bott. Crustal Structure in the Vicinity of South-west England. Geophysical Journal International (1971) 23 (5): 465-489, doi: 10.1111/j.1365-246X.1971.tb01838.x. By permission of Oxford University Press on behalf of the Royal Astronomical Society. Please visit: https://academic.oup.com/gji/article/23/5/465/677462. This figure is not included under the Creative Commons CC-BY license of this publication. For permissions, please contact journals.permissions@oup.com

Deep offshore seismic reflection profiles from the South West Approaches Traverse (SWAT) crossed south-west England. SWAT 6 crossed the Cornubian Batholith (Prive, 1986). A normal incidence seismic reflection survey was conducted over two lines to investigate the internal structure of the Cornubian Batholith (Willis-Richards et al., 1989). The two lines cross at the Rosemanowes site, passing over the HDR reservoir (see Figure 3.1 in Willis-Richard et al., 1989). The purpose of the survey was to investigate the structure of the granite between 4–8 km and determine the size and shape of the granite. The seismic section displays many short reflectors within the killlas where it reaches a thickness of >0.5 km (Jones, 1989). This was as anticipated, based on its known compositional variation (Willis-Richards et al., 1989). These reflectors are apparent down to about 4.5 km in the killas or appear to stop at the killas/granite boundary if it is shallower than this (Jones, 1989). However, the actual granite/killas contact was not imaged, as it is not reflective. This is because the seismic reflection technique is based on measurements of acoustic impedance. Acoustic impedance is a product of the density and the seismic velocity. The killas has a significantly higher density than the granite (making gravity modelling a good technique for determining the shape of the granite), but the granite has a much higher seismic velocity than the killas, therefore the acoustic impedance is very similar for both lithologies (Willis-Richards et al., 1989). There are no reflectors in the granite, which appears to be seismically featureless to a depth of 14 km (Jones, 1989; Willis-Richards et al., 1989) (see Figure 3 in Jones, 1991). Despite the normal incidence reflection data containing no evidence of structures at depths of 4–8 km, the wide angled reflection interpretation i.e. Brooks et al. (1984) does identify a feature (R1) at a depth of between 6–8 km (Jones, 1991). Resistivity data from Beamish (1990) (see below) suggests this depth represents a change from

an interconnected joint/pore network at hydrostatic pressures to a regime of isolated pores at lithostatic pressures. This could cause a decrease in seismic velocity, consistent with the presence of the R1 reflector in the wide angled data. This change would occur over too large a depth interval to produce a normal-incidence reflection, hence its absence in this dataset (Jones, 1991).

4.1.2.3 Magnetotellurics

A magnetotelluric (MT) survey was undertaken over the Carnmenellis granite in 1988 by BGS. MT uses natural variations in the earths EM field as its source. The way in which the EM source is modified by the rocks being surveyed is used to determine the resistivity of the rock as a function of depth. The most significant findings were that the granite appears very homogenous on a broad scale and that below a depth 1 km resistivity values increase down to a depth of about 6 km. Below 6 km the resistivity values remain fairly consistent down to 12–14 km. Importantly, it was concluded that the results are consistent with joint closure by a depth of 7 km, with a change to pore-dominated resistivity below this depth (see Figure 6 in Beamish, 1990). The electrical base of the granite was modelled at 14 km, which is consistent with gravity modelling (Beamish, 1990).

4.1.2.4 Natural seismicity

The British Geological Survey has monitored natural seismicity in Cornwall since 1980. Natural seismicity can be used to confirm the direction of the regional principal stresses and provide information on stress anisotropy at depth. Based upon events monitored between 1981–1987, those within the granite batholith cluster between 4–6 km depth, with some recorded at a depth of in excess of 8 km. Hypocentres located in the killas do not have a similar depth grouping. Focal mechanisms, are consistent with the maximum compressive stress being directed from the SE (Willis-Richards et al., 1989). Willis-Richards et al. (1989) notes that the magnitude of deviatoric stress in a deep (6 km) geothermal reservoir is an important parameter that will influence stimulation of the reservoir. It is considered unlikely that deviatoric stresses will exist in a granite for geologically significant time periods at temperatures above 200–220°C. It is suggested that this corresponds well with the observations based on natural seismicity. It is concluded that the transition from brittle to ductile conditions is probably occurring 'within the region of interest for geothermal exploitation', and at reservoir temperatures and over human time-scales the granite will behave elastically (Willis-Richards et al., 1989).

4.2 Tellus magnetics data reassessment

Given the importance of structure to EGS the TellusSW magnetics data was reassessed during this review. Figure 32 shows the geology and corresponding TellusSW aeromagnetic data over the north-eastern margin of the Carnmenellis granite. The country rocks are predominantly hornfelsed slates and siltstones of the MSF, with some metabasaltic rocks present. In the extreme NE of the district, metamorphosed mudstones and sandstones of the Gramscatho Formation are also present. Both granites and country rocks are intruded by a predominantly NE-trending suite of felsite dykes (Figure 32A).

The magnetic anomaly map (Figure 32B) shows that areas of granite are generally magnetically 'quiet', with little evidence of coherent features. Those magnetic features that are present over the granite are generally bullseye features that can be correlated with cultural structures (for example farm buildings) identified on Ordnance Survey (OS) topographic maps. Such anomalies that do not relate to cultural features are considered likely to arise from unmapped sources, which are potentially shallowly-buried. Comparison of the geology map with the magnetic anomaly map shows that the felsite dykes are, as would be expected on compositional grounds, not associated with linear magnetic anomalies. In areas that are not underlain by granite, there is a

good correlation between magnetic anomalies and mapped metabasaltic rocks, with additional anomalies that have no obvious geological correlation, potentially reflecting unmapped or buried magnetic units. The NE margin of the Carnmenellis granite is associated with a fairly broad NW-SE-trending linear feature (Figure 32B).

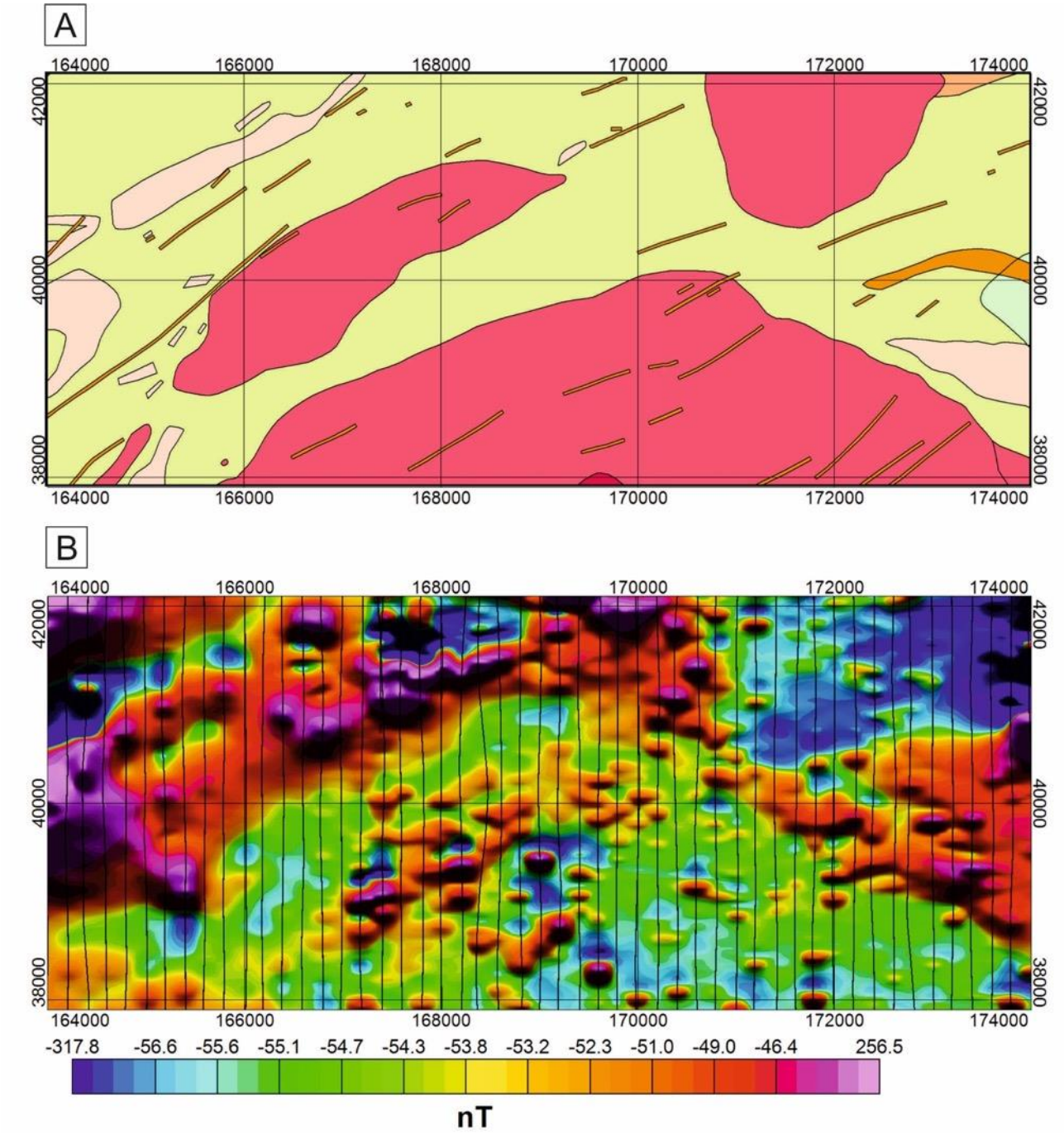

Figure 32: Geology and magnetic response over the north-eastern margin of the Carnmenellis granite. A. 1:50 000 scale solid geology. B. The TellusSW aeromagnetic data of the same area, with N-S flight lines displayed, produced from the TellusSW airborne geophysical survey data (Beamish et al., 2014). British Geological Survey © UKRI.

In order to examine this linear feature in a regional context, the TellusSW data for a 40 km x 40 km area enclosing the primary area of interest were examined. Figure 33 shows the reduced-to-pole total magnetic

intensity (TMI) anomaly and illustrates that the NW-SE-trending feature along the NE margin of the Carnmenellis granite forms part of a longer, regional NW-SE-trending feature that crosses Cornwall. Figure 34 shows the tilt-derivative of the TMI anomaly (Miller and Singh, 1994), further illustrating this linear magnetic feature.

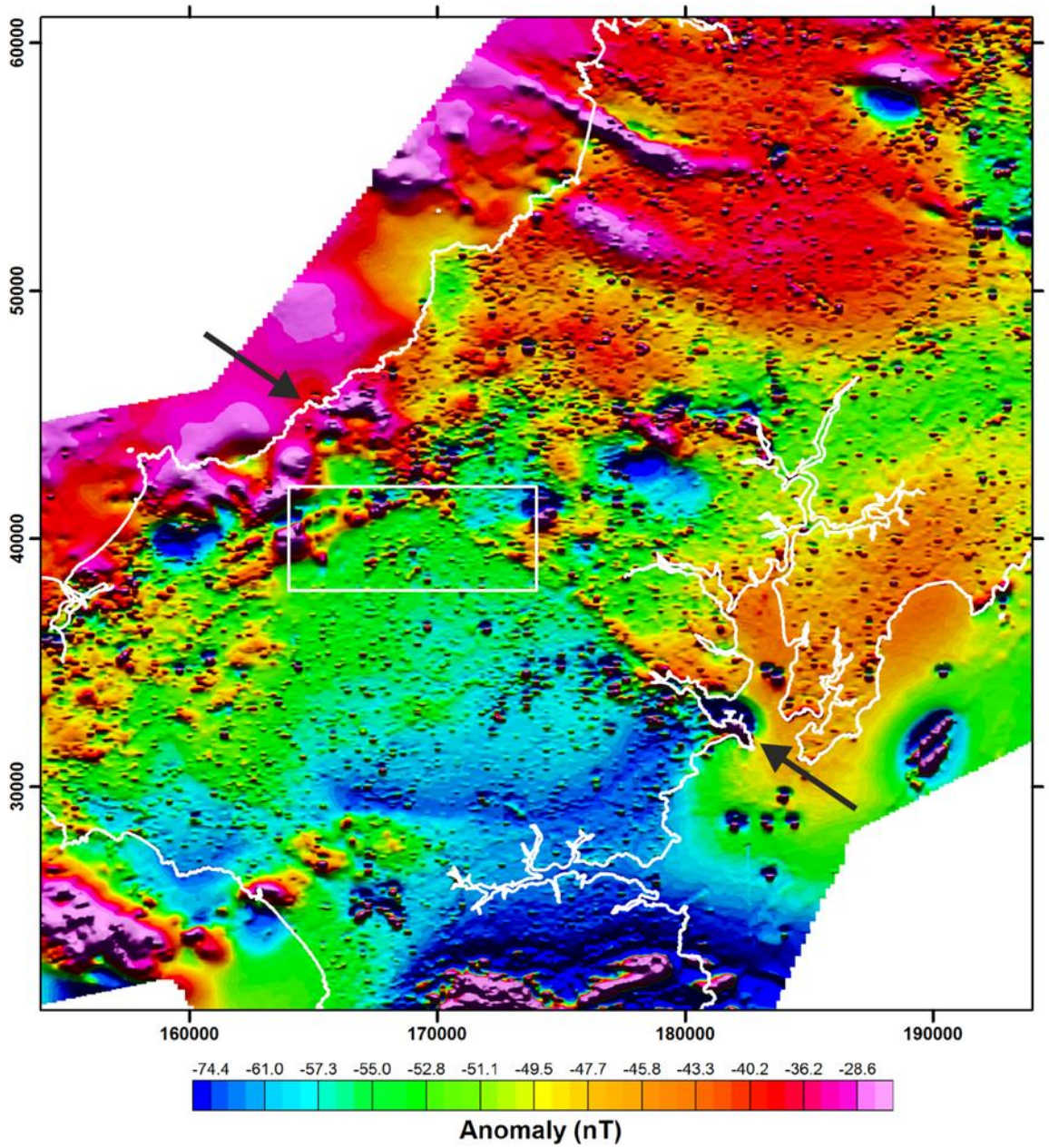

Figure 33: Regional reduced-to-pole total magnetic intensity anomaly from the Tellus SW aeromagnetic data. The white rectangle shows the area shown in Figure 32, and the two arrow indicate the regional magnetic lineament described in the text. Contains Ordnance Data © Crown Copyright and database rights [2019]. Ordnance Survey Licence no. 100021290. Contains British Geological Survey materials © NERC [2019].

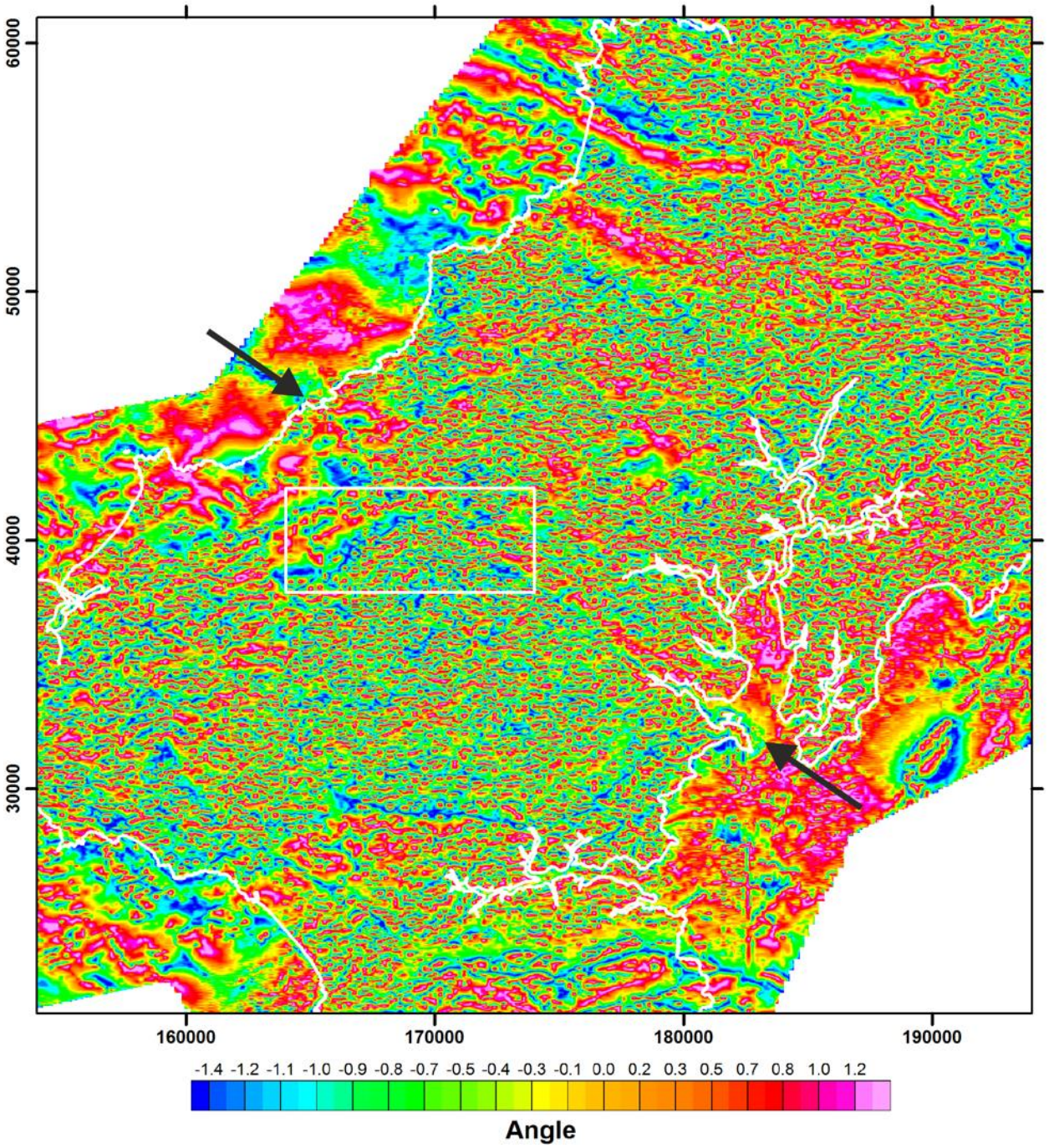

Figure 34: Tilt-derivative of the regional TMI anomaly. The two arrows indicate two arrows indicate the regional NW-SE-trending magnetic lineament described in the text. Contains Ordnance Data © Crown Copyright and database rights [2019]. Ordnance Survey Licence no. 100021290. Contains British Geological Survey materials © NERC [2019].

In common with the aeromagnetic data, cultural interference and associated anomalies are a challenge for interpretation of the TellusSW radiometric data (Figure 35). This is illustrated by the radiometric (potassium) data to the east of Redruth. A significant anomaly coincides with an area of made ground on the OS map. This is a landfill site that has been covered by china clay waste, which results in the elevated potassium signal (Figure 35).

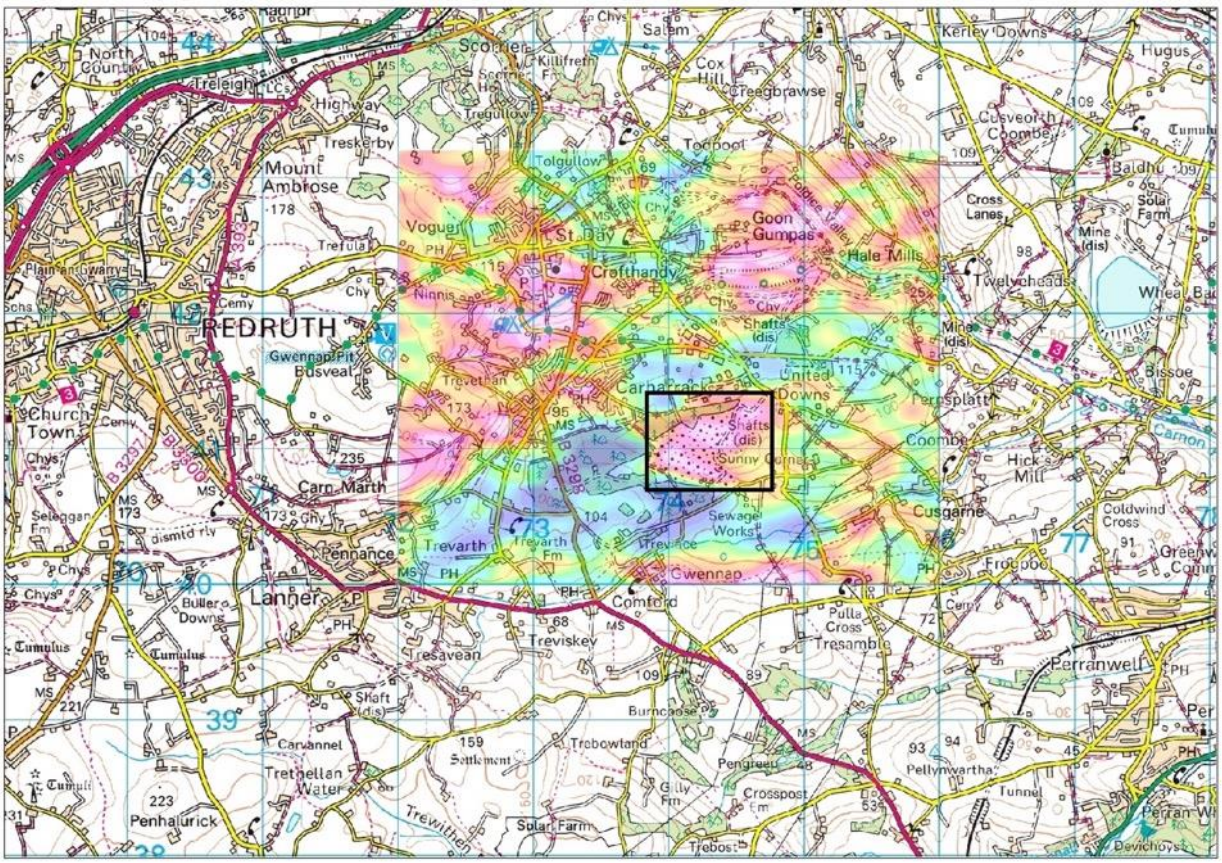

Figure 35: An example of a cultural artefact seen in airborne radiometric (potassium) data. The area in the rectangle is a historic landfill site that has been capped with china clay, which results in a strong positive signal. Contains Ordnance Data © Crown Copyright and database rights [2019]. Ordnance Survey Licence no. 100021290. Contains British Geological Survey materials © NERC [2019].

5 Deep metal enrichment

5.1 Types of mineralisation in the CHPM2030 study area

The CHPM2030 study area hosts two principal types and phases of mineralisation: i) granite-related mineralisation, which was largely formed during the Early to Mid-Permian; and ii) Mid-Triassic mineralisation, resulting from fracture-controlled migration of basinal brines from the Permo-Triassic basins into older rocks, which formed the so called 'cross-course' veins. Both types are abundant in the Camborne-Redruth area of Cornwall, which is located in the study area (Figure 7).

5.1.1 Granite-related mineralisation

Granite-related mineralisation, also termed 'main stage' mineralisation, is abundant in the study area (Figure 7). It primarily resulted from the migration and mixing of magmatic hydrothermal and other fluids within fractures in the granites and metasedimentary host rocks. It is considered a globally important, type example, of mineralisation associated with granitic magmatism, and has been termed 'Cornwall-type' mineralisation.

The majority of metal production, including tin, copper, zinc, arsenic and tungsten, from the Cornubian orefield has been obtained from exploitation of these large syn-granite fissure veins, termed 'lodes'. The term lode implies that both the vein and the altered wall-rock that hosts it are mineralised. Many of the endogranitic systems can be described as lode zones, which often contain multiple, inter-related veins rather than a single continuous vein structure (Dominy and Camm, 1998). This mineralisation style can be broadly defined as quartz–wolframite and tourmaline–quartz–cassiterite veins (Figure 6C), with subordinate Cu, As, and minor Bi, Ag, and Pb that is related to high-level, high-heat producing granites (Romer and Kroner, 2016). The lodes generally have exploitable strike lengths of a few hundred to a thousand metres (and exceptionally up to 6000 m e.g. the Great Flat lode) and dip lengths of 100–500 m (up to 2000 m e.g. Dolcoath Main lode). Lode widths range from a few tens of centimetres to 20 m, but are typically in the range 0.5–2 m. The lodes typically occupy steeply-dipping (more than 65°) faults or fractures, however, shallow-dipping (less than 50°) structures may also carry significant mineralisation. Lodes typically occur in swarms, for example, over 30 subparallel lodes occur in the Camborne-Redruth district (Figure 7) (Jackson et al., 1989). The Great Flat Lode (Figure 36) is a very large ore-bearing body, situated to the south of Carn Brea, and tilted at an angle of about 45°. Typically lodes are found perpendicular to the ground surface or at angles of about 60°. The low angle of the Great Flat lode meant that mines could be placed at the optimum locations to extract the tin or copper ore whilst minimising the amount of waste removed.

It is thought that 90–100 per cent of the total Sn, Cu, and As production of the region is derived from within 1500 m of a granite contact (Willis-Richards and Jackson, 1989). Lodes in which quartz ± chlorite ± fluorite form the principal gangue minerals, and which host variable combinations of cassiterite, chalcopyrite, arsenopyrite, sphalerite, galena and sporadic wolframite are the dominant type of lode mineralisation in the country rock surrounding the granites, but also occurs within the granite plutons XX. These lodes were the main source of Cu and As, as well as substantial Sn, occasionally present as stannite. Lodes with a primary tourmaline-quartz-cassiterite ± rutile ± arsenopyrite ± fluorite ± specular hematite assemblage have been a significant source of Sn production from granites and, to a lesser extent, from the metasedimentary rocks. Examples include the lower parts of Dolcoath Main Lode, the Great Flat Lode, and the 'numbered' lodes at the South Crofty Mine (Edmonds et al., 1985).

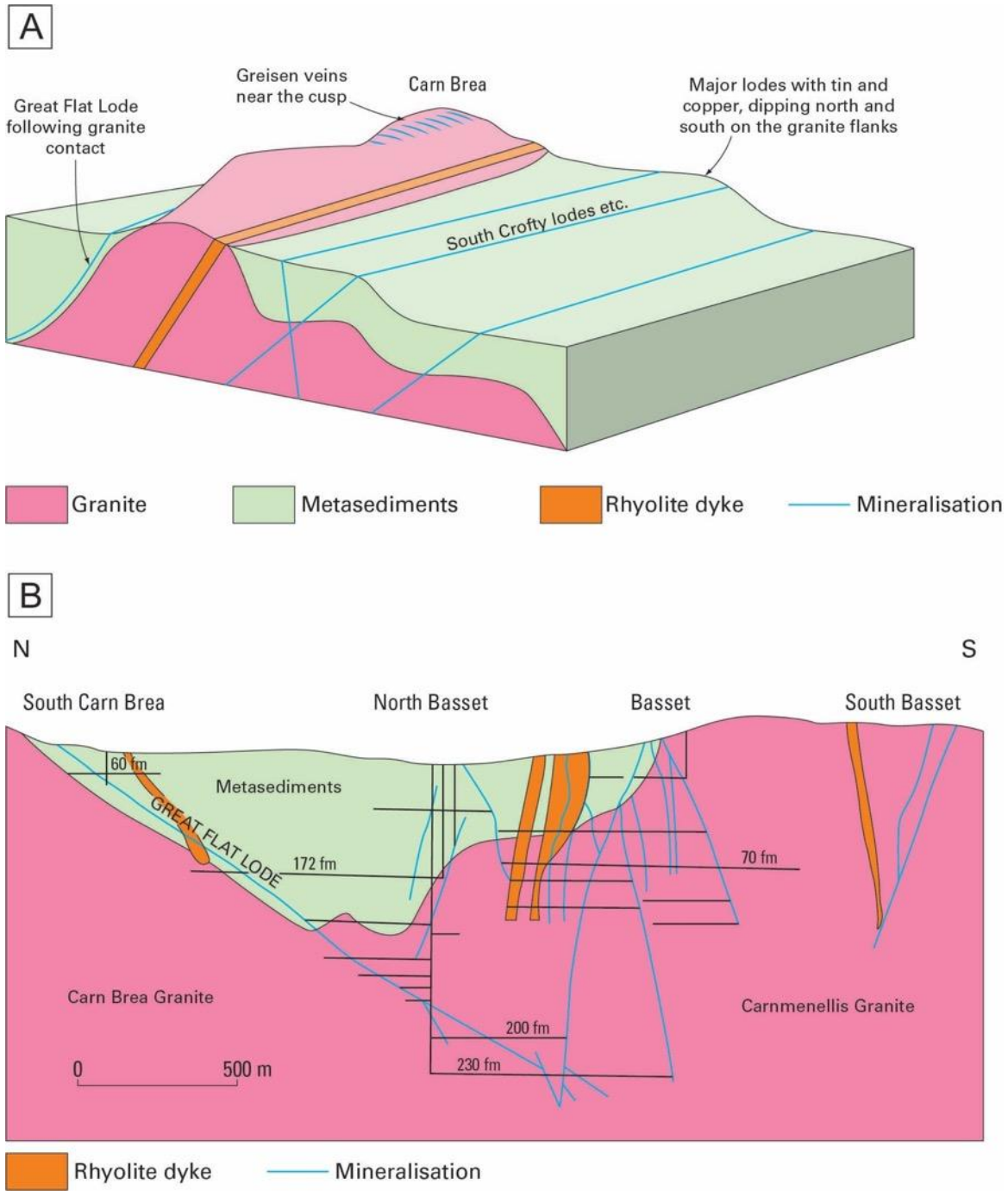

Figure 36: The Carn Brea area and its mineralisation. (A) Schematic diagram of the geology of the Carn Brea area, identifying the major lodes in the region. (B) Schematic cross-section through the Great Flat Lode, which is predominantly hosted in metasedimentary rocks between the Carn Brea granite to the north and the Carnmenellis granite to the south. Redrawn from webpages accessed July 2017 (no longer accessible online). Credit: Dr Nick Le Boutillier (BSc PhD MCSM EurGeol CGeol FGS).

In some areas as the mines deepened, copper production from near surface quartz-chlorite-fluorite sulfide assemblages transitioned in to tin production from tourmaline-dominated assemblages. The change from a 'copper zone' to 'tin zone' typically occurs in the vicinity of the granite–host rock boundary, but can be significantly higher or lower, and include a mixed zone containing both Cu and Sn assemblages (Figure 37).

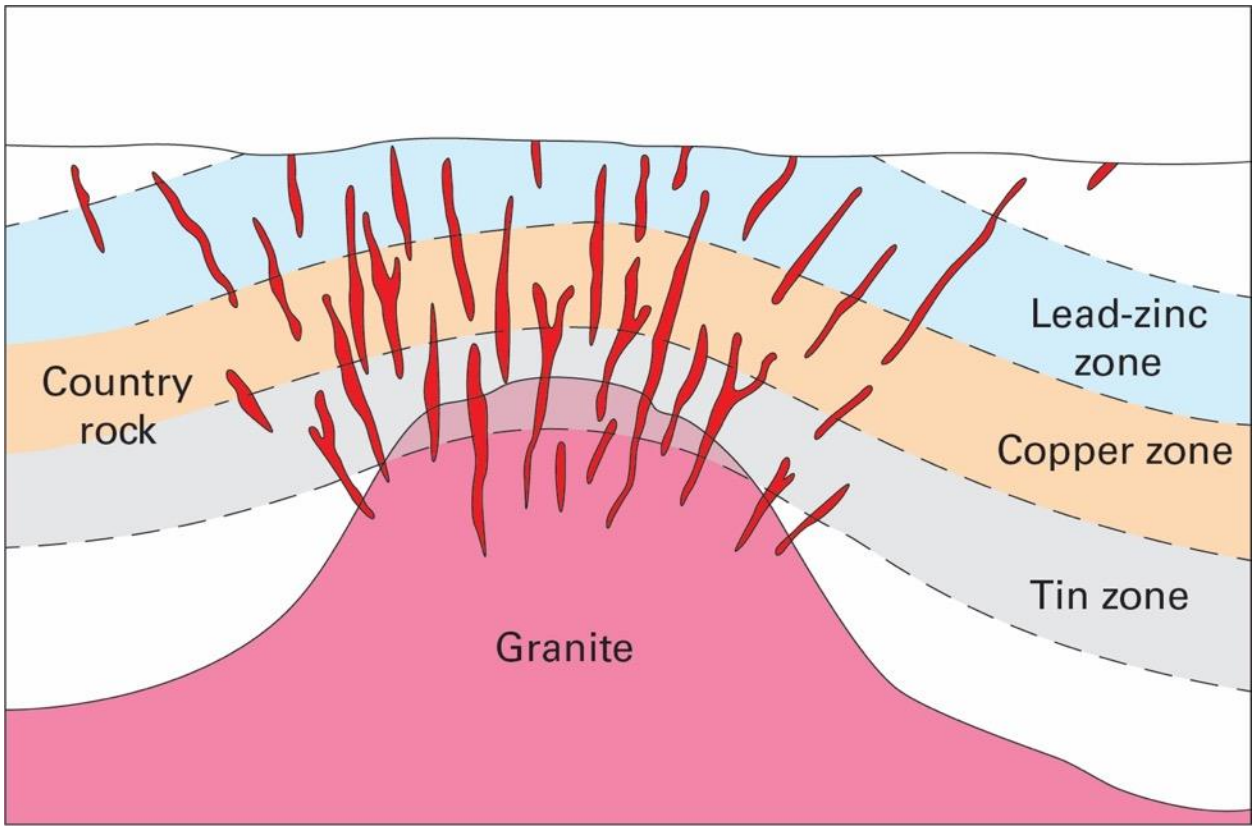

Figure 37: Schematic diagram illustrating the regional zonation of metals in vein deposits in south-west England. Redrawn from Sinclair (1995). Copy of the version available at [http://publications.gc.ca/collections/collection_2016/rncan-nrcan/M40-49-8-23-eng.pdf].

In addition to the Sn and Cu that dominated metal production in the region, cobalt was produced from Wheal Sparnon, located in Redruth town. This is one of few known mines that solely produced cobalt, with intermittent production between 1808–1827 (Jenkin, 1979). Little information is available on the deposit, however, cobalt was hosted in a range of mineral phases, including cobaltite, erythrite, skutterudite and safflorite (Tindle, 2008), with mineralisation extending to a depth of >120 m (NAMHO, 2013).

The Camborne-Redruth district was the most productive in the region, with hundreds of mines being developed from the mid-19th Century onwards. It also includes some mines with the longest life span in the region. In the Carn Brea area, some of the larger mines represent an amalgamation of hundreds of once independent workings. These larger mines were often also consolidated, for example Dolcoath and East Pool were later merged (in 1936) with South Crofty to form the South Crofty Mine. Figure 38 shows a grade–tonnage diagram to illustrate the size and grade of the major mines of south-west England, relative to tin-tungsten deposits globally.

In Cornwall between 1852–1914 more than 210 000 tonnes of contained copper metal was produced, and between 1848–1920 about 800 000 tonnes of tin ore was mined (Burt et al., 2014). Many mines closed in the early 20th Century and with declining tin prices the deposits became increasingly uneconomic, with the last mine in the region, the South Crofty Mine, ceasing operation in 1998.

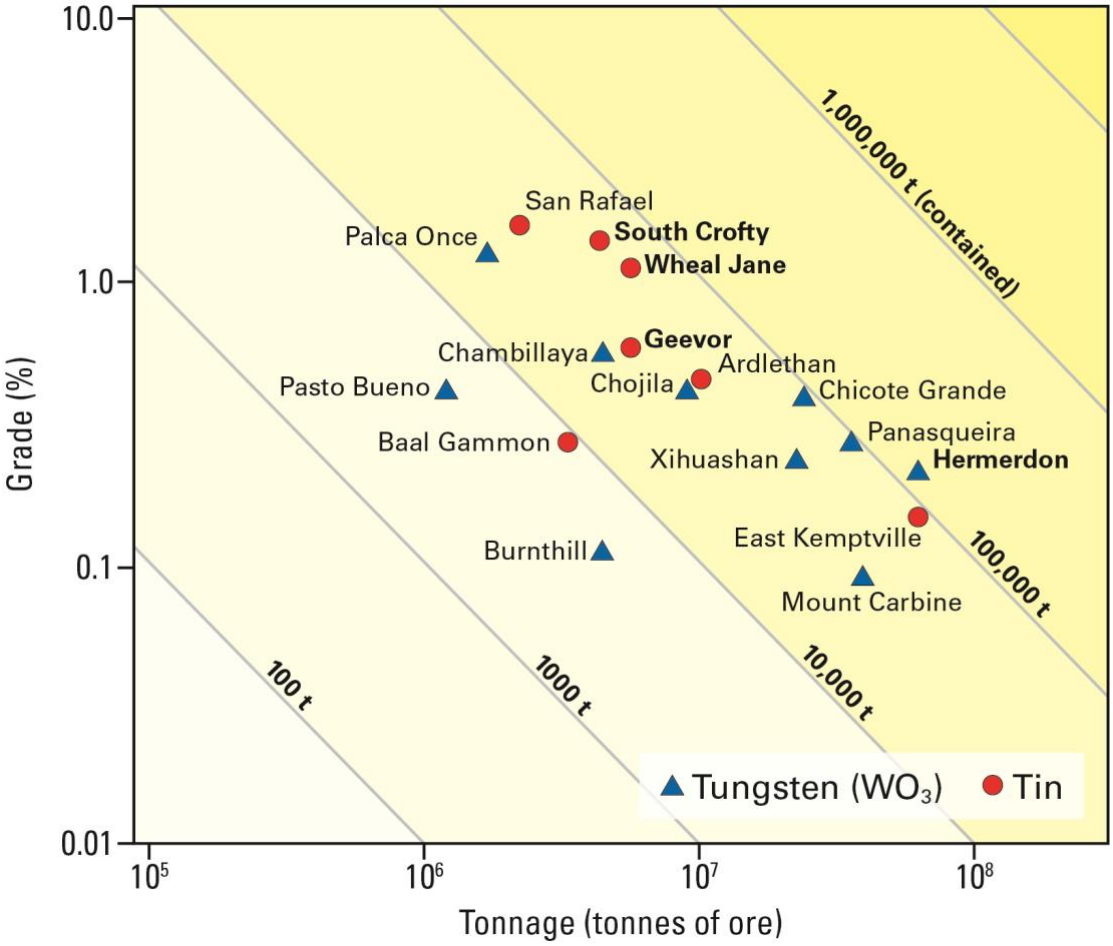

Figure 38: Grade versus tonnage diagram for vein-stockwork tin-tungsten deposits from south-west England and globally. Modified from Sinclair (1995). Copy of the version available at [http://publications.gc.ca/collections/collection_2016/rncan-nrcan/M40-49-8-23-eng.pdf].

5.1.2 Triassic 'cross-course' mineralisation

In the area to the NW of the Carnmenellis granite there are significant NNW-trending structures that cross-cut the granite-related mineralisation (Figure 22, Figure 39). Their structural characteristics are described in Section 3.3.2.2. These structures are variably mineralised (barren, non-metalliferous veins are commonly associated with the Mid-Triassic mineralising event), which means they have produced less total metal than the granite-related, main-stage mineralisation. They have been primarily exploited for lead, zinc, silver, fluorite and barite. In the Camborne-Redruth area these structures are vertical- to sub-vertical (Figure 22) and displace the 'main-stage' mineralisation by up to 100 m (Dines, 1956). There are two types of cross-course structure in the area: i) fracture zone cross-courses; and ii) extensional cross-courses. The 100 m wide Great Cross-course

represents a fracture zone cross-course that comprises networks of intense micro fractures and quartz veins with variable amounts of argillic and haematitic alteration (Dominy et al., 1994). The extensional cross-courses are the most common type in this area, with veins ranging in width from a few centimetres to about 2 m. With the exception of a small amount of localised silicification and kaolinisation there is little wallrock alteration associated with these veins. These fissures, contain open-space, and are principally filled by quartz and chalcedony, with variable quantities of fluorite, pyrite, chlorite, siderite, calcite and haematite (Dominy et al., 1994) (Figure 40).

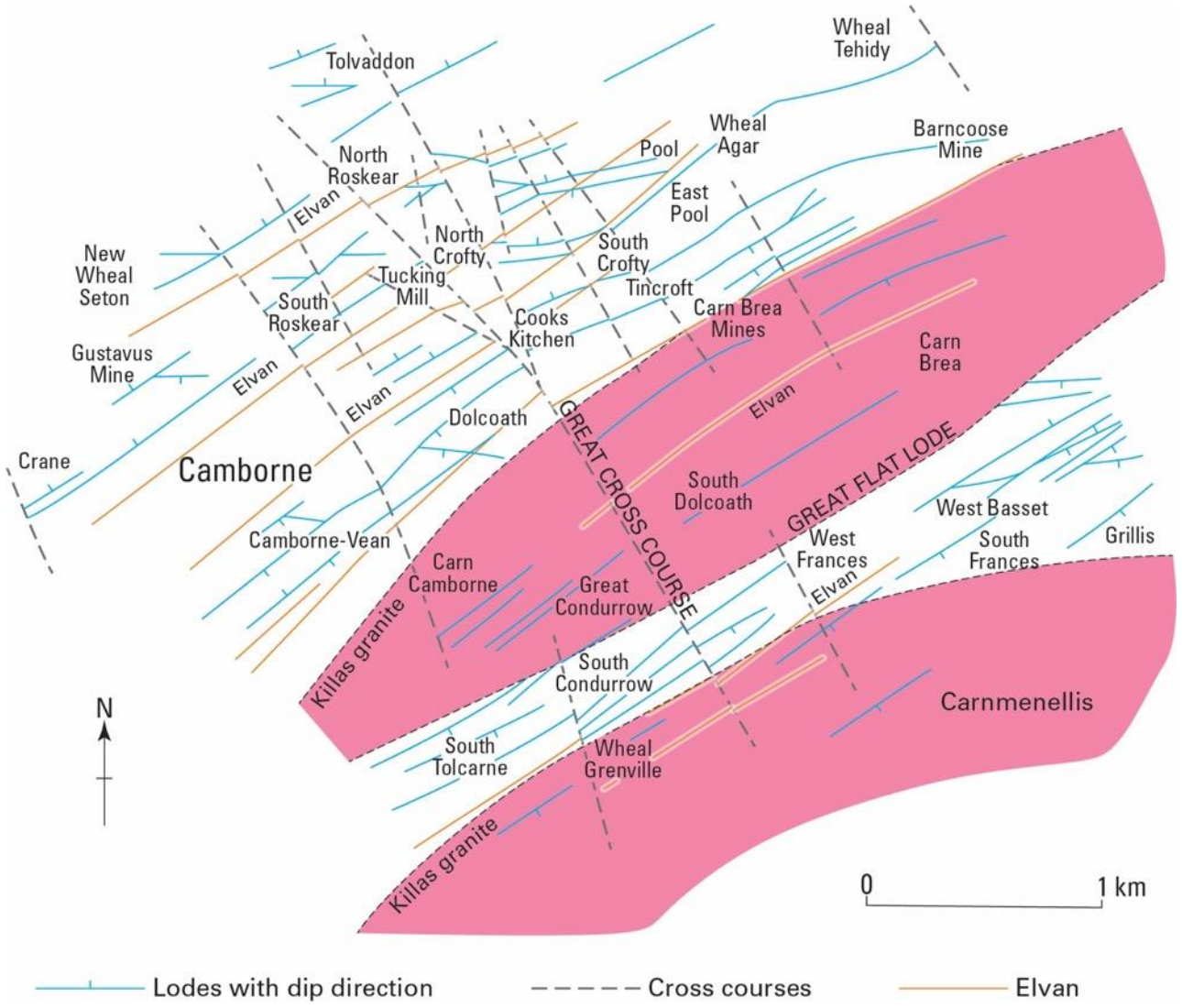

Figure 39: Map of the main lodes and cross-course veins in the area NW of the Carnmenellis granite. Redrawn from Dominy et al. (1994).

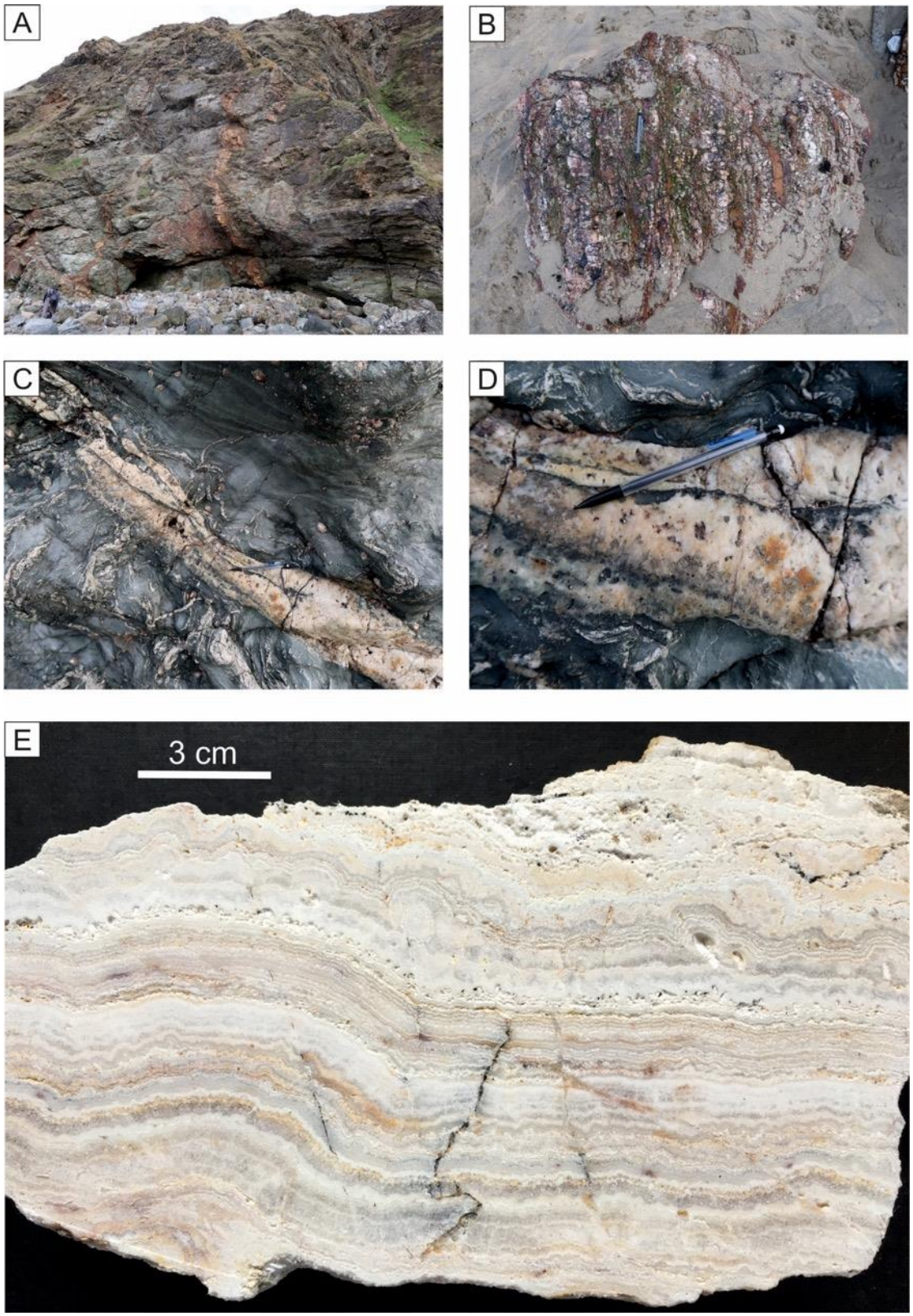

Figure 40: Typical cross-course mineralisation. A. Mineralisation in the cliff near Cotty's Point, Perranporth. B. Block of cross-course mineralisation on the beach at Cotty's Point. C. Mineralised cross-course vein in the metasedimentary rocks at St Agnes. D. Detail of the vein shown in C, which contains abundant pyrite. E. A cut vein sample, from Cotty's Point, primarily composed of multiple layers of quartz and chalcedony. British Geological Survey © UKRI.

5.2 Controls on mineralisation

In the Camborne-Redruth area over 35 sub-parallel veins, or lodes, are present (Dines, 1956). Both single in-filled fractures and composite systems are present in the area, with the latter being more common (Dominy and Camm, 1998). Lodes are typically orientated E–W and the strong preferred orientation of the lode vein systems is a clear indication that the host fractures were produced within a regional confining stress field. The weakest principal stress appears to be oriented normal to the axis of each portion of the batholith, and the maximum principal stress oriented between the vertical and the horizontal, in a plane parallel to the axial trace of the batholith (Jackson et al., 1989). Fracturing is thought to result from hydraulic stresses related to individual plutons (Moore, 1975). Moore (1975) suggested that the magmatic fluids exited the granite via pre-existing faults, and enlarged primary igneous joints and extensional fractures and faults created by the emplacement of the intrusion. Once developed, the fracture systems acted as high permeability corridors exerting a profound control on the movement of fluids around and through the batholith (Jackson et al., 1989). Fluids were drawn into active fault zones during the dilation phase prior to faulting and were transmitted along the faults after the seismic event (Sibson et al., 1975). Controls on ore localisation are complex and related to the many stages of structural reactivation that are present within a vein. A number of variable factors, including host-rock fracture geometry, lithology and physiochemical conditions of the wall rocks and fluids exerted control on the formation of mineralisation (Dominy and Camm, 1998).

5.3 Potential for deep metal enrichment

The deepest mine in south-west England is the Dolcoath mine, located in the area north of Carn Brea (Figure 7), where mine workings reached a depth of approximately 1000 m. Zonation of the mineralisation in the mine (copper in the upper zone and tin in the deeper zone) resulted in initial production of copper with subsequent production of tin. This zoning is attributed to pressure-temperature regimes along the granite metasediment contact (Dominy and Camm, 1998), and is supported by fluid inclusion data which demonstrate that the deeper tin zone is related to generally higher temperature fluids (Scrivener et al., 1986). The Dolcoath Main Lode was the largest tin-bearing structure in the region at 12 m wide (Dines, 1956). The mine produced some 2.5–3 million tonnes of ore, at a grade of about 1.6 per cent Sn (40,000 tonnes Sn metal) (Dominy and Camm, 1998). Between 800–900 m the lode consists of tourmaline-cassiterite veins. These comprise cassiterite, hydrothermal schorl-buergerite tourmaline (LeBoutillier et al., 2002 and reference therein), fluorspar and quartz, and quartz tourmaline breccia, which is crosscut by veins of clear quartz and fluorspar. At greater depths the schorl-buergerite tourmaline is replaced by a tourmalinised breccia. Vein paragenesis comprises: i. quartz + cassiterite + tourmaline; ii. multiple generations of brecciation with influxes of cassiterite and tourmaline; and iii. cementation by quartz with chalcopyrite (Dines, 1956). The wall rock for 1.5 m on either side of the lode fissures is brecciated, with localised areas being completely chloritised or tourmalinised and impregnated with cassiterite (Dines, 1956). In the deepest part of the mine tourmaline lodes varied in width from 5–30 m (Dominy and Camm, 1998).

The deepest drilling in Cornwall was undertaken during the HDR research programme. Three holes were drilled at the Rosemanowes Quarry in the Carnmenellis granite. The deepest hole reached 2610 m and a review of the single, partial, log (only one borehole has an available log, BH RH15 available digitally from the BGS, see Appendix 2 for further details) was undertaken as part of this project. Three mentions of sulfide are made in the log between 2213 and 2610 m (core samples are available for review, Figure 3E,F), and these are described as being associated with vein structures. However, no further details on the ‘sulphide mineralisation’ are described in the log. The CHPM concept does not necessarily require an ore body in the traditional sense. Any

metal enriched geological formation or reservoir of metals is a potential target for leaching. Accordingly, the following section provides a general overview of the distribution of metals in the Cornish granites.

5.4 The batholith as a metal reservoir

5.4.1 Granite geochemistry

The most recent geochemical analyses of the granites in south-west England has been undertaken by Simons et al. (2017; 2016), and the resulting new categorisation into five groups (types G1 to G5), based on their mineralogy, is described in Section 3.1.1.1. Simons et al. (2016) present data on the major elements (SiO_2, Al_2O_3, TiO_2, Fe_2O_3, MnO, MgO, CaO, Na_2O, K_2O, P_2O_5), trace elements (Ba, Pb, Rb, Sr, Nb, Th, U, Zr), and the rare earth elements (REE). Simons et al. (2017) includes new geochemical data on the fractionation of Li, Be, Ga, Nb, Ta, In, Sn, Sb, W and Bi in the G1–G5 granites of the Cornubian Batholith (Simons et al., 2017). The Cornubian granite has previously been identified as bismuth enriched, with Bi concentrations in south-west England granites two orders of magnitude higher than world average estimates for granites. The average concentration of Bi in south-west England granites ranges from 1–2ppm, whilst the global mean concentration of Bi in granites is about 0.05ppm (Ball et al., 1982). Regionally, there is a strong enrichment in Li in all the granites, whereas the G2 and G5 granites are enriched in W. Gallium, In and Sb plot towards expected UCC abundances. Beryllium, Nb, Ta, Sn and Bi are slightly enriched in the least evolved G1 and G3 granites, typically increasing for the G2, G4 and G5 granites. Average values for the peri-Gondwanan Devonian Gramscatho Basin (GB) plot around average UCC abundances (Simons et al., 2017). Examination of trace trace element distribution across the granites, highlights the abundance of many of the metals in the G5 (topaz) granites and the enrichment of Be in G2 (muscovite) granites. The enrichment of Li, Ga, Nb, Ta, Sn and W in the G5 (topaz) granites is explained by the high-F content of these granites.

5.4.2 Disseminated mineralisation

Granites that evolve towards or have high-F contents may contain disseminated magmatic mineralisation, depending on depth of intrusion, with limited partitioning of metals such as Sn and W into fluids exsolved from the melt (Pollard et al., 1987; Simons et al., 2017). With increased fractionation, the distribution of less compatible elements such as Tb and Nb is controlled by accessory phases such as rutile and columbite, which can occur as common magmatic phases, disseminated throughout a granite body with high levels of fractionation (Simons et al., 2017). Disseminated Nb and Ta phases have been found in the G4 (tourmaline) and G5 (topaz) granites (Simons et al., 2017). The G5 (topaz) granites of the batholith evolve towards very low-grade disseminated Sn–Ta–Nb–(W) magmatic mineralisation, which to date, has not been exploited (Simons et al., 2017).

5.4.3 Silicate-hosted metals

Fractionation, dominated by biotite and feldspars, increases Be, Nb, Ta, In, Sn, W and Bi in the G1 (two-mica) and G2 (muscovite) granites. Lithium is dominantly hosted by trioctahedral micas (i.e. biotite, lepidolite and zinnwaldite) in all the granites of the Cornubian Batholith. Gallium is fairly evenly distributed between all major silicates. Niobium and tantalum partition into muscovite in the G1–G2 granites; biotite, lepidolite and zinnwaldite micas into the G3 (biotite) granites, and accessory minerals into the G4 (tourmaline) and the G5 (topaz) granites. Fe-Ti oxides are an important host of these metals in all the south-west England granite types, and columbite-tantalite host Nb and Ta in the G5 (topaz) granites. Indium, Sn and W follow Nb and Ta, with the exception of the G4 (tourmaline) granites, in which they are incorporated into trioctahedral micas (Simons

et al., 2017). In the G2 (muscovite) granites the metals partition dominantly into muscovite, with limited disseminated magmatic mineralisation (Simons et al., 2017).

Although very limited data exists on deep (>1000 m) metal enrichment in the Cornubian orefield, the short review above indicates that some of the host rocks (i.e. the granite) to the hydrothermal mineralisation contain either disseminated metal-bearing phases, most common in the younger, more fractionated granites, or metals are incorporated into the structure of common silicate minerals, such as biotite and feldspar. Preliminary research to assess the potential for mobilising these metals from rock-forming minerals in the granites, in a CHPM-types system, is described in Section 5.5.

The Carnmenellis granite is a two-mica granite that predominantly comprises quartz, orthoclase feldspar, biotite (5–10 modal %), muscovite (up to 6 modal %) and about 1 modal per cent tourmaline. Accessory minerals typically include zircon, monazite, xenotime, andalusite, apatite, ilmenite, fluorite and topaz (Simons et al., 2017). However, disseminated sulfides are extremely rare, meaning the potential for extracting metals from sulfides contained in the Carnmenellis granite during circulation of an EGS fluid is limited. Another potential 'target' mineral that may host appreciable concentrations of minor and rare metals is mica. Micas are known to be important sinks for many minor metals, especially in granitic rocks. For example, Simons et al. (2017) showed that biotite in the Carnmenellis granite is enriched in Li (up to 3,450 ppm), Ga (105 ppm), and Nb (up to 182 ppm). Whereas, muscovite from the same study contains less lithium (up to 1,300 ppm), Ga (up to 170 ppm) and Nb (up to 73 ppm), but is more enriched in Sn (up to 60 ppm) and W (up to 69 ppm).

5.4.3.1 Preliminary leaching experiments

Based on the results of the study by Simons et al. (2017) and the abundance of mica (between 11 and 16 modal %) in the Carnmenellis granite, leaching experiments were conducted at the British Geological Survey to evaluate the potential for recovering metals such as Li, Ga, Nb and Sn from micas in the Carnmenellis granite. A large (approximately 8 kg) sample of fresh Carnmenellis granite was jaw crushed to a nominal grain size of 10 mm and then sieved to produce a sub-sample with a grain size of 500–250 µm. A rough mixed mica (biotite and muscovite) concentrate was extracted from an approximately 750 g sample of the 500–250 µm sieved material using an automated panning machine. After drying overnight at 40°C about 9 g of mica concentrate was loaded into a titanium reaction vessel with 350 ml of 0.1 M acetic acid. The vessel was pressurised to 200 bar with N2 and held at a constant temperature of 200°C for approximately six weeks. After six weeks the fluid in the vessel was sampled and analysed by ICP-MS at the BGS for a range of major and trace elements, including lithium.

ICP-MS results (Table 2) show that acetic acid at a concentration of 0.1 M is not particularly effective for leaching metals from mica at a temperature of 200°C and a pressure of 200 bar. With the exception of Si and Na the concentrations of the other major elements (i.e. Ca, Mg, and K) in the leachate do not exceed 50 ppm, whereas the concentrations of the minor and trace elements in the leachate are typically very low (i.e. <0.5 ppm). However, only one lixiviant was tested under fixed conditions (i.e. concentration, temperature and pressure), and it is possible that using alternative lixiviants (e.g. EDTA) and/or a different set of experimental conditions would liberate a higher concentration of metals.

Table 2: ICP-MS data (ppm) for a sample of Carnmenellis granite analysed during the CHPM2030 project.

Element	Ca	Na	K	Si	Cu	Li	Sn	Ga	Nb
Concentration in ppm	50.0	67.0	33.6	239	0.184	0.007	0.089	0.01	0.008

5.5 Applicable leaching agents based on WP2

A key aspect of the CHPM2030 concept is that metals can be transported in solution and extracted at the surface. The extraction process will be more efficient with higher dissolved metals concentrations, but this could result in problems with precipitation in the production boreholes and surface infrastructure. An entire work package (WP2) in the CHPM2030 project was devoted to investigating metal mobilisation using mild leaching agents (Kilpatrick et al., 2017). Three mineralised samples from Cornwall were used in the experimental work: i) from the South Caradon Mine, which is located on Bodmin Moor. This was one of the major copper producing mines in Cornwall. The sample was dominated by quartz, containing pyrite and arsenopyrite, and was selected to represent the 'main-stage' mineralisation; ii) a composite sample from Herodsfoot Pb-Ag-Zn-Cu mine, SE of Bodmin, composed of metasedimentary rock and quartz vein material. This sample, represents 'cross-course' mineralisation, and was dominated by quartz. Galena was the dominant sulfide mineral, with minor pyrite and sphalerite also present. Antimony is associated with the base metals, predominantly occurring in bournonite (Deady and Moore, 2015; Knight et al., 2016); and iii) from Cligga Head to represent tin-tungsten mineralisation (Moore and Jackson, 1977). This sample was dominated by quartz, but contained cassiterite, columbite and ferberite.

Seven experiments using acetic acid at concentrations of 0.1 M and of 0.001 M, at 70°C in a rotating mixer, and at 150°C in a pressurised batch vessel were conducted on the Cornish samples of mineralisation. For the sample of 'main-stage' mineralisation the spread of elements extracted during both experiments are broadly similar, with detectable concentrations of some elements considered 'critical', along with a broader range of elements that are associated with mineralisation in south-west England. It was concluded that acetic acid concentration and pH had very little influence on the concentration of elements liberated during the experiments. Three experiments were carried out using the sample of 'cross-course' mineralisation. Two used acetic acid at a concentration of 0.1 M, and the other an acid concentration of 0.001 M. Experiments employed the following varying conditions: 70 °C, atmospheric pressure, and 150 °C/200 bar. Acid concentration significantly affected the number of elements recovered in the leachate and their concentration, with the stronger acid performing best. Cobalt, gallium, molybdenum and antimony were detected in the leachates. Notably, concentrations of cobalt, gallium, lead and some REE were greater in the leachate produced by the 70°C experiment, than in the 150°C experiment, possibly indicating that formation of a precipitate occurred during the higher temperature experiment, which resulted in scavenging of some of these elements (Figure 41). All of the experiments on the sample of 'cross-course' mineralisation leached a greater number of elements than was achieved from the other sample types. Experiments on the tin-tungsten mineralised sample, resulted in notable differences in the concentrations of metals liberated from the sample depending on the acetic acid concentration used. The number of elements detected in the leachate were limited, but a greater number of elements at higher concentrations were detected in the 0.001 M experiment. However, with the exception of tungsten, no other critical metals were detectable in the leachates arising from either experiment on the tin-tungsten mineralisation. Copper, arsenic, tungsten and iron were relatively abundant in the leachates, reaching concentrations of about 2E-5 M, 2E-6 M, 8E-7 M, 7E-7 M and 1E-4 M, respectively,

in the experiment that used the more concentrated acid. Complete details of the experimental methods and results can be found in Kilpatrick et al. (2017).

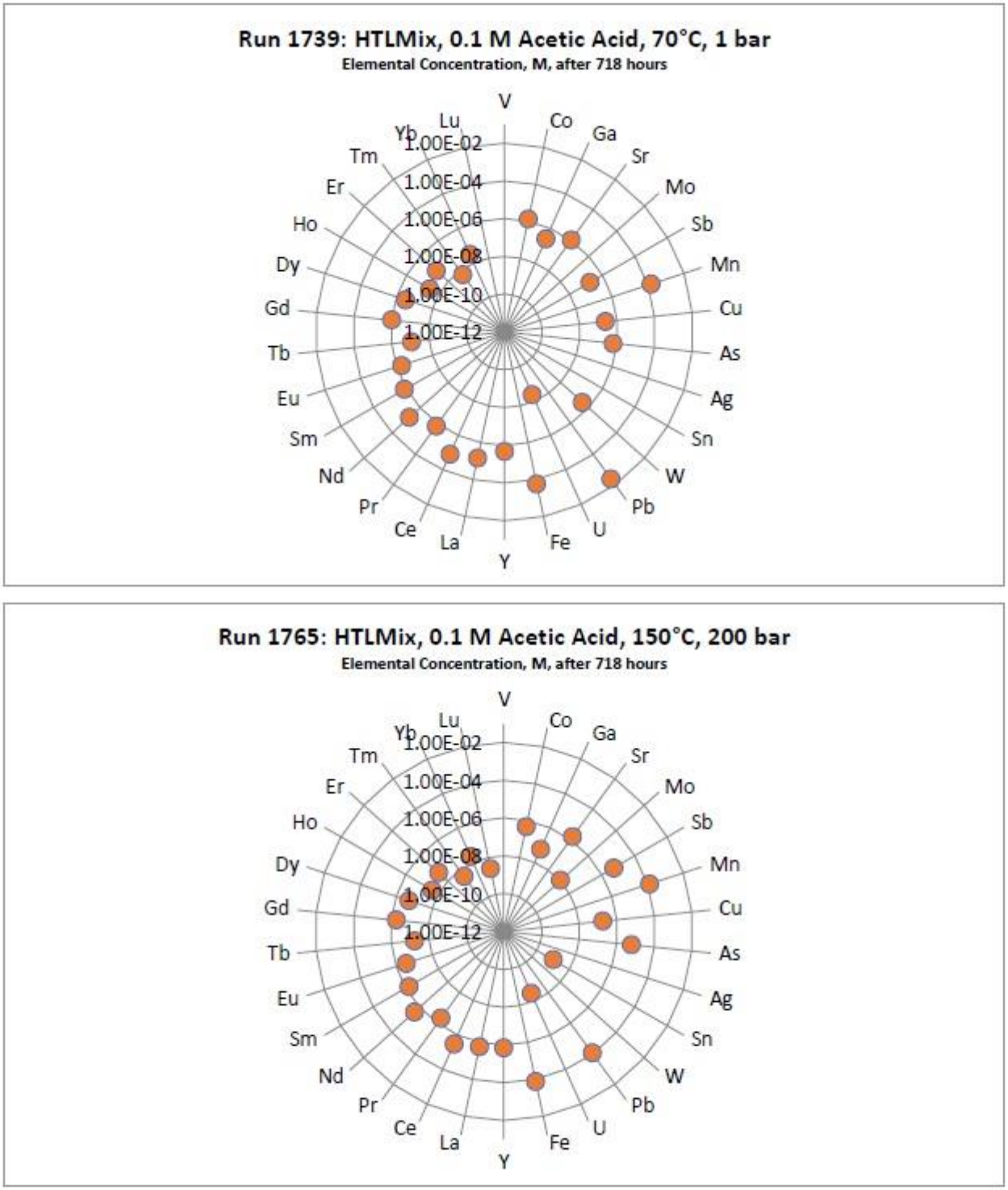

Figure 41: Concentration of selected metals in the leachates arising from experiments on a sample of 'cross-course' mineralisation from Cornwall (Kilpatrick et al., 2017). British Geological Survey © UKRI.

6 EGS potential

6.1 Geothermal characteristics of the area

6.1.1 Temperature gradient and heat flux

The mean heat flow of the Cornubian Batholith is 117 ± 8 mW m^{-2} (Beamish and Busby, 2016). A programme of relatively shallow (100–303 m, the majority 100 m deep) borehole measurements were undertaken across the Cornubian Batholith during the 1980s, as part of the HDR research programme. The heat production and heat flow data obtained are presented in Wheildon et al. (1981) and Thomas-Betts et al. (1989). The locations of the boreholes on the Cornubian Batholith are shown in Figure 42. Deeper heat flow values are also available from the South Crofty (650 m) and Geevor mines (403 m) (Downing and Gray, 1986; Tammemagi and Wheildon, 1974). This data is reviewed in Downing and Gray (1986) and Lee et al. (1987).

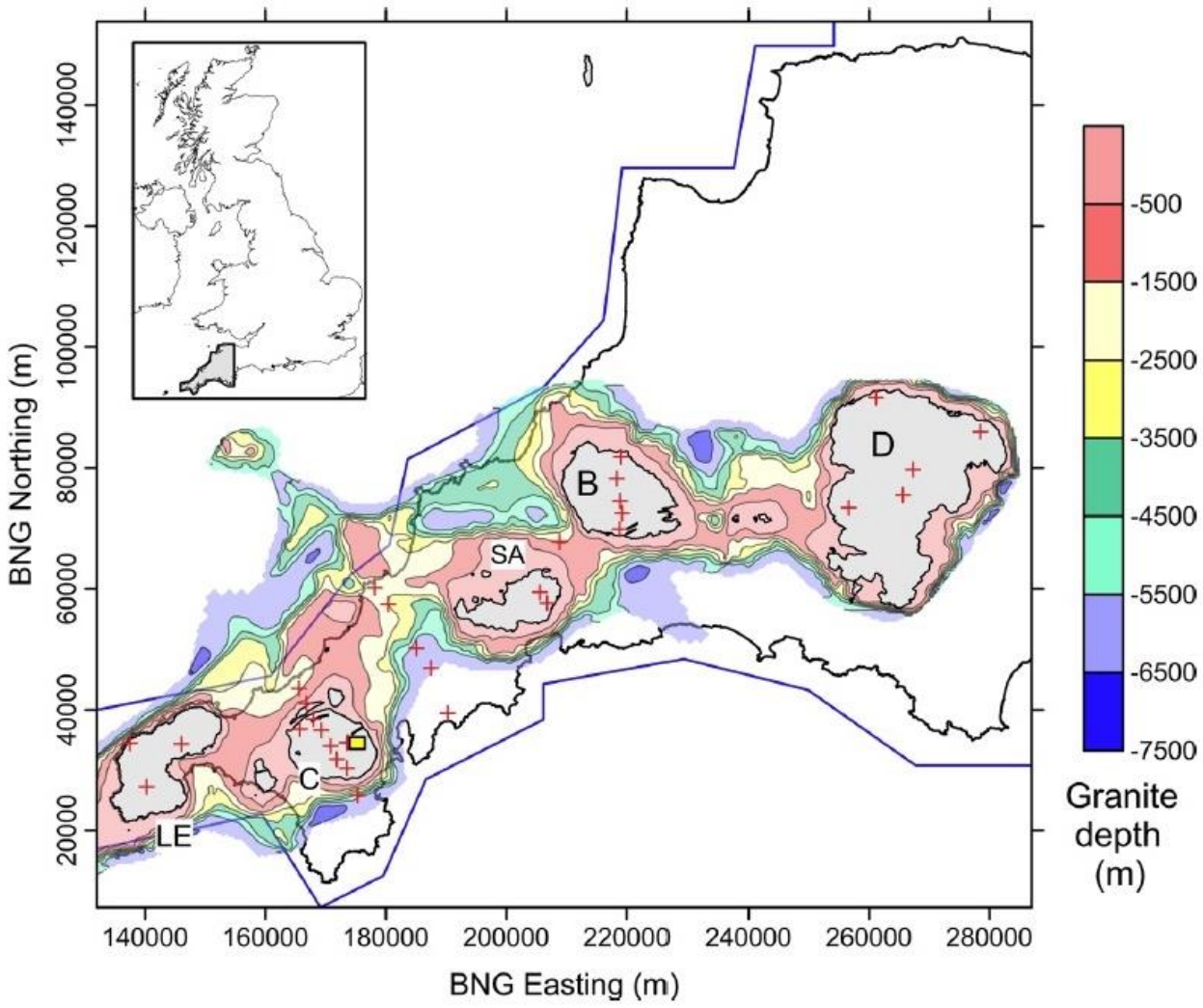

Figure 42: South-west England and geothermal borehole locations. Coloured contours show the depts. Below ground of a model of the batholith obtained from the 3D gravity model. Granite outrcrops are shown in grey with labels, LE (Land's End), C (Carnmenellis), SA (St Austell), B (Bodmin) and D (Dartmoor). Reproduced, unmodified from Beamish and Busby (2016), under Creative Commons Attribution 4.0 International License (http://creativecommons.org/ licenses/by/4.0/). © Beamish and Busby. 2016.

Beamish and Busby (2016) reassessed the published data on heat flow values and heat production from 34 boreholes, using the latest paleoclimate reconstruction, and provide revised estimates of heat at depth. They discard the data from the two mine sites as the temperature gradient is likely to have been affected by the extensive period of mining activity. The recalculated heat flows and borehole-derived heat production data have been used to estimate temperatures at 5 km depth for each of the granites. The temperatures at 5 km depth range from 185°C for the Dartmoor granite to 221°C for the St Austell granite. The temperature of the Carnmenellis granite at 5 km depth was estimated to be 200°C (Beamish and Busby, 2016) (Figure 43).

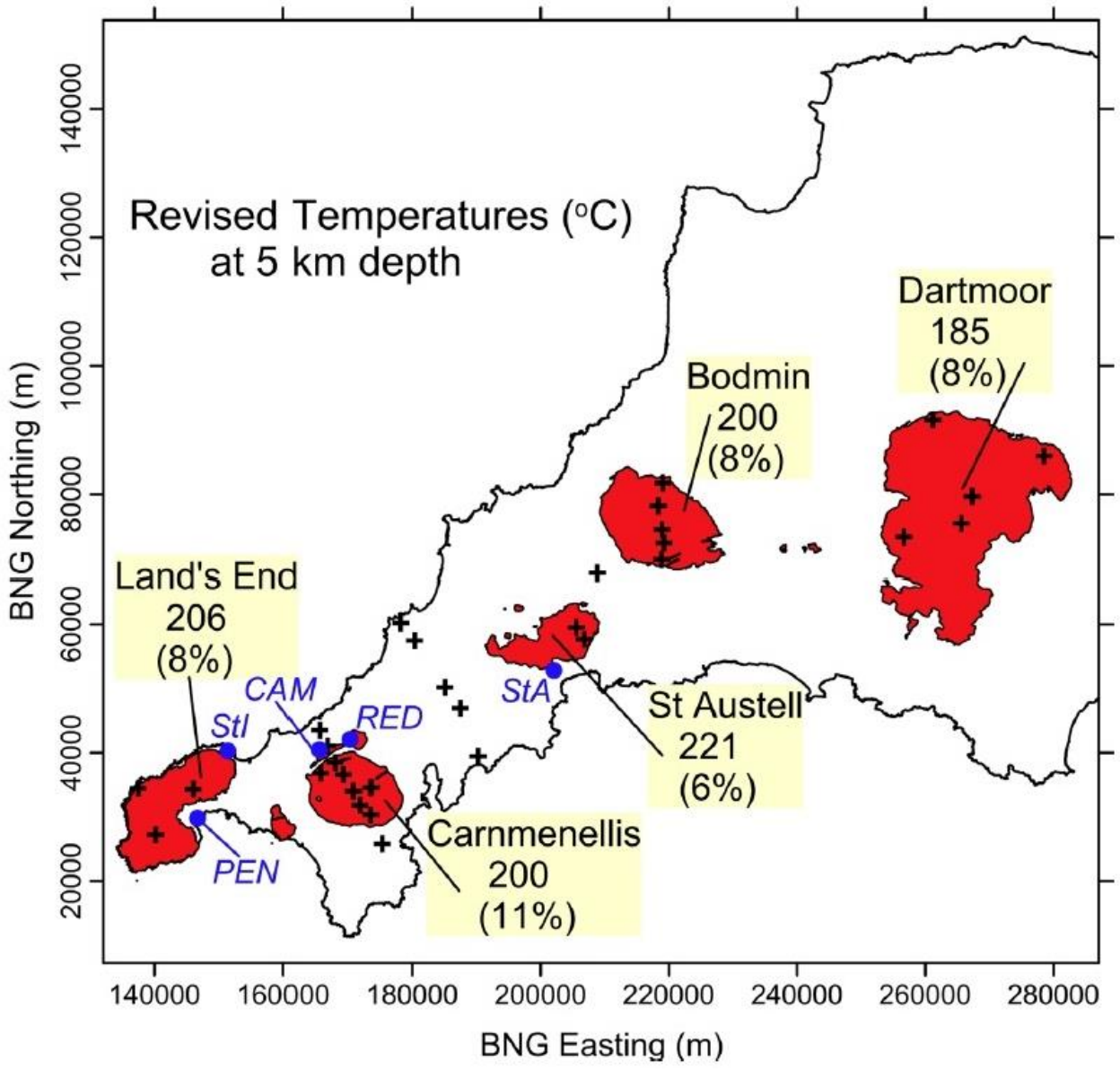

Figure 43: Revised granite-average tempetures (in °C) at a depth of 5 km and percentage increases (in brackets) over previously publicshed estimates. Reproduced, unmodified from Beamish and Busby (2016), under Creative Commons Attribution 4.0 International License (http://creativecommons.org/licenses/by/4.0/). © Beamish and Busby. 2016.

For validation purposes, the only deep temperature measurements that exist for the Cornubian Batholith are those from the HDR boreholes at the Rosemanowas quarry in the Carnmenellis granite. RH12 reached a depth of 2.1 km at which the rock temperature was 79°C. A subsequent drill hole (RH15) extended to 2.6 km, at which depth the rock temperature was 100°C (Barker et al., 2000). The revised heat flow estimates for the shallow holes at the Rosemanowas site are consistent with this, as the constant heat production with depth model, returns subsurface temperatures that are only slightly higher than the temperatures measured in the deep holes, of about 84°C and 102°C at 2.1 km and 2.6 km, respectively (Beamish and Busby, 2016). Beamish and Busby (2016) also consider the borehole heat production values in the context of the TellusSW radiometric data, which provides ground concentration estimates of the heat-producing radioelements. They use the relatively sparse borehole data as a control to correct the airborne estimates. The corrected airborne heat production estimates provide a heat production map, based on uniformly acquired data, in which it is possible to identify zones of high heat production at a detailed scale (Figure 44). Previous observations based on the borehole data alone suggested that the greatest areas of heat production within the granites was towards the granite/country rock contact. Using the heat production maps it is possible to define clear zones with the highest values (Figure 45). Whilst these zones have associations with the granite margins they also extend across the granite bodies (Beamish and Busby, 2016). The expected temperature of 200°C at 5 km depth in the Carnmenellis granite is too low to have a significant effect on the granite strength and brittle behaviour (Pine and Kwakwa, 1989).

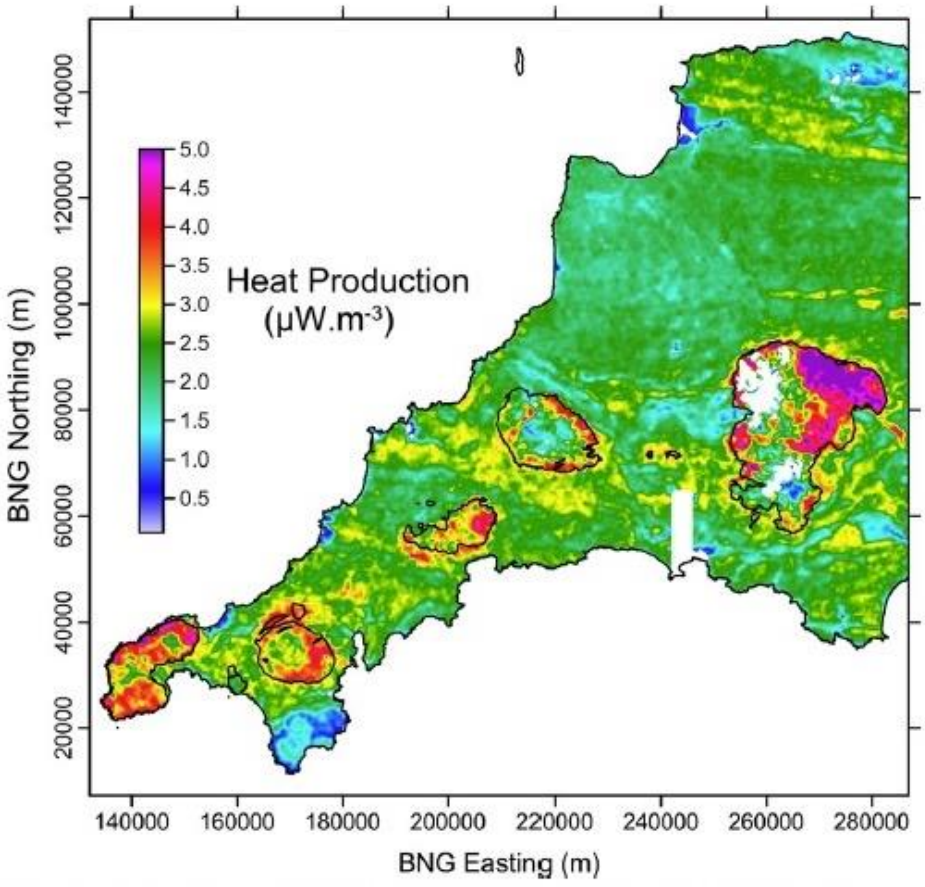

Figure 44: Revised heat production estimates for south-west England. Reproduced, unmodified from Beamish and Busby (2016), under Creative Commons Attribution 4.0 International License (http://creativecommons.org/ licenses/by/4.0/). © Beamish and Busby. 2016.

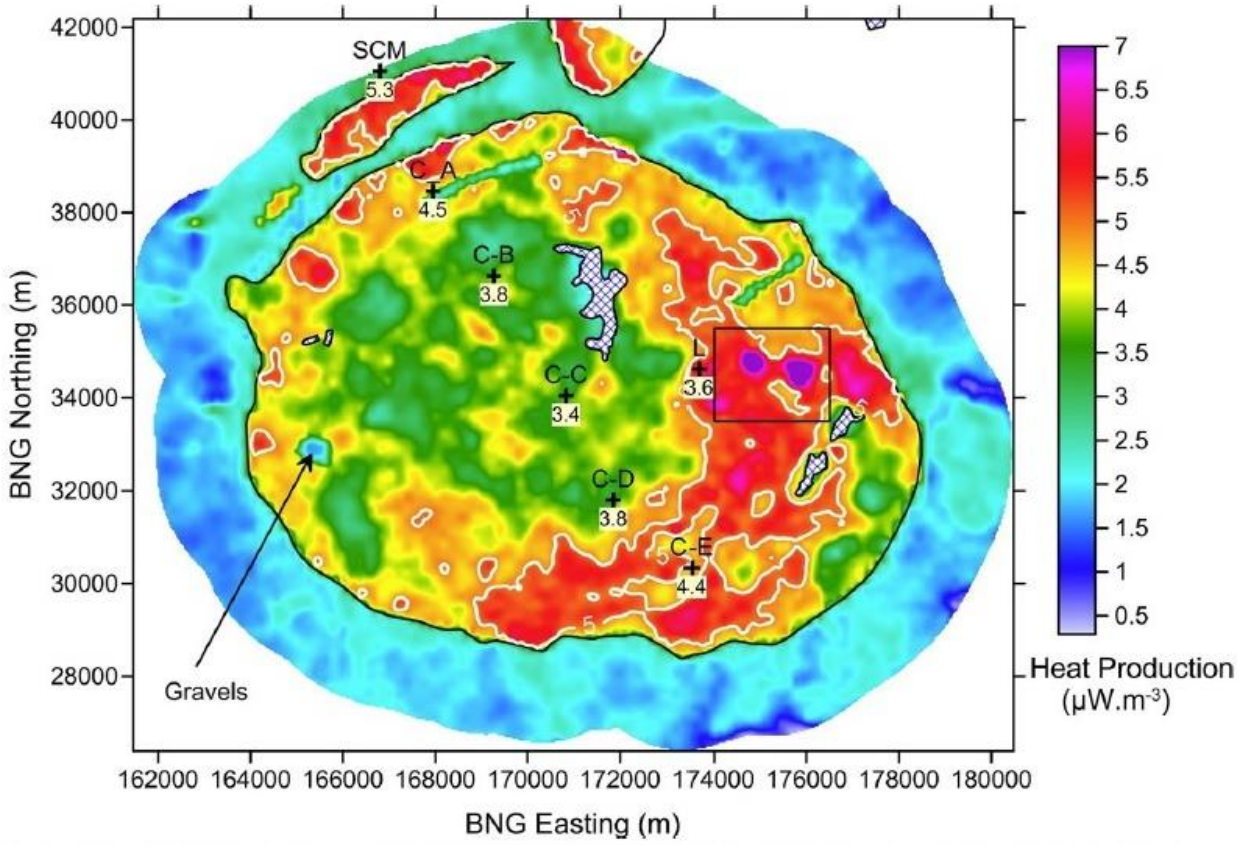

Figure 45: Area of the Carnmenellis granite outcrop, radially extended by 2 km. Continuous colour image of BH-correct heat production. Reproduced, unmodified from Beamish and Busby (2016), under Creative Commons Attribution 4.0 International License (http://creativecommons.org/ licenses/by/4.0/). © Beamish and Busby. 2016.

6.1.2 Stress field

The magnitude and orientation of the in-situ stresses exert the dominant control on the shape, extent and orientation of the growth of a HDR reservoir (Pine et al., 1983b). An extensive programme of both direct and indirect stress measurement was undertaken in the Carnmenellis granite during the HDR project. Hydraulic fracture or hydrofracture stress tests were conducted in borehole RH 12, at progressively deeper levels to a maximum depth of 2550 m, in the Carnmenellis granite at Rosemanowes quarry. The tests provides values for the minimum horizontal stress and estimates of the maximum horizontal stress, and its variation with depth. Stress anisotropy was very significant in the parts of the hole tested, with maximum and minimum horizontal stresses at a vertical depth of 2000 m of about 70 and 30 MPa, respectively. The overburden stress at this depth was estimated to be 52 MPa (Batchelor and Pine, 1986; Pine et al., 1983a). The results of the hydrofracture measurements gave the following trends with depth: maximum horizontal stress (MPa) = 15 + 27.5 d; minimum horizontal stress (MPa) = 6 + 11.8 d; and vertical stress (MPa) = 26 d. The maximum shear stress was found to increase rapidly with depth, and this stress condition was considered vital for strike slip shearing during hydraulic stimulation at Rosemanowes quarry. If the stress field at depth is compared with Mohr's envelope for the intact granite, it shows that that compressive failure of the borehole wall should not occur. In contrast, if 'effective' stress conditions apply (i.e. borehole pressure equals the pore fluid pressing the surrounding rock), then shear failure of the rock is predicted. Examination of the boreholes with dip-meter,

four-arm calliper and borehole televiewer did not identify any breakouts prior to the wells being exposed to the high hydraulic pressures (Batchelor and Pine, 1986).

Overcoring rock stress measurements were conducted at the South Crofty mine (about 10 km from the Rosemanowes test site), at a depth of 790 m. Two types of overcoring technique were used, but the average principal stress directions, based on the four best tests using the Commonwealth Scientific and Industrial Research Organisation of Australia (CSIRO) system are shown in Table 3. The direction of maximum principal stress was 130–320°. A significant anisotropy exists between the two horizontal principal stresses, and the conditions were mainly attributed to tectonics arising from the Alpine orogeny. The direction of maximum principal stress, of about 130°, and the stress magnitudes determined by overcoring measurements (Table 3) were close to those measured by the hydrofracture tests at the same depth (~770 m) (Batchelor and Pine, 1986; Pine et al., 1983a).

Table 3: Average principal stress directions based on the four best CSIRO overcoring tests undertaken in South Crofty mine. σ_1 = maximum principal stress; σ_3 = minimum principal stress (Pine et al., 1983b).

Stress	Magnitude (MPa)	Azimuth (°)	Dip (°)
σ_1	37.7	129.8	5.0
σ_2	18.5	−13.1	84.4
σ_3	11.3	40. 5	−3.2

However, Evans et al. (1992) urge caution regarding the direction of maximum horizontal stress reported in earlier publications arising from the HDR project (e.g. Pine and Batchelor, 1984). This is due to their reliance on over coring data from the South Crofty Mine (which is located well outside the main Carnmenellis pluton) as it was not possible to image the fractures that developed during the hydrofracture stress measurements in RH12 (Evans et al., 1992). Subsequent data collection, including imaging of induced fractures in RH15 (N156°E±10), hydraulic fracture measurements at the Carwynnen test site in the Carnmenellis granite (N147°E±7) (Haimson et al., 1989), and data arising from inversion of focal mechanism solutions of induced seismicity at the Rosemanowas site (143–180°) (Pine et al., 1990) suggest that N150°E±10° is a more appropriate orientation for the direction of maximum horizontal stress in the Carnmenellis pluton (Evans et al., 1992).

The differential strain analysis (DSA) technique can be used to derive strain orientation data from orientated core. However, during the HDR drilling programme it was not possible to obtain orientated core. Hence the available core could not be used to derive true orientation data. Despite this, the principal strain directions can be estimated if it is assumed that one of the principal strains is vertical. Granite cubes were cut from the cores taken from depths ranging from 1500–2400 m. Figure 46 shows the stresses based on the DSA measurements compared with the results from the hydrofracturing and over-coring tests. The stress measurements from the cubes at about 1500 m are similar to those from the hydraulic stress tests. However, at greater depths the results from the DSA did not agree with the overall trend. Some of the deeper cores obtained were heavily 'disked' and the data obtained from cubes containing disking would give excessive strain values parallel to the core axis and an underestimate of the horizontal stresses. This appears to be the case at depths below 1700 m, where the data from the DSA is not consistent with the results from the other techniques (Batchelor and Pine, 1986).

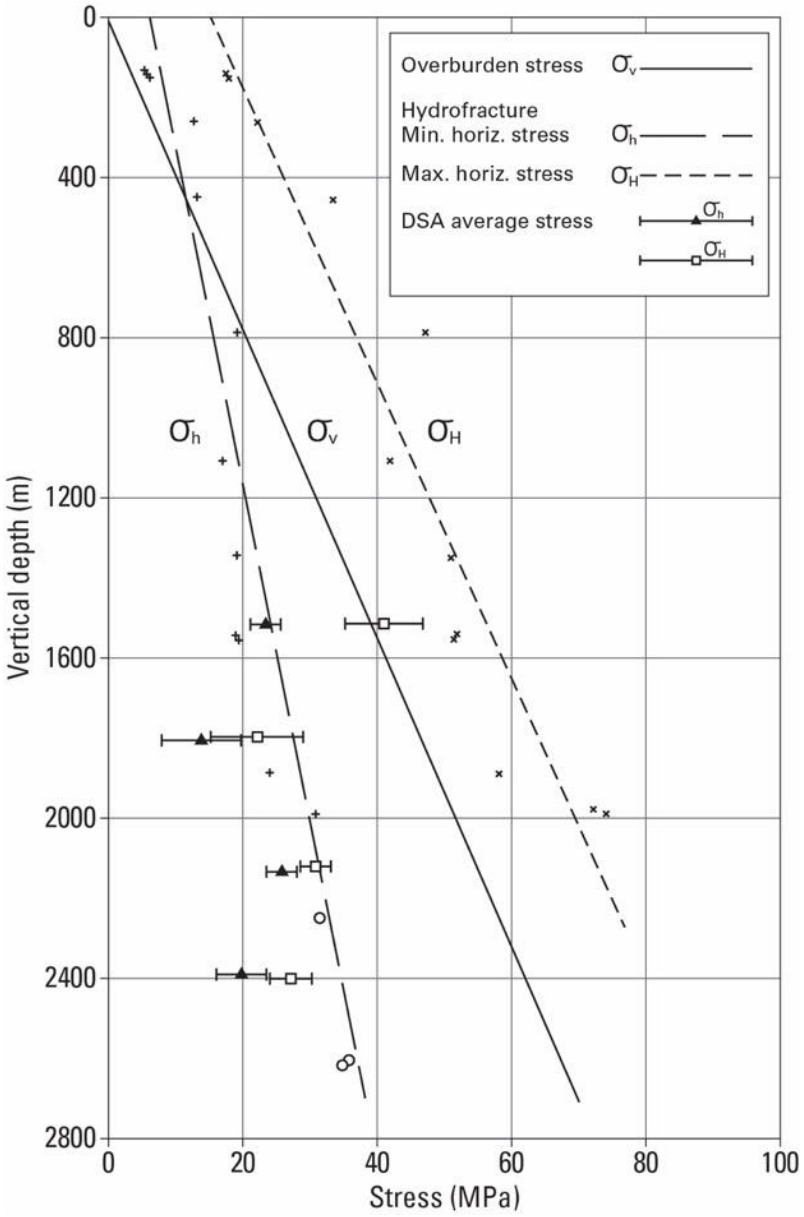

Figure 46: Depth vs. stress plot for the three principal stresses, showing data obtained from DSA, hydrofracturing and over-coring measurements. Redrawn from Batchelor and Pine (1986), Figure 4, ©International Society for Rock Mechanics.

The relationship between injection flow rate and injection pressure was studied during the hydraulic injection tests at the HDR site. During one test, involving repeated pressurisation of a single feature in a short packed off section of well, a significant increase in flow rate occurred above 8 MPa. The open hole lengths of the three HDR project holes were 357 m, 722 m and 575 m. Flow measurements and temperature logging over these intervals indicated that water entered or exited the well on joints that were within 30° of the direction of the maximum principal stress. However, not all joints at this orientation permit water to leave or enter the well. The threshold pressure of joint opening was determined by plotting pressure change as a function of the square root of the flow rate, and for RH12 this indicated a minimum effective stress of 7.0 MPa at 1800 m depth (Batchelor and Pine, 1986).

A major hydraulic stimulation operation was undertaken on HDR well RH15 to produce a fracture at a depth of 2370 m. This involved pumping 5500 m^3 of viscous fluid into the well over a period of 8 hours. Following the injection, the well was closed (shut in), and the pressure decay was observed over a 24 hour period (Figure 47). The well closure pressure (minimum pressure required to keep fractures open) was determined to be 30.25 MPa, after about 5 hours of closure. The hydrostatic pressure at 2370 m was 20.55 MPa, which means closure occurred at a well head pressure of 9.7 MPa (Batchelor and Pine, 1986).

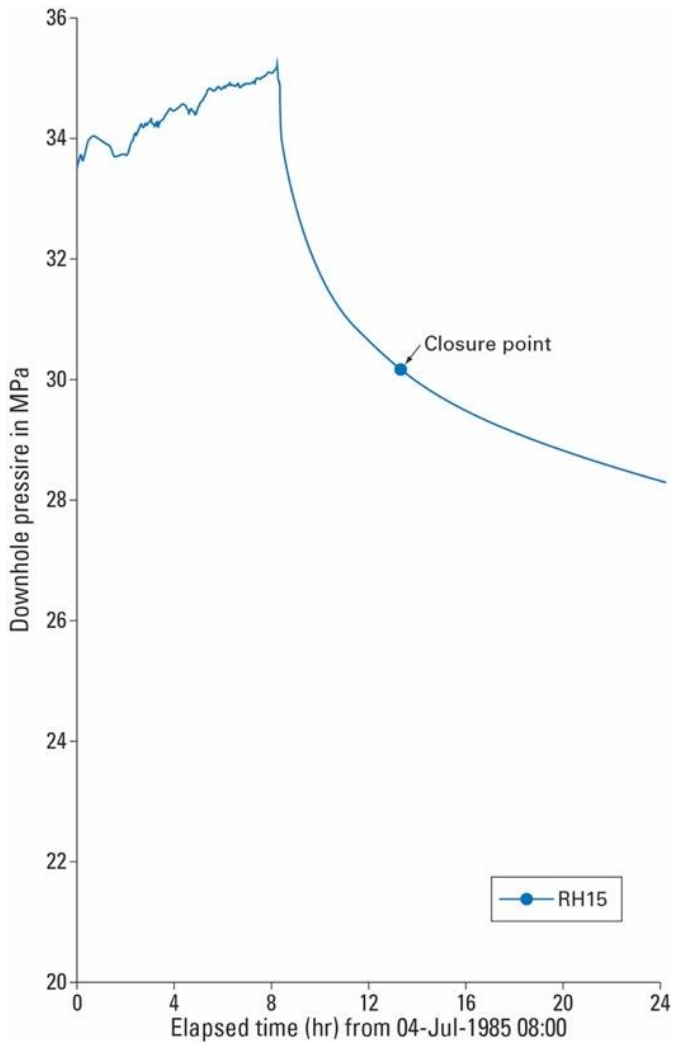

Figure 47: Downhole pressure for 24 hours covering the 8 hours of injection and the first 16 hours of well shut in. Redrawn from Batchelor and Pine (1986), Figure 7, ©International Society for Rock Mechanics.

A microseismic network was established to monitor the injection operations at the HDR site. It was active throughout the Phase 2A (studies at intermediate depths, 2500 m, focussed on assessing the feasibility of creating a subsurface heat exchanger; MacDonald et al. 1992) injections and recorded about 30 000 events. 5260 events were located and provided information on the reservoir geometry. Figure 48 shows that most of the events occurred beneath the wells. This was attributed to the shearing along natural joints, in response to the highly anisotropic stress field (Mines, 1988).

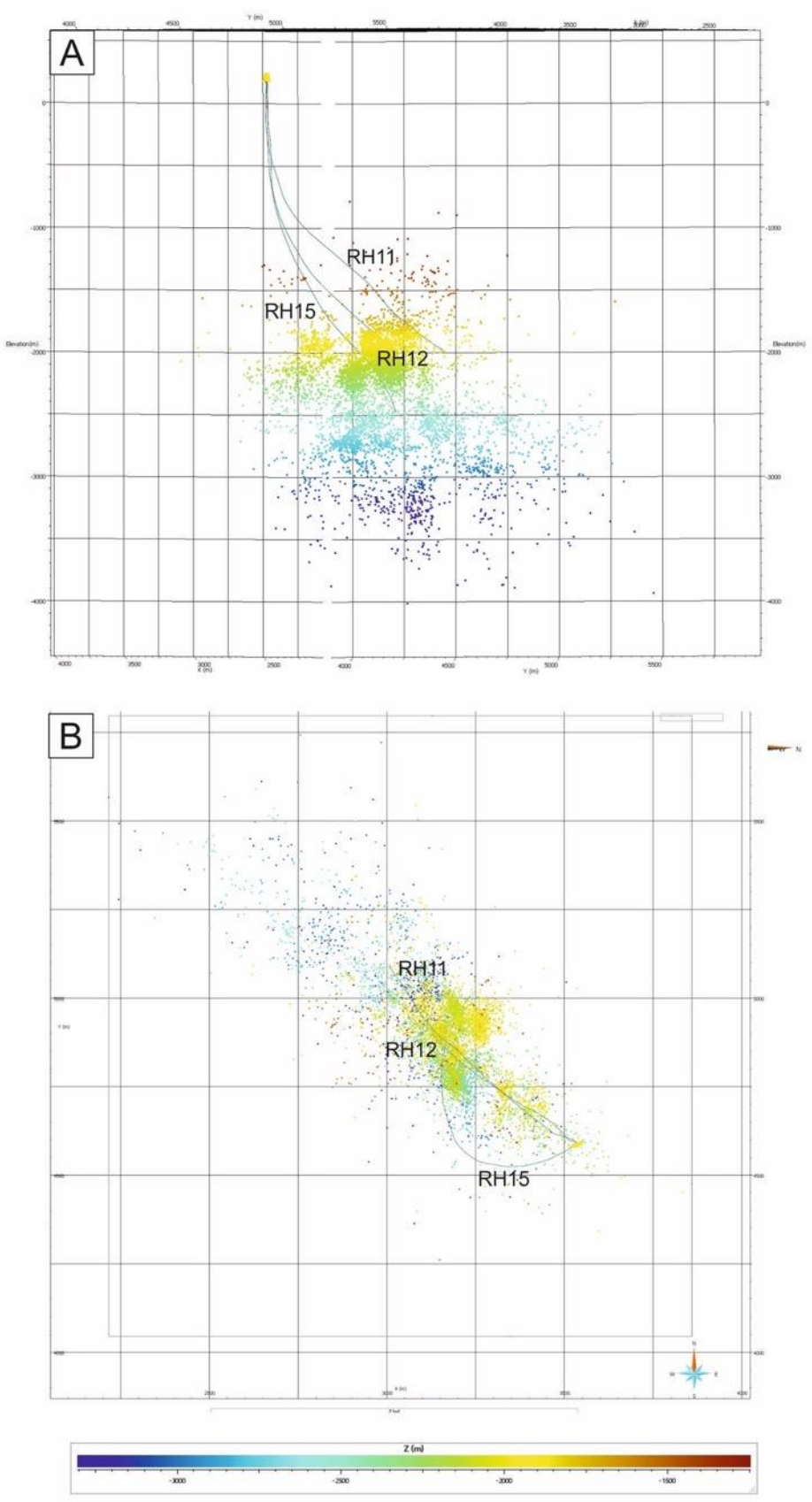

Figure 48: Microseismic event locations and well trajectories. A. View in the plane. B. Plan view. British Geological Survey © UKRI.

P-wave first motion data collected by seismic networks can be used to determine fault plane solutions (a way of showing the fault and the direction of slip on it from a seismic event). P-wave first motions, based on a 'double couple' mechanism will define two orthogonal planes. The monitoring network at the HDR site had insufficient sensors to determine faults plane solutions for individual seismic events. However, the complete data set collected was used to generate a composite solution to determine the predominant fault mechanism. The seismic data collected during the major, viscous hydraulic stimulation experiment in HDR well RH15 (described above) is presented in Baria et al. (1985). The fault plane solution based on this data indicates that either left or right lateral strike slip motion on close to vertical faults planes has occurred. The two planes defined have strike orientations of 353° and 263°. The plane at 353° has an orientation similar to one of the major joint sets observed at 2000 m depth using a borehole televiewer. It was concluded that 353° is the orientation of the majority of the 'mobile joints'. Fault plane solutions based on data from other injection experiments are consistent with these findings. The fault plane solutions indicate that the maximum principal stress direction is located to the west of 353°, in the dilatational quadrant. More than 80 per cent of the events measured indicate a strike slip motion and if the friction between joint surfaces is assumed to be at an angle of 35–45° it results in a stress direction of 320–330°. This agrees with the directions measured by the overcoming experiments described above (Batchelor and Pine, 1986).

When plotted the microseismic events form a cloud with a general strike of 135–315°. The combination of the orientations of the major joint sets and the stress regime shown in Figure 49, limited the growth of the hydraulically stimulated reservoir to a direction that predominantly lies between the maximum principal stress direction and the joint set that strikes at about 330°. However, detailed examination of the reservoirs internal structure indicates groups of planes strike at about 350°, but have an overall pattern more comparable to the stress direction (Batchelor and Pine, 1986).

Rock stress measurements have also been made at the Carwynnen experimental site, close to the NW margin of the Carnmenellis granite. This location has vertical boreholes to a depth of 700 m (Tunbridge et al., 1989). Two series of hydraulic fracturing stress measurements were made here in the late 1980s, one at a shallow level (74–134 m) and the other at a deeper level (602–685 m). They calculated the principal horizontal stresses, which were indicative of a compressive stress regime with a NW maximum horizontal stress direction, and a ratio greater than 2:1 between the horizontal stresses. The relative principal stress magnitudes in the deeper level zone would favour strike-slip faulting. The stress directions and relative stress magnitudes obtained from the Carwynnen experiment were consistent with the existing stress measurements for the Carnmenellis granite (Rosemanowes site and South Crofty Mine). They conclude that the stress measurements obtained from the Carwynnen site represent the regional stress regime and the conditions in the upper kilometre of the Carnmenellis granite. Additionally, agreement between the independent measurements (see Figure 7 in Haimson et al., 1989), are indicative of the reliability of the data and the uniformity of the stress field in the Carnmenellis granite (Haimson et al., 1989).

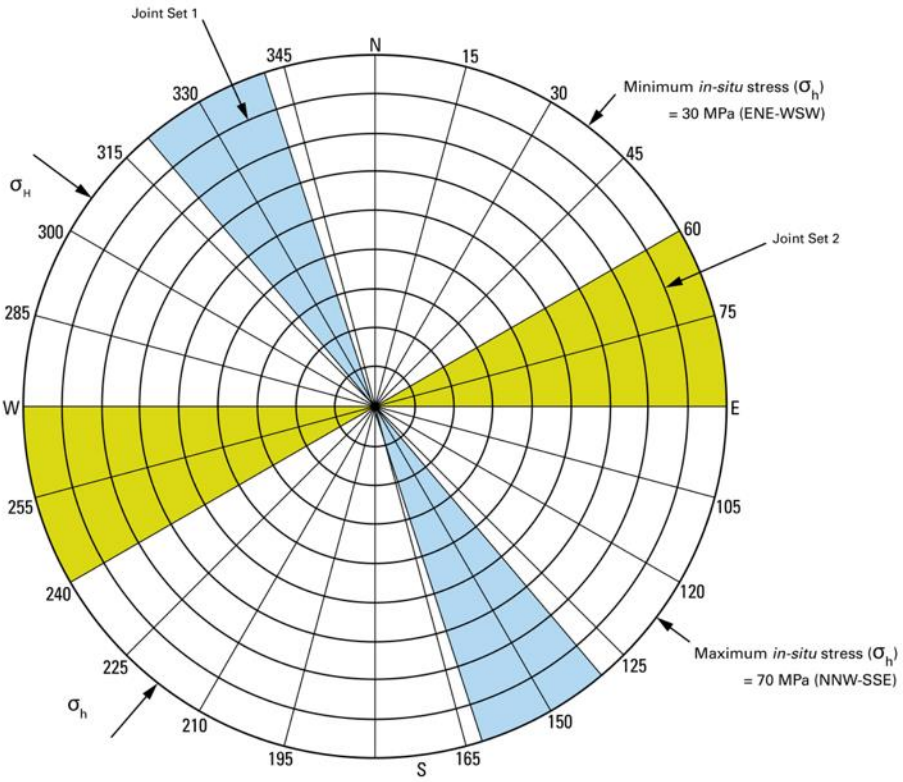

Figure 49: Strike directions of the major joint sets and principal stress orientation (note a more recent review i.e. Evans et al., 1992 suggests a more appropriate orientation for the direction of maximum horizontal stress in the Carnmenellis pluton is N150°E±10°, see Section 6.1.2) and magnitude in the Carnmenellis granite as determined by in-situ hydraulic fracture tests at the Rosemanowes HDR test site. Redrawn from Batchelor and Pine (1986), Figure 10, ©International Society for Rock Mechanics.

6.1.2.1 Implications for fracture systems at greater depth and crustal permeability

It was originally calculated that the microseismic events extended to depths of over 4 km (Figure 48) and no significant changes in their directions were apparent. It was concluded that this is evidence that there is no significant rotation of the stress field at depth (up to 6 km; Pine and Kwakwa, 1989) in the Carnmenellis granite, major structures extend to these depths, and the stress field is 'critically anisotropic', with fluids occurring in near vertical structures. However, the researchers note that even with the 'substantial and comprehensive data set there can be no great confidence in the extrapolation of all aspects of the stress tenor [to much greater depth]'. Despite this uncertainty they conclude that the 'persistence of the serve anisotropy and the direction of the stresses can be predicted and minimum horizontal stress trend may well persist in the 3000–7000 m depth range' (Batchelor and Pine, 1986). Pine and Kwakwa (1989) reviewed the hydrofracture stress measurements (HFSM) made during the HDR project, to assess the implications for measuring stress at depths of up to 6 km. They considered there to be too few data points at 2.6 km to be confident about stress magnitudes at this depth and extrapolating these values to depths of great than 3–4 km is high-risk. Despite this they indicate that extrapolation to 6 km depth based on data from the 0–4 km depth range in the same rock type (i.e. Carnmenellis granite) the measurements were made in 'should be sufficiently accurate'.

However, this assumes that no major stress discontinuity exists at depth, but they postulate that such as discontinuity would be the result of a major lithological change, or the occurrences of a major structure, which should be obvious from surface geophysics or drilling (Pine and Kwakwa, 1989). It is important to note that a more recent reassessment of the microseismic data, using information from an additional measurement station, which improved vertical accuracy to less than 20 m, relocates the seismic events to a maximum depth of the 3 km (Evans et al., 1992).

6.2 Evidence for deep fluids

6.2.1 Deep-saline fluids

Warm (up to 55°C), high-salinity groundwaters have been found at depths of up to 820 metres, primarily issuing from NNW-SSE-trending cross-courses and lodes in mines at the northern edge of the Carnmenellis granite. These flows occur in mines in both the granite and in the killas. Some of the cross-course flows have been discharging for more than 30 years. Crosscourse bines typically discharge at about 1–10 l/s at temperatures between 40–45°C, and with salinities of about 2000 mg/l, suggesting that a large reservoir of saline, thermal water exists at depth. These deep spring waters are mildly acidic to neutral (pH 5.4–7.7), and compositionally they are dominated by Na, Ca and Cl (Smedley et al., 1989) (Table 4).

The Na/K geothermometer indicates an equilibrium temperature of 54 °C for the water, which suggests a depth of origin of 1.1 to 1.2 km, or some 440 m below the depth of discharge into the South Crofty Mine (Burgess et al., 1982b). Stable oxygen ($\delta^{18}O$) and hydrogen ($\delta^{2}D$) isotope studies indicate that these waters are not derived from seawater, but are more likely diluted palaeobrines, which have flowed through cross-course structures within the granite and killas. Their chemical and isotopic signatures also indicate mixing and dilution by circulation of local meteoric water (Alderton and Sheppard, 1977; Smedley et al., 1989). Isotope (^{4}He and U series) studies by Burgess et al. (1982b), Edmunds et al. (1984), and Smedley and Allen (2004) identify components of the deep-brines with ages of between 10000 and 1000000 years old. The presence of tritium and $\delta^{14}C$ isotopes indicate that up to 40 per cent of the deep-brines, by volume, comprise more recent (1953–1978) meteoric water, which indicates mixing of fluids (Burgess et al., 1982a). The mixing of these waters also points to percolation of modern waters to a depth of at least 700 metres below ground level, where it mixed with older, deeper saline fluids (Burgess et al., 1982b; Downing, 1986; Smedley and Allen, 2004). Historically these waters have only been analysed for a limited suite of major and minor elements, which means that the concentration of metals of economic interest in these deep fluids remains enigmatic. One exception is lithium. The concentration of lithium, up to 125 mg/l^{-1} in deep spring waters from South Crofty (Edmunds et al., 1984), is of current interest to Cornish Lithium Ltd., a private company actively exploring south-west England for brine-hosted lithium resources. It is thought that the relatively high concentrations of lithium in these waters is a function of mica breakdown during fluid-rock reaction (Edmunds et al., 1984). This is also of interest to future geothermal projects in south-west England, as lithium may be a metal that could be leached, and recovered, by CHP operations.

Table 4: Summary of deep, mine water compositions from mines around the northern edge of the Carnmenellis granite, including South Crofty (1, 2 and 3), Clifford United (4), and Wheal Seton (5). Data from Alderton and Shepherd (1977) and Smedley et al. (1989). *Tr.* = trace and *n.d.* = not determined.

	1	2	3	4	5
	mg l^{-1}				
Na	2000	3210	457	2043	230
K	87.6	138	25.1	111	83
Ca	1070	1670	287	1166	2,,490
Mg	33.2	51.6	24.7	32	44
Fe	1.92	1.82	0.1	*Tr.*	2
Al	<0.4	<0.4	<0.1	*Tr.*	182
Si	14.4	19.6	12	24	13
Mn	2.58	3.03	1.2	*Tr.*	*Tr.*
Sr	17.6	27.6	1.3	*n.d.*	*n.d.*
Li	59.6	97.2	9.9	61	80
Cl	5800	8750	1260	5,628	9,168
Br	*n.d.*	*n.d.*	*n.d.*	*n.d.*	*Tr.*
HCO3	*n.d.*	*n.d.*	126	*n.d.*	*n.d.*
F	*n.d.*	*n.d.*	3.6	*n.d.*	*n.d.*
SO4	126	107	92	124	21
B	7.60	*12.2*	0.8	*n.d.*	*n.d.*
TDS	9,226	14,099	2,306	9,189	14,441
pH	6.61	6.79	6.85	*n.d.*	*n.d.*
Depth (m)	690	690	618	448	330
Temp (°C)	41.6	45.3	35	52	33

6.2.2 Fluid circulation models

Palaeo-fluid flow in and around the Carnmenellis granite can be divided in to four main stages (Figure 50): (i) Expulsion of early magmatic fluids associated with the emplacement of the granite, which led to the formation of sheeted Sn-W greisens in the granite roof zone and overlying metasedimentary rocks. Hydrothermal convection of formation waters starts to occur in response to the thermal anomaly created by the granite emplacement; (ii) Copper, zinc and sulphur are leached from the host rocks. Formation waters are drawn down through the granite as the system begins to cool, resulting in the deposition of Cu-Zn- sulfides in veins; (iii) Main-stage, polymetallic lodes are emplaced within the granite roof zone by further expulsion of magmatic fluids; and (iv) Formation waters start to circulate through the granite in response to cooling of the system, resulting in the deposition of Cu-Zn- sulfides in steeply dipping fissures (Smedley et al., 1989). Post-magmatism basinal brines circulate through N–S-trending structures within the granite and killas, mixing with meteoric waters. These fluids deposited Pb-Zn-rich mineralisation within the so-called cross-course veins (Gleeson et al., 2000; Gleeson et al., 2001; Scrivener et al., 1994).

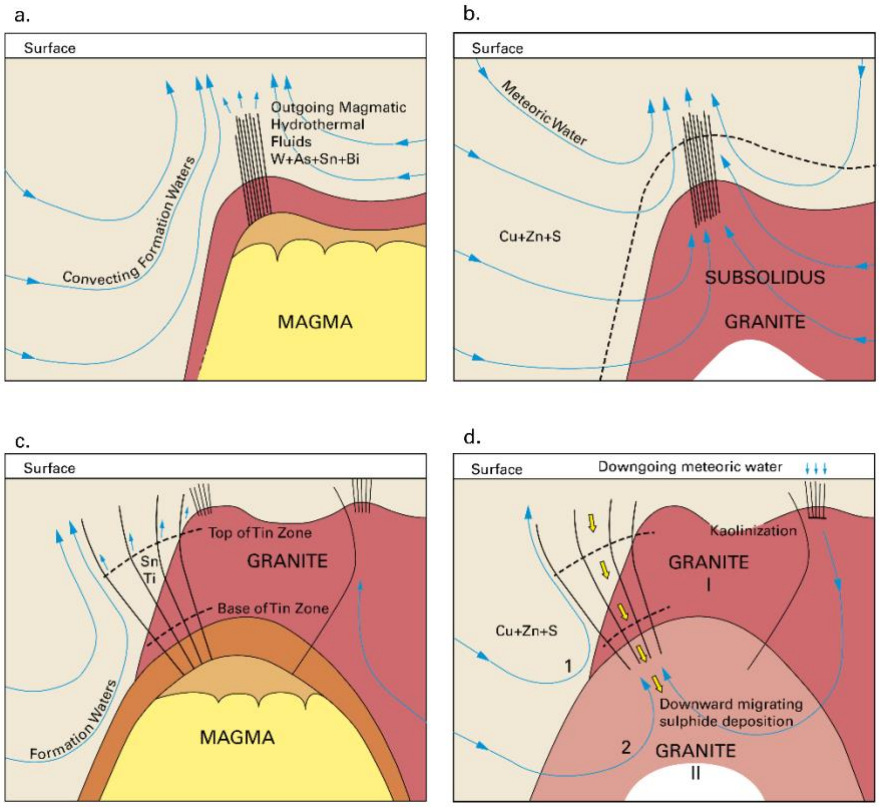

Figure 50: Schematic diagram illustrating fluid flow regimes in relation to emplacement of the Carnmenellis granite. (A) Expulsion of magmatic fluids forming Sn-W greisen's and generation of hydrothermal convection in the overlying groundwater. (B) Leaching of metals and sulphur from the host rocks. Cooling of the system permits meteoric waters to move down into the granite pluton. (C) Main stage, polymetallic lodes form in the roof zone of the granite pluton from expulsion of magmatic fluids. (D) Meteoric waters circulate through the granite as the system cools. Cu-Zn sulfides are deposited in a series of lodes. Re-drawn from Smedley et al. (1989). British Geological Survey © UKRI.

7 Integrated modelling

Modelling of the Cornubian Batholith was undertaken as part of the CHPM2030 project to improve understanding of its geothermal properties. This work involved the development of three models: a regional model, and two site-specific models, one based on the HDR project site, and the other on the ongoing United Downs Deep Geothermal Power (UDDGP) project. Here we outline the data used, methodology and limitations of the three models. The models were developed in a range of modelling software packages, including Fracman, Move4D, Petrel, and SKUA-GoCAD, with each piece of software bringing its own strengths to the modelling.

7.1 Regional model

The regional model was constructed to understand the spatial relationship of key geological parameters that feed directly into the site-scale models. The model covers the Cornubian Batholith, including the Dartmoor, Bodmin, Carnmenellis, St. Austell, and Lands' End granites, but excludes the Scilly Isles (Figure 51). It consists of a 3D Geospatial Information Dataset, containing the most relevant information for this project and future research in the region.

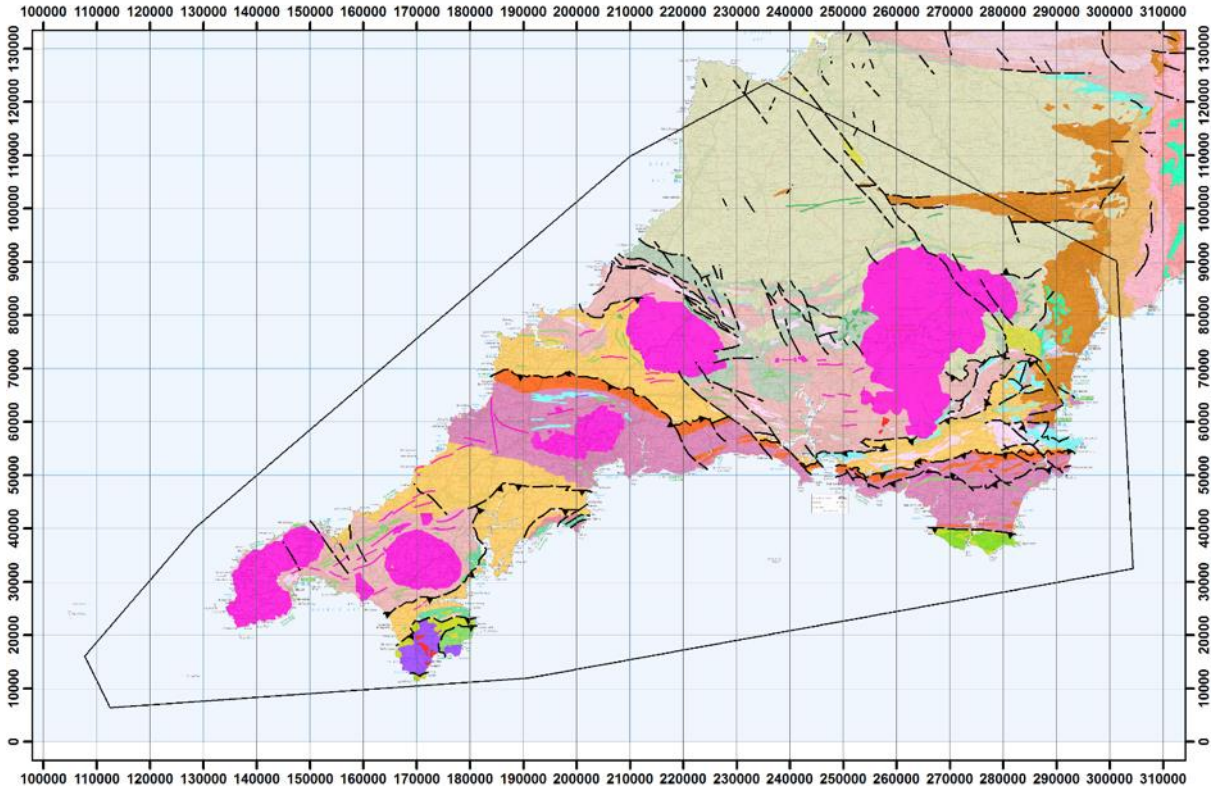

Figure 51: Geological map showing the extent of the regional model (black line) covering Cornwall and southern Devon, and the mapped location of the granite (pink). Contains Ordnance Data © Crown Copyright and database rights [2019]. Ordnance Survey Licence no. 100021290. Contains British Geological Survey materials © NERC [2019].

The model consists of two geological units: granite and killas. The granite surface was derived from the regional gravity model (Camborne School of Mines, 1988; Willis-Richards and Baria, 1989) and enhanced with five higher resolution gravity models for south-west Dartmoor (Tombs, 1977), the area between Dartmoor and Bodmin Moor (Rollin, 1988), Hayle-Leedstown (Tombs, 1977), and St. Agnes (Tombs, 1977) and St. Austell (Tombs, 1977), and the top granite contact based on 50 boreholes records (see Section 3.3.1.2 and Figure 17) (Figure 52). The surface extent of the granite was based on BGS 1:50 000 scale onshore mapping data and 1:250 000 offshore mapping data for the Land's End granite. Properties were calculated on the surface, including curvature, slope and aspect.

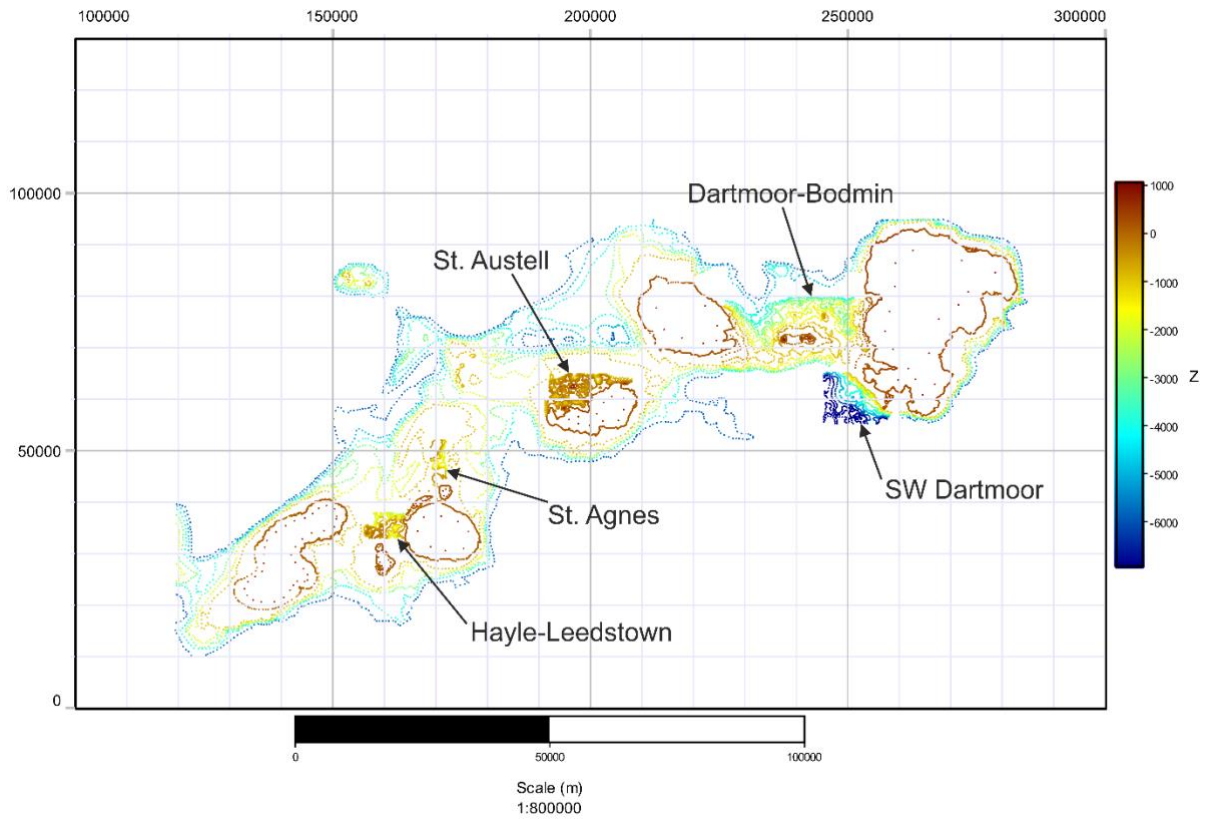

Figure 52: Points of the top granite contact used for modelling the top granite surface. Arrows indicate the location of the additional higher resolution gravity models mentioned in the text. British Geological Survey © UKRI.

The land surface and bathymetry data is derived from the General Bathymetric Chart of the Oceans (GEBCO; The GEBCO_2014 Grid, version 20150318, http://www.gebco.net) and was used as the capping surface to the model (Figure 53). Additionally this surface was used to drape the boundary polygons, and fault network. Using the GEBCO bathymetry data allowed the offshore Lands' End granite to be modelled. The base of the granite has been investigated through seismic (Brooks et al., 1984; Jones, 1991), MT (Beamish, 1990), and gravity modelling (Taylor, 2007; Willis-Richards and Baria, 1989). There is ambiguity regarding the exact location of the base of the granite. The seismic data identify a seismically homogeneous granite with three reflectors at a depth of; 6–8km, 12–15 km and 30 km; the latter reflecting the Moho (Brooks et al., 1984). The magnetotelluric survey shows resistivity increasing to a depth of 6 km, at which point joints and cracks close, and by 7 km pore-related resistivity dominates (Beamish, 1990). The electrical base of the granite lies at 14 km.

Gravity modelling by Willis-Richards and Baria (1989) suggests the base of the granite is located at between 12–15 km. Taylor (2007) suggests that the granite consists of two sheets, with an upper granite, with a base at 6–8 km, and a lower more extensive granite sheet, with a base at 12–15 km. This is supported by the magnetotelluric and seismic data. Based on the seismic data of Brooks et al. (1984), both the upper granite base and the lower granite base have been modelled (Figure 54). The base of the lower granite has been interpolated across the model extent and forms the base of the model. The surfaces of the base of the granite show a general deepening to the SE, and the lower granite thins towards the north. However, the surfaces are based on limited data and further work is required to improve understanding of the base of the granites and the shape of the two granite sheets if deeper geothermal reservoirs are to be explored.

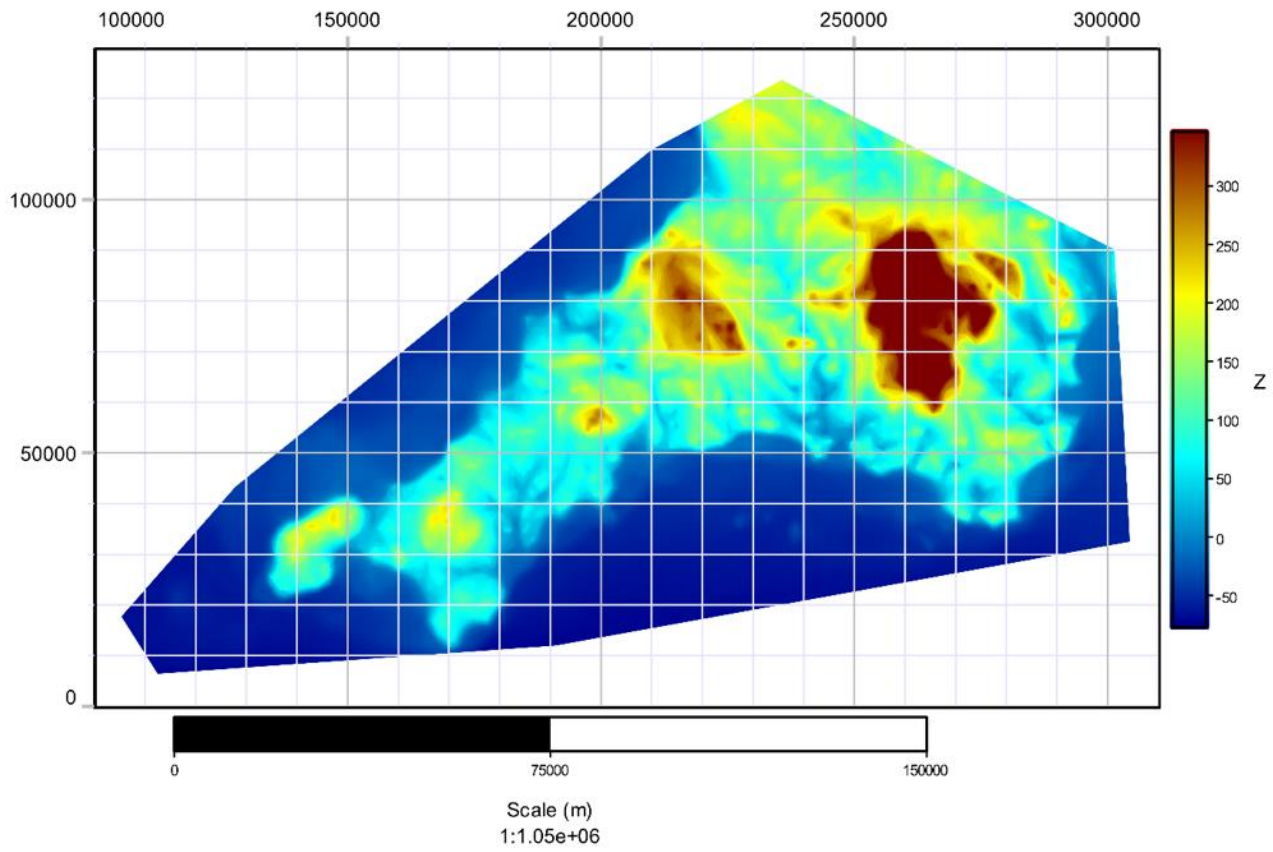

Figure 53: Modelled topographic surface. The granite intrusions can be identified as higher ground. British Geological Survey © UKRI.

Modelled surfaces were constructed using the GoCAD/SKUA implicit method with a spatial sampling of 500 m. The relative difference between the input data and output surfaces were calculated to estimate the error and uncertainty associated with the modelled surface (Table 5). There was good agreement between the modelled topography and input data, but the top granite surface had a larger error. The top granite surface is based on the interpretation of geophysical models and relatively sparse data, and given the scale of the regional model and the surface resolution (>500 m) the error is not considered to present an issue.

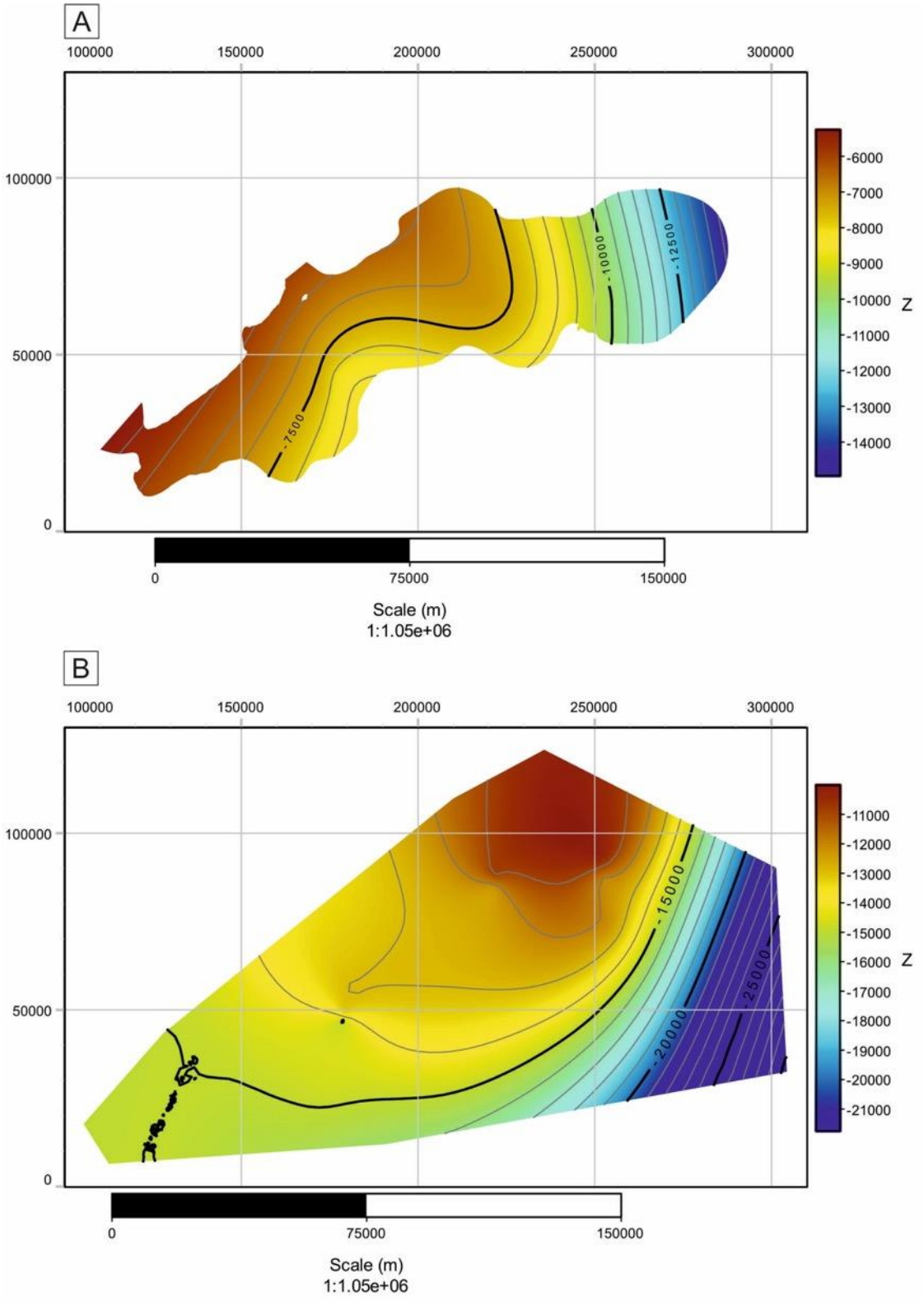

Figure 54: The granite surface used in the model. A. Upper granite surface. B. Lower surface granite surface, which has been extended across the model and also represents the base of the model. British Geological Survey © UKRI.

Table 5: Computed difference between input data and modelled granite surfaces.

Data	Error
Topography	Mean = -0.149066 m SD = 4.80127
Granite	Mean = 12.1854 m SD = 111.487

The model area is crosscut by numerous faults that would be impractical to model at a regional scale and it was therefore decided that only larger faults would be modelled (Figure 55). Major structural orientations across Cornwall include NE-SW-trending thrusts, E–W-trending thrusts, E–W-trending normal faults, and NE-SW-trending and NW-SE-trending strike-slip faults. The Cornubian granite is primarily affected by the NW-SE-trending strike-slip faults and the 19 most prominent faults identified in Camborne School of Mines (1988) were included in the regional model. These faults were modelled as vertical structures that transect the model from the topographic surface to the base of the model. Although additional faults could be incorporated into the model, for the purpose of this study, the number used were considered sufficient to show the general trend of the structures that cut the granite.

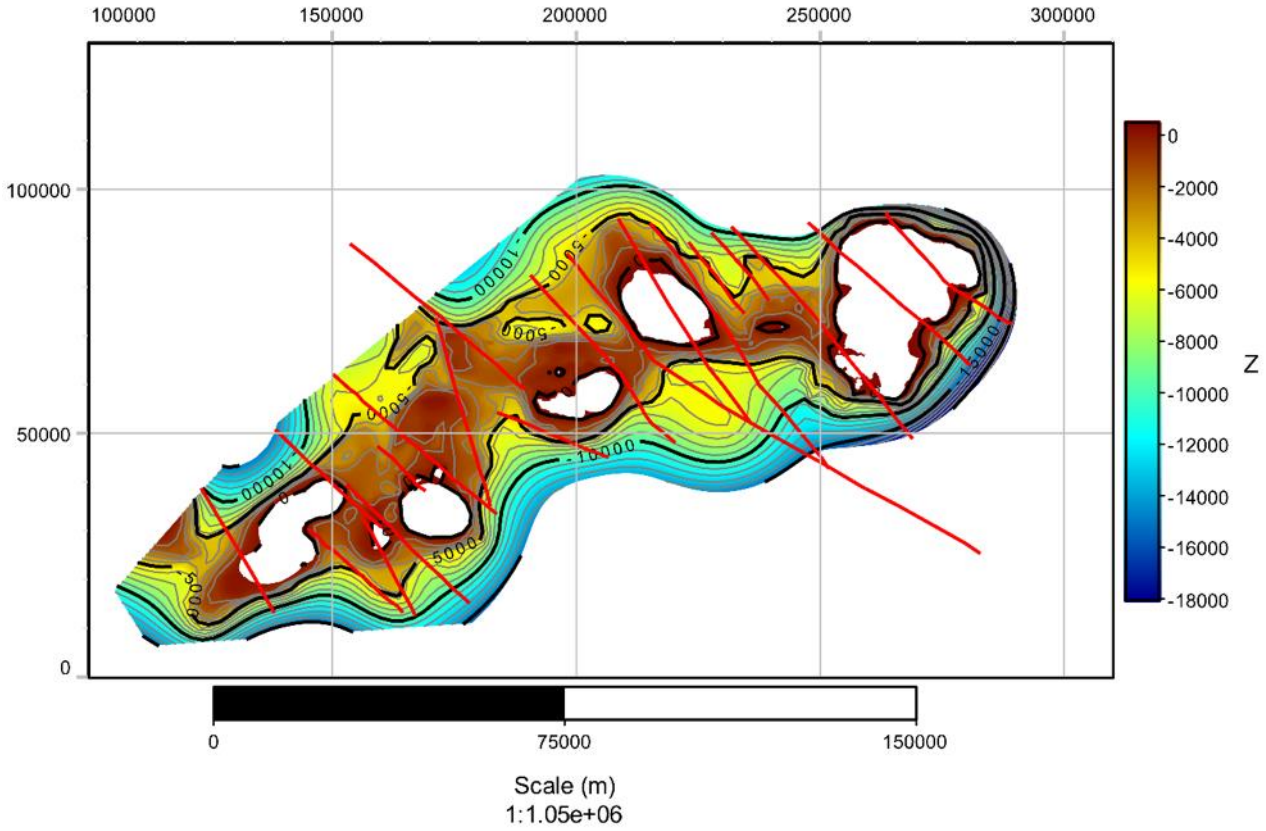

Figure 55: Map view of the top granite surface and principal large faults (red lines; after CSM, 1988). British Geological Survey © UKRI.

Once the geometrical model was established and built the model was voxelated and properties assigned. The voxel model represents an area of 207,543 km^3 with a voxel size of 1065x639x160 m (XxYxZ) resulting in 1,906,068 voxels (Figure 56). With the framework built, physical properties, including heat production, heat flow, and temperature were interpolated or simulated into the voxelated volume (Appendix 3).

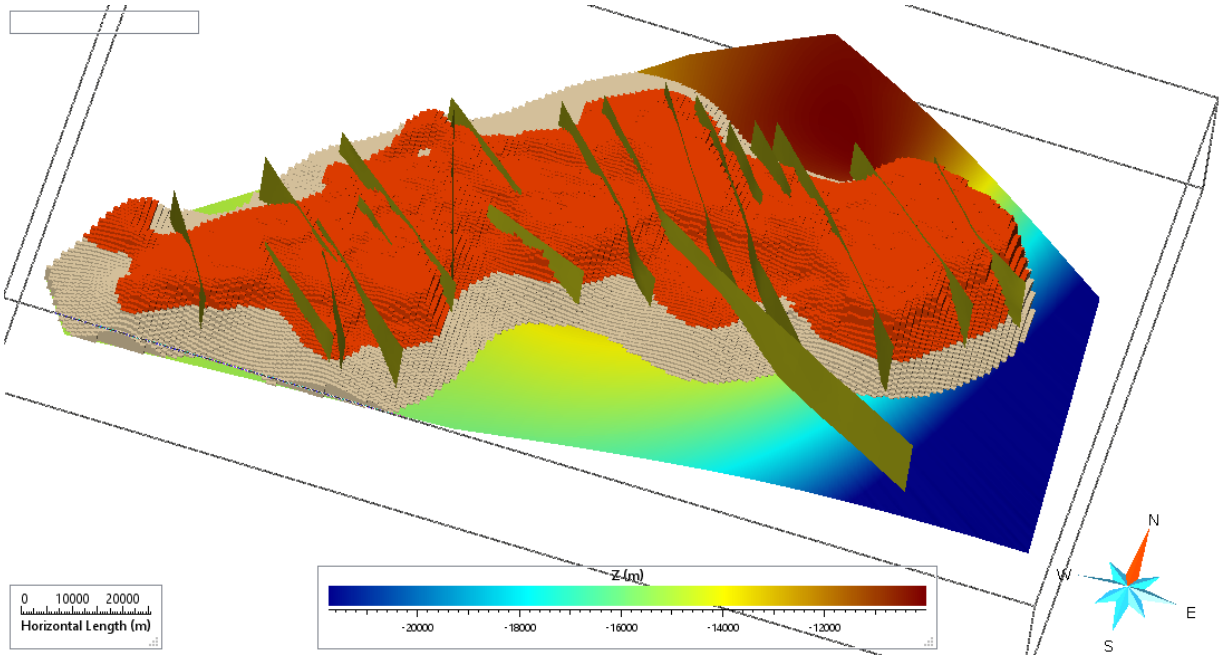

Figure 56: 3D view of the voxelated granite model showing the two granite sheets and the SE dipping base of the granite. British Geological Survey © UKRI.

7.1.1 Fracture data

Fractures are the predominant flow pathway within the granite and understanding the spatial properties of the fracture network is important for modelling the fracture network and upscaling the network for flow simulations (

Figure 57). The fracture modelling focuses on the Carnmenellis granite as the two site-scale models are both located within this pluton. However, there is a requirement to extend the fracture characterisation across the extent of the Cornumbian Batholith if the entire geothermal potential of the granite is to be examined. A number of studies on the fractures in the Carnmenellis granite have shown that there are three dominant fracture sets; two near vertical and one that is sub-horizontal (Camborne School of Mines, 1986). The two high angle fracture sets trend NNW-SSE and ENE-WSW, and dip at 80–90 degrees (Figure 20). The sub-horizontal fracture set is limited to the near surface and therefore at reservoir depths is unlikely to be a contributing factor in the reservoir flow model, and is therefore not included in the model. The two principal fracture sets are identifiable in the downhole image logs from RH12 and RH15 (Figure 58). RH12 was drilled towards the NW and therefore there is a bias in the data towards the ENE-aligned fracture set. In contrast RH15 was drilled in a spiral to intersect the microsesimic cloud resulting from the stimulation of RH12. Terzaghi (1965) correction was applied to both wells to reduce the bias within the dataset. Fracture intensity (fracture per m) was calculated from the fracture logs and upscaled to 5 m intervals for each fracture set (Figure 59). There is no indication of a mechanical stratigraphy with the cumulative frequency plot showing a uniform slope. Therefore, there was no need to subdivide the granite into discreet fracture stratigraphy.

Figure 57: Coastal exposure of fractured Lands' End granite. British Geological Survey © UKRI.

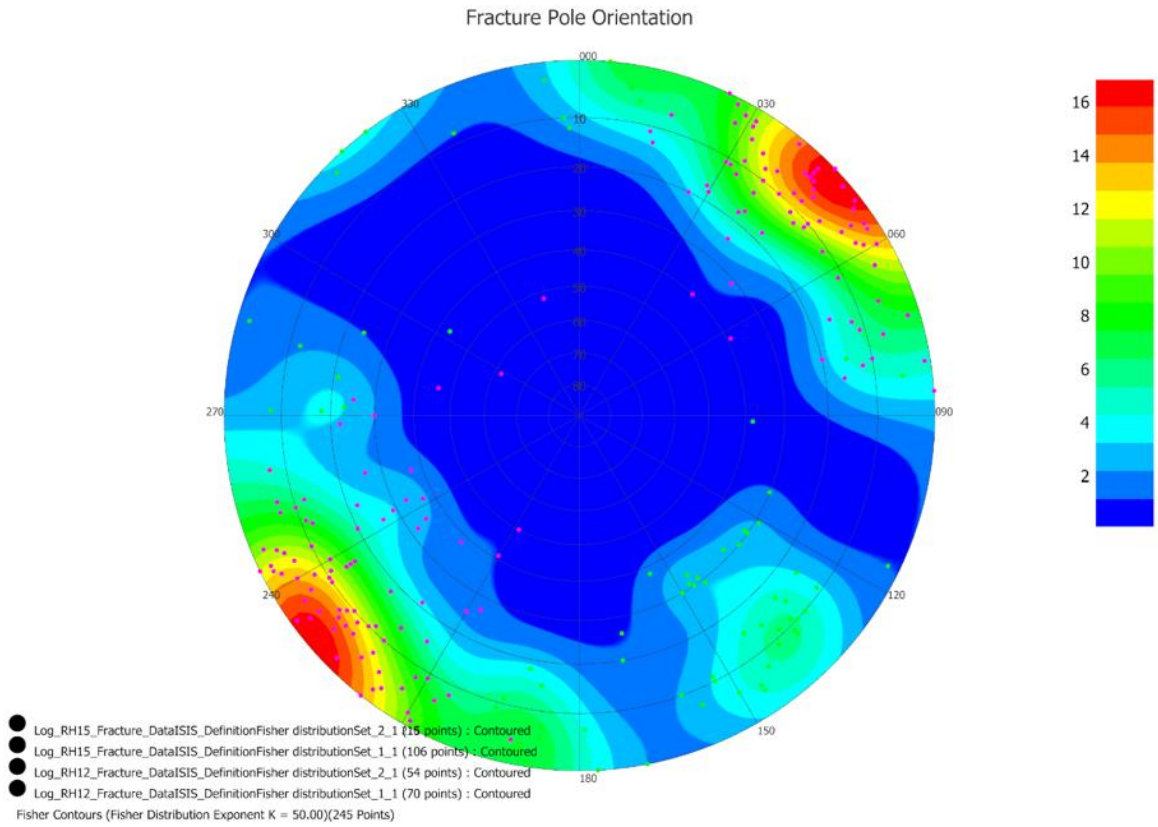

Figure 58: Lower hemisphere stereonet showing the poles to fractures from the downhole image logs for RH12 and RH15. Two primary fracture sets can be identified striking NW-SE and NE-SW, which matches with the known surface fracture orientations for the Carnmenellis granite. British Geological Survey © UKRI.

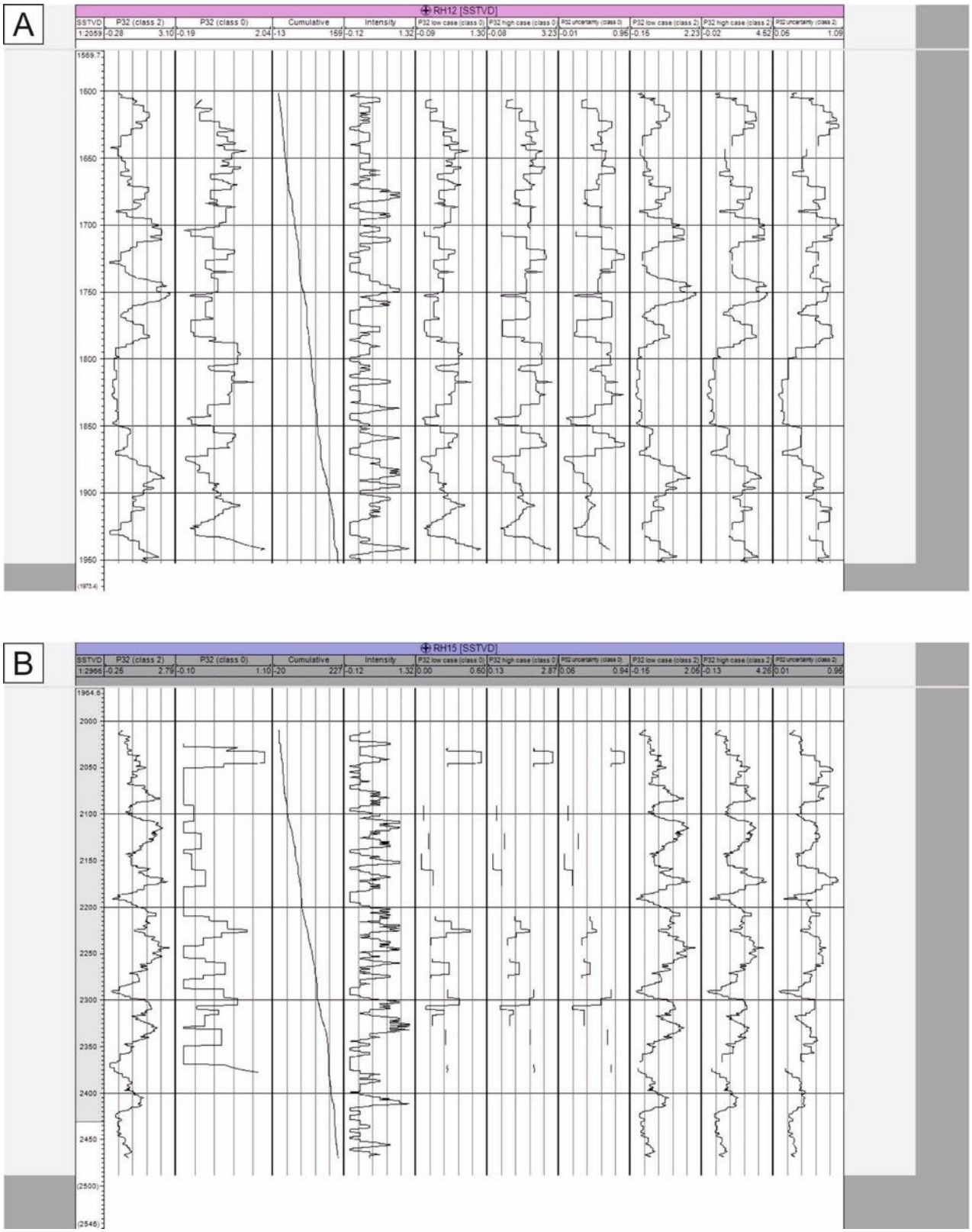

Figure 59: Derived fracture intensity, cumulative frequency, density, and uncertainty for the two fracture sets identified from the downhole image logs. A. RH 12. B. RH 15. British Geological Survey © UKRI.

The fracture density (P32; m^2/m^3) was calculated from the intensity providing a mean density per 5 m interval. Low (P10) and high (P90) confidence intervals were also calculated, providing three models that account for the recorded fracture intensity (Appendix 4). There is no direct evidence to account for the changes in fracture density and therefore it is assumed that density is random within the granite, at least at the site scale. Histograms of the computed fracture density reflect a truncated normal distribution. Fracture density within the model was randomly drawn from the corresponding distribution, with a given mean, standard deviation and upper and lower limits.

In addition to the fracture set definition, orientation and density, it is necessary to estimate the fracture length, shape and aperture for Discrete Fracture Network (DFN) modelling. Although the fracture azimuth and dip are relatively well constrained within the granite there is limited information on the fracture length or fracture aperture distribution, especially at reservoir depths.

Fracture lengths were measured in four quarries and are reported in Camborne School of Mines (1986). If all fractures are considered, both the horizontal and vertical length fit a lognormal distribution (Figure 60) with a maximum recorded length of 300 m.

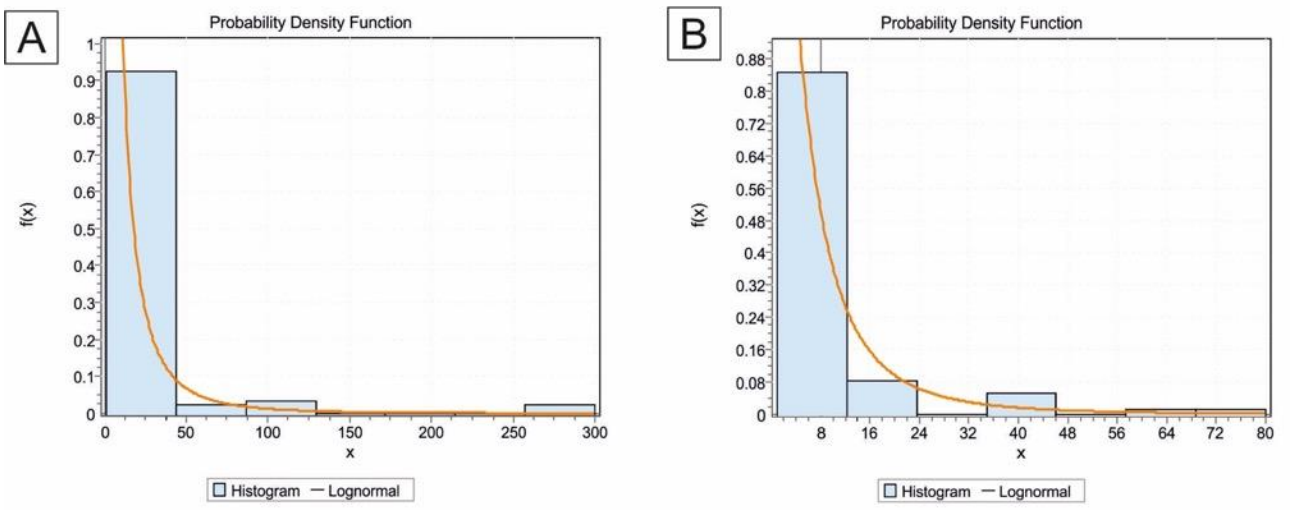

Figure 60: Lognormal horizontal fracture length distributions for all fractures. A. Left. B. Right. British Geological Survey © UKRI.

If each fracture set is considered independently, assuming that length still follows a lognormal distribution, we can calculate the mean and standard deviation for each fracture set (Figure 61). The aspect ratio for each fracture set was calculated by dividing the mean horizontal length by the mean vertical length. Fracture aperture is very poorly constrained and data on fracture aperture only exists from the surface or relatively near-surface mines, which will over estimate fracture aperture. However, results from numerical modelling and hydraulic testing at the HDR project site provide estimates for fracture aperture at reservoir depths, which ranges between 5–50 µm with a mean of 10 µm (Pine and Nicol, 1993). Additionally, it is known that

permeability prior to stimulation was 10^{-6} µm^2 but post stimulation this increased to 0.5*10^{-3} µm^2. Given a flow fracture spacing of 10 m (based on data from flow logging data), the hydraulic aperture is 40 µm (Evans et al., 1992).

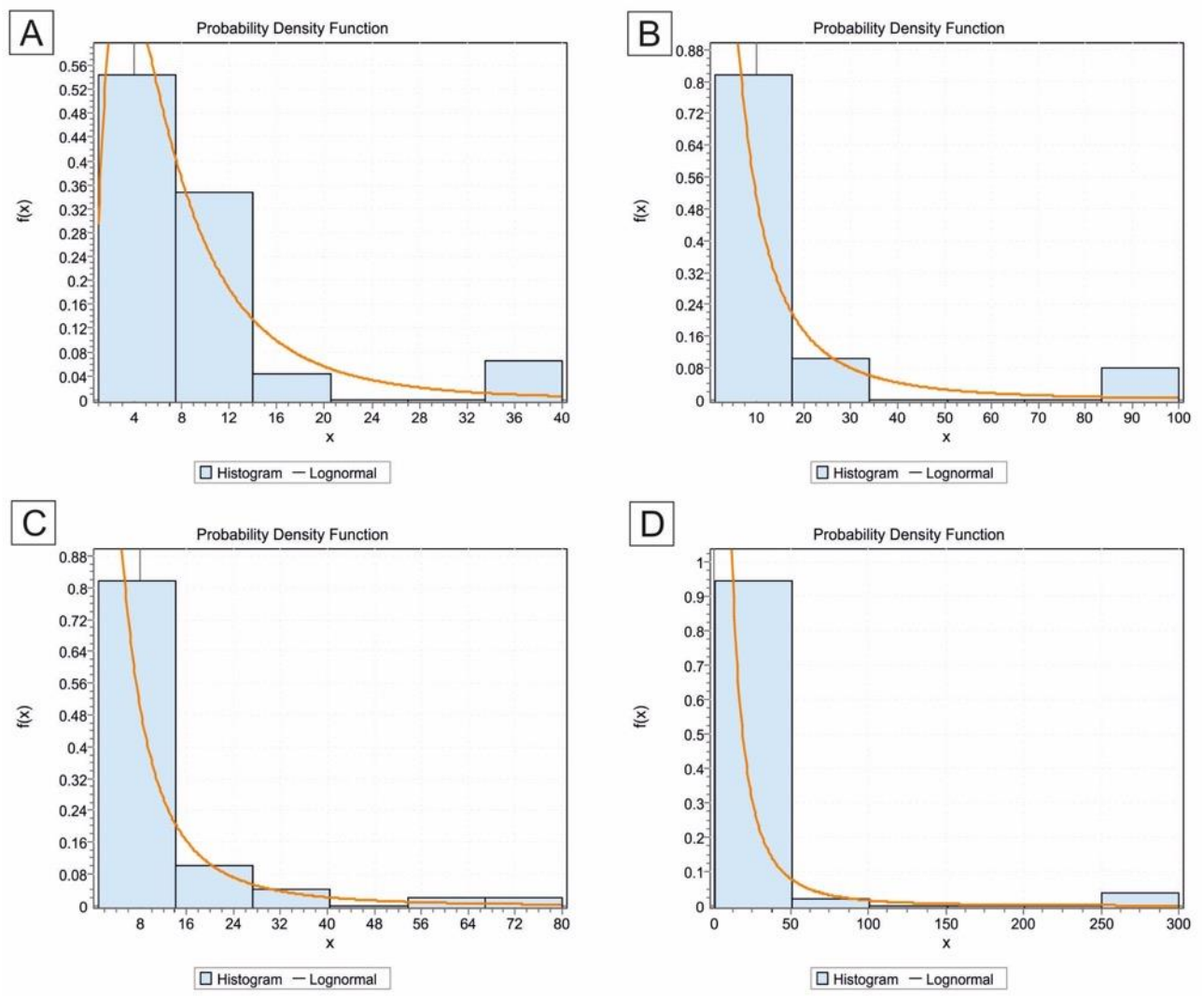

Figure 61: Calculated lognormal distributions for two fracture sets. A. Fracture set 1 for vertical lengths. B. Fracture set 1 for horizontal lengths. C. Fracture set 2 for vertical lengths. D. Fracture set 2 for horizontal lengths. British Geological Survey © UKRI.

It is also known that the flow is predominantly along the NNW-SSE-trending fractures (Evans et al., 1992). Given that these are approximately parallel to the maximum compressive direction, they will have a higher dilation tendency (Ferrill and Morris, 2003; Morris et al., 1996) (Figure 62) and therefore a larger aperture. Low flow rate hydraulic tests at low injection pressures indicated permeabilities between 1–10 µD at up to 0.7 MPa fluid overpressure. Permeability subsequently increased to 60 µD at a pressure of 3 MPa, prior to the onset of significant discontinuous behaviour at pressures over 5 MPa (Parker, 1999). The pumping test data show that the aperture is strongly controlled by the in-situ stress conditions. This supports the dilation tendency results, with fractures aligned parallel to the direction of maximum compression becoming

increasingly open as injection pressure increases. It is assumed that fractures perpendicular to the maximum compressive stress direction will have an aperture in the order of a tenth of the fractures parallel to the maximum compressive stress direction (Figure 63).

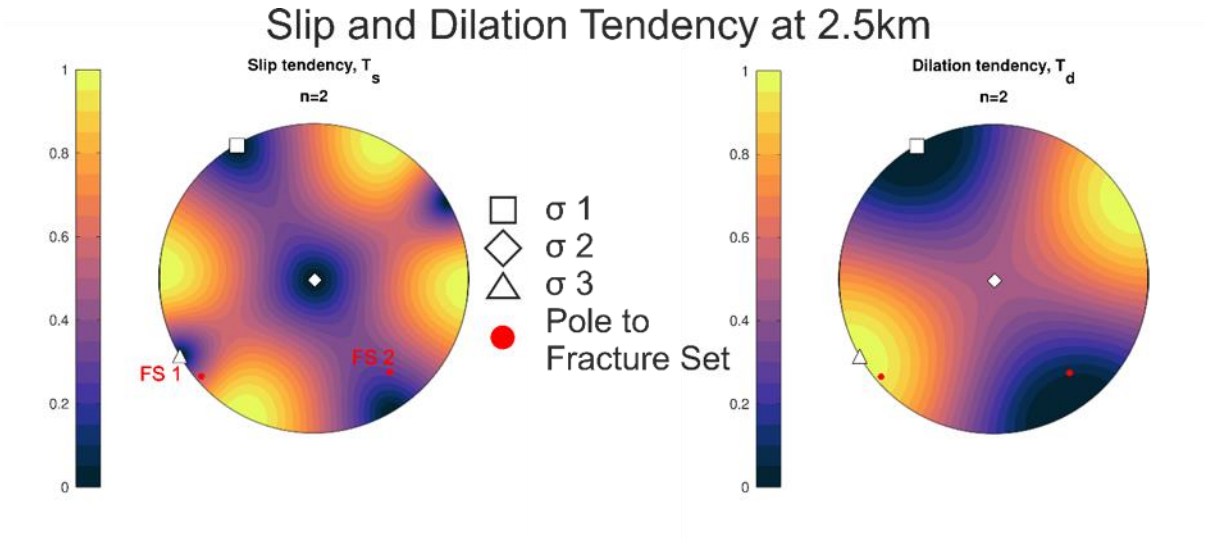

Figure 62: Slip tendency and dilation tendency analysis and the two fracture sets (FS1 and FS2) based on insitu stress equivalent to 2 km at the Hot Dry Rock project site and the revised direction of maximum compression as measured in RH 15 of 150 degrees ± 10 degrees. Note that fracture set 1 is optimally aligned for dilation. Neither fracture set are preferentially aligned for slip reactivation. British Geological Survey © UKRI.

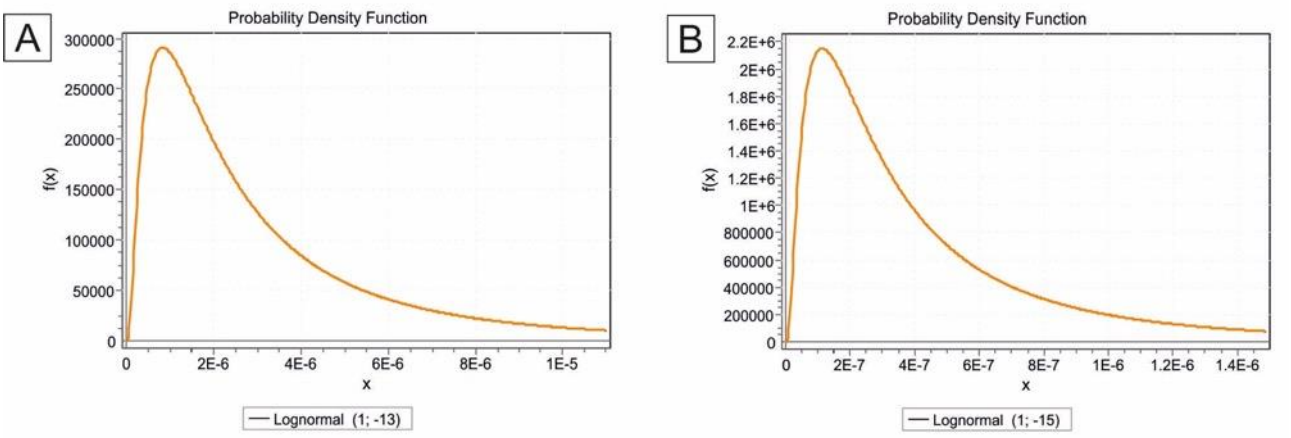

Figure 63: Assumed aperture distribution. A. Fracture set 1 (parallel to maximum compressive direction). B. Fracture set 2. British Geological Survey © UKRI.

7.2 Hot dry rock project site model

The HDR project site model is a site-scale model that includes fracture data from two of the three deep boreholes drilled as part of the HDR project; RH 12 and RH 15. The model covers a volume of 2.6 km^3, centred on the wells and has a depth range of -1000 to -3000 mbsl (

Figure 64). The region was gridded with a cell size of 13x10x10m and properties were transferred from the regional model. The HDR project site model also includes site-specific parameters related to the hydrological properties of the system. As previously discussed, fracture flow is the predominant flow mechanism within the granite. Therefore the statistics and assumptions on the fracture network described above were used to generate three discreet fracture network models for the HDR reservoir. These were up scaled to include porosity and permeability to understand the likely flow pathways within the reservoir. In order to facilitate future geomechanical modelling the model was orientated parallel to the regional direction of maximum horizontal compressive stress.

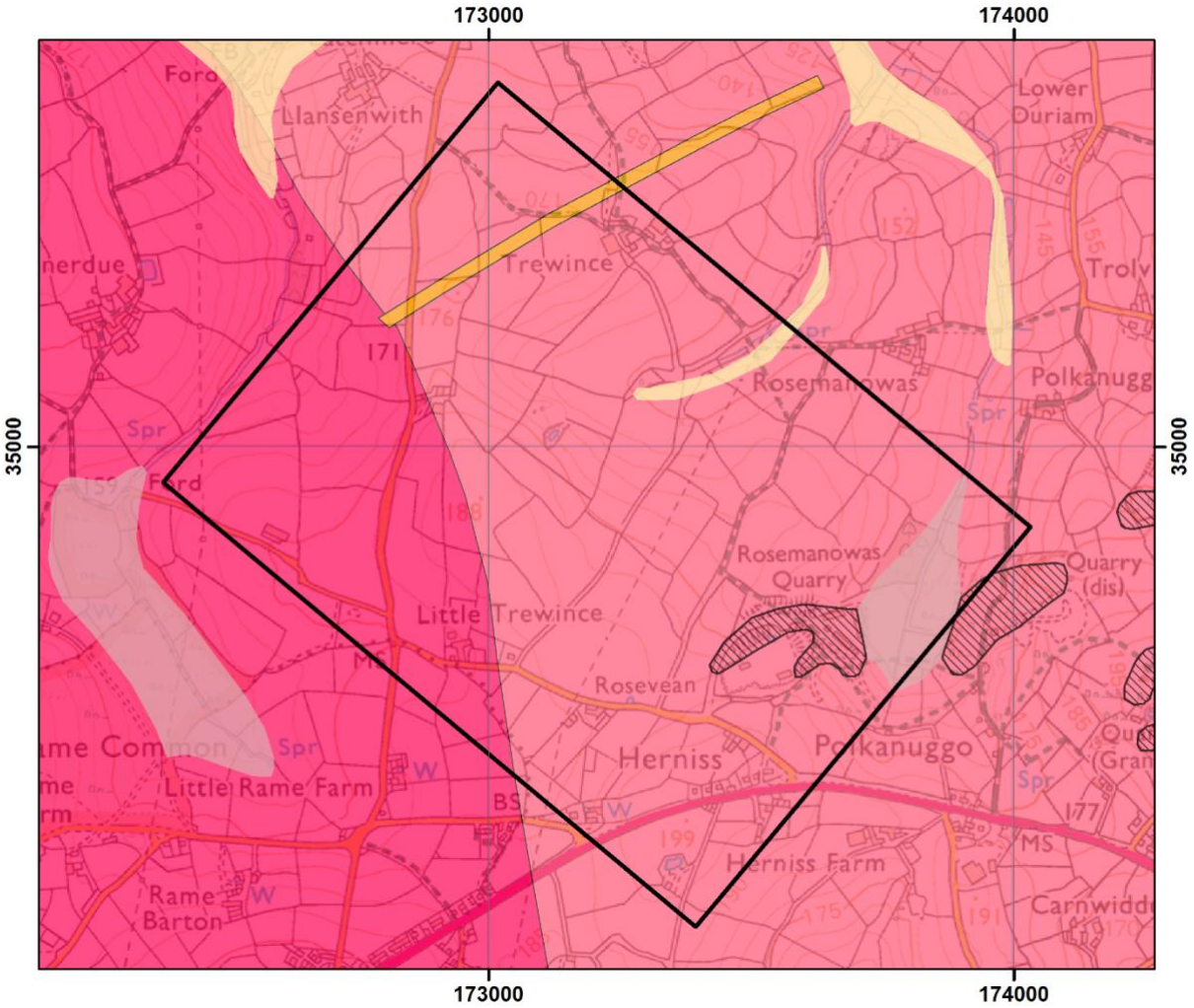

Figure 64: 1:50 000 scale geological map of the HDR project site showing the lack of faults and uniform geology. The area covered by the HDR project site model is shown by the black outline. Contains Ordnance Data © Crown Copyright and database rights [2019]. Ordnance Survey Licence no. 100021290. Contains British Geological Survey materials © NERC [2019].

The modelling parameters for the stochastic simulation of the DFN are presented in Appendix 5 and are based on the above discussion. Evans et al. (1992) state that only 10 per cent of the imaged fractures had appreciable flow, and a spacing of approximately 10–15 m. Given the focus on the dominant flow pathways, fracture permeability and porosity was calculated for fractures with a length greater than 150 m, but less than 300 m,

resulting in a spacing of about 10–15m. The resulting permeability is within good agreement with the 1–10uD reported by Parker (1999).

Once the fracture network was generated, the resulting DFNs were upscaled into the voxel volume (Appendix 6). A number of methods are available for upscaling including the Oda method (Oda, 1985), the flow-based method (Lough et al., 1997), and a corrected Oda method (Ghahfarokhi, 2017). The Oda method is considered a good first pass for upscaling DFN for porosity and permeability, as it is quick to calculate but it tends to overestimate the permeability and porosity as it does not take into account the connectivity of the fracture network. The flow-based method is more accurate, but very slow especially when the model contains a large number of voxels. To reduce the over estimation the corrected Oda method can be applied, which up scales the fracture network using the faster Oda method, but corrects the results based on a subsample of cells to which the flow-based method is applied. This has the advantage of being relatively quick and reducing the over estimation issue associated with the classical Oda method.

7.3 United Downs Deep Geothermal Power project site model

The UDDGP project site model considers an area located to the NW of the Carnmenellis granite. However, the target reservoir is still considered to be within the Carnmenellis granite. The site is located near historical mine workings and the area is cut by a number of NNW-SSE-trending faults and ENE-WSW-trending mineralised zones. The site-scale model covers a volume of 12 km^3, including the drilling pad and the SW extent of the drilling with a depth range of -1500 to -5500 mbsl (Figure 65). The region was voxelated with a voxel size of 15x20x10 m and properties were transferred from the regional model.

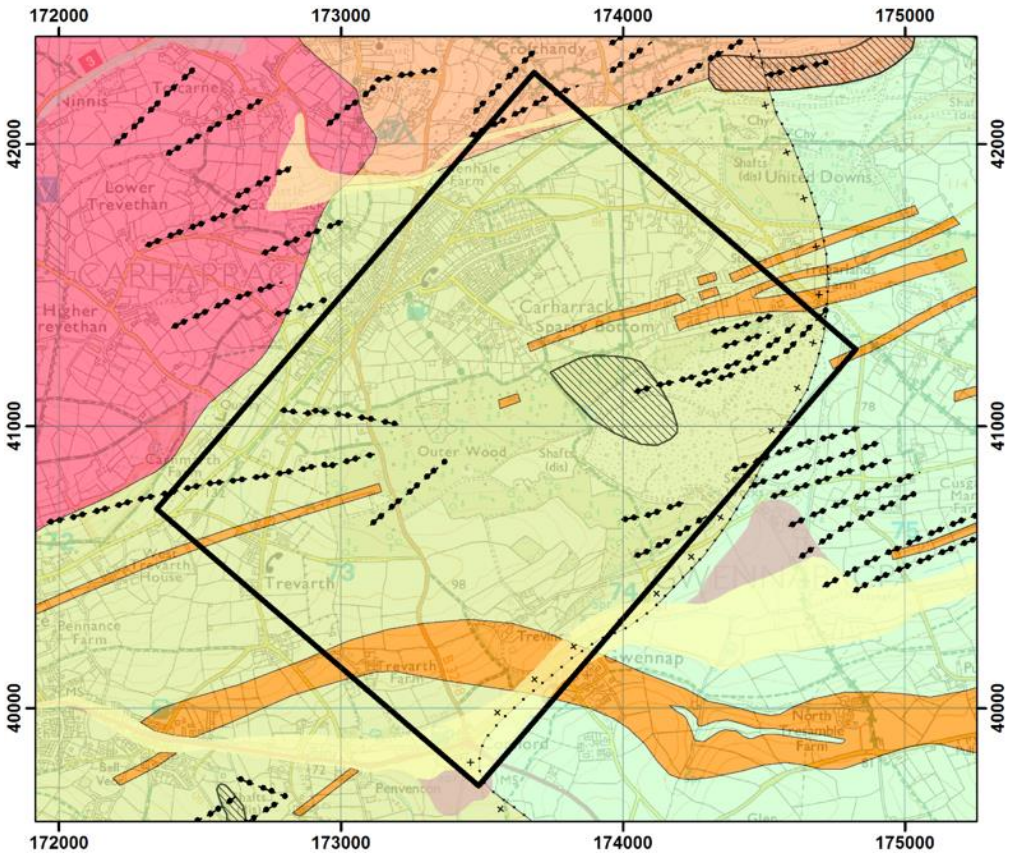

Figure 65: BGS 1:50 000 scale geological map of the UDDGP project site model area (thick black line) showing the general structure with NE-SW-trending mineral veins (dotted lines) and felsic intrusions (orange polygons) in the killas (green and blue). Note that no faults are shown on this map. Granite is coloured red and orange. Contains Ordnance Data © Crown Copyright and database rights [2019]. Ordnance Survey Licence no. 100021290. Contains British Geological Survey materials © NERC [2019].

There is not currently any published data on the fracture network in the UDDGP project target reservoir. However, given the consistency of the mapped fractures at surface across the Carnmenellis granite it was assumed that the fracture parameters will be similar to those used in the HDR project site model that is described above (Appendix 7). The workflow for the UDDGP project site model replicates that of the HDR project site model except for the addition of a fault zone, which is discussed in more detail below. In order to facilitate future geomechanical modelling the model was orientated so that it was parallel to the regional direction of maximum horizontal compressive stress. The UDDGP project is targeting a fault zone within the granite that may be more densely fractured, resulting in higher permeability and flow rates that will be sufficient development of a geothermal system, without the need for hydraulic stimulation of the reservoir.

The UDDGP project drilling target is an inferred 500 m wide fault zone located to the south-west of the site, and termed the Porthtowan Fault Zone (PTFZ). The faults have been mapped at surface as a series of smaller faults forming a board fault zone. The fault zone trends NNW-SSE and is aligned with the general trend of the cross-courses and strike-slip faults, such as the Sticklepath-Lustleigh fault zone near Dartmoor. These faults are considered to have been active during the Cenozoic and represent the most recent recorded fault movement within the area. However, there are inconsistencies between the mapped extent of the faults shown on the published 1:10 000 scale geological map (Figure 66) and a map published by Geothermal Engineering Ltd (Figure 67). The latter has been used in the modelling. The PTFZ is modelled as a volume of rock between two bounding fault surfaces located to the east and west, respectively. There is limited information on the vertical extent of the faults and the PTFZ has been modelled by the vertical projection of surface fault traces through the model. There is a large uncertainty regarding the presence, location and nature of the fault zone at reservoir depths that only drilling can reduce.

As the target reservoir for the UDDGP project is the Carnmenellis granite, and surface mapping has shown consistent fracture patterns across the granite, it is assumed that the two fracture sets used in the HDR project site model will persist across the UDDGP project site. This includes consistency in fracture density, length, aperture distributions and aspect ratio. However, the target fault zone adds additional complexity to this area.

Considering the uncertainty associated with the location of the faults within the PTFZ it was considered more appropriate to consider the fault zone and associated damage zone as a fractured volume of rock and therefore DFN modelling methods can be applied to attempt to represent the fault zone within the model. In addition to the two primary fracture sets identified in the HDR project site model, a third fracture set that is parallel to the fault strike was introduced. Studies of faults have shown that they tend to characterised by a fault core, surrounded by a region of damaged rock before transitioning into host rock. The density of fractures will be greatest close to the fault plane, reducing away from the fault. It was assumed that the fracture density within the fault zone is equivalent to the maximum density observed within well RH12 and RH15, which was 4.14 m^2/m^3. It was also assumed that the fault-related fracture density will reduce with distance from the fault. Accordingly, the inverse of the cube root of the distance from the fault scaled by 4.14 was used so that the maximum fracture density is at the fault plane and reduces smoothly away from the fault zone (Figure 68).

This is a conceptual model of the potential fracture density of the fault zone, which needs to be validated with additional data.

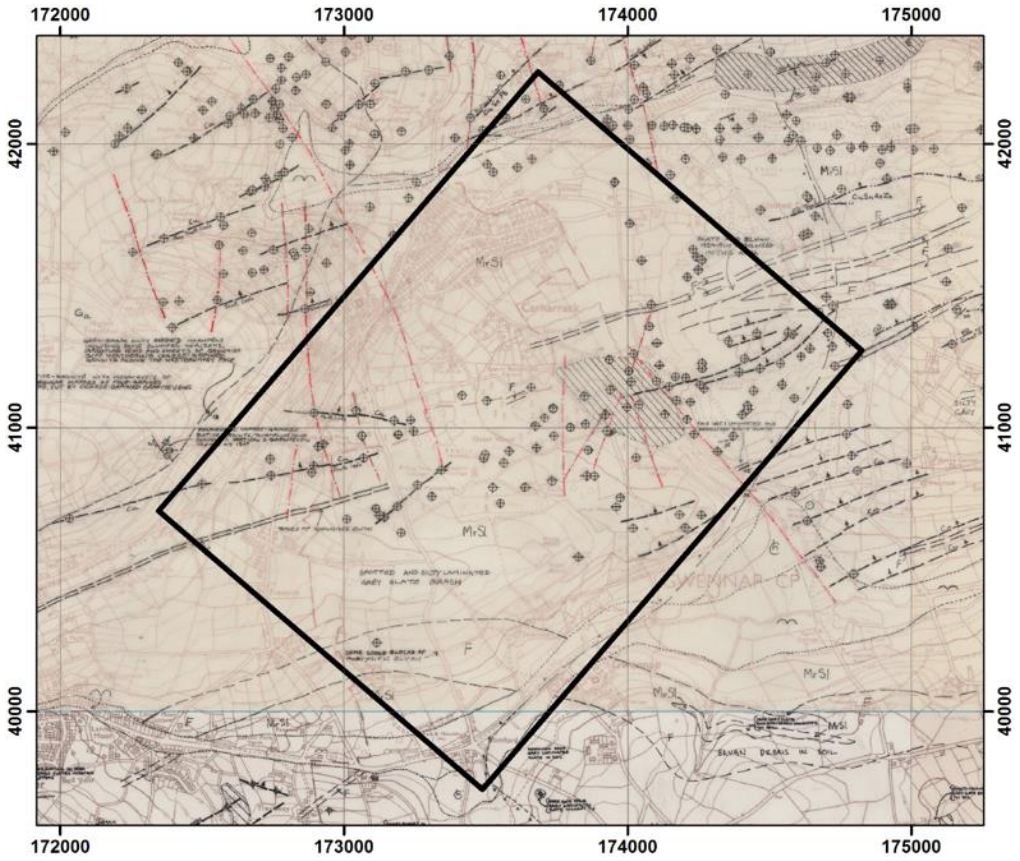

Figure 66: BGS published 1:10 000 scale mapped faults and veins across the area covered by the UDDGP project site model. Contains Ordnance Data © Crown Copyright and database rights [2019]. Ordnance Survey Licence no. 100021290. Contains British Geological Survey materials © NERC [2019].

Once the fracture network was generated, the resulting DFNs were up scaled into the voxel volume (Appendix 8) using the same approach described above for the HDR site project model. The up scaled permeabilities show a clear increase within the fault zone relative to the HDR site project model, despite the background permeability being similar. However, the model is likely to overestimate the permeability in the deeper reservoir as the fracture apertures used in the modelling are based on the measured flow within the shallower HDR wells. As previously discussed the fracture permeability is strongly controlled by the insitu stress, which increases with depth and may result in smaller effective apertures and therefore reduced permeability.

7.4 Uncertainties and limitations

There are a number of uncertainties and limitations to the current models. These include the range of assumptions used during the modelling workflow and the generalisation of the data. In terms of the regional model the greatest uncertainty remains the shape and extent of the granite. Although a revised top granite

surface has been developed, this is still largely based on the original gravity inversion with only minor corrections based on the additional data. At the borehole-scale there is likely to be a significant difference between the modelled granite surface and the depth at which granite is intersected. However, the top granite surface was only ever intended to be used for regional studies and at this scale it is considered to be adequate.

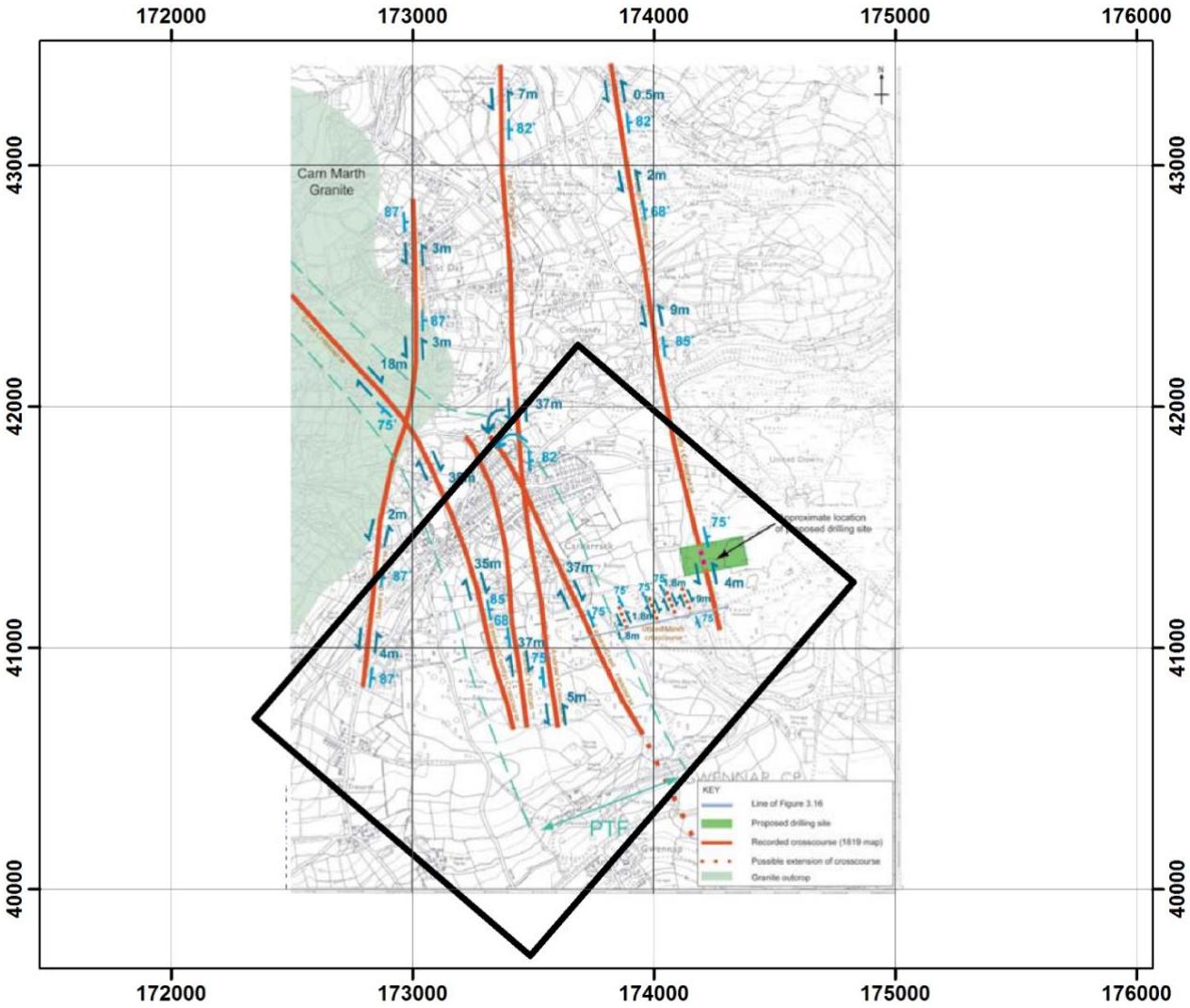

Figure 67: Map of the area of the UDDGP project site showing a number of NNE-SSW faults (orange) and the interpreted position of the Porthtowan Fault Zone (PTZ; Blue). Reproduced with permission of Geothermal Engineering Ltd 2018.

There are still large uncertainties regarding the depth of the base of the granite and the nature of the contact between the granites. A conservative depth to the base of the granite, of 12–15 km, was used in the modelling, which is based on one of the interpreted seismic reflectors. Additional research is required to better constrain the base of the granite, as future geothermal drilling in Cornwall may target even deeper, potentially higher temperature zones in the granite. If the base of the granite is shallower than predicted there is a risk that these deeper wells could extend through the base of the granite. In the current modelling the Cornubian Batholith is modelled as one contiguous granite body. However, it is known from surface mapping that the granite

consists of a number of distinct plutons. It is unclear what the shape of the individual granites is or how they potentially connect at depth. Only detailed exploration is likely resolve this.

Based on the modelled properties it is apparent that there is limited information on heat flow and heat production with depth, both of which have a significant impact on the assessment of the potential heat resource that could be extracted. The current drilling at the UDDGP project site and the associated data produced, including radiometric downhole surveys should significantly improve understanding of heat production at depths greater than 2.6 km in the Cornubian Batholith. The location of the UDDGP project boreholes on the flanks of the granite will also provide information on the thermal blanketing effect of the killas. The new data should also improve understanding of the consistency of the geothermal gradient across a larger area, and whether it is valid to extrapolate these values across the Cornubian granite, as has been done in the CHPM2030 project modelling.

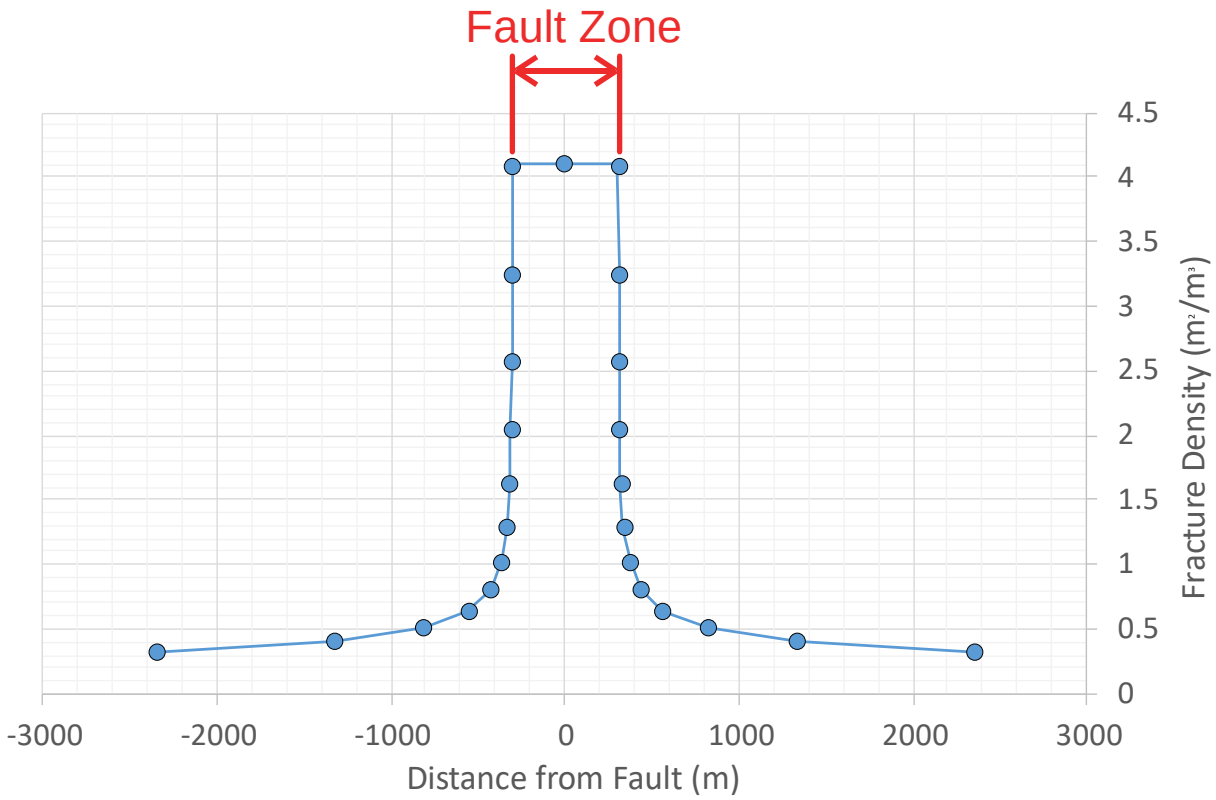

Figure 68: Idealised model of the change in fracture density with distance from the Porthtowan Fault Zone. British Geological Survey © UKRI.

At a regional scale the large faults in Cornwall are relatively well understood, however, their frequency and effect on the granite at depth is unknown. In the current modelling the faults are projected through the granite and over the full depth of the model, however, this may not be valid. It is possible that the faults may interact differently with the granite at depth, contrasting with how they behave in the near surface environment or in the metasedimentary country rocks.

For the site-scale models the greatest uncertainty relates to the position and properties of structures at depth. The nature of the fault-related fracturing has not been measured, and the data used in the UDDGP project site model represents an idealised system. Additional investigation is required to improve understanding of fault-related fracture systems and spatial relationships with the fault zone. This is considered essential for the concept on which the UDDGP project is based on (i.e. exploiting the natural permeability of a fault zone) to become widely accepted by the geothermal community.

Although the fracture system within the Carnmenellis granite is reasonably well understood the regional fracture system across the south-west is poorly defined. The least well understood fracture parameters include density, length and aperture. Further studies of fracture systems in granites across south-west England are essential for informing regional geothermal exploration. Although the site-scale models provide a qualitative assessment of the reservoirs, detailed numerical simulations are required to calibrate the models in order to understand how the reservoirs will evolve during production and to optimise development of the resource. This information could be used to better predict the thermal drawdown and the life expectancy of the reservoir. Flow and pumping data exists from the HDR project. This could be used to validate the models produced, providing confidence in the methodology and assumption used. As additional data becomes available this will need to be integrated into the UDDGP project site model, and calibration and validation can be undertaken.

8 Information for CHPM technology development

The UK HDR project, based at Rosemanowes Quarry, near Penryn in west Cornwall, aimed to demonstrate the feasibility of establishing a 'full-scale prototype' HDR power station in Cornwall. The project comprised three phases: i) focussed on experiments at shallow depth (300 m) that aimed to improve the permeability of the reservoir; ii) deeper (2500 m) studies focussed on the development of a HDR subsurface heat exchanger; and iii) development of a 'commercial depth' (~6 km deep) HDR prototype system. Phase 3A is particularly relevant to CHPM2030 as it examined the feasibility of creating an underground HDR heat exchanger, techniques for enhancing hydraulic performance and addressing the challenge of 'short circuits' in these systems, and modelling system performance, resource size and economic criteria (MacDonald et al., 1992).

8.1 Underground heat exchanger and metal enrichment

8.1.1 Expected reservoir characteristics

The philosophy for developing HDR systems in Cornwall has evolved substantially since the HDR research project, particularly the type of geological environment being targeted for the development of these systems and the requirement for artificial stimulation of the rock mass. The Rosemanowes test site is located in the eastern part of the Carnmenellis granite, away from any identified geological structures, in what was considered to be 'virgin' rock. Initial experimental work during the HDR project (Phase 1) focussed on enhancing the permeability of the rock mass surrounding the boreholes. Tests on boreholes at a depth of 300 m, employing a combination of explosives, hydraulic fracturing and water circulation, demonstrated that the impedance of the system could be reduced by a factor of 50 relative to the natural rock mass. The lowest flow impedance achieved at Rosemanowes was about 0.1 MPa per 1/s. However, it was noted at the time that the shallow level of the testing was unrepresentative of a deeper system (>400 m depth), in which the minimum principal stress would typically be horizontal, causing fractures to preferentially develop in the vertical plane.

Phase 2 in the HDR project, extending over an eight year period, focussed on development of a 'commercial-scale' heat exchanger. At the time, it was considered necessary to drill to a depth of 6 km to establish a 'commercial' system. However, to reduce drilling costs two boreholes to a depth of about 2 km were drilled. It was hoped that the results of this study would have relevance to the geological conditions at 6 km depth, but the limitations of these relatively shallow holes were acknowledged. During this phase defined as '2A', two holes (RH11 and RH12), deviated from the vertical by 30° were drilled to 2 km depth, and maintained at a separation of 300 m apart (Figure 69). Hydraulic fracturing was conducted in the lower borehole, with the aim of opening near-vertical joints that potentially rose upwards, joining it to the upper borehole.

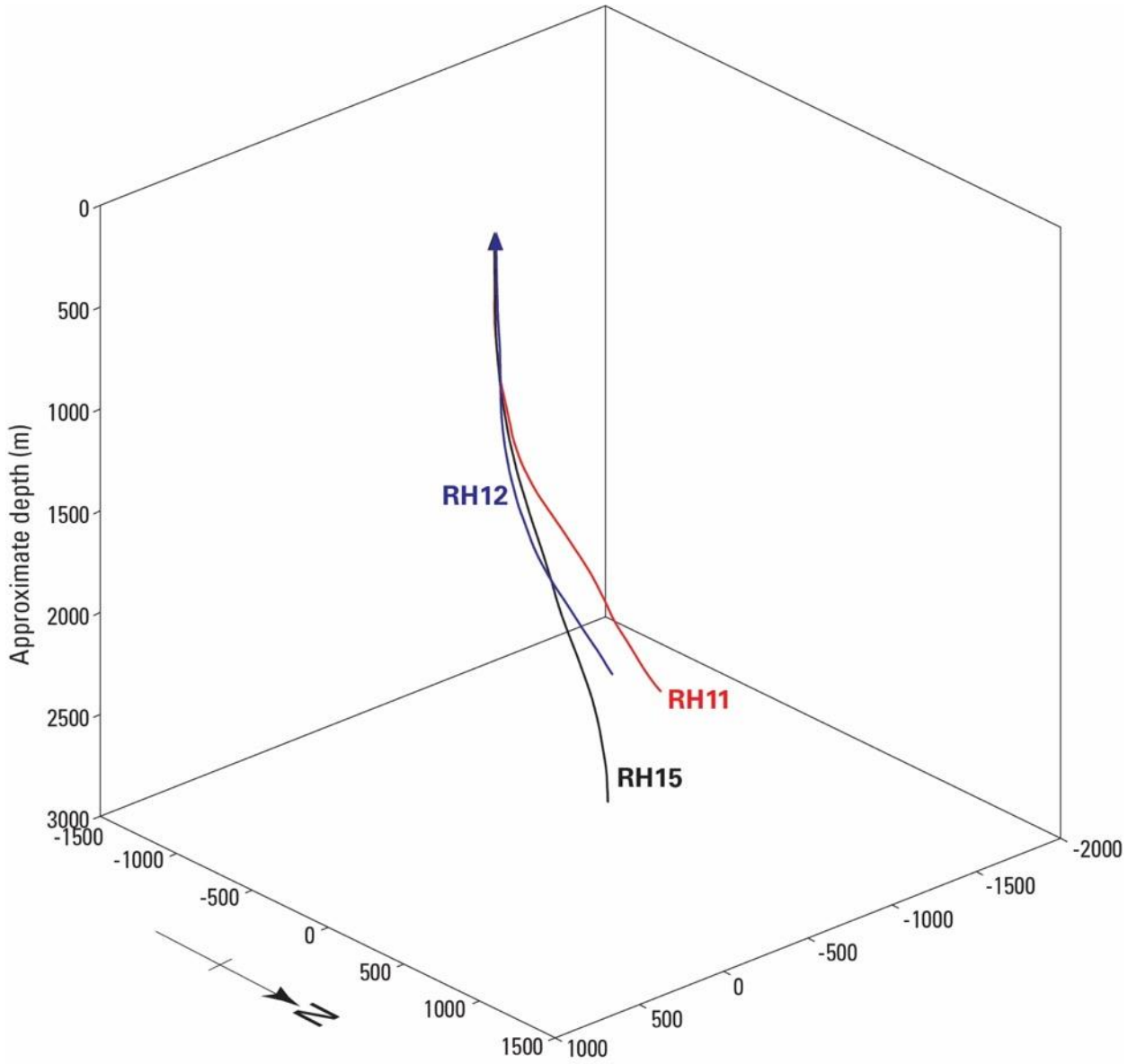

Figure 69: Configuration of the HDR project boreholes. Based on information supplied by Avalon Geoscience Ltd. British Geological Survey © UKRI.

However, when water circulation commenced fluids losses were excessive and the pumping pressures required to maintain circulation were excessive. It is reported that it was not possible 'to get within a factor of ten of the target production flow rate of 75 l/s. The poor connectivity between the boreholes was confirmed from pumping and tracer tests. Subsequent stress measurements indicated that the direction of maximum principal stress in the granite was closely aligned with the borehole deviation, the least desirable combination for intersecting joints that could easily be opened by hydraulic stimulation. As a result the project moved into Phase 2B, in which another borehole (RH15) was drilled to 2600 m depth. In an attempt to maximise the number of joint intersections, its trajectory crossed the microsesimic cloud (measured beneath each of the shallower boreholes during the stimulation and circulation tests, Figure 48), and was perpendicular to the vertical plane of the first two boreholes. A medium-viscosity gel was used to try and open up the volume of rock between borehole RH15 and the deeper of the two earlier holes (RH12). Using this new configuration

injection and production flow rates in the system were measured over a continuous four year period (Figure 70).

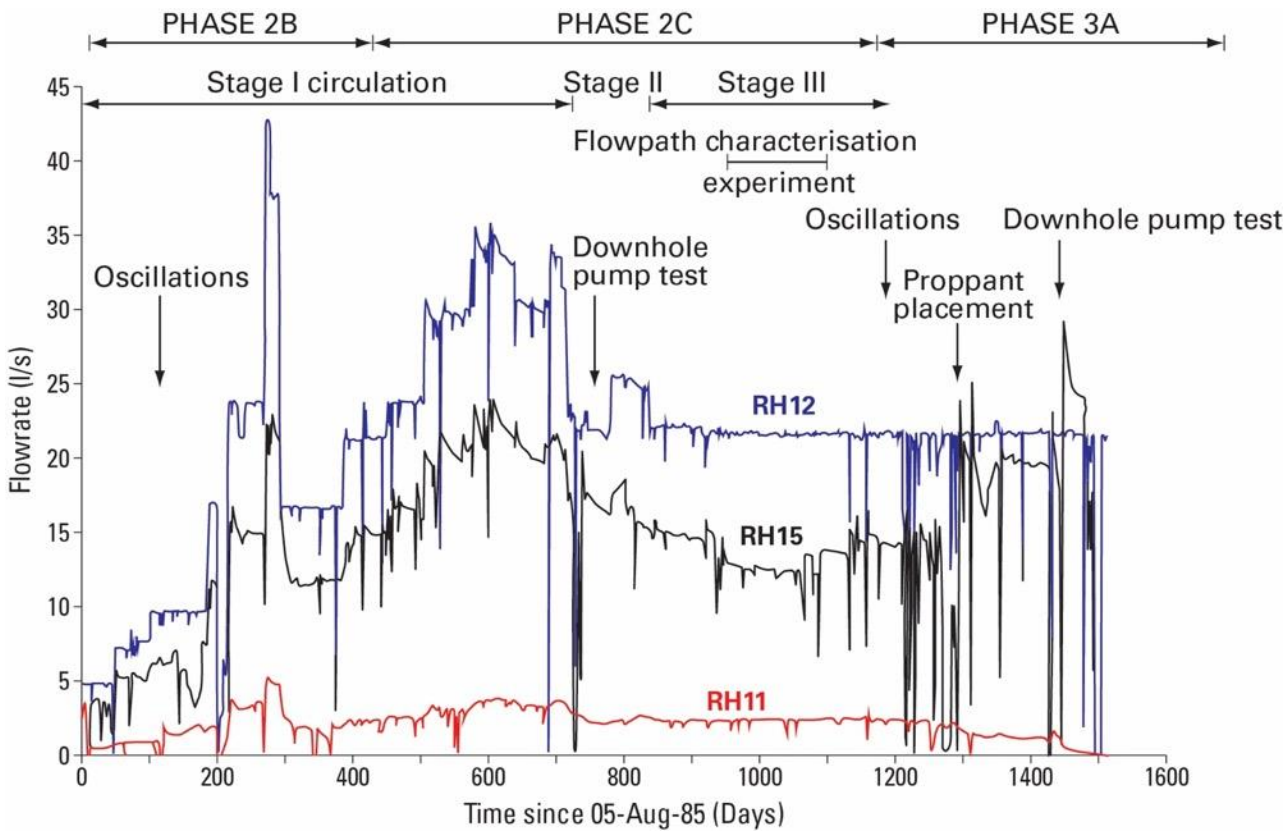

Figure 70: Injection and production flow rate measured in the Rosemanowes system, during the HDR project. Modified from Parker (1990), Contains public sector information licensed under the Open Government Licence v3.0.

The data showed that during Phase 2B there was a gradual increase in the injection flow rate (Figure 70). As the project progressed into Phase 2C and the injection pressure and flow rate increased, impedance in the system declined. It also demonstrated that at injection pressures exceeding 10 MPa above hydrostatic pressure water losses from the system were too great. It was concluded that the 'optimum hydraulic performance' that could be achieved at the Rosemanowes site was an injection flow rate of 24l/s, with impedance of 0.6 MPa per l/s and with a water loss of 21 per cent. This level of hydraulic performance was considerably lower than that considered desirable for a 'commercial' prototype. A further concern was that although the RH12/RH15 system had lower impedance and water losses than the previous configuration (circulation between RH11 and RH12) there was a decline in thermal performance. Over a three year period the temperature at the top of the of production borehole declined from 80°C to 55°C. Flow path modelling of the system using tracer and subsequent thermal modelling showed that a 'short circuit' existed between the boreholes, significantly reducing its effectiveness as a heat exchanger. It was concluded that the granite surrounding the area of the short circuit had cooled more quickly than the rest of the reservoir causing cooler water to enter the production borehole. Towards the end of Phase 2 a review of the programme examined the status of HDR technology in south-west England, and identified the following specific issues: i) the size of the subsurface heat exchanged available was considerably smaller than required for a 'commercial' system; ii) short circuiting reduced the thermal efficiency of the heat exchanger and water losses were too great; iii) the

experimental work had not managed to demonstrate the concept of being able to engineer a underground heat exchanger; and iv) a 'commercial'-scale system may require the development of a number of underground 'modules' operated in parallel. Despite these problems the experimental work continued into a third phase (3A). An experiment in Phase 3A involved injecting sand, as a proppant material, into the joints surrounding the production well. The sand was introduced into the system using a high viscosity (700 cP) gel during a secondary stimulation stage. This stimulation reduced water loss and impedance of the system, but exacerbated the short circuiting and caused a further decline in the water temperature from the production borehole (Figure 71). Another experiment attempted to address the short circuiting by shutting off the problematic section of the production borehole using a temporary packer assembly. Subsequent flow testing showed that the short circuit had been sealed off, but a very low flow rate resulted, which was not be corrected by further stimulation. It was concluded that this stimulation failed to establish a connection with the previously stimulated zone that ran parallel to it. Phase 3A of the project also resulted in a conceptual design for a 6 km deep, 'commercial' HDR prototype power station and cost modelling for a HDR power station are described in Section 9.2 (MacDonald et al., 1992).

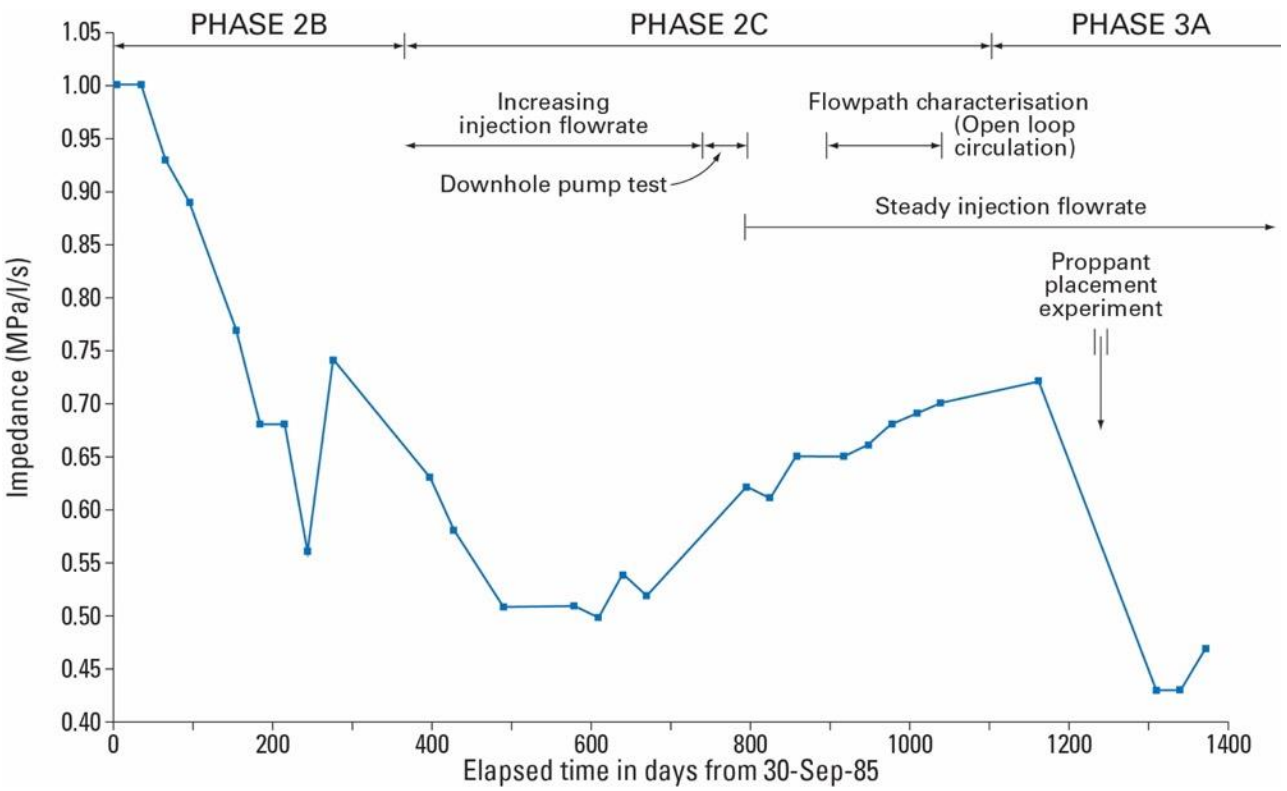

Figure 71: Impedance in the RH12/RH15 system. Modified from Parker (1990), Contains public sector information licensed under the Open Government Licence v3.0.

Whilst building on the experience and expertise developed during the HDR project the current (drilling commenced in November 2018) United Downs Deep Geothermal Power (UDDGP) project, operated by Geothermal Engineering Limited (GEL) plans to test a new concept for EGS development in Cornwall. From the reconnaissance stage it was assumed that the rock matrix being targeted for an EGS in Cornwall would have

low to very low porosity and permeability. In fact there is little evidence for the granite in south-west England having sufficient transmissivity for geothermal circulation without reservoir stimulation. However, it is acknowledged that the existing lack of evidence largely results from limited deep subsurface investigation, which could identify fault, fracture and weathered zones creating natural permeability that is exploitable as a geothermal reservoir (Atkins, 2013). Accordingly, development of a geothermal reservoir in the Cornubian Batholith would be dependent on the presence of fracture-controlled permeability, and this would have to be of an adequate size to host a commercial-scale heat exchanger, and extend deep enough to reach sufficient temperatures (Ledingham et al., 2019).

The UDDGP, located to the east of the Carnmarth granite (Figure 7), is actively targeting a structurally complex zone, with the objective of exploiting the natural permeability that exists in the fracture system to circulate water between two boreholes. The target geological structure is termed the 'Porthtowan Fault Zone' (PTFZ), which is located about 800 m to the west of the United Downs drilling site (Geothermal Engineering Ltd, 2018e). GEL describe the PTFZ as 'a geological structure which extends across Cornwall from Porthtowan on the north coast to Falmouth on the south coast. It is no longer active but it should contain a concentration of natural fractures…' (Geothermal Engineering Ltd, 2018b). It is a >15 km long NNW-SSE orientated strike-slip fault. It unlikely to represent a discreet structure, but rather a 200–500 m wide feature, comprised of several anastomosing faults. It is assumed to be near-vertical and extend to EGS depths, based upon its linearity. It is reportedly mapped along the NE side of the Carnmenellis granite and has been identified in some of the mines in the area. Cross-course structure identified in the mines, which have the same orientation as the PTFZ frequently result in bad ground, as a result of fracturing and are zones of fluid flow. It is hoped that the PTFZ shares these characteristics (Ledingham et al., 2019). Estimates of the permeability and transmissivity of the PTFZ have been made based on a number of assumptions. Ledingham et al. (2019) indicate that if the PTFZ is assumed to have true width of 200 m and two fractures occur every metre that have an aperture of 90 µm, the entire zone would have a transmissivity of 123 mD, resulting in a transmissivity of about 25 Dm. It is acknowledged that this transmissivity value is relatively low for a productive geothermal reservoir (Ledingham et al., 2019). For comparison, drilling for geothermal exploration in the Weardale granite of northern England, also targeting a major, linear, sub-vertical structure encountered a highly permeable zone at a depth of about 400 m and a transmissivity of 4000 Dm (= 3×10^{-9} m^2 m) was obtained from a 21 m interval in the borehole. This is more than 20 times greater than maximum value reported elsewhere from granites and other crystalline rocks. However, in terms of the entire granite sequence drilled (almost 600 m) more than 99 per cent of the total transmissivity is accounted for by the fracture zone in the 21 m interval (Younger and Manning, 2010).

GEL conducted heat flow modelling of the United Downs area, and at a vertical depth of 4500 m (the bottom of the production well) it is predicted that the temperature will be between 180–220°C (at a 90 per cent confidence level). Based on this, and the expected transmissivity the project aims to produce water at the surface at about 175°C, with a circulation flow rate of between 20–60 l/s (Ledingham et al., 2019).

8.1.2 Expected types of mineralisation and metal enrichment

The only information available on the potential for deep (>1 km) metal enrichment in Cornwall comes from drilling and logs from the HDR experiments, and the current UDDGP project. Minor sulfide was logged in RH15 at depths in excess of 2200 m. Limited published information is available on the UD-1 well to a depth of about 2000 m. The initial 210 m of the hole was dominated by killas. Persistent, steeply dipping quartz veins were encountered in this section. Granite was first intersected at a depth of 210–230 m. It was a fine-grained

kaolinised microgranite. It is reported that in the upper 1000 m of UD-1 'a number of predicated mineral lodes and cross-course structures….were encountered.' (Ledingham et al., 2019). These were presumably 'predicted' on the basis of the known abundance of mineralisation in the United Downs area. Below 250 m depth the near-bit gamma log showed peaks that corresponded with the observation of 'mineralization' in the drill chippings. A chlorite-rich zone at 750 m correlates with a gamma ray peak and is described in the evaluation log as a 'hydrothermal quartz-chlorite lode', containing 50–75 per cent quartz, with accessory phases including chlorite, tourmaline, muscovite, arsenopyrite, chalcopyrite and cassiterite, and no oxidation present. A feature described as a 'sulphide-rich lode' was also encountered at 1325–1335 m depth. Apparently mineralised chippings coincided with an increase in the rate of drilling progress, a peak in the gamma log and decline in the weight on bit. In the drill evaluation log this 'hydrothermal lode' is described as containing pyrite, cassiterite, tourmaline, quartz, biotite, and muscovite, with no evidence of mineral oxidation (Ledingham et al., 2019). Despite this encouraging information, at the time of writing, no direct evidence exists for the existence of substantial mineralisation at EGS reservoir depths (4–5 km) in Cornwall. However, equally there is currently no reason to conclude that it does not extend to these depths. There is a growing body of global of evidence to suggest that fracture-controlled fluid flow, and therefore the potential for mineral deposit formation, can occur at depths of several to tens of kilometres (Barnes, 1997). Assuming the abundant near-surface, metallic mineralisation of the Cornubian orefield (Section 5.1) is stable under the pressures and temperature at 4–5 km, in order to proceed with the CHPM concept and other components of the design, it should be assumed that any mineralisation occurring at reservoir depths is most likely to be of similar style and composition. The release of additional data from the UDDGP project may help to verify this.

8.2 Production and injection wells

In the original design for the HDR project the injection borehole (RH12) was below the production borehole (RH11), because it was assumed that the injected water would move upwards (Figure 69). In contrast this experiment demonstrated that the water migrated downwards, along favourably orientated joints. The position of RD15, below RH12 attempted to correct for this issue. The stress regime at the UDDGP project location will be the same as at Rosemanowes, therefore, downward migration of injected water is expected, although if necessary this could be facilitated by temporary increases of the injection pressure (Ledingham et al., 2019).

The UDDGP project aims to drill two boreholes that will both intersect the PTFZ (Figure 72). A borehole to about 2500 m will be used for water injection, whilst a deeper hole extending to about 4500 m will be used for production (Geothermal Engineering Ltd, 2018e). A downhole pump in the production well will drive the UDDGP system. This will result in a pressure sink around the production well, causing water to migrate towards it from the injection well and the broader rock mass. It is predicted that even moderate injection pressures will result in shearing on favourably orientated fractures, which likely to occur at pressures as low as 5 Mpa (Ledingham et al., 2019).

Well spacing is a major consideration in EGS design and is dependent on range of factors, including the expected permeability of the reservoir. The UDDGP project concept is based on the assumption that the natural fracture-controlled permeability, resulting from the PTFZ, will be sufficient to permit fluid circulation over a large vertical distance. High permeability coupled with a large (c. 2000 m) separation between the injection and production wells is hoped to result in a sufficiently large natural heat exchanger for a commercial-

scale operation. The large separation should also reduce the risk of short-circuiting of flow from the injector to producer wells, which is detrimental to system performance (Ledingham et al., 2019).

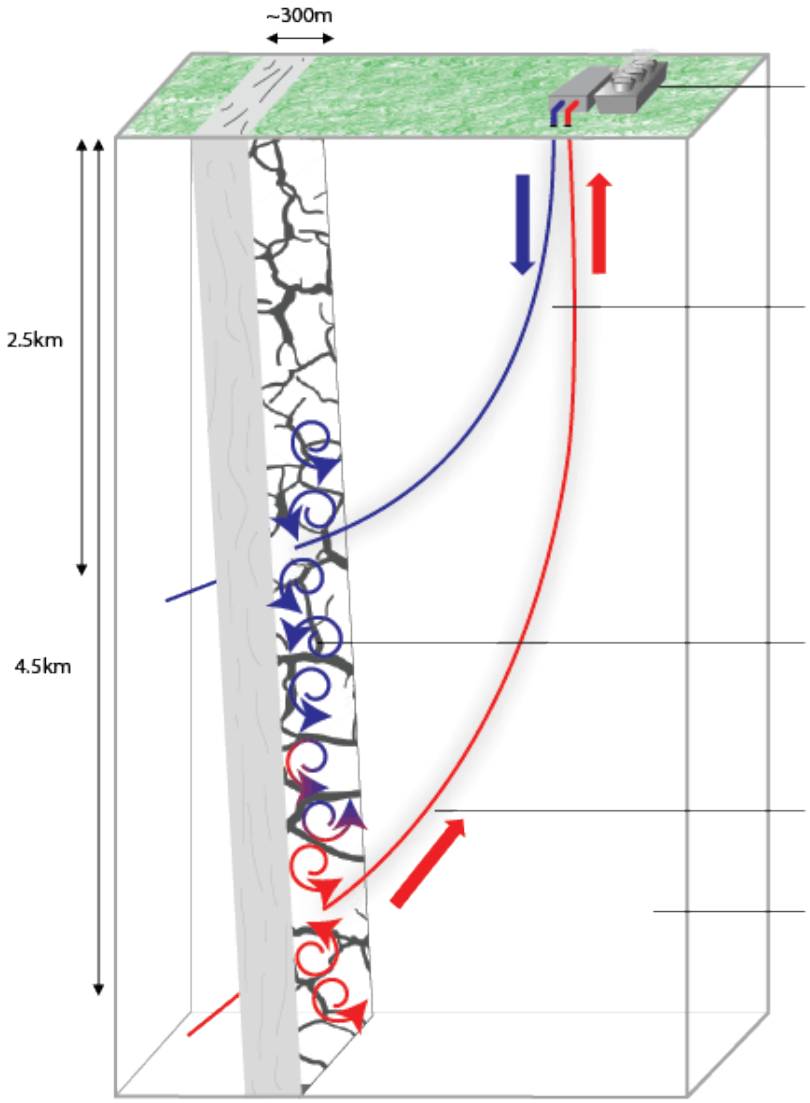

Figure 72: Schematic representation of the planned EGS system for the United Downs Deep Geothermal Power project. Water will be injected into the ground through the shallower injection well (blue), obtain heat from the rocks and return to the surface up a deeper production well (red), fed through a heat exchanger and then re-injected into the ground to collect more heat in a continuous cycle. The extracted heat will be used to supply a demonstration power plant. Reproduced with permission of Geothermal Engineering Ltd 2018.

At surface the well centres are only 8 m apart, which is a function of the space limitations on the site. Initially the wells will be 24 inches (609.6 mm) in diameter and vertical, but as they become deeper they will be deviated towards the SW to try and intersect the PTFZ (predicted to be about 700 m way from the well centres), and gradually narrowed in diameter (Table 6) (Geothermal Engineering Ltd, 2018a). The kickoff points for the wells will be 1110 m and 3400 m for the injection and production wells, respectively (Ledingham et al.,

2019). The two holes will be steel cased for the majority of their length, with the last few hundred metres being open hole, with a terminal diameter of 8.5 inches (Geothermal Engineering Ltd, 2018a).

Table 6: The planned completions for the two wells that will be drilled at the United Downs Deep Geothermal Power project. Reproduced from Ledingham et al. (2019).

Injection well			Production well		
Drilled diameter (mm)	Depth	Casing size (mm)	Drilled diameter (mm)	Depth	Casing size (mm)
24" (609.6)	250 m	18 5/8" (473.07)	24" (609.6)	250 m	18 5/8" (473.07)
17 ½" (444.5)	900 m	13 5/8" (346.07)	17 ½" (444.5)	900 m	13 5/8" (346.07)
12 ¼" (311.15)	4000 m	9 5/8" (244.47)	12 ¼" (311.15)	4000 m	9 5/8" (244.47)
8 ½" (215.9)			8 ½" (215.9)		

8.3 Power plant and local energy demand

If establishing an operational geothermal system is successful the UDDGP project plans to construct a demonstration power plant to supply power to the UK national grid. Initial plans are to establish a 1MWe plant, whilst considering the potential to expand the size to 3MWe (this limit of the available grid connection), subject to system performance and availability of further funding. Preliminary plans for plant design involve the use of a binary power plant (Geothermal Engineering Ltd, 2018d). Cornwall Council published a technical paper on energy projection for the county. Total final energy demand in Cornwall (excluding aviation and shipping) was projected to fall by nine per cent from 1,030 kilo tonnes of oil equivalent (ktoe) in 2007 to 939 ktoe in 2030. Considering increases in population, final energy demand per person in Cornwall was projected to decrease from 1.954 toe in 2007 to 1.490 toe in 2030. Final energy demand per household was projected to decrease from 4.496 toe in 2007 to 3.172 toe in 2030. Demand for renewables and bio-fuels was projected to increase in Cornwall from 5 ktoe in 2007 to 101 ktoe in 2030 (Table 7) (Cornwall Council, 2013b).

8.4 Salt gradient power generation

The concept of salinity gradient power relies on the existence of two solutions with large differences in salt concentration. Freshwater represents a low salinity solution that could be used in this process. The south-west of England experiences average annual rainfall values in the range of 1000 and 1500 mm, meaning access to water in the CHPM study area is unlikely to be a problem. Surface drainage in the study area is characterised by a radiating pattern of small rivers that drain off the high-ground of the granite (c. 300 m above sea-level) towards the coast (c. 60 m above sea level). The majority of water used in the study area is derived from surface water sources, for example Stithians Reservoir, which has a capacity of about 5 million litres. Very little water is sourced from underground aquifers (i.e. groundwaters), because the rocks that comprise the study area have very low-primary permeability and are therefore classified as low productivity aquifers. Historically water has been drawn from disused mine shafts and adits for public supply and agricultural uses, although it is unclear if this practice still takes place. Similarly, shallow (10–15 m deep) groundwaters held in weathered and fractured granite and country rock (killas) has also been used as a local water source; however, borehole yields are typically very low. For example, the average yield from 73 boreholes in the Carnmenellis granite was about 37 m^3 per day (Leveridge et al., 1990).

Table 7: Energy demand by final user in kilo tonnes of oil equivalent. For details of the calculations and data sources used and table notes see (Cornwall Council, 2013b). Reproduced from Cornwall Council (2013b).

		2007	2010	2015	2020	2025	2030
Domestic	Electricity	116	114	90	87	94	105
	Gas	146	160	131	126	132	139
	Petroleum	65	73	29	17	18	15
	Coal/ Manufactured fuels	5	5	5	5	5	7
	Renewables	0	4	28	35	36	37
	TOTAL	**332**	**356**	**283**	**270**	**285**	**303**
Industrial and commercial	Electricity	131	123	132	136	141	149
	Gas	113	107	100	81	77	80
	Petroleum	102	78	74	60	56	54
	Coal/ Manufactured fuels	5	5	4	4	3	3
	Renewables	5	8	18	57	57	57
	TOTAL	**356**	**327**	**331**	**326**	**323**	**332**
Transport	Electricity	0	1	1	2	1	1
	Petroleum (Rail)	10	9	10	10	9	9
	Petroleum (Road)	336	312	294	280	282	276
	Bio-fuel	0	3	9	16	6	7
	TOTAL	**346**	**325**	**314**	**308**	**298**	**293**
TOTAL	Electricity	247	238	223	225	236	255
	Gas	259	266	232	207	209	219
	Petroleum	513	472	407	367	365	355
	Coal/ Manufactured fuels	10	10	9	9	8	9
	Renewables and bio-fuels	5	15	55	108	99	101
	TOTAL	**1,034**	**1001**	**926**	**916**	**917**	**939**

The composition of shallow groundwater in the study area is largely controlled by the bedrock lithology, and to a lesser extent metallic mineralisation and farming practices. The groundwaters are typically low-salinity, mildly acidic and have relatively low total dissolved solids (TDS) content. However, groundwaters from the country rock (killas) have a higher TDS content and major ion concentration than those from the granite. Groundwaters from both rock types are typically soft, with $CaCO_3$ contents of between 24 and 116 mg l^{-1}. However, groundwaters from the granite tend to have lower $CaCO_3$ contents (24–43 mg l^{-1}) and are therefore more acidic (pH between 4 and 7), than those from the country rock (pH between 5 and 8) (Leveridge et al., 1990) (Table 8). Further details about groundwater and surface water chemistry can be found in Smedley et al. (1989).

Table 8: A summary of selected parameters for granite-hosted and country rock (killas) hosted groundwaters. Data from Leveridge et al. (1990).

	Granite groundwaters			Country rock (killas) groundwaters		
Temperature (°C)	15.6	10.8	14.5	12.5	18.5	13.8
pH	6.78	5.13	5.70	6.94	6.62	6.32
SEC (µS/cm)	200	210	112	210	120	340
TDS (mg l^{-1})	97.2	70.2	83.4	92.5	128	198
Total hardness (mg l^{-1} $CaCO_3$)	43	24	37	45	58	116
Sodium (mg l^{-1})	13.4	13.7	18.8	13.9	30.9	20.6
Chloride (mg l^{-1})	24	22	28	23	41	36
Silica (mg l^{-1})	1.0	4.1	4.1	2.2	11.4	2.5

9 Operational characteristics

9.1 Environmental, social and political background

9.1.1 Environmental

The HDR project took place in a quarry, which was chosen because it was on the exposed Carnmenellis granite and no major structural features were evident at the surface (Parker, 1991). The quarry is principally surrounded by arable farmland, traversed by a number of minor roads, with the A394 to its immediate south. A number of villages and smaller settlements are located within a 1 km radius of the site. Three reservoirs are located less than 3.5 km from the quarry (Figure 73). Although it is unclear whether it was a criteria for site selection at the time, the quarry setting represented a brownfield site, and would have significantly shielded the operations that took place for some 14 years. The location in the base of the quarry would have helped to reduce the visual impact of the drilling rig and well towers (Figure 3A and Figure 74).

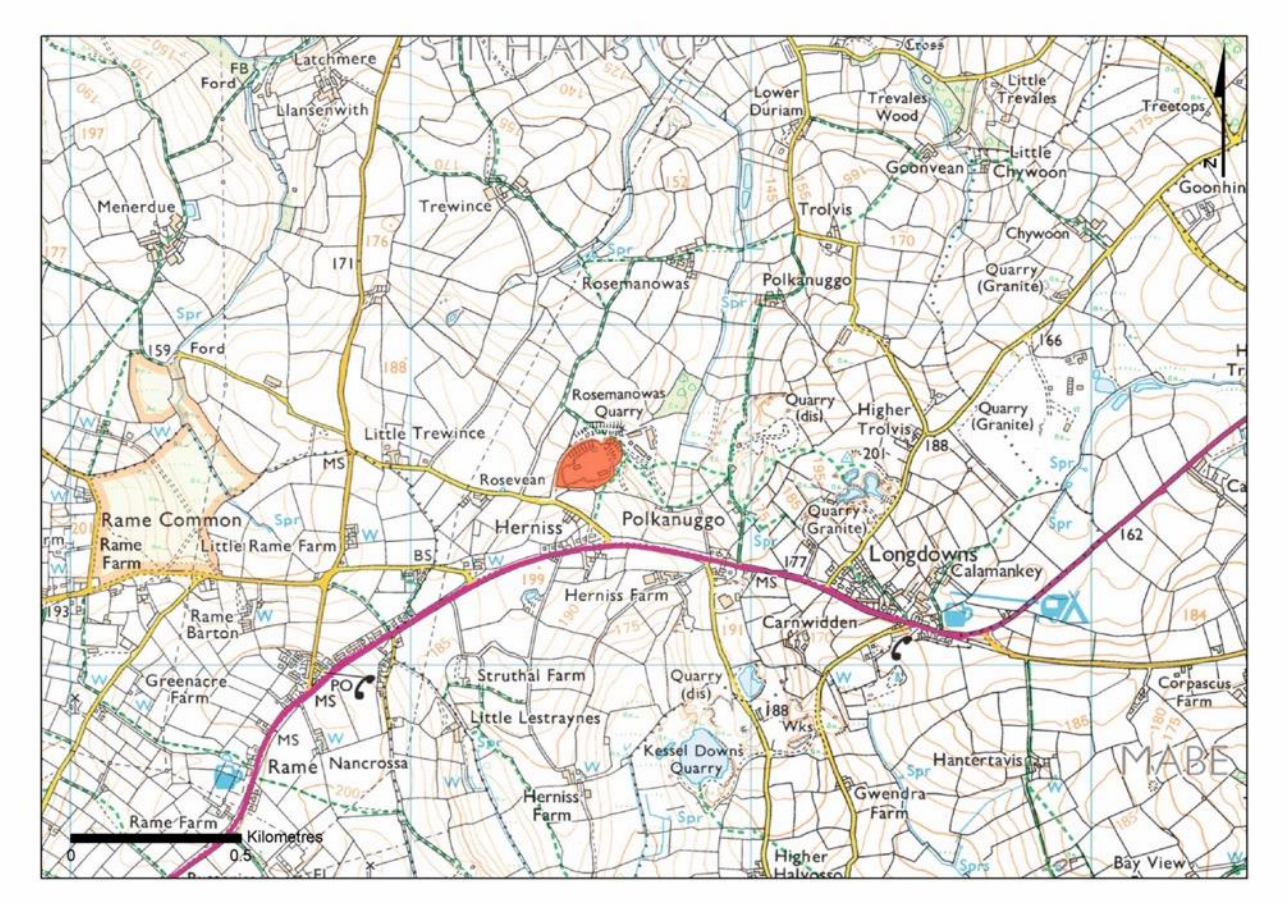

Figure 73: Location of Rosemanowes Quarry (shaded red) and the surrounding land use and infrastructure. Contains Ordnance Data © Crown Copyright and database rights [2019]. Ordnance Survey Licence no. 100021290. British Geological Survey © UKRI.

The location of the UDDGP project site, its extent and the current development provide the best indications of the potential environmental impacts of future geothermal resource development in Cornwall. The UDDGP project site is located 4.1 km east of Redruth and about 7 km north of the old HDR project site (Figure 7 and Figure 75).

Figure 74: Operations at the Rosemanowes HDR project site during the 1980s and 1990s. A/B. Aerial view of the quarry during drilling operations. C. View across the quarry and of the two towers. D. Steamy water being generated at a wellhead. E. Construction of the cistern for the boreholes. F. The cascade and water lagoon at the site. Images reproduced from the HDR project photo archive held by the British Geological Survey.

There were several locations in the area from which the PTFZ could have been targeted with drilling. However, with the exception of the United Downs Industrial Estate these were all greenfield sites. Given the existence of a brownfield site strong justification would be required for selection of an alternative (pers. comm.). Geothermal Engineering Ltd (2018) indicate that other considerations were good road access, sufficient space for the drilling rig, a relatively flat site, proximity to the National Grid and availability of services.

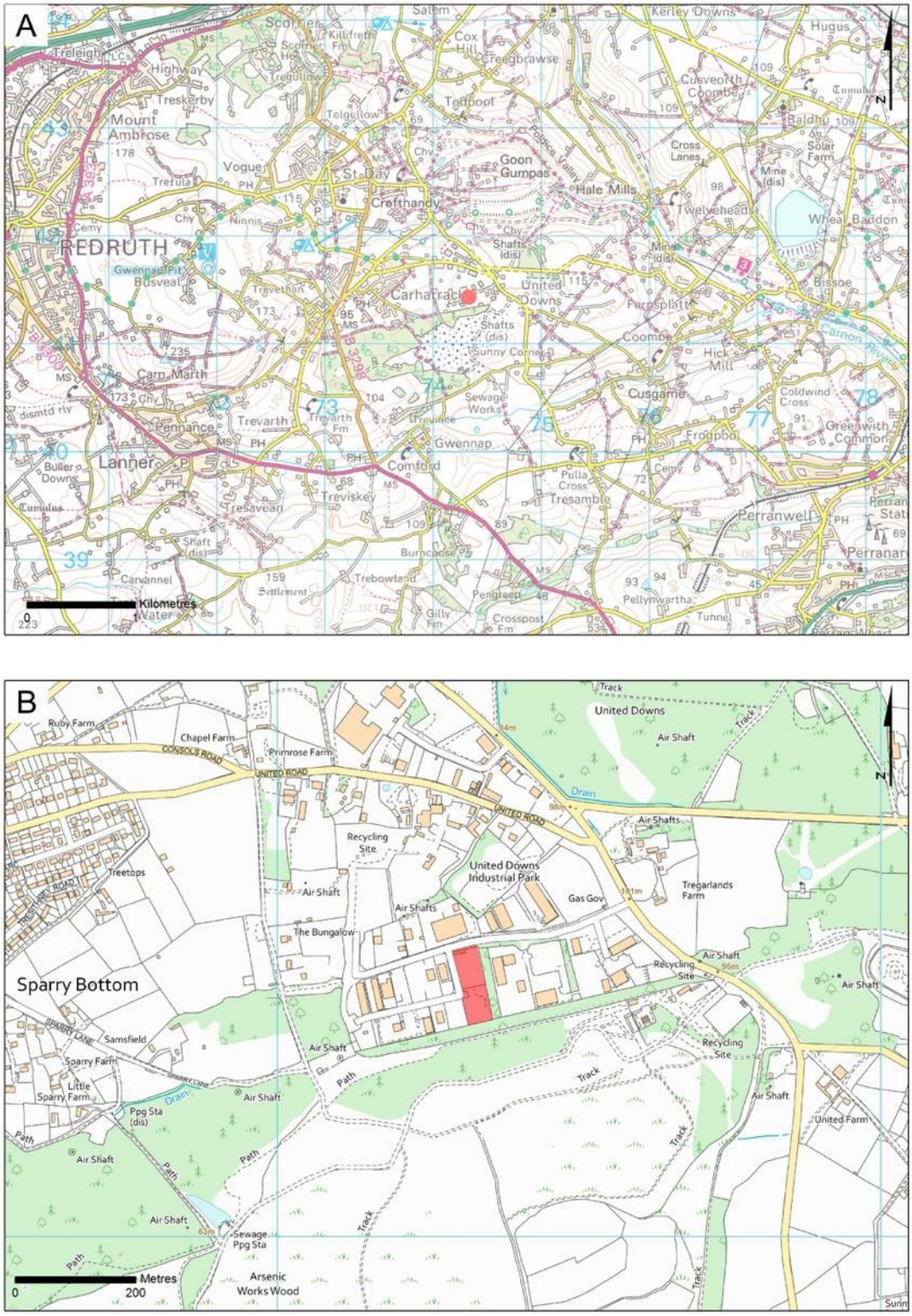

Figure 75: Location of the United Downs Deep Geothermal Power project and the surrounding land use and infrastructure. A. General location of the site (red circle) east of Redruth. B. Position of the site on the United Down Industrial Park. Contains Ordnance Data © Crown Copyright and database rights [2019]. Ordnance Survey Licence no. 100021290. British Geological Survey © UKRI.

In March 2010 Geothermal Engineering Ltd (GEL) submitted a 'hybrid' (comprising part detail, part 'outline') planning permission application (NR/10/00056/GEO) to Cornwall Council for geothermal exploration and development on, on an unoccupied plot on the United Downs Industrial Estate (Figure 76). The 'detailed' part of the application covered the drilling of the wells and associated pumping and test equipment. Whilst only 'outline' information was provided for the development of a power generating plant, pumping equipment and electrical infrastructure etc. The scheme received no objections from both statutory consultees and local residents, and planning permission was granted in October 2010 (Cornwall Council, 2012). All planning application documents are available online from Cornwall Council (Cornwall Council, 2019). These include specific documents relating to ecology, landscape and visual impact, geology and hydrology, noise and vibration and public consultation.

Figure 76: Nature of the land use surrounding the United Downs Deep Geothermal Power project site (outlined in red). British Geological Survey © UKRI.

9.1.1.1 Noise and microseismic monitoring at the UDDGP project

Geothermal Engineering Ltd (2018b) indicate that the principal environmental impacts associated with the UDDGP project relate to the exploration of the geothermal resource, which requires the drilling of two boreholes. The drilling rig and its diesel power generators represent a potential source of noise and it has a visual impact. The industrial site on which the drilling rig is located is noisy during the day, but not active over night or at weekends. Private housing exists along the western, northern and eastern perimeter of the industrial estate. The closest properties are about 300 m from the site, and the nearest village of Carharrach is less than 1 km to the west (Figure 75

Figure 75). The planning consent specifies the maximum acceptable noise levels during day and night. Background monitoring and predictive modelling was undertaken to predict the noise levels in the area surrounding the site (Ledingham et al., 2019). The drilling rig being used for the UDDGP project is a new generation semi-automated hydraulic rig. The H. Anger's Söhne Innova rig was constructed in 2007 and according to the manufacturer it has been designed to minimise environmental impact, as the space required to install the rig is much smaller than is necessary for conventional rigs; and it produces considerably less noise, making it beneficial for use in urban and noise-sensitive environments (H. Anger's Söhne, 2019), such as United Downs. In addition a range of noise mitigation and attenuation measures have been implemented at the drilling site, including the use of acoustic barriers. Continuous noise monitoring is taking place during the drilling phase, with sensors positioned on site and remotely (Ledingham et al., 2019). GEL have published a project 'noise management information sheet' (Geothermal Engineering Ltd, 2018f). Ledingham et al. (2019) indicates that only on a 'handful' of occasions have noise levels from drilling approached or exceeded the pre-set limits. GEL have established a noise reporting system, and it is reported that some local residents have complained about noise resulting from the drilling rig, despite the noise levels being below the threshold set in the planning consent (Ledingham et al., 2019).

The drilling rig comprises a mast, substructure, top drive, substructure, generators, pumps, drilling mud system, waste handling and data recording and has sufficient drill pipe to drill to more than 5000 m. The height of the mast of the rig is 51.8 m above ground level, meaning it is visible for some distance from the site (Figure 77). Drilling the two wells is anticipated to take six to seven months, operating 24 hours a day, 7 days a week (Geothermal Engineering Ltd, 2018b), therefore these specific impacts associated with the rig are short-term in nature. A further impact arising from the rig relates to its transportation to the UDDGP project site by road. This means during mobilisation and demobilisation of the rig there will be many (~70) large transport vehicles accessing the site over a 10–14 day period (Geothermal Engineering Ltd, 2018f).

Induced seismicity is a concern in all projects that involve deep drilling and water circulation through fractures. Geothermal Engineering Ltd (2018b) indicate that 'Testing and operating the geothermal reservoir will cause some micro-earthquakes but nearly all will be too small to be felt at surface.' During the HDR project tens of thousands of micro-events were recorded, however, it is reported that only two were felt at the surface (Geothermal Engineering Ltd, 2018b). In the planning consent for the project the local planning authority included a requirement for both seismic monitoring and for a monitoring and control protocol. A monitoring network has been installed on and around the site that combines microseismic and ground vibration monitoring systems. This will be capable of detecting seismic events down to magnitude 0.0 at a depth of 5 km around the reservoir, and to magnitude of 1.0 across a wider, 10 km x 10 km area. Background monitoring commenced several months before the drilling started. Data is transmitted from each station to a central processing centre, where a system automatically detects events. Data from the monitoring system is transferred to the British Geological Survey who make them publically available via their website (Ledingham et al., 2019).

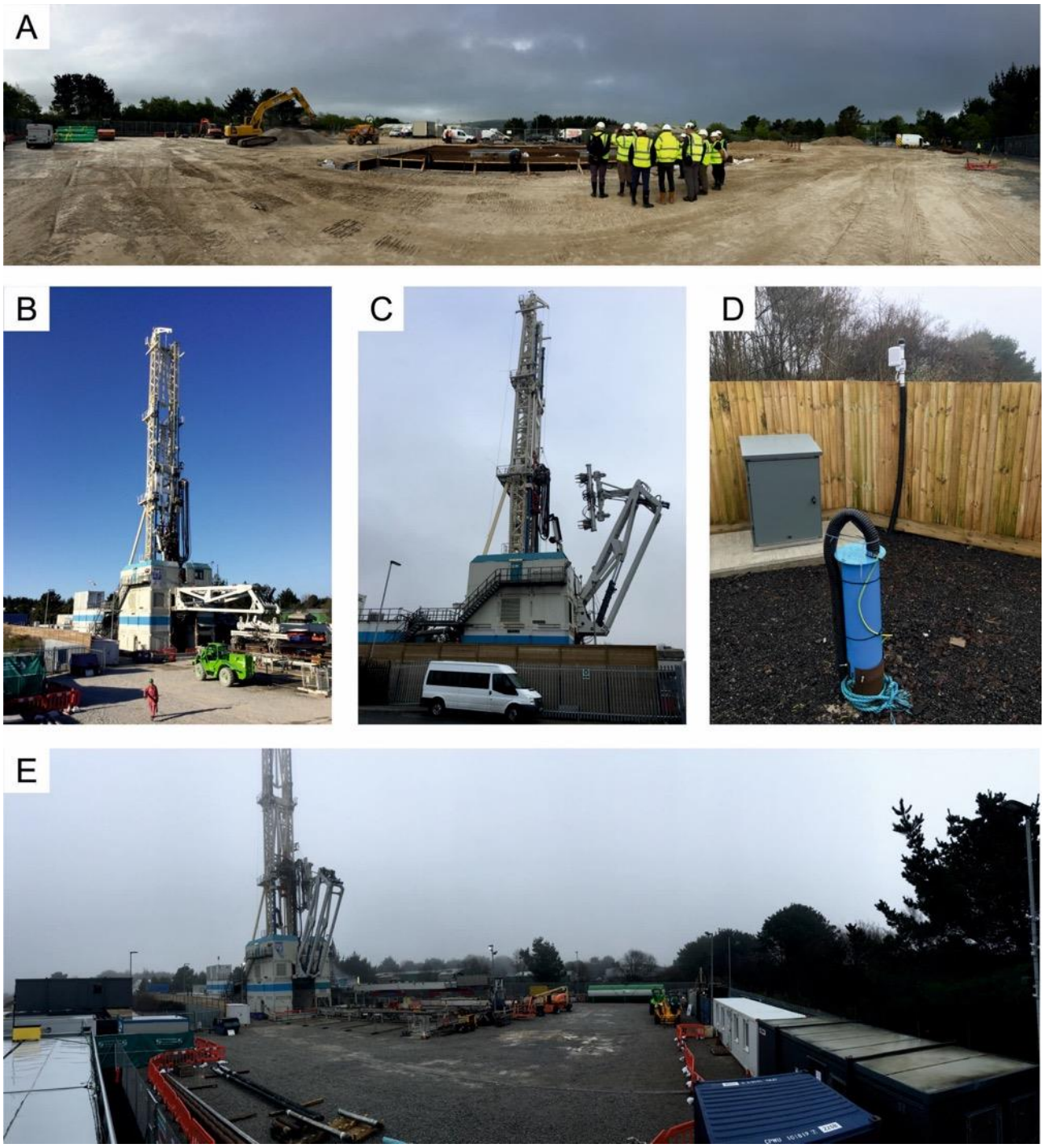

Figure 77: The United Downs Deep Geothermal Power project site. A. Site preparation and construction of the concrete drill pad in May 2018. H. Anger's Söhne Innova rig installed on the site. C. The height of the mast of the rig is more than 50 m above ground level, meaning it is visible for some distance from the site. D. Part of the ground vibration monitoring system at the site. E. View across the site. The trees to the right of the image mark the southern boundary of the site (Figure 76). British Geological Survey © UKRI.

9.1.2 Social

The history of mining in south-west England stretches back for millennia (Figure 78). The fact that UNESCO World Heritage Site status has been granted to the Cornwall and West Devon mining landscape is testament to the impact mineral extraction has had on the development of the region. The landscape of Cornwall and West Devon was transformed during the 18th and early 19th centuries as the copper and tin mining industry developed. The extensive underground mine workings, engine houses, which litter the landscape, new towns, ports and harbours and their associated industries reflect the importance of the region in terms of its 19th century metal production and the contribution it made to supplying raw materials for the Industrial Revolution in Great Britain (UNESCO, 2006). Of all the counties in the England Cornwall has experienced the most metalliferous mining. In addition the UK was the ninth largest producer of kaolin in the world in 2017 and made a more significant contribution to global supply in the past (Brown et al., 2019). Koalin resources in Great Britain are confined to the granites of south-west England and the deposits are world class in terms of size and quality. All the main granite intrusion have been worked to some extend in the past, but production has historically been based on the central and western parts of the St Austell granite and south-western margin of the Dartmoor granite. The kaolin production has had a strong impact on the Cornish landscape (Figure 79). Kaolinisation on the south-western part of the Dartmoor granite is adjacent to and extends into the Dartmoor National Park. In 2001, the two companies working in the area announced their intention to relinquish their planning permissions within the National Park because of the impact that these workings would have on a sensitive area. There are several SSSIs (mainly geological) located within the operational area in Cornwall. Goss and Tregoss Moor Special Area of Conservation is located just to the NE of the main kaolin extraction area (Bloodworth and Wrighton, 2009) (Figure 79). The last decade has seen a renewed interest in metals in south-west England. The most notable development, is the Drakelands Mine, formerly known as the Hemerdon Mine, near Plymouth. Hemerdon is one of the world's largest tungsten deposits and an open-pit mining operation was established here in 2015 to primarily produce tungsten and tin. There are also plans to reopen the South Crofty Mine. The South Crofty project is fully permitted, with an underground mining licence valid until 2071, planning permission to construct a new process plant and a permit from the Environment Agency to dewater the historical mine workings. The extent of mineral extraction in south-west England and its impact on the heritage of the region means local communities probably have a relatively receptive attitude towards natural resource development, mining projects and geothermal operations. Furthermore, factors such as income, unemployment levels, health, education, skills and training, and living environment can have an influence on local attitudes to developments that could have potential socio-economic benefits. Cornwall has a number of area with consistently high levels of deprivation (Cornwall Council, 2017b). It is noted that the Camborne and Redruth community network has the highest number of neighbourhoods in the most deprived 20 per cent in England. The number of deprived neighbourhoods in Cornwall has increased since 2010. This is attributed to a number of factors, including income and employment and a slight delay between the economic recovery in Cornwall and the rest of the country (Cornwall Council, 2015).

The most up to date information on the attitudes of communities in Cornwall to deep geothermal power development are provided by the consultation programme that was undertaken to support the proposed development of the UDDGP project. The consultation process involved disseminating information on geothermal energy to local stakeholders, outlining the plans for the geothermal power plant development, providing the community with an opportunity to discuss and interrogate the proposal, assessing the views and concerns of the community, and communicating the benefits and local impacts of the proposed plan.

Figure 78: Evidence of the strong influence of mining on the landscape of south-west England. A. There is extensive evidence of Cornwall's long mining history along the coastline. View along the coast towards Cligga Head. B/C. The Crowns mine at Botallack forms one of the most spectacular historic mining scenes in Cornwall with the engine house perched precariously on the rocks just above the sea (Figure 6A). D. The Wheal Jane water treatment facility, which was constructed to treat the polluted water from this underground mine. E. China clay workings, Great Pit, Lee Moor, south Dartmoor. F. Part of the old china clay workings in the kaolinised granite of Tregonning Hill, on or near the site of the first china clay workings in Cornwall. Steep narrow quartz and greisen veins cut the altered granite. G. Development works during the construction of the Drakelands Mine, formerly known as the Hemerdon Mine in 2014. British Geological Survey © UKRI.

Figure 79: China clay working to the NE of St Austell, Cornwall. Towns are labelled for reference. British Geological Survey © UKRI.

The Planning Application Document on the public consultation concluded that: 'The overwhelming response from the community consultation programme has been positive.' and 'The local politicians have been supportive.' It is also indicate that based on a consultation questionnaire completed by 88 people 'There was overwhelming support for geothermal energy with 89 per cent supporting the development of geothermal energy in the locality and only 6 per cent objecting'. Concerns about the project primarily focussed on traffic and noise, although it is emphasised that 'many people listed no concerns at all.' (Wardell Armstrong, 2010b).

Plymouth University, in south-west England are studying the issues relating to public perception of geothermal energy exploitation in the UK. The research will consider both the psychological and social factors that influence public opinion, and the influence of the media. The latter will examine how to improve communications between resource companies and affected residents that live close to potential geothermal sites (Geothermal Engineering Ltd, 2018g). GEL have undertaken an extensive education and community outreach programme targeting the full cross-section of potential stakeholders. More details can be found in Ledingham et al. (2019)

9.1.3 Political and regulatory framework

Geothermal heat has the potential to make a significant contribution to meeting the UK's legally binding emissions targets set out in the UK Climate Change Act (Abesser et al., 2018).

9.1.3.1 National context

Heat

Abesser et al. (2018) indicate that geothermal heat needs to be managed and regulated in a similar way to other natural resources such as oil, gas, coal and water. This requires clear definition of the term 'geothermal energy' as well as a clear understanding of ownership. One of the key challenges with ownership and regulation of geothermal heat in the UK is that it is regarded as a physical property, not a recoverable material such as a metallic mineral ore. As such, 'heat' is not a legally-defined entity and this causes some difficulties for assigning legal ownership and regulating it. Abesser et al. (2018) suggest that revision of geothermal regulations is one of a number of measures required to encourage exploitation of geothermal resources in the UK. Regulations enact the law, and a change to UK law is needed so that it better defines heat, and thereby allows implementation of such regulations. Currently, heat is not dealt with in UK law, except as a pollutant. Such cases are covered by the EU Water Framework Directive and UK groundwater regulations. Detrimental impact of geothermal schemes on other users (e.g. neighbouring schemes) are covered by 'private nuisance', i.e. they are a civil issue (Abesser et al., 2018). Abesser et al. (2018) indicate that early development risks are one of the main reasons why so few geothermal energy projects have been implemented in the UK to date.

In terms of the current regulatory approach in the UK for deep geothermal, the same requirements for environmental permissions and licences from the Environment Agency apply as for the open-loop, shallow geothermal systems (which abstract groundwater and return discharge it to the ground after it has been used for heating or cooling). They fall under environmental permitting and groundwater regulations, as defined by the Water Framework Directive, in EU countries. In the UK, the regulatory control of abstraction and discharges, required for open-loop systems, is solely aimed at protecting groundwater, not regulating heat (Abesser et al., 2018).

Minerals

Mineral exploration of fluctuating intensity has been undertaken in Great Britain over the last fifty years and there are several areas where exploration has identified potentially economic resources of a number of metals. Although many significant discoveries were made during this period, the last tin mine in Great Britain, South Crofty, in Cornwall, closed in 1998 (Colman and Cooper, 2000), and with the exception of a small gold deposit in Northern Ireland and the Drakelands tin-tungsten mine in Devon no new operations have since been commissioned.

The rights to non-energy minerals in Great Britain, with the exception of gold and silver, are mainly in private ownership although a significant proportion is owned by the Crown and by Government departments and agencies (Colman and Cooper, 2000). In Great Britain only the mineral rights owner can legally grant rights to explore and mine (Robertson, 1983). Hence a critical stage in the exploration and development process is determination of mineral ownership. Great Britain has no minerals title registry or system and although mineral rights in Great Britain are typically held by the surface landowner, they may have been retained by previous landowners when the surface freehold was sold. The beneficiaries of such rights are often unknown

to the surface owners and the titles to the mineral rights may have been lost or destroyed. In some regions, particularly those with a long history of mineral extraction such as Cornwall this issue can be compounded by several parties potentially having interests in the mineral rights of a particular area (undivided interests). The process of determining mineral ownership in Great Britain can be time consuming and costly and is a potential deterrent to investment. In Great Britain granting of an exploration agreement confers not rights of entry and the applicant has to negotiate access with surface rights owners. Severed land and mineral rights ownership in Great Britain can result in access problems.

The National Planning Policy Framework (NPPF) establishes the overarching context for the development of Local Planning policy and guidance in England. In relation to renewables and low carbon energy and heat it states that Local Planning Authorities should develop positive strategies to help increase the use and supply. It states that local planning policies should be designed to maximise deployment of renewables and low carbon energy, while ensuring that adverse impacts are addressed satisfactorily. The NPPF contains support for community-led initiatives for renewable and low carbon energy (Cornwall Council, 2016b). The National Planning Practice Guidance adds further context to the NPPF, and helps local councils in developing policies to support the framework. Whilst the NPPG reinforces the role that planning has in the delivery of renewable and low energy infrastructure, it states that renewable energy developments should be acceptable for their proposed location (Cornwall Council, 2016b). The Guidance on 'Renewable and low carbon energy' states that 'Community initiatives are likely to play an increasingly important role and should be encouraged as a way of providing positive local benefit from renewable energy development.' (Ministry of Housing Communities & Local Government, 2015). The Overarching National Policy Statement (NPS) for Energy (EN-1) sets out national policy for the delivery of major energy infrastructure. It states that 'As part of the UK's need to diversify and decarbonise electricity generation, the Government is committed to increasing dramatically the amount of renewable generation capacity'. It emphasises that renewable energy generation is 'essential to enable the UK to meet its commitments under the EU Renewable Energy Directive', and 'will also help improve our energy security by reducing our dependence on imported fossil fuels'. The NPS includes a list of generic impacts that must be considered by energy development proposals (Department of Energy and Climate Change, 2011). Whilst the NPS specifically identifies a range of technologies from which future large-scale renewable energy generation is likely to come, geothermal energy is not mentioned.

9.1.3.2 Cornwall future growth and energy strategy

Cornwall Council became a signatory of the 'Nottingham Declaration' on climate change in 2010. Cornwall Council commissioned a study that was published in 2012 to better understand the potential for geothermal resource development in the county. It considered technology, policy and commercial considerations that impact the sector. It identified a number of reasons for the slow development of deep geothermal in Cornwall, strategies the Council could take to stimulate the deep geothermal sector and presented three options for future development (ARUP, 2012). In 2013 Cornwall Council released the 'Sustainable Energy Action Plan (SEAP)'. This indicates that Cornwall has an annual energy demand estimated to be about £1.4 billion. It states that 'Cornwall Council has the responsibility to lead by example and inspire the businesses and communities in Cornwall to drive down emission and energy demand.' It describes the importance of 'Supporting and promoting geothermal opportunities' and how the Council is seeking to better understand the potential of the resource, and if appropriate, to support development of this sector in line with the green energy aspirations of the county (Cornwall Council, 2013a). Since 2015 Cornwall has had devolved powers. In 2018 the Council released a 'New Frontiers' plan, which describes how 'Cornwall…will continue their economic, social and environmental transformation…'. It emphasises the importance of clean growth and environmental

management, and states 'Our peninsula is energy rich, with strong established and emerging renewable energy sectors including solar, wind and geothermal.' (Cornwall Council, 2018).

9.1.3.3 Planning policy in Cornwall

The Cornwall Local Plan was formally adopted on 22 November 2016. It provides the overarching planning policy framework for Cornwall, and covers the period up to 2030. The Cornwall Local Plan Strategic Policies 2010–2030 ('The Local Plan') sets out the Council's vision and strategy for Cornwall until 2030 and policies that will be used in determining planning applications. The Plan contains a specific 'Renewable and low carbon energy' policy, which seeks to increase the use and production of renewables and low carbon energy generation. In terms of context it states that more than 14 per cent of households in Cornwall spend more than 10 per cent of their income on fuel for domestic heating and that the county uses an estimated £500 million of energy annually. It emphasises that renewable and low carbon electricity and heat generation is reliant on continued access to the natural resources. With respect to geothermal it states that careful management is necessary to ensure that new developments do not harm the integrity of deep geothermal reservoirs. This is supported by another specific policy on 'Safeguarding renewable energy' that states 'New development, where appropriate, should show that it does not significantly harm the performance of any existing facility…or the availability of their resource (where the operation is dependent on uninterrupted flow of energy to the installation).' (Cornwall Council, 2016a). Cornwall Council also provides planning policy guidance, commonly referred to as Supplementary Planning Documents (SPD), which provide more detailed advice and guidance to supplement policies and proposals contained in the Local Plan. In 2016 the Council published the SPD: 'Cornwall Renewable Energy Planning Advice'. The Planning Advice contains general guidance, which is relevant to planning for all renewable energy technologies. The general guidance considers 'community energy' i.e. a model focussed on a 'local energy economy', with a shift of ownership to local people. The Council believes this model of renewable energy deployment should receive particular support at the planning decision stage. It also focuses on 'optimising renewable energy' i.e. minimising its impact by maximising its efficiency (Cornwall Council, 2016b). The Local Plan specifically states that renewable energy development will be supported where they 'maximise the use of the available resource by deploying installations with the greatest energy output practicable' (Cornwall Council, 2016a). The general guidance also emphasises the importance of 'co-location' (Cornwall Council, 2016b), since the Local Plan is particularly supportive of developments that 'create opportunities for colocation of energy producers with energy users, in particular heat, and facilitate renewable and low carbon energy innovation.' (Cornwall Council, 2016a). The SPD indicates that examples where co-location between heat generation and consumption is likely to be encouraged include geothermal energy (Cornwall Council, 2016b). A section of the SPD is devoted to 'deep geothermal', which discusses the importance of optimisation and co-location, and potential impacts, including on landscape, ecology and biodiversity, the historic environment, and noise emissions. In terms of used of land it indicates that 'whenever geological and thermal conditions allow, geothermal development should be sited on previously developed/brownfield sites, contaminated land…and industrial land.' It 'should avoid significant loss of Best and Most Versatile agricultural land.' It also provides more detailed advice and guidance on flood management, rights of way and highways, traffic, and the impacts of drilling and the requirement for seismic hazard assessment (Cornwall Council, 2016b). The SPD describes the importance of 'safeguarding' renewable energy resources, in line with the specific policy in the Local Plan (see above). However, it indicates that 'Deep geothermal operations may also conflict with the interests of minerals safeguarding areas' (Cornwall Council, 2016b), for which there is also a specific policy ('Minerals safeguarding') in the Local Plan, which states 'Important mineral resources and reserves…shall be safeguarded from sterilisation by other forms of

incompatible development.' (Cornwall Council, 2016a). The SPD indicates that 'Where deep geothermal developments are proposed within, or near to minerals safeguarding areas, it is recommended that the issue be addressed as part of the pre-application process with the Council and, if necessary, through engagement with the land owner and relevant mineral operator.' (Cornwall Council, 2016b).

9.2 Financial aspects

MacDonald et al. (1992) indicates that cumulative expenditure (to April 1991) on phases 1 to 3A of the HDR project was more than £35 million. When this historical price is converted into equivalent present-day prices (2018) by using historical inflation rates, the expenditure is more than £73 million. An alternative source estimates that government and European Union support for this project was about £50 million (Law, 2011). During Phase 3A of the HDR project work was undertaken on the economic costs of HDR systems. The capital cost associated with a 'post-prototype' commercial-scale HDR power station was estimated to be about £45 million in 1990. An alternative cost model estimated it be £35 million (MacDonald et al., 1992). Conversion of these historical prices to 2018 prices places current capital cost at between about £71–100 million.

A study commissioned by the Department of Energy and Climate Change, included a review of the costs associated with exploration, exploitation and potential investment returns for deep geothermal. The research took a case study-based approach, with the low permeability granites of south-west England being selected as one of the case studies. A high level techno-economic model was developed to assess the expected financial returns. This report concluded that south-west of England has a development potential of 100MW of electricity generation (Atkins, 2013). A previous study by Sinclair Knight Merz (2012) concluded that Cornwall's generating capacity could be up to 4GW of electricity, with a by-product of 13GW of heat (ERDF, 2016). ERDF (2016) indicate that a 100MW geothermal resource could provide electricity to about 150 000 homes and 4GW would be greater than Cornwall's total energy demand. It is emphasised how development of geothermal resources could result in more affordable heat and power. This could result in Cornwall becoming an attractive destination for power dependent industries and those seeking to lower energy costs. It is suggested that development of a geothermal industry will produce 'high value' jobs resulting in both direct and indirect employment, arising from down-stream industries (ERDF, 2016). For the UDDGP project the Planning Application Document on the 'Socio-economic and environmental benefits' indicates that Geothermal Engineering are seeking a partner to utilise a portion of the renewable heat that is generated from the power plant, and would be provided 'at a very low cost'. It indicates that potential industrial partners include: agriculture for glasshouses, industrial drying facilities, laundry services, breweries and industries with significant cooling requirements e.g. IT data centres (Wardell Armstrong, 2010a).

The electricity grid in Cornwall has spare capacity on the network to take more locally generated renewable energy. However, because of existing connection agreements, which are yet to be used, and the time required to make upgrades to the grid, there is very little capacity actually available for new connections. The Council indicates that delivering geothermal in the capacities that appear achievable will take many years, because each 5–10 MW project will require 4–6 years of construction time. They suggest that potential solutions include reviewing connection agreements, improved network management, energy storage schemes, as well as general infrastructure improvements. The UDGP project has secured a grid connection (Cornwall Council, 2017a).

The costs associated with the UNDGP project provide the most recent estimates of the expenditure associated with geothermal exploration and development in Cornwall. The project has a total cost of £18 million, which has obtained from three funding sources. The European Regional Development Fund has provided £10.6 million under its Priority Axis 4 ('Supporting the Shift Towards a Low Carbon Economy in All Sectors'). Cornwall Council has provided £2.4 million in support of its economic development programme and its vision for a low carbon energy future. The remaining £5 million has been provided by private investors (Geothermal Engineering Ltd, 2018c). The Planning Application Document on the 'Socio-economic and environmental benefits' of the UDDGP project outlines the level of economic investment required to establish a 10 MWe geothermal plant. It was estimated the geothermal power plant would annually generate more than 55,188 MWh of electrical output (sufficient to supply the electrical requirements of more than 9000 homes) and 65,043 MWh of thermal output. In 2010 it was estimated that the total investment required for the project would be about £44 million. At this time the borehole drilling and exploration was estimated to be in the order of £8 million (then GEL were proposing to develop up to three wells). It is indicated that once operational the power station would provide 4–5 permanent jobs (Wardell Armstrong, 2010a).

10 References

ABESSER, C, SCHOFIELD, D, BUSBY, B, BONSOR, B, AND WARD, R. 2018. Who owns (geothermal) heat? *British Geological Survey*.

ALDERTON, D, AND SHEPPARD, S. 1977. Chemistry and origin of thermal waters from southwest England. *Transactions of the Institute of Mining and Metallurgy Section B-Applied Earth Science*, Vol. 86, B191-B194.

ALEXANDER, A, AND SHAIL, R. 1996. Late-to post-Variscan structures on the coast between Penzance and Pentewan, South Cornwall. *Proceedings of the Ussher Society*, Vol. 9, 6.

ANDERSEN, J, STICKLAND, R, ROLLINSON, G, AND SHAIL, R. 2016. *Indium mineralisation in SW England: Host parageneses and mineralogical relations*. No. 78.

ARUP. 2012. Cornwall Geothermal Options Report. *Ove Arup & Partners Ltd* (London, United Kingdom).

ATKINS. 2013. Deep Geothermal Review Study Final Report.

BALL, T, BASHAM, I, BLANK, D, AND SMITH, T. 1982. Aspects of the geochemistry of bismuth in South-West England. *Proceedings of the Ussher Society*, Vol. 5, 376-382.

BARIA, R, HEARN, K C, LANYON, G N, AND BATCHELOR, A S. 1985. Microseismic Results

BARKER, J A, DOWNING, R A, GRAY, D A, FINDLAY, J, KELLAWAY, G A, PARKER, R H, AND ROLLIN, K E. 2000. Hydrogeothermal studies in the United Kingdom. *Quarterly Journal of Engineering Geology and Hydrogeology*, Vol. 33, 41-58.

BARNES, H L. 1997. *Geochemistry of hydrothermal ore deposits*. (New York: Wiley.) ISBN 047157144X 9780471571445

BARNES, R, AND ANDREWS, J. 1981. Pumpellyite-actinolite grade regional metamorphism in south Cornwall. *Proceedings of the Ussher Society*, Vol. 5, 139-146.

BATCHELOR, A. 1978. The engineering properties of the southwestern granites related to artificial geothermal exploitation. *Proc. Ussher Soc*, Vol. 4, 355-361.

BATCHELOR, A, AND PINE, R. 1986. The results of in situ stress determinations by seven methods to depths of 2500 m in the Carnmenellis granite. *ISRM International Symposium*, International Society for Rock Mechanics.

BEAMISH, D. 1990. *A deep geoelectric survey of the Carnmenellis granite*. No. 102.

BEAMISH, D, AND BUSBY, J. 2016. The Cornubian geothermal province: heat production and flow in SW England: estimates from boreholes and airborne gamma-ray measurements. *Geothermal Energy*, Vol. 4, 4.

BEAMISH, D, HOWARD, A, WARD, E K, WHITE, J, AND YOUNG, M E. 2014. Tellus South West airborne geophysical data (British Geological Survey).

BEAMISH, D, AND WHITE, J. 2014. TellusSW : airborne geophysical data and processing report. . *British Geological Survey* (Keyworth, Nottingham).

BEER, K E, BURLEY, A J, AND TOMBS, J M C. 1975. The concealed granite roof in south-west Cornwall. *Institute of Geological Sciences*, 1 (Keyworth, Nottingham).

BLOODWORTH, A, AND WRIGHTON, C. 2009. Mineral Planning Factsheet Kaolin.

BOTT, M H P, DAY, A A, MASSON-SMITH, D, AND DUNHAM, K C. 1958. The geological interpretation of gravity and magnetic surveys in Devon and Cornwall. *Philosophical Transactions of the Royal Society of London. Series A, Mathematical and Physical Sciences*, Vol. 251, 161-191.

BOTT, M H P, HOLDER, A P, LONG, R E, AND LUCAS, A L (editors). 1970. *Crustal structure beneath the granites of south-west England. In Mechanism of igneous intrusion*. Geol. J., special issue.

BOTT, M H P, AND SCOTT, P (editors). 1964. *Recent geophysical studies in south-west England*. Present view of some aspects of the geology of Cornwall. (Truro: Blackford.)

BRITISH GEOLOGICAL SURVEY. 1990. Geological Survey of England and Wales 1:63,360/1:50,000 geological map series, New Series. Falmouth. Sheet number 352. 1:50 000.

BROMLEY, A V, THOMAS, L J, SHEPHEARD, T J, AND DARBYSHIRE, D P F. 1989. Geochemistry in relation to Hot Dry Rock development in Cornwall, Volume 5. Mineralogy and geochemistry of the Carnmenellis Granite. *British Geological Survey*, British Geological Survey Research Report SD/89/2.

BROOKS, M, DOODY, J J, AND AL-RAWI, F R J. 1984. Major crustal reflectors beneath SW England. *Journal of the Geological Society*, Vol. 141, 6.

BROOKS, M, MECHIE, J, AND LLWELLYN, D J (editors). 1983. *Geophysical investigations in the Variscides of Southwest Britain*. The Variscan foldbelt in the British Isles. (Bristol: Adam Hilger Ltd.)

BROWN, T, IDOINE, N, RAYCRAFT, E, HOBBS, S, SHAW, R, EVERETT, P, KRESSE, C, DEADY, E, AND BIDE, T. 2019. World Mineral Production 2013-2017. *British Geological Survey*.

BURGESS, W G, EDMUNDS, W M, ANDREWS, J N, AND KAY, R L F. 1982a. The origin and circulation of grounwater in the Carnmenellis Granite: the hydrogeochmeical evidence. *British Geological Survey*, WJ/GE/82/004.

BURGESS, W G, EDMUNDS, W M, ANDREWS, J N, KAY, R L F, AND LEE, D J. 1982b. origin and circulation of groundwater in the Carnmenellis granite: the hydrogeochemical evidence. *nstitute of Geological Sciences* (London).

BURT, R, BURNLEY, R, GILL, M, AND NEILL, A. 2014. *Mining in Cornwall and Devon: Mines and Men*. (University of Exeter Press.) ISBN 085989889X

BUSBY, J. 2010. Geothermal Prospects in the United Kingdom. Proceedings World Geothermal Congress Bali, Indonesia.

BUSBY, J, AND TERRINGTON, R. 2017. Assessment of the resource base for engineered geothermal systems in Great Britain. *Geothermal Energy*, Vol. 5, 7.

CAMBORNE SCHOOL OF MINES. 1986. Jointing in the Carnmenellis granite (Report 2A-59). 2A-46 (Camborne, United Kingdom).

CAMBORNE SCHOOL OF MINES. 1988. Resource evaluation (Report 2C-7). 2A-46 (Camborne, United Kingdom).

CHAPPELL, B W, AND HINE, R. 2006. The Cornubian Batholith: an Example of Magmatic Fractionation on a Crustal Scale. *Resource Geology*, Vol. 56, 203-244.

CHEN, Y, CLARK, A H, FARRAR, E, WASTENEYS, H A H P, HODGSON, M J, AND BROMLEY, A V. 1993. Diachronous and independent histories of plutonism and mineralization in the Cornubian Batholith, southwest England. *Journal of the Geological Society*, Vol. 150, 1183-1191.

CHESLEY, J T, HALLIDAY, A N, SNEE, L W, MEZGER, K, SHEPHERD, T J, AND SCRIVENER, R C. 1993. Thermochronology of the Cornubian batholith in southwest England: Implications for pluton emplacement and protracted hydrothermal mineralization. *Geochimica et Cosmochimica Acta*, Vol. 57, 1817-1835.

CLARK, A, CHEN, Y, FARRAR, E, AND NORTHCOTE, B. 1994. Refinement of the time/space relationships of intrusion and hydrothermal activity in the Cornubian Batholith. *Abstracts Volume, Ussher Society Annual Meeting, Minehead*.

COLMAN, T B, AND COOPER, D C. 2000. Exploration for metalliferous and related minerals in Britain: a guide. *British Geological Survey*.

CORNWALL COUNCIL. 2012. Renewable Energy Planning Guidance Note 8 The Development of deep geothermal.

CORNWALL COUNCIL. 2013a. Sustainable Energy Action Plan (SEAP) for a Green Cornwall. *Cornwall Council* (Cornwall, United Kingdom).

CORNWALL COUNCIL. 2013b. Technical Paper E1 (b) Energy Projections for Cornwall. *Cornwall Council* (Cornwall, United Kingdom).

CORNWALL COUNCIL. 2015. Indices of Multiple Deprivation 2015. Cornwall, Cornwall Council 6.

CORNWALL COUNCIL. 2016a. Cornwall Local Plan - Strategic Policies 2010-2030. *Cornwall Council* (Cornwall, United Kingdom).

CORNWALL COUNCIL. 2016b. Cornwall Renewable Energy Planning Advice. *Cornwall Council* (Cornwall, United Kingdom).

CORNWALL COUNCIL. 2017a. Deep geothermal FAQ's. https://www.cornwall.gov.uk/media/16892627/faqs-210617.pdf

CORNWALL COUNCIL. 2017b. Deprivation. [cited 03 April]. https://www.cornwall.gov.uk/council-and-democracy/data-and-research/data-by-topic/deprivation

CORNWALL COUNCIL. 2018. New Frontiers - An inclusive approach to an economy, environment and society that works for everyone in Cornwall and the Isles of Scilly. *Cornwall Council* (Cornwall, United Kingdom).

CORNWALL COUNCIL. 2019. Planning – Planning Application Documents. http://planning.cornwall.gov.uk/online-applications/applicationDetails.do?activeTab=documents&keyVal=KYLN1FFG0DT00

CORNWELL, J D, KIMBELL, S F, EVANS, A D, AND COOPER, D C. 1995. A review of detailed airborne geophysical surveys in Great Britain. *British Geological Survey* (Keyworth, Nottingham).

DANGERFIELD, J, AND HAWKES, J. 1981. The Variscan granites of south-west England: additional information. *Proceedings of the Ussher Society*, Vol. 5, 116-120.

DARBYSHIRE, D, AND SHEPHERD, T. 1987. Chronology of magmatism in south-west England: the minor intrusions. *Proceedings of the Ussher Society*, Vol. 6, 431-438.

DARBYSHIRE, D P F, AND SHEPHERD, T J. 1985. Chronology of granite magmatism and associated mineralization, SW England. *Journal of the Geological Society*, Vol. 142, 1159-1177.

DE LA BECHE, H T. 1839. Report On the Geology of Cornwall, Devon and West Somerset.

DE LA BECHE, H T. 1846. Geological Survey of England and Wales 1:63,360 geological map series [Old Series]. [South Coast, from Polperro to St. Neverne, N. Coast, St. Agnes Head to Portreath, Truro, Falmouth, the Mining Districts of St. Austell, Fowey, Camborne, Redruth, showing Lodes.] Sheet number 31. 1:63 360.

DEADY, É, AND MOORE, K R. 2015. The Key to Understanding Antimony Mineralisation in South West England — the North Herodsfoot Mine? Applied Earth Science, Taylor & Francis. **124** 20-59.

DEPARTMENT OF ENERGY AND CLIMATE CHANGE. 2011. Overarching National Policy Statement for Energy (EN-1). (London, United Kingdom).

DINES, H G. 1956. *The metalliferous mining region of south-west England*. No. 1. (HM Stationery Office.)

DOMINY, S, AND CAMM, G. 1998. Controls on ore localization in tin-bearing veins: a review. *PROCEEDINGS-USSHER SOCIETY*, Vol. 9, 241-249.

DOMINY, S, SCRIVENER, R, LE BOUTILLIER, N, BUSSELL, M, AND HALLS, C. 1994. Crosscourses in South Crofty Mine, Cornwall: further studies of paragenesis and structure. *Proceedings-Ussher Society*, Vol. 8, 237-237.

DOWNING, R A. 1986. *Geothermal energy: The potential in the United Kingdom*. (HMSO.)

DOWNING, R A, AND GRAY, D A. 1986. *Geothermal energy : the potential in the United Kingdom*. (London: H.M.S.O.) ISBN 0118843664 9780118843669

DUNHAM, K, BEER, K E, ELLIS, R A, GALLAGHER, M J, NUTT, M J C, AND WEBB, B C. 1978. United Kingdom. *Mineral deposits of Europe*. HASLAM, H W, KVALHEIM, A, AND BOWIE, S H U (editors). Volume 1 (Northwest Europe). (London: Institution of Mining and Metallurgy and Mineralogical Society.) ISBN 0900488441

DURRANCE, E M. 1985a. Hydrothermal circulation and isostasy, with particular reference to the granites of southwest England. . *Institution of Mining and Metallurgy Conference on High heat production (HHP) granites, hydrothermal circulation and ore genesis; St. Austell (UK); 22-25 Sep 1985*.

DURRANCE, E M. 1985b. A possible major Variscan thrust along the southern margin of the Bude Formation, south-west England. *Proceedings of the Ussher Society*, Vol. 6, 173-179.

EDMONDS, E A, MCKEOWN, M C, WILLIAMS, M, AND DEWEY, H. 1985. *British Regional Geology. South-west England. Fourth edition. Reprinted 1985 with additional references*.

EDMUNDS, W, ANDREWS, J, BURGESS, W, KAY, R, AND LEE, D. 1984. The evolution of saline and thermal groundwaters in the Carnmenellis granite. *Mineralogical Magazine*, Vol. 48, 407-424.

EDWARDS, J. 1984. Interpretations of seismic and gravity surveys over the eastern part of the Cornubian platform. *Geological Society, London, Special Publications*, Vol. 14, 119-124.

ERDF. 2016. Vision for geothermal energy in Cornwall. European Regional Development Fund Convergence http://www.erdfconvergence.org.uk/_userfiles/files/GrowthProgramme/Geothermalvisionjan2016update.pdf

EVANS, C D R. 1990. The geology of the western English Channel and its western approaches. *British Geological Survey*, United Kingdom offshore regional report (London).

EVANS, K F, KOHL, T, HOPKIRK, R J, AND RYBACH, L. 1992. Modelling of energy production from Hot Dry Rock systems. *Eidgenössische Technische Hochschule (ETH)* (Zürich, Switzerland).

EXLEY, C S, AND STONE, M (editors). 1982. *Hercynian intrusive rocks*. Igneous rocks of the British Isles. (Chichester: Wiley.)

FERRACCIOLI, F, GERARD, F, ROBINSON, C, JORDAN, T, BISZCZUK, M, IRELAND, L, BEASLEY, M, VIDAMOUR, A, BARKER, A, ARNOLD, R, DINN, M, FOX, A, AND HOWARD, A. 2015. LiDAR based Digital Terrain Model (DTM) data for South West England. CENTRE, N E I D.

FERRILL, D A, AND MORRIS, A P. 2003. Dilational normal faults. *Journal of Structural Geology*, Vol. 25, 183-196.

FLOYD, P A, EXLEY, C S, AND STYLES, M. 1993. The igneous rocks of south-west England. 1-7 in *Igneous Rocks of South-West England*. (Springer).

FRANKE, W. 1989. Tectonostratigraphic units in the Variscan belt of central Europe. *Geol Soc Am Spec Pap*, Vol. 230, 67-90.

GEOTHERMAL ENGINEERING LTD. 2018a. Drilling the wells. https://www.uniteddownsgeothermal.co.uk/drilling-the-wells

GEOTHERMAL ENGINEERING LTD. 2018b. Frequently asked questions. https://www.uniteddownsgeothermal.co.uk/frequently-asked-questions

GEOTHERMAL ENGINEERING LTD. 2018c. Funding. https://www.uniteddownsgeothermal.co.uk/funding-objectives

GEOTHERMAL ENGINEERING LTD. 2018d. Generating Electricity. https://www.uniteddownsgeothermal.co.uk/generating-electricity

GEOTHERMAL ENGINEERING LTD. 2018e. Project Overview. https://www.uniteddownsgeothermal.co.uk/project-overview

GEOTHERMAL ENGINEERING LTD. 2018f. UDDGP Noise Management Information Sheet 2.

GEOTHERMAL ENGINEERING LTD. 2018g. University of Plymouth research. [cited 03 April]. https://www.uniteddownsgeothermal.co.uk/plymouth-university-research

GERARD, F. 2014. PROJECT: PM_1478 Processing of LIDAR data for the South West TELLUS Project.

GHAHFAROKHI, P K. 2017. The structured gridding implications for upscaling model discrete fracture networks (DFN) using corrected Oda's method. *Journal of Petroleum Science and Engineering*, Vol. 153, 70-80.

GHOSH, P K. 1934. The Carnmenellis Granite: Its Petrology, Metamorphism and Tectonics. *Quarterly Journal of the Geological Society*, Vol. 90, 240-276.

GLEESON, S, WILKINSON, J, SHAW, H, AND HERRINGTON, R. 2000. Post-magmatic hydrothermal circulation and the origin of base metal mineralization, Cornwall, UK. *Journal of the Geological Society*, Vol. 157, 589-600.

GLEESON, S, WILKINSON, J, STUART, F, AND BANKS, D. 2001. The origin and evolution of base metal mineralising brines and hydrothermal fluids, South Cornwall, UK. *Geochimica et Cosmochimica Acta*, Vol. 65, 2067-2079.

H. ANGER'S SÖHNE. 2019. HAS Innova rig. [cited 23/03]. http://www.angers-soehne.com/?page_id=4793&lang=en

HAIMSON, B C, TUNBRIDGE, L W, LEE, M Y, AND COOLING, C M. 1989. Measurement of rock stress using the hydraulic fracturing method in Cornwall, U.K.—Part II. Data reduction and stress calculation. *International Journal of Rock Mechanics and Mining Sciences & Geomechanics Abstracts*, Vol. 26, 361-372.

HAWKES, J. 1981. A tectonic 'watershed'of fundamental consequence in the post-Westphalian evolution of Cornubia. *Proceedings of the Ussher Society*, Vol. 5, 128-131.

HAWKES, J, AND DANGERFIELD, J. 1978. The Variscan granites of south-west England: a progress report. *Proceedings of the Ussher Society*, Vol. 4, 158-171.

HEATH, M J. 1985. Geological control of fracture permeability in Carnmenellis granite, Cornwall: implications for radionuclide migration. *Mineralogical Magazine*, Vol. 49, 233-244.

HILLIS, R, AND CHAPMAN, T. 1992. Variscan structure and its influence on post-Carboniferous basin development, Western Approaches Basin, SW UK Continental Shelf. *Journal of the Geological Society*, Vol. 149, 413-417.

HOLDER, A P, AND BOTT, M H P. 1971. Crustal Structure in the Vicinity of South-west England. *Geophysical Journal of the Royal Astronomical Society*, Vol. 23, 465-489.

HOLDER, M T, AND LEVERIDGE, B. 1986. Correlation of the Rhenohercynian Variscides. *Journal of the Geological Society*, Vol. 143, 141-147.

HOLDER, M T, AND LEVERIDGE, B E. 1994. A framework for the European Variscides. *British Geological Survey*, Technical Report WA/94/24 (Keyworth, Nottingham).

JACKSON, N J, WILLIS-RICHARDS, J, MANNING, D A, AND SAMS, M S. 1989. Evolution of the Cornubian ore field, Southwest England; Part II, Mineral deposits and ore-forming processes. *Economic Geology*, Vol. 84, 1101-1133.

JENKIN, A K H. 1979. *Mines and miners of Cornwall (Vol. 10 Camborne and Illogan)*. (Truro Bookshop.)

JONES, R H. 1989. Camborne Geothermal Energy Project 2C-7 Resource Evaluation: Seismic Reflection Survey. *Camborne School of Mines*.

JONES, R H. 1991. A seismic reflection survey as part of a geophysical investigation of the Carnmenellis Granite. Annual Conference of the Ussher Society, January 1991 418-420.

KILPATRICK, A, ROCHELLE, C, RUSHTON, J, LACINSKA, A, FŰZÉRI, D, CHENERY, S, MARRIOT, A, HAMILTON, E, WATTS, M, MOUNTNEY, I, AND KEMP, S. 2017. Report on metal content mobilisation using mild leaching.

KIMBELL, S F, COOPER, D C, AND SCRIVENER, R C. 2000. *The digitisation and interpretation of data from the 1957/9 airborne radiometric survey of south-west England: British Geological Survey, Regional Geophysics Series, Technical Report WK/00/04*.

KIMBELL, S F, COOPER, D C, AND SCRIVENER, R C. 2003. *The digitisation and geological interpretation of data from the 1957-9 airborne radiometric survey of south-west England*. No. 10.

KNIGHT, H, DEADY, É, GUNN, A G, MOORE, K, AND NADEN, J. 2016. Ore fluid characteristics of antimony deposits in South West England: new insights into ore genesis in Wadebridge-Port Isaac and Herodsfoot. *Applied Earth Science*, Vol. 125, 89-89.

LAW, R. 2011. Deep geothermal UK - United Downs Project, Redruth. Ground Source Live June 8th 2011.

LeBoutillier, N, Camm, G, Shail, R, Bromley, A, Jewson, C, and Hoppe, N. 2002. Tourmaline-quartz-cassiterite mineralization of the Land's End Granite at Nanjizal, west Cornwall.

LeBoutillier, N G. 2002. The Tectonics of Variscan Magmatism and Mineralisation in South West England. University of Exeter.

Ledingham, P, Cotton, L, and Law, R. 2019. The United Downs Deep Geothermal Power Project. 44th Workshop on Geothermal Reservoir Engineering. Stanford University, Stanford, California 1-11.

Lee, M K, Brown, G C, Webb, P C, Wheildon, J, and Rollin, K E. 1987. Heat flow, heat production and thermo-tectonic setting in mainland UK. *Journal of the Geological Society*, Vol. 144, 35-42.

Leveridge, B, and Hartley, A. 2006. *0 The Variscan Orogeny: the development and deformation of Devonian/Carboniferous basins in SW England and South Wales The Variscan of SW England*.

Leveridge, B E. 2002. *Geology of the Plymouth and south-east Cornwall area: memoir for 1:50 000 geological sheet 348*. (London: H.M.S.O.) ISBN 0118845608 9780118845601

Leveridge, B E, Holder, M T, Goode, A J J, Scrivener, R C, and Monkhouse, R A. 1990. *Geology of the country around Falmouth: memoir for the 1:50000 geological sheet 352*. (London: H.M.S.O.) ISBN 0118844679 9780118844673

Lough, M F, Lee, S H, and Kamath, J. 1997. A New Method To Calculate Effective Permeability of Gridblocks Used in the Simulation of Naturally Fractured Reservoirs. *SPE Reservoir Engineering*, Vol. 12, 219-224.

MacDonald, P, Stedman, A, and Symons, G. 1992. The UK geothermal hot dry rock R&D programme. Proceedings, Seventeenth Workshop on Geothermal Reservoir Engineering. Stanford University, Stanford, California 5-11.

Manning, D A C. 1998. Granites and associated igneous activity. 15 in *The Geology of Cornwall and the Isles of. Scilly*. Selwood, E B, Durrance, E M, and Bristow, C M (editors). (Exeter: Exeter University Press.)

Manning, D A C, Hill, P I, and Howe, J H. 1996. Primary lithological variation in the kaolinized St Austell Granite, Cornwall, England. *Journal of the Geological Society*, Vol. 153, 827-838.

Middleton, G V, and Hampton, M A. 1976. Subaqueous sediment transport and deposition by sediment gravity flows. 21 in *Marine sediemnt transport and environmental management*. Stanley, D J, and Switt, D J P (editors). (New York: John Wiley.)

Miller, H G, and Singh, V. 1994. Potential field tilt—a new concept for location of potential field sources. *Journal of Applied Geophysics*, Vol. 32, 213-217.

Mines, C S o. 1988. Camborne Geothermal Energy Project Viscous Stimulation of Hot Dry Rock Reservoir.

Ministry of Housing Communities & Local Government. 2015. Guidance Renewable and low carbon energy. (London, United Kingdom).

MOORBATH, S E. 1962. Lead isotope abundance studies on mineral occurrences in the British Isles and their geological significance. *Phil. Trans. R. Soc. Lond. A*, Vol. 254, 295-360.

MOORE, J M. 1975. A mechanical interpretation of the vein and dyke systems of the SW England orefield. *Mineralium Deposita*, Vol. 10, 374-388.

MOORE, J M, AND JACKSON, N. 1977. Structure and mineralization in the Cligga granite stock, Cornwall. *Journal of the Geological Society*, Vol. 133, 467-480.

MORRIS, A, HENDERSON, D B, AND FERRILL, D A. 1996. Slip-tendency analysis and fault reactivation. *Geology*, Vol. 24, 275-278.

NAMHO. 2013. The Archeology of Cobalt Mining - Cobalt assessment.

NEACE, E R, NANCE, R D, MURPHY, J B, LANCASTER, P J, AND SHAIL, R K. 2016. Zircon LA-ICPMS geochronology of the Cornubian Batholith, SW England. *Tectonophysics*, Vol. 681, 332-352.

ODA, M. 1985. Permeability tensor for discontinuous rock masses. *Géotechnique*, Vol. 35, 483-495.

PARKER, R H (editor). 1989. *Hot Dry Rock Geothermal Energy, Phase 2B Final Report of the Camborne school of Mines Project*. (Pergamon Press.)

PARKER, R H (editor). 1990. *Progress in hot dry rock technology for application in south west England (1987-1989)*.

PARKER, R H. 1991. Problems in the development of artificial geothermal energy exploitation in Cornwall. Annual Conference of the Ussher Society 316-320.

PARKER, R H. 1999. The Rosemanowes HDR project 1983–1991. *Geothermics*, Vol. 28, 603-615.

PINE, R J, JUPE, A, AND TUNBRIDGE, L W. 1990. An evaluation of in situ stress measurements affecting different volumes of rock in the Carnmenellis granite.
effects in rock masses. Loen. Norway. June 1990. International Society for Rock Mechanics first international workshop on scale.

PINE, R J, AND KWAKWA, K A. 1989. Experience with hydrofracture stress measurements to depths of 2.6 km and implications for measurements to 6 km in the Carnmenellis granite. *International Journal of Rock Mechanics and Mining Sciences & Geomechanics Abstracts*, Vol. 26, 565-571.

PINE, R J, LEDINGHAM, P, AND MERRIFIELD, C M. 1983a. In-situ stress measurement in the Carnmenellis granite—II. Hydrofracture tests at Rosemanowes quarry to depths of 2000 m. *International Journal of Rock Mechanics and Mining Sciences & Geomechanics Abstracts*, Vol. 20, 63-72.

PINE, R J, AND NICOL, D A C. 1993. Analytical and Numerical Modeling of High Pressure Fluid-Rock Mechanical Interaction in HDR Geothermal Energy Reservoirs. 523-546 in *Surface and Underground Project Case Histories*. HOEK, E (editor). (Oxford: Pergamon.) ISBN 978-0-08-042068-4

PINE, R J, TUNBRIDGE, L W, AND KWAKWA, K. 1983b. In-situ stress measurement in the Carnmenellis granite—I. Overcoring tests at South Crofty mine at a depth of 790 m. *International Journal of Rock Mechanics and Mining Sciences & Geomechanics Abstracts*, Vol. 20, 51-62.

POLLARD, P, PICHAVANT, M, AND CHAROY, B. 1987. Contrasting evolution of fluorine-and boron-rich tin systems. *Mineralium Deposita*, Vol. 22, 315-321.

PRIVE, E. 1986. Sesimic interpretation and gravity modelling of BIRPS SWAT lines 5 and 6. *British Geological Survey*.

RICHARDS, H G, WILLIS-RICHARDS, J, AND PYE, J. 1991. A review of geological investigations associated with the UK Hot Dry Rock programme
Annual Conference of the Ussher Society.

ROBERTSON, K F. 1983. Obtaining Mineral Prospecting Permissions in Southwest England. *Occasional Papers of the Institution of Mining and Metallurgy*, Vol. Legal aspects of prospecting in the United Kingdom, 1-6.

ROLLIN, K. 1988. A detailed gravity survey between Dartmoor and Bodmin Moor: the shape of the Cornubian granite ridge and a new Tertiary basin. *Proceedings of the Geologists' Association*, Vol. 99, 15-25.

ROLLIN, K E, O'BRIEN, C F, AND TOMBS, J M C. 1982. Seismic and gravity surveys over the concealed granite ridge at Bosworgy, Cornwall. *Institute of Geological Sciences*, 49 (Keyworth, Nottingham).

ROMER, R L, AND KRONER, U. 2016. Phanerozoic tin and tungsten mineralization—tectonic controls on the distribution of enriched protoliths and heat sources for crustal melting. *Gondwana Research*, Vol. 31, 60-95.

SCRIVENER, R, DARBYSHIRE, D, AND SHEPHERD, T. 1994. Timing and significance of crosscourse mineralization in SW England. *Journal of the Geological Society*, Vol. 151, 587-590.

SCRIVENER, R C (editor). 2006. *Cornubian Granites and Mineralisation of SW England*. The Geology of England and Wales. (London: The Geological Society.)

SCRIVENER, R C, SHEPHERD, T J, AND GARRIOCH, N. 1986. Ore genesis at Wheal Pendarves and South Crofty Mine, Cornwall—a preliminary fluid inclusion study. *Proceedings of the Ussher Society*, Vol. 6, 412-416.

SELWOOD, E B, DURRANCE, E M, AND BRISTOW, C M (editors). 1998. *The Geology of Cornwall and the Isles of. Scilly.* (Exeter: Exeter University Press.)

SHAIL, R, MCFARLANE, J, HASSALL, L, THIEL, H, STOCK, T, SMETHURST, M, TAPSTER, S, SCRIVENER, R, LEVERIDGE, B, AND SIMONS, B. 2017. The geological setting of the Hemerdon W–Sn deposit. *Applied Earth Science*, Vol. 126, 92-92.

SHAIL, R K, AND ALEXANDER, A C. 1997. Late Carboniferous to Triassic reactivation of Variscan basement in the western English Channel: evidence from onshore exposures in south Cornwall. *Journal of the Geological Society*, Vol. 154, 163-168.

SHAIL, R K, ANDERSEN, J O, SIMONS, B, AND WILLIAMSON, B. 2014. EUROGRANITES 2014 – Granites and mineralisation of SW England. *University of Exeter* (United Kingdom).

SHAIL, R K, AND LEVERIDGE, B E. 2009. The Rhenohercynian passive margin of SW England: Development, inversion and extensional reactivation. *Comptes Rendus Geoscience*, Vol. 341, 140-155.

SHAW, R A, DEADY, E, BATEMAN, K, AND LUSTY, P. 2016. Report on data availability: South-west England.

SHEPHERD, T, MILLER, M, SCRIVENER, R, AND DARBYSHIRE, D. 1985. Hydrothermal fluid evolution in relation to mineralization in southwest England with special reference to the Dartmoor-Bodmin area. *High Heat Production (HHP) Granites, hydrothermal circulation and ore genesis*, 345-364.

SIBSON, R, MOORE, J M M, AND RANKIN, A. 1975. Seismic pumping—a hydrothermal fluid transport mechanism. *Journal of the Geological Society*, Vol. 131, 653-659.

SIMONS, B, ANDERSEN, J, AND SHAIL, R. 2013a. *Concentrations of critical metals in the Carnmenellis biotite granite, Cornwall, UK*.

SIMONS, B, ANDERSEN, J, AND SHAIL, R. 2013b. *Distribution of critical metals in biotite and Li mica granite from Cornwall, UK*.

SIMONS, B, ANDERSEN, J, AND SHAIL, R. 2014. *Fractionation of critical metals in the granites of SW England*.

SIMONS, B, ANDERSEN, J C, SHAIL, R K, AND JENNER, F E. 2017. Fractionation of Li, Be, Ga, Nb, Ta, In, Sn, Sb, W and Bi in the peraluminous Early Permian Variscan granites of the Cornubian Batholith: precursor processes to magmatic-hydrothermal mineralisation. *Lithos*, Vol. 278, 491-512.

SIMONS, B, SHAIL, R K, AND ANDERSEN, J C Ø. 2016. The petrogenesis of the Early Permian Variscan granites of the Cornubian Batholith: Lower plate post-collisional peraluminous magmatism in the Rhenohercynian Zone of SW England. *Lithos*, Vol. 260, 76-94.

SINCLAIR KNIGHT MERZ. 2012. Geothermal Energy Potential in Great Britain and Northern Ireland. 174.

SINCLAIR, W. 1995. Vein-stockwork tin, tungsten. 409-420 in *Geology of Canadian Mineral Deposit Types*. ECKSTRAND, O R, SINCLAIR, W D, AND THORPE, R I (editors). (Geological Survey of Canada.)

SMEDLEY, P, AND ALLEN, D. 2004. Baseline report series. 16, the granites of south-west England.

SMEDLEY, P L, BROMLEY, A V, SHEPHEARD, T J, EDMUNDS, W M, AND KAY, R L F. 1989. Geochemistry in relation to Hot Dry Rock development in Cornwall, Volume 4. Fluid circulation in the Carnmenellis granite: hydrogeological, hydrogeochemical and palaeofluid evidence. *British Geological Survey*, British Geological Survey Research Report SD/89/2.

STONE, M. 1995. The main Dartmoor granites: Petrogenesis and comparisons with the Cammenellis and Isles of Scilly granites. *Proceedings-Ussher Society*, Vol. 8, 379-379.

STONE, M. 1997. A geochemical dichotomy in the Cornubian batholith. *Proceedings-Ussher Society*, Vol. 9, 206-210.

STONE, M. 2000a. The early Cornubian plutons: A geochemical study, comparisons and some implications. *Geoscience in South-West England*, Vol. 10, 37-41.

STONE, M. 2000b. Petrogenetic implications from biotite compositional variations in the Cornubian granite batholith. *Mineralogical Magazine*, Vol. 64, 729-735.

STONE, M, AND EXLEY, C S (editors). 1985. *High heat production granites of south-west England and their associated mineralisation: a review*. High Heat Production (HHP) Granites, hydrothermal circulation and ore genesis. (London: Institution of Mining and Metallurgy.)

TAMMEMAGI, H Y, AND WHEILDON, J. 1974. Terrestrial Heat Flow and Heat Generation in South-west England. *Geophysical Journal of the Royal Astronomical Society*, Vol. 38, 83-94.

TAYLOR, G K. 2007. Pluton shapes in the Cornubian Batholith: new perspectives from gravity modelling. *Journal of the Geological Society*, Vol. 164, 525-528.

TERZAGHI, R D. 1965. Sources of Error in Joint Surveys. *Géotechnique*, Vol. 15, 287-304.

THOMAS-BETTS, A, WHEILDON, J, AND SAMS, M S. 1989. Further heatflow measurement and geothermal modelling in the vicinity of Carnmenellis granite. . *Camborne School of Mines*.

TIMÓN, S, LÓPEZ MORO, F J, L. ROMER, R, RHEDE, D, FERNÁNDEZ-FERNÁNDEZ, A, AND MORO BENITO, M C. 2019. Late-Variscan multistage hydrothermal processes unveiled by chemical ages coupled with compositional and textural uraninite variations in W-Au deposits in the western Spanish Central System Batholith. No. 17.

TINDLE, A G. 2008. *Minerals of Britain and Ireland*. (Terra Publishing.) ISBN 190354422X

TOMBS, J M C. 1977. A study of the space form of the Cornubian granite batholith and its application to detailed gravity surveys in Cornwall. *Institute of Geological Sciences*, 11 (Keyworth, Nottingham).

TUNBRIDGE, L W, COOLING, C M, AND HAIMSON, B C. 1989. Measurement of rock stress using the hydraulic fracturing method in Cornwall, U.K.—Part I. field measurements. *International Journal of Rock Mechanics and Mining Sciences & Geomechanics Abstracts*, Vol. 26, 351-360.

UNESCO. 2006. Nomination of the Cornwall and West Devon Mining Landscape for inclusion on the World Heritage List.

WARDELL ARMSTRONG. 2010a. 4 Socio-economic and environmental benefits NR/10/00056/GEO. Planning Application Documents. cornwall.gov.uk.

WARDELL ARMSTRONG. 2010b. 11 Public consultation NR/10/00056/GEO. Planning Application Documents. cornwall.gov.uk.

WESTHEAD, K, HOLDEN, A, SCHOFIELD, D, HASLAM, R, LOVELESS, S, BLOOMFIELD, J P, LEE, J R, BAPTIE, B, SHAW, R P, BIDE, T, AND MCEVOY, F M. 2017. National Geological Screening: South-

west England region. *British Geological Survey*, Commissioned Report CR/17/095 (Keyworth, Nottingham).

WHEILDON, J, M.F., F, J.R.L, E, AND A., T-B. 1981. Investigation of the S.W. England thermal anomaly zone. CEC Final Report, Contract No 097-76 EGUK, 568-78-1 EGUK. (Brussels).

WILLIS-RICHARDS, J, AND BARIA, R. 1989. Camborne Geothermal Energy Project 2C-7 Resource Evaluation: Gravity and Themal Modelling. *Camborne School of Mines*.

WILLIS-RICHARDS, J, AND JACKSON, N J. 1989. Evolution of the Cornubian ore field, Southwest England; Part I, Batholith modeling and ore distribution. *Economic Geology*, Vol. 84, 1078-1100.

WILLIS-RICHARDS, J, JONES, R H, AND BARIA, R. 1989. Camborne Geothermal Energy Project 2C-7 Resource Evaluation: Overview. *Camborne School of Mines*.

WILSON, A, AND TAYLOR, R. 1976. *Stratigraphy and sedimentation in west Cornwall*.

YEOMANS, C. 2017. *Tellus South West data usage: a review (2014–2016)*. No. 3.

YEOMANS, C. 2018. Enhancing the Geological Understanding of Southwest England Using Machine Learning Algorithms. University of Exeter.

YEOMANS, C M, MIDDLETON, M, SHAIL, R K, GREBBY, S, AND LUSTY, P A J. 2019. Integrated Object-Based Image Analysis for semi-automated geological lineament detection in southwest England. *Computers & Geosciences*, Vol. 123, 137-148.

YOUNGER, P L, AND MANNING, D A C. 2010. Hyper-permeable granite: lessons from test-pumping in the Eastgate Geothermal Borehole, Weardale, UK. *Quarterly Journal of Engineering Geology and Hydrogeology*, Vol. 43, 5-10.

Appendix 1 Borehole data used to determine the depth to granite surface.

Bore hole name	BGS ID	Hyperlink	Granite intersection depth m	**Total depth**	Azimuth	Inclination	Easting	Northing
Baltrink 11	658977	http://bgsintranet/ImageConverter/ScanToPdf?group_id=658977&type=0	0	244	314	-55	150470	37420
Bosworgy 1	622890	http://bgsintranet/ImageConverter/ScanToPdf?group_id=622890&type=0	170.76	214		vertical	158060	33670
CLV 17	702987	http://bgsintranet/ImageConverter/ScanToPdf?group_id=702987&type=0	155.83	695.4	301	-45	164200	37170
CM1	689090	http://bgsintranet/ImageConverter/ScanToPdf?group_id=689090&type=0	205	346	327.5	-45	165276	37859
CM3	689091	http://bgsintranet/ImageConverter/ScanToPdf?group_id=689091&type=0	33	1040.7	327	-45	165733	38078
CTL 18	689068	http://bgsintranet/ImageConverter/ScanToPdf?group_id=689068&type=0	217	236.22	330	-55	165470	38060
CTL10	689064	http://bgsintranet/ImageConverter/ScanToPdf?group_id=689064&type=0	2.5	663	338	-55	166660	39180
CTL11	689065	http://bgsintranet/ImageConverter/ScanToPdf?group_id=689065&type=0	21.5	121.92	328	-50	166480	39060
CTL13	689066	http://bgsintranet/ImageConverter/ScanToPdf?group_id=689066&type=0	0	144.78	330	-55	165950	37950
CTL17	689067	http://bgsintranet/ImageConverter/ScanToPdf?group_id=689067&type=0	0	124.96	338	-75	166660	39180
CTL19	689069	http://bgsintranet/ImageConverter/ScanToPdf?group_id=689069&type=0	0	647.09	338	-55	166580	39400
CTL22	689070	http://bgsintranet/ImageConverter/ScanToPdf?group_id=689070&type=0	214	459.02	330	-55	165470	37710
CTL27	689073	http://bgsintranet/ImageConverter/ScanToPdf?group_id=689073&type=0	0	429.15	330	-60	165990	38010

CTL27	689059	http://bgsintranet/ImageConverter/ScanToPdf?group_id=689059&type=0	0	217.32	328	-50	166780	38870
CTL4	689060	http://bgsintranet/ImageConverter/ScanToPdf?group_id=689060&type=0	0	193.54	328	-49	166550	38710
CTL6	689061	http://bgsintranet/ImageConverter/ScanToPdf?group_id=689061&type=0	0	121.92	309	-48	16690	38940
CTL7	689062	http://bgsintranet/ImageConverter/ScanToPdf?group_id=689062&type=0	0	171.6	328	-50	166660	38810
D3	618452	http://bgsintranet/ImageConverter/ScanToPdf?group_id=618452&type=0	556	793	358	-50	242740	73320
East pool new shaft Taylors	714113	http://bgsintranet/ImageConverter/ScanToPdf?group_id=714113&type=0	353	573	unknown	unknown	167420	41870
GFL1	689087	http://bgsintranet/ImageConverter/ScanToPdf?group_id=689087&type=0	114.24	340		vertical	165630	38160
GFL2	689088	http://bgsintranet/ImageConverter/ScanToPdf?group_id=689088&type=0	191.23	330		vertical	165470	38040
IMS 14	610069	http://bgsintranet/ImageConverter/ScanToPdf?group_id=610069&type=0	25.6	159.1	357	-45	226280	71430
IMS 16	610070	http://bgsintranet/ImageConverter/ScanToPdf?group_id=610070&type=0	6	237.74	0	-55	226240	71190
IMS 6	618442	http://bgsintranet/ImageConverter/ScanToPdf?group_id=618442&type=0	0	238.65	164.5	-50	242090	71840
IMS20	610071	http://bgsintranet/ImageConverter/ScanToPdf?group_id=610071&type=0	0	134.25	0	-45	226820	71210
IMS22	610072	http://bgsintranet/ImageConverter/ScanToPdf?group_id=610072&type=0	0	160.02	180	-50	226740	71150
IMS30	610073	http://bgsintranet/ImageConverter/ScanToPdf?group_id=610073&type=0	0	124.96	180	-45	226640	71220
IMS7 Calstock	618443	http://bgsintranet/ImageConverter/ScanToPdf?group_id=618443&type=0	249	481.58	147	-45	240460	71650

KB 83-1A	658491	http://bgsintranet/scripts/ida/boreholescan/dispBorehole.cfm?bgsID=658491	456	429		-90	236020	71490
KB85-3	658437	http://bgsintranet/ImageConverter/ScanToPdf?group_id=658437&type=0	265.7	400	True north	-45	236320	71270
KB86-4	658438	http://bgsintranet/scripts/IDA/boreholescan/dispBorehole.cfm?bgsid=658438	317	493.25	177	-45	236130	71880
MENNOR 1	658973	http://bgsintranet/ImageConverter/ScanToPdf?group_id=658973&type=0	43	150.57	358	-45	152690	36600
Pendarves P4	689078	http://bgsintranet/ImageConverter/ScanToPdf?group_id=689078&type=0	155	172	147	-45	165040	37550
Pendarves B1	702962	http://bgsintranet/ImageConverter/ScanToPdf?group_id=702962&type=0	64	304.8	147	-45	165810	39050
Pendarves B2	702963	http://bgsintranet/ImageConverter/ScanToPdf?group_id=702963&type=0	128	257.25	147	-45	164910	38920
Pendarves B9	702956	http://bgsintranet/ImageConverter/ScanToPdf?group_id=702956&type=0	150	243.23	147	-45	164580	38590
Pendarves DDH 200	689092	http://bgsintranet/ImageConverter/ScanToPdf?group_id=689092&type=0	0	261	151.5	1	165020	38010
Pendarves DDH 201	689093	http://bgsintranet/ImageConverter/ScanToPdf?group_id=689093&type=0	0	152.37	151.5	36	165020	38010
Pendarves DDH 202	689094	http://bgsintranet/ImageConverter/ScanToPdf?group_id=689094&type=0	0	271	141	-1	165160	38090
Pendarves DDH 208	689096	http://bgsintranet/ImageConverter/ScanToPdf?group_id=689096&type=0	0	210	95.5	21	165160	38090
Pendarves E1	702960	http://bgsintranet/ImageConverter/ScanToPdf?group_id=702960&type=0	182	203	333	-45	164480	38730
Pendarves F1	702957	http://bgsintranet/ImageConverter/ScanToPdf?group_id=702957&type=0	0	151.48	327	-45	164820	38160
Pendarves F2	702966	http://bgsintranet/ImageConverter/ScanToPdf?group_id=702966&type=0	97	142.95	327	-45	164780	38250
Pendarves F4	702983	http://bgsintranet/ImageConverter/ScanToPdf?group_id=702983&type=0	185	316.38	329	-45	164550	38130

Pendarves G1	702967	http://bgsintranet/ImageConverter/ScanToPdf?group_id=702967&type=0	340.5	343.2	147	-45	164260	39000
Pendarves G2	702980	http://bgsintranet/ImageConverter/ScanToPdf?group_id=702980&type=0	257.18	265	147	-45	166440	38860
Pendarves Q2	702946	http://bgsintranet/ImageConverter/ScanToPdf?group_id=702946&type=0	94	161.54	147	-45	164930	37980
Pendarves Q3	702947	http://bgsintranet/ImageConverter/ScanToPdf?group_id=702947&type=0	23	170	327	-45	164880	38070
Pendarves Q4	702943	http://bgsintranet/ImageConverter/ScanToPdf?group_id=702943&type=0	36	152.7	327	-45	164550	37730
Pendarves Q5	702944	http://bgsintranet/ImageConverter/ScanToPdf?group_id=702944&type=0	30.5	151.79	327	-45	164500	37700
Pendarves Q6	702945	http://bgsintranet/ImageConverter/ScanToPdf?group_id=702945&type=0	25	150.57	327	-45	164450	37670
Pendarves R4	702952	http://bgsintranet/ImageConverter/ScanToPdf?group_id=702952&type=0	125	152.7	147	-45	164600	38560
Pendavres DH 203	689095	http://bgsintranet/ImageConverter/ScanToPdf?group_id=689095&type=0	0	351	115	-1	165160	38090
RADNOR 16	657228	http://bgsintranet/ImageConverter/ScanToPdf?group_id=657228&type=0	362	850	337	-75	172000	44300
RADNOR 3	657226	http://bgsintranet/ImageConverter/ScanToPdf?group_id=657226&type=0	428.5	609.6	329	-50	172160	44300
RADNOR 5	657230	http://bgsintranet/ImageConverter/ScanToPdf?group_id=657230&type=0	439	467.56	343	-50	171720	44230
RH15	625306	http://bgsintranet/ImageConverter/ScanToPdf?group_id=625306&type=0	0	2610.5	357.7	29.4	173555	34590
RH6	625300	http://bgsintranet/ImageConverter/ScanToPdf?group_id=625300&type=0	0	309	unknown assume vertical		173464	34548
RH8(B)	625301	http://bgsintranet/ImageConverter/ScanToPdf?group_id=625301&type=0	0	304	unknown assume vertical		173468	34567
RH9(D)	625302	http://bgsintranet/ImageConverter/ScanToPdf?group_id=625302&type=0	0	305	unknown assume vertical		173484	34569

RM80-11	658489	http://bgsintranet/ImageConverter/ScanToPdf?group_id=658489&type=0	482.15	500	356	-45	360700	71130
RM82-29	658481	http://bgsintranet/ImageConverter/ScanToPdf?group_id=658481&type=0	522	699.5	177	-50	235990	71440
Roughter D2	608638	http://bgsintranet/ImageConverter/ScanToPdf?group_id=608638&type=0	50.55	114	unknown	-60	216350	82770
Roughtor D4	608640	http://bgsintranet/ImageConverter/ScanToPdf?group_id=608640&type=0	89.85	117	unknown	-74	216210	82810
S.C. 1	689054	http://bgsintranet/ImageConverter/ScanToPdf?group_id=689054&type=0	0	416.05	330	-50	166520	39530
S.C. 3	689056	http://bgsintranet/ImageConverter/ScanToPdf?group_id=689056&type=0	0	422.14	330	-60	166230	39380
S.C. 4	689057	http://bgsintranet/ImageConverter/ScanToPdf?group_id=689057&type=0	0	403.86	335	-60	166090	39320
S.C.2	689055	http://bgsintranet/ImageConverter/ScanToPdf?group_id=689055&type=0	0	354.17	330	-60	166310	39530
S.C.5	689058	http://bgsintranet/ImageConverter/ScanToPdf?group_id=689058&type=0	0	533.09	330	-50	166360	39760
SJ1	615290	http://bgsintranet/ImageConverter/ScanToPdf?group_id=615290&type=0	421.17	846.98	251	-45	135070	31770
SJ2	615291	http://bgsintranet/ImageConverter/ScanToPdf?group_id=615291&type=0	0	557.78	247	-45	135380	31380
SJ3	615292	http://bgsintranet/ImageConverter/ScanToPdf?group_id=615292&type=0	649.41	355.32	267	-45	136580	34220
SJ4	615293	http://bgsintranet/ImageConverter/ScanToPdf?group_id=615293&type=0	133.01	322	44	-45	136660	34010
SJ5	615294	http://bgsintranet/ImageConverter/ScanToPdf?group_id=615294&type=0	1161	1192	267	-45	136690	34390
Stithians	625307	http://bgsintranet/ImageConverter/ScanToPdf?group_id=625307&type=0	0	309	unknown assume vertical		173460	34540
TRDD2013001	19905551	http://bgsintranet/ImageConverter/ScanToPdf?group_id=19905551&type=0	484	544.5	294	-65	191920	60741

Trebowland Manor	618330	http://bgsintranet/ImageConverter/ScanToPdf?group_id=618330&type=0	0	110	No data	No data	173100	38900
TS1	658962	http://bgsintranet/ImageConverter/ScanToPdf?group_id=658962&type=0	0	271.27	306.5	-75	150540	37350
TS12	658972	http://bgsintranet/ImageConverter/ScanToPdf?group_id=658972&type=0	0	198	314	-50	150720	37660
TS3	658964	http://bgsintranet/ImageConverter/ScanToPdf?group_id=658964&type=0	0	375.51	306.5	-72	150580	37280
TS4	658965	http://bgsintranet/ImageConverter/ScanToPdf?group_id=658965&type=0	0	223.11	306.5	-65	150750	37830
TS5	658966	http://bgsintranet/ImageConverter/ScanToPdf?group_id=658966&type=0	0	375.81	306.5	-72	150690	37340
TS6	658967	http://bgsintranet/ImageConverter/ScanToPdf?group_id=658967&type=0	43	308.15	306.5	-72	150800	37390
TS7	658968	http://bgsintranet/ImageConverter/ScanToPdf?group_id=658968&type=0	0	366.36	313	-72	150920	37430
Wheal Grenville No 25	689072	http://bgsintranet/ImageConverter/ScanToPdf?group_id=689072&type=0	78.5	436.77	330	-60	165960	38370
Wheal Vor CTL 15	612498	http://bgsintranet/ImageConverter/ScanToPdf?group_id=612498&type=0	330	347.77		vertical	161510	29900
Wheal Vor CTL 35	612500	http://bgsintranet/ImageConverter/ScanToPdf?group_id=612500&type=0	350	429.15	155	-50	161650	29880

Appendix 2 Extracts from the RH15 core log.

7356 3459

HOT DRY ROCK GEOTHERMAL ENERGY PROJECT
CAMBORNE SCHOOL OF MINES

Measured Depth (MD) 2274.4 - 2284.7 m
Trud Depth (TD) 2185.4 - 2194.4 m

WELL RH15
Core L
Sheet 1 of 3

Machine National 80UE, Kenting Rig K31
Core Barrel Hycalog 6½ in x 2⅜ in x 45 ft, double swivel
Bit Design Security H99F, 8½ x 2⅜ in 6-cone TC insert

Wellhead Coordinates SW 173555 34594
Wellhead Elevation 161.83 m AOD
Inclination 28.6° Azimuth 359.5°

Core Photograph	Fracture/Vein Relative Dip (vein width)	Fracture/Vein Relative Azimuth	Physical Description of Discontinuities	Symbolic Fracture Log	Lengths of Matching Core	Core Length (m)	Geological Description: Rock Fabric	Geological Description: Alteration	Geological Description: Vein/Fracture Mineralogy
			smooth to rough, rounded drilling break			0.00			
	1: 75° (<0.5 mm)	Ref	1 vein				Fine-medium grained equigranular granite		1: Reddened vein
			2 fresh, hackled drilling break						
	3: 75°	0°	3 smooth to rough, planar						3: Reddened
			4 smooth, rounded, drilling break					Slight Reddening	
			5 rough drilling break, some grinding			0.50			
			6 fresh, hackled drilling break						
	7: 85°	Ref	7 rough, planar						7: Chlorite
	8: 20°	+180°	8 rough drilling break, some grinding						
			9 smooth, planar drilling break					Reddening decreases	
	10: 90° (1 mm)		10 vein						10: Quartz/Chlorite
	11: 70° (1 mm)	Ref	11 vein						11: Quartz/Chlorite
	12: 70° (1 mm)	0°	12 vein			1.00			12: Quartz/Chlorite
	13: 50°	-150°	13 rough, planar drilling break?						13: None
	14: 75°	+90°	14 rough, planar						14: Trace light green mineral
	15: 40°	+30°	15 fresh, hackled drilling break					Trace Reddening	
			16 rough drilling break, some grinding						
	17: 55°	Ref	17 rough, angular						17: Reddened
	18: 85° (<0.5 mm)	-150°	18 vein						18: Chlorite
	19: 85° (<0.5 mm)	-150°	19 vein			1.50			19: Chlorite
			20 fresh, angular drilling break						
	21: 90°		21 smooth, planar						21: None
			22 fresh, hackled drilling break						
	23: 90°	Ref	23 fresh, hackled drilling break						
			24 smooth, planar drilling break						
	25: 80° (2 mm)	Ref	25 vein						25: Tourmaline?
	26: 80° (1 mm)	-140°	26 vein			2.00			26: Quartz/Chlorite Sulphides
	27: 30°	-140°	27 fresh, planar drilling break?						27: None
			28 rough to smooth, planar drilling break						
			29 fresh, hackled drilling break						
	30: 70°	+90°	30 rough, planar						30: None
			31 rough to smooth, planar drilling break						
	32: 80° (1 mm)	-140°	32 vein						32: Chlorite/Quartz
			33 fresh, hackled drilling break			2.50			
	34: 70°	-40°	34 rough, planar						34: None
	35: 80° (1 mm)	-140°	35 vein						35: Chlorite/Quartz
	36: 80° (1 mm)	-140°	36 vein						36: Chlorite/Quartz
			37 vein						
	38: 80°	-140°	38 rough, some grinding						3: Chlorite
			39 smooth, rounded, drilling break			2.90			

Total Solid Recovery (%) 64

Logged by RMcC
Date Jan 1985

SW 73 SW/11
7356 3459

HOT DRY ROCK GEOTHERMAL ENERGY PROJECT
CAMBORNE SCHOOL OF MINES

Measured Depth (MD) 2274.4 - 2284.7 m
True Depth (TD) 2185.4 - 2194.4 m

WELL RH15
Core L
Sheet 2 of 3

Machine National 80UE, Kenting Rig K31
Core Barrel Hycalog 6½ in x 2⅝ in x 45 ft, double swivel
Bit Design Security H99F, 8⅜ x 2⅝ in 6-cone TC insert

Wellhead Coordinates SW 173555 34594
Wellhead Elevation 161.83 m AOD
Inclination 28.6° Azimuth 359.5°

Core Photograph	Fracture/Vein Relative Dip (vein width)	Fracture/Vein Relative Azimuth	Physical Description of Discontinuities	Symbolic Fracture Log	Lengths of Matching Core	Core Length (m)	Geological Description: Rock Fabric	Geological Description: Alteration	Geological Description: Vein/Fracture Mineralogy
						2.90			
	40: 85° (0.5 mm)	Ref	40 vein	40			Fine-medium grained equigranular granite		40: Chlorite/Quartz
			41 fresh, hackled drilling break	41					
			42 fresh, hackled drilling break	42					
			43 fresh, hackled drilling break						
	44: 70°	-100°	44 smooth, planar	43					44: Chlorite
			45 rough, drilling break						
			46 rough drilling break, some grinding	44		3.50			
			47 rough drilling break, some grinding	45 47 46					
			48 smooth, planar drilling break	48					
			49 smooth, planar drilling break	49					
			50 rough to smooth, drilling break	50					
	51: 70°	Ref	51 rough, planar			4.00		Trace Reddening	51: Chlorite with silicified margin
			52 rough drilling break, some grinding	51					
			53 smooth, rounded, drilling break	52 53					
	54: 70° (1 mm)	0°	54 vein	54					54: Chlorite/ Sulphides
			55 rough to smooth, rounded, drilling break						
	56: 30°	Ref	56 rough to smooth, rounded, drilling break	55 56		4.50			
			57 rough drilling break, some grinding	57 58					
	58: 75°	Ref	58 rough, planar					Slight Reddening	Brown 58: Carbonate
			59 smooth, planar drilling break						
			60 rough, drilling break	59		5.00			
			61 smooth, planar drilling break	60 61					
	62: 60° (1 mm)	Ref	62 vein	62				Slight Reddening with silicified zone	62: Chlorite
	63: 60° (1 mm)	+10°	63 vein	63					63: Chlorite
			64 smooth, planar drilling break	65 64		5.50			
			65 smooth, planar drilling break						
	66: 50°	Ref	66 rough, planar	66				Trace Reddening	66: None
			67 smooth, planar drilling break	67		5.70			

Total Solid Recovery (%) 64

Logged by RMcC
Date Jan 1985

7356 3459

HOT DRY ROCK GEOTHERMAL ENERGY PROJECT
CAMBORNE SCHOOL OF MINES

Measured Depth (MD) 2274.4 - 2284.7 m
True Depth (TD) 2185.4 - 2194.4 m

WELL RH15
Core L
Sheet 3 of 3

Machine National 80UE, Kenting Rig K31
Core Barrel Hycalog 6½ in x 2⅝ in x 45 ft, double swivel
Bit Design Security H99F, 8⅜ x 2⅝ in 6-cone TC insert

Wellhead Coordinates SW 173555 34594
Wellhead Elevation 161.83 m AOD
Inclination 28.6° Azimuth 359.5°

Core Photograph	Fracture/Vein Relative Dip (vein width)	Fracture/Vein Relative Azimuth	Physical Description of Discontinuities	Symbolic Fracture Log	Lengths of Matching Core	Core Length (m)	Geological Description: Rock Fabric	Geological Description: Alteration	Geological Description: Vein/Fracture Mineralogy
	68: 75°	Ref	68 rough, planar drilling break			5.70	Fine-medium grained equigranular granite		
	69: 75° (2 mm)	-90°	69 vein					Silification	69: Chlorite
	70: 60°	+180°	70 rough, planar drilling break						
			71 smooth, planar drilling break						
			72 smooth, drilling break					Slight Reddening	
						6.00			
	73: 65°	Ref	73 rough, planar						Brown 73: Carbonate
			74 smooth, planar drilling break				Low mafic content	Trace Reddening	
			75 smooth, rounded, drilling break						
			76 angular rough to smooth drilling break					Medium Reddening	
								Strong Reddening	
	77: 65°	Ref	77 smooth, rounded, drilling break			6.50			
			78 smooth, planar drilling break						
	79: 70° (<0.5 mm)	Ref	79 vein						79: Chlorite
	80: 70°	0°	80 rough, angular						80: Chlorite
			81 smooth, rounded, drilling break						
	82: 70°		82 smooth, angular drilling break						
	83: 70° (5 mm)	Ref	83 vein						83: Chlorite/Quartz
			84 smooth, rounded, drilling break						

Total Solid Recovery (%) 64

Logged by RMk
Date Jan 198[illegible]

Appendix 3 Properties simulated, interpolate or calculated through the model volume.

Property	Source	Units	Method
BrazillianTensileStrength	CSM Report 2A-46 Mechanical Properties of the Carnmenellis Granite HDR Report 3,3,1	MPa	BrazillianTensileStrength = 10.6 + 1.1 * (DepthBelowSurface / 1000)
DepthBelowSurface		m	Calculated from model
DistancetoFault		m	Calculated from model
DistancetoGranite		m	Calculated from model
GraniteDensity	CSM Report 2A-46 Mechanical Properties of the Carnmenellis Granite HDR Report 3,3,1	Kg/m^3	Granite = 2640
GraniteThickness		m	Calculated from model
HeatFlow	Wheildon and Rollins 1986. eq 2.5 and 2.6	mWm^{-2}	For depths Greater than 300m below ground level HeatFlow= (2 * 833.33 * ThermalConductivityMean * log ((TemperatureHDRGradient + 823.33) / 833.33) + (HeatProductionBeamishCoKrig * pow((DepthBelowSurface / 1000), 2)))/(2 * (DepthBelowSurface / 1000))
HeatFlowInverse	Wheildon and Rollins 1986. eq 2.5 and 2.14	mWm^{-2}	For depths Greater than 300m below ground level HeatFlowInverse = (ThermalConductivityMean * 833.33 * log(((TemperatureHDRGradient + 823.33) / 833.3))+(HeatProductionBeamishCoKrig / pow(0.1,2) * (1-(0.1 * (DepthBelowSurface / 1000) + 1)*(1 - (log(0.1 * (DepthBelowSurface / 1000) + 1))))))/(DepthBelowSurface / 1000);}
HeatFlowMeanNormDistCorrAFrancis1980	Francis (1980)	mWm^{-2}	Simulated from a Normal Distribution Granite – Mean = 116 SD=9 Killas – Mean =59 SD=10

HeatFlowRichardsonOxburgh1979	In Francis (1980) eq5.6 (after Richardson and Oxburgh 1979)	mWm^{-2}	HeatFlowRichardsonOxburgh1979= 27 + (16.6 * HeatProductionBeamishCoKrig); This is known to under estimate the heat flow (Beamish and Busby, 2016)
HeatProductionBeamishCoKrig	Beamish and Busby (2016)	uWm^{-3}	Co-Kriging simulation of the Heat production model from beamish cross correlated with log of the inverse distance from granite with a correlation coefficient of 0.5. The variogram had sill of 0.501789, exponential, R1 = 14422.9, R2 = 18585.6, R3 = 262196 and an azimuth of 3.15886 and nugget of 0.
HeatProductionBeamishCoKrigExpoDecrease	Wheildon and Rollins 1986. eq 2.9	uWm^{-3}	HeatProductionBeamishCoKrigExpoDecrease = HeatProductionBeamishCoKrig * exp(-(DepthBelowSurface / 1000) / 16.6);
HeatProductionBeamishCoKrigInverse	Wheildon and Rollins 1986. eq 2.13	uWm^{-3}	HeatProductionBeamishCoKrigInverse = HeatProductionBeamishCoKrig / (0.1 * (DepthBrlowSurface / 1000) +1);
PoissonsRation	Parker 1991		For granite only. PoissonsRatio = urand(0.22 ,0.27);
PoissonsRationTemperatureYu2014	Yu 2014		Change in Poissons Ratio in response to increase in temperature PoissonsRatioTemperatureYu2014 = 0.0004 * TemperatureKHDRGeothermalGradient + 0.22;

Regions			Calculated from model 1=Killas 2=Upper Granite 3=Lower Granite
SHMaxAzimuth		°	Based on SHINE (Carafa et al., 2014) interpolation of World Stress Map 2016 data (Heidbach et al. 2016)
SHMaxMagnitude	Parker 1991	MPa	SHmax = 15 + 28 * (DepthBelowSurface / 1000)
ShminAzimuth		°	Based on SHINE (Carafa et al, 2014) interpolation of World Stress Map 2016 data (Heidbach et al. 2016)
ShminMagnitude	Parker 1991	MPa	Shmin = 6 + 12*(DepthBelowSurface / 1000)
SpecificHeatCapacity	Lindroth and Krawza 1971 in Jackson et al. 1989	$Jg^{-1}K^{-1}$	SpecificHeatCapacity= 4.186 * (0.209334 + 0.000131034 * TemperatureHDRGradient);
SurfaceTemperature	Francis 1980	°C	11
SvMagnitude	Parker 1991	MPa	SvMagnitude = 26 * (DepthBelowSurface / 1000)
TemperatureHDRGradient	Parker 1991	°C	TemperatureHDRGradient = 0.035 * DepthBelowSurface + 12;
TemperatureHaenel1980	Haenel 1980 (Francis 1980 eq5.1)	°C	TemperatureHaenel1980 = SurfaceTemp + (HeatFlowMeanNormDistCorrAFrancis1980 * (-1 * (DepthBelowSurface / 1000)) / ThermalConductivityMean) - (HeatProductionBeamishCoKrig * (-1 * DepthBelowSurface / 1000)/(2 * ThermalConductivityMean));
TemperatureHaenel1980RichardsonOxbughHeatFlow	Francis 1980 eq5.4	°C	Change in Temperature with constant heat production but with temperature dependant thermal conductivity TemperatureHaenel1980Richardson = SurfaceTemperature + ((HeatFlowRichardsonOxburgh1979 * (DepthBelowSurface / 1000)) / ThermalConductivity) - ((HeatProductionBeamishCoKrig * pow(DepthBelowSurface / 1000,2)) / (2 * ThermalConductivity));
TemperatureKHDRGradient	Parker 1991	K	Temperature at depth in Kelvin based on HDR geothermal gradient TemperatureKHDRGradient = TemperatureHDRGradient + 273.15;
ThermalDiffusivity	Vosteen and Schellschmidt 2003 Eq. 3	m^2s^{-1}	ThermalDiffusivity = ThermalConductivity / (GraniteDensity * SpecificHeatCapacity);

ThermalConductTempKappelmyerHaenel1974	Kappelmeyer and Haenel, 1974 in Wheildon and Rollins 1986	$Wm^{-1}K^{-1}$	ThermalConductTempKappelmyerHaenel1974 = ThermalConductivityMean * 833.33 / (823.33 + TemperatureHDRGradient);
ThermalConductivity	Granite – Francis 1980 Killas - Kappelmeyer and Haenel, 1974	$Wm^{-1}K^{-1}$	Granite ThermalConductivity = -0.41 * log(TemperatureHDRGradient) + 4.0; Killas - Perpendicular to bedding ThermalConductivity= -0.056 * log(TemperatureHDRGradient) + 2.0302;
ThermalConductivityMean	Francis 1980	$Wm^{-1}K^{-1}$	Granite – ThermalConductivity = 3.33 Killas – ThermalConductivity = 2.5
ThermalConductivitySartori1983	Sartori 1983 in Jackson et al. 1989	$Wm^{-1}K^{-1}$	Granite ThermalConductivitySartori1983 = 574.8 / TemperatureKHDRGradient + 1.30;
ThermalExpansionCoefficientHeuze1983	Heuze 1983 in Jackson et al. 1989	K-1	Granite ThermalExpansionCoefficientHeuze1983 = 0.000005 + (TemperatureHDRGradient / 920) * 0.000018;
ThicknessLowerGranite		m	Calculated from model
ThicknessUpperGranite		m	Calculated from model
TriaxialCompressiveStrength	Mechanical Properties of the Carnmenellis Granite HDR Report 3,3,1	MPa	Granite TriaxialCompressiveStrength = 132 + (37 * (DepthBelowSurface / 1000));
UniaxialCompressiveStrength	Mechanical Properties of the Carnmenellis Granite HDR Report 3,3,1	MPa	Granite UniaxialCompressiveStrength = 32 * (DepthBelowSurface / 1000) + 103:
UniaxialCompressiveStrengthTemperatureYu2014	Yu et al. 2014	MPa	Granite UniaxialCompressiveStrengthTemperatureYu2014 = -0.0001 * pow(TemperatureHDRGradient,2) - 0.0284 * TemperatureHDRGradient + 103;
YoungsModulus	Mechanical Properties of the Carnmenellis Granite HDR Report 3,3,1	GPa	Granite YoungsModulus = 54 + (4 * (DepthBelowSurface / 1000));

YoungsModulusTemperatureHeuze1983	Heuze 1983 in Jackson et al. 1989	GPa	Granite YoungsModulusTemperatureHeuze1983 = ((90 + (4 * (DepthBelowSurface / 1000))) * (1000 - TemperatureKHDRGradient)) / 1000;
YoungsModulusTemperatureYu2014	Yu et al. 2014	GPa	Granite YoungsModulusTemperatureYu2014 = -0.0002 * pow(TemperatureHDRGradient,2) + 0.0515 * TemperatureHDRGradient + 54;

Appendix 4 Fracture density statistics and histograms from calculated fracture density.

Property	Mean	SD	Low Cut off	High Cut off	
FS1 Low	0.354883	0.222659	0	1.18521	

					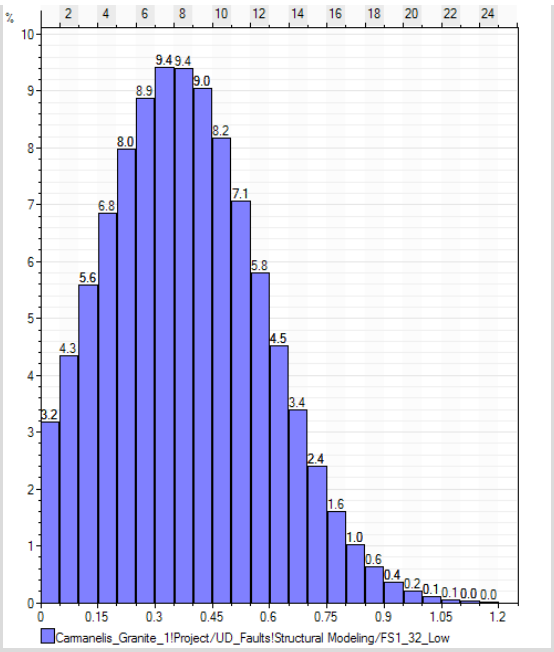
FS1 Mean	0.493334	0.403768	0	1.85008	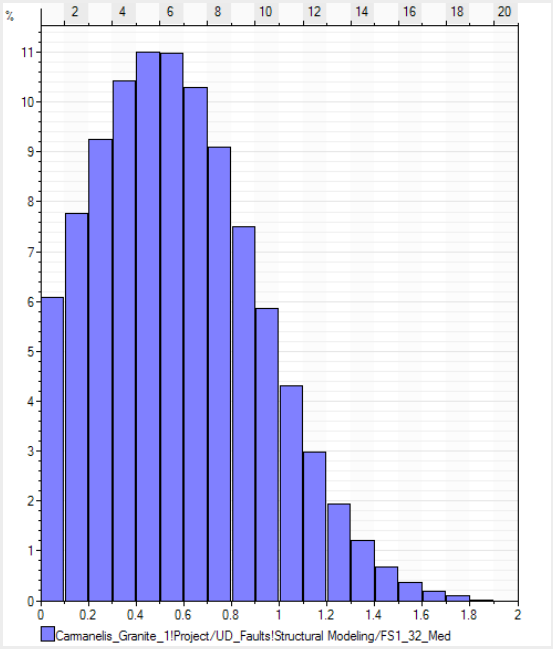
FS1 High	1.51089	0.64597	0	2.9548	

					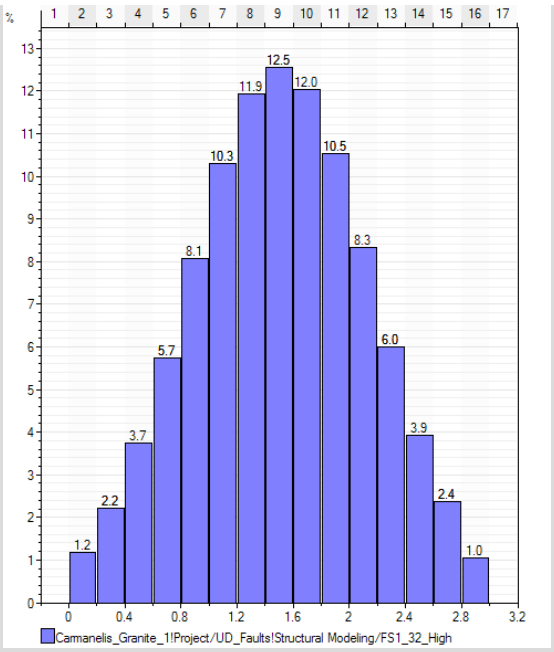
FS2 Low	0.732625	0.435894	0	2.02774	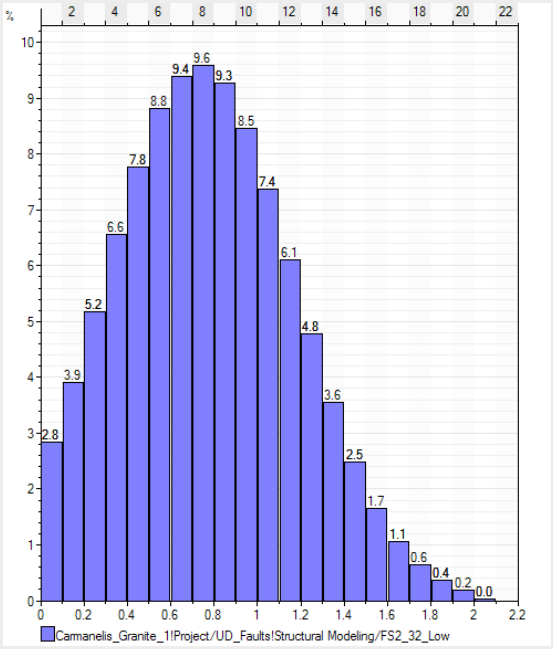

FS2 Mean	1.11078	0.614915	0	2.8212	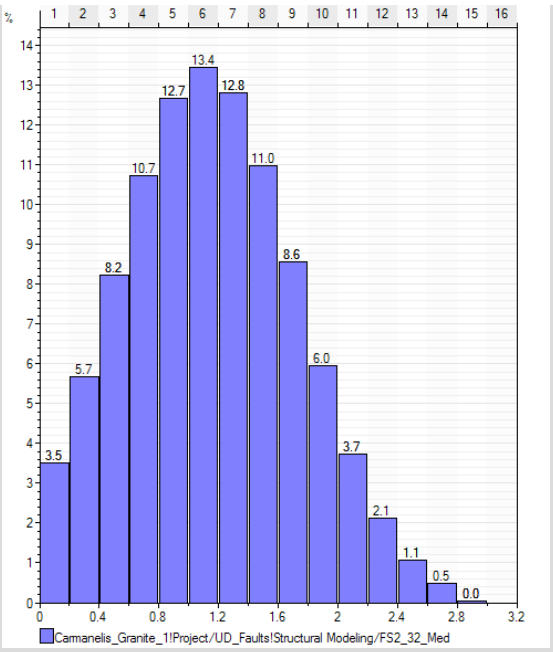
FS2 High	2.030668	0.862203	0	4.14364	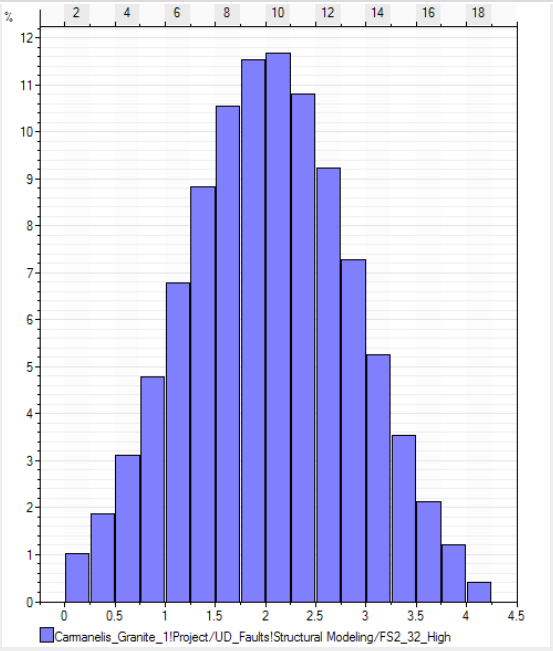

Appendix 5 The parameters used for the three DFN models for the HDR site. Note the three density models used in the three models.

	FS1	FS2
Density	P32 Low, Med, High	P32 Low, Med, High
Sides	4	4
Elongation ratio	2	1.7
Length Distribution	Lognormal	Lognormal
Length Distribution – Mean	13.925	13.357
Length Distribution - SD	33.89	25.018
Maximum Length of Implicit	150m	150m
Maximum Length	300m	300m
Orientation – Dip Azimuth	49.49	321.75
Orientation – Dip	86.36	67.22
Orientation – Concentration	15.91	8.40
Aperture Distribution	Lognormal	Lognormal
Aperture Distribution – Mean	3.7267E-6	5.0435E-7
Aperture Distribution – SD	4.885E-6	6.6112E-7
Aperture Distribution - Max	0.00005	0.000025
Aperture Distribution - Min	0	0

Appendix 6 Calculated permeability in each of the principal grid orientations (i, j, k) and for each of the HDR model based on the corrected Oda method for fractures with a horizontal length greater than 150m.

Model	Direction	Mean Permeability (mD)	SD		
HDR Low	Ki	0.0051	0.0279	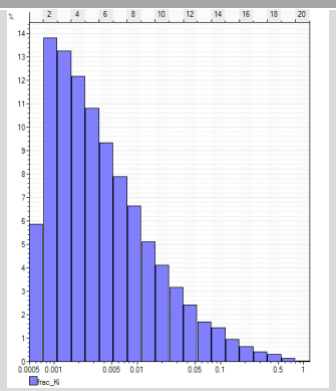	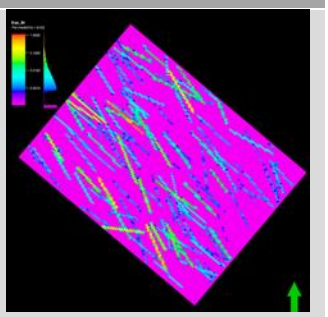
	Kj	0.0009	0.0068	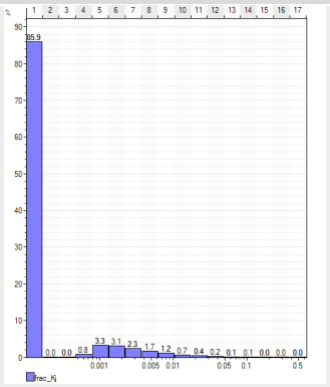	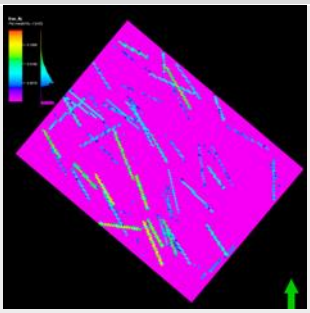
	Kk	0.0070	0.0375	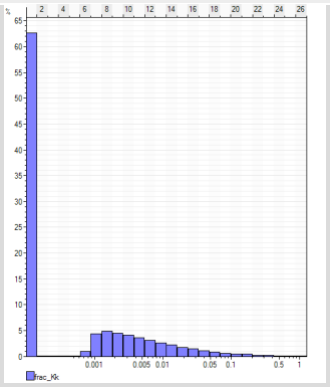	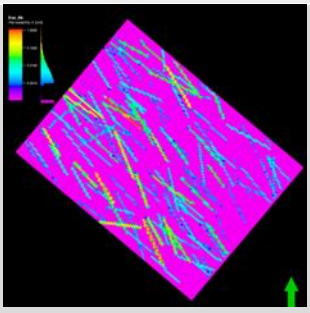

HDR Mean	Ki	0.0082	0.0346	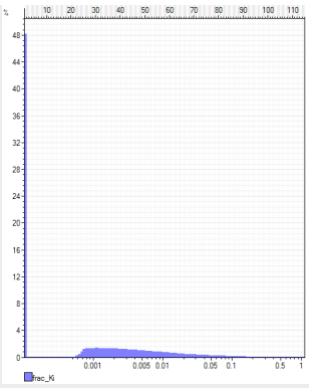	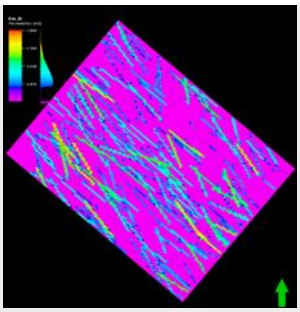
	Kj	0.0014	0.0081	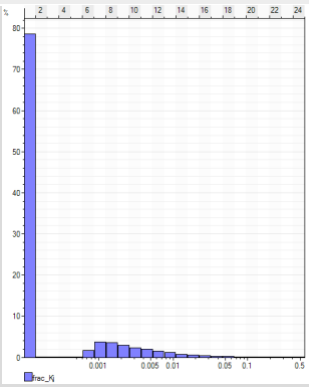	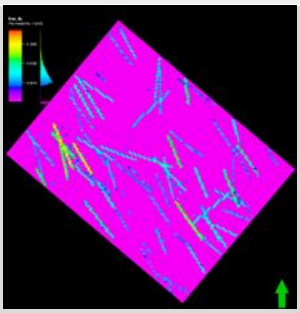
	Kk	0.0110	0.0468	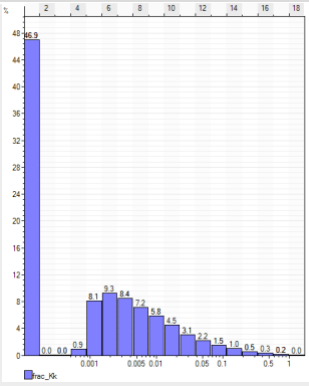	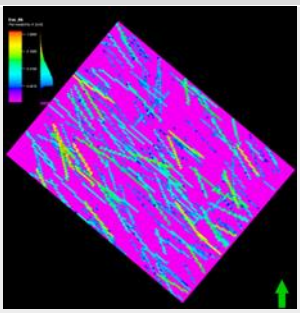
HDR High	Ki	0.0230	0.0592	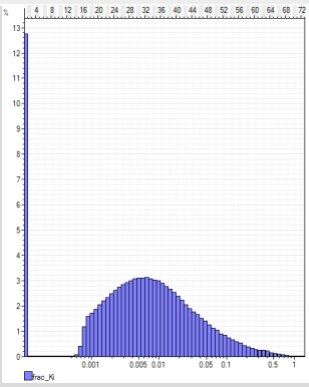	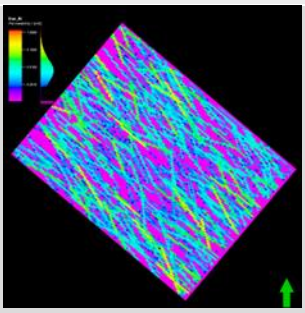

	Kj	0.0038	0.0130	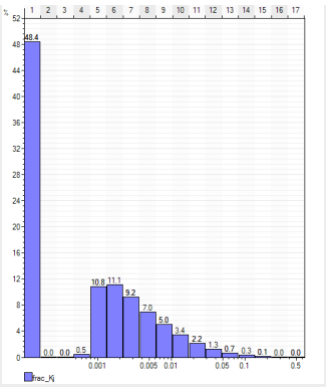	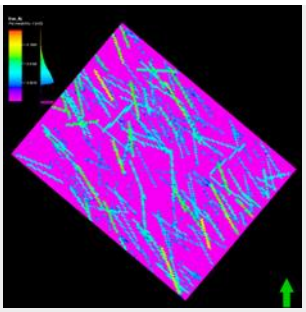
	Kk	0.0280	0.0703	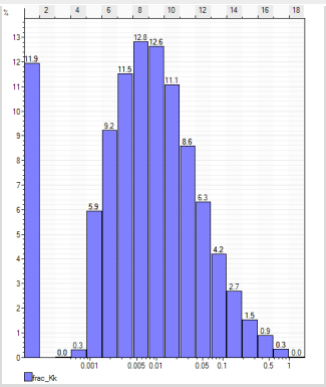	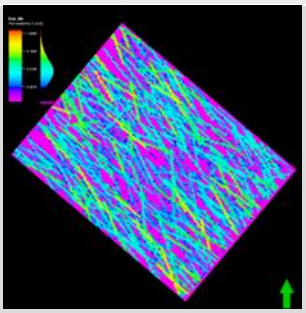

Appendix 7 Calculated permeability in each of the principal grid orientations (i, j, k) and for each of the UD model based on the corrected Oda method for fractures with a horizontal length greater than 150m.

	FS1	FS2	Fault Zone
Density	P32 Low, Med, High	P32 Low, Med, High	P32 = 4.14 within the fault zone and the inverse of the cube root of the distance to fault multiplied by the 4.14
Sides	4	4	4
Elongation ratio	2	1.7	2
Length Distribution	Lognormal	Lognormal	Lognormal
Length Distribution – Mean	13.925	13.357	13.925
Length Distribution - SD	33.89	25.018	33.89
Maximum Length of Implicit	150m	150m	150m
Maximum Length	300m	300m	300m
Orientation – Azimuth	49.49	321.75	Perpendicular to the fault strike
Orientation – Dip	86.36	67.22	85
Orientation – Concentration	15.91	8.40	50
Aperture Distribution	Lognormal	Lognormal	Log-Normal
Aperture Distribution – Mean	3.7267E-6	5.0435E-7	3.7267E-6
Aperture Distribution – SD	4.885E-6	6.6112E-7	4.885E-6
Aperture Distribution - Max	0.00005	0.000025	0.00005
Aperture Distribution - Min	0	0	0

Appendix 8 Modelled permeabilaties for the UD model

Model	Direction	Mean Permeability (mD)	SD		
UD Low	Ki	0.0242	0.0499	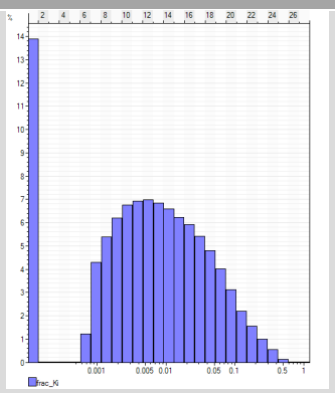	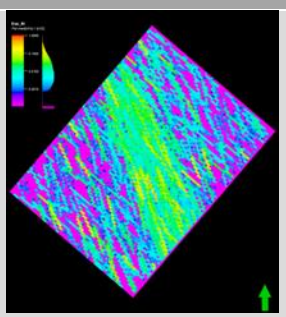
	Kj	0.0047	0.0112	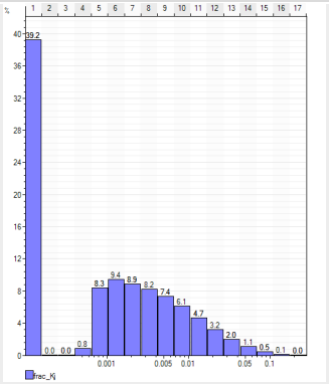	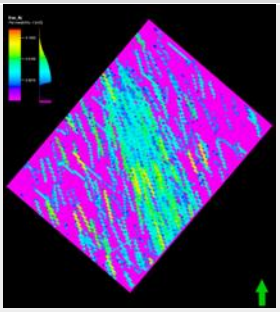
	Kk	0.0323	0.0646	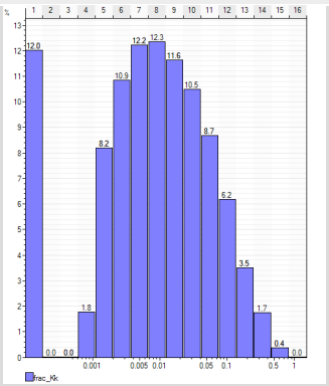	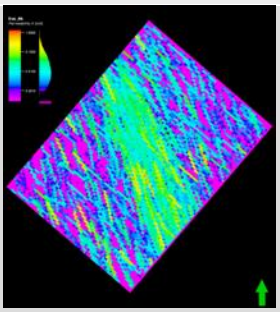
UD Mean	Ki	0.0274	0.0524	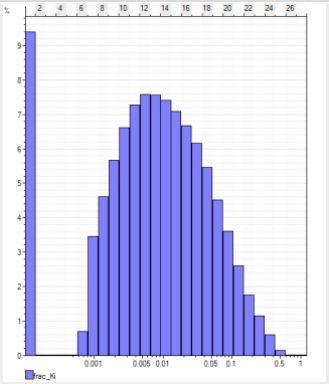	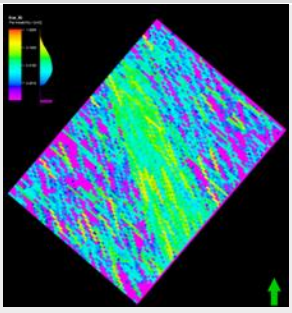

	Kj	0.0055	0.0123	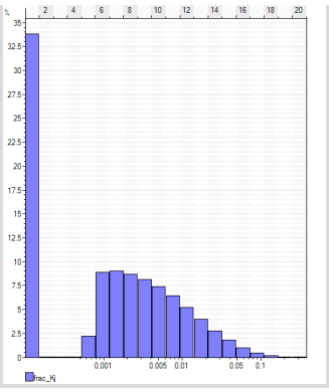	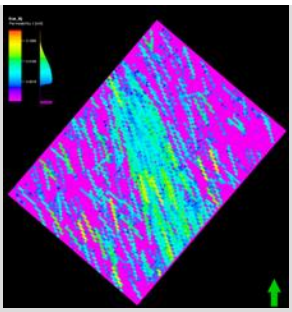
	Kk	0.0355	0.0665	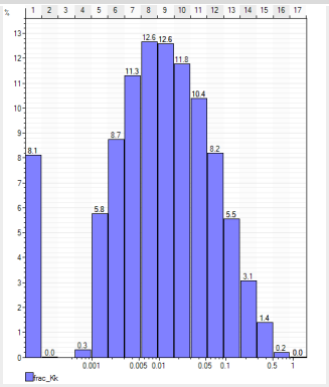	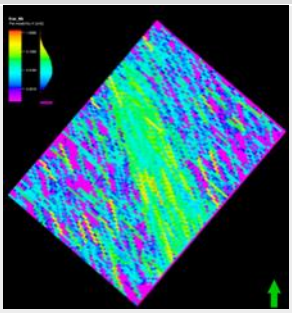
UD High	Ki	0.0449	0.0671	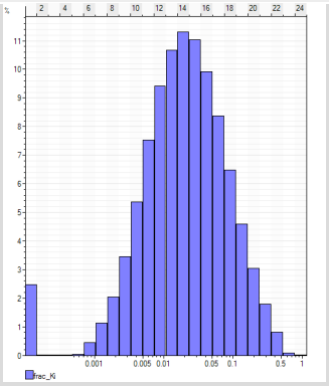	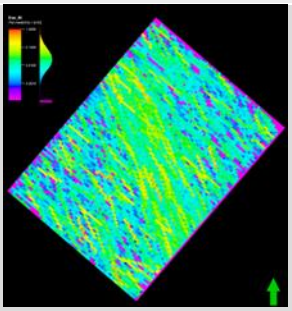
	Kj	0.0083	0.0150	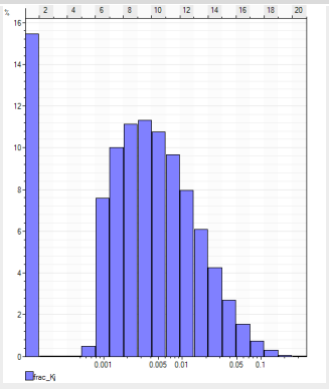	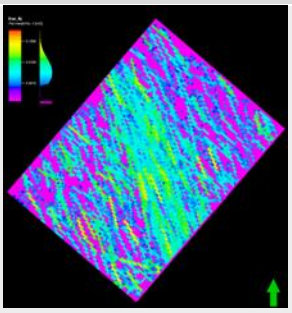

	Kk	0.0530	0.0788